Dendritic Cells in Autoimmune Diabetes

by

Simon Janendra Prasad

A thesis submitted for the degree of
Doctor of Philosophy of the Australian National University

John Curtin School of Medical Research
Australian National University
Canberra, Australia

March 2000

Statement

This thesis presents the results of research undertaken at the Medical Genome Center, Division of Molecular Medicine of the John Curtin School of Medical Research, Australian National University, Canberra. The research was undertaken between May 1996 and March 2000 while I was a recipient of an Australian National University PhD scholarship and a tution waiver from the John Curtin School of Medical Research.

The results and analyses presented in the thesis are my own work accomplished under the supervision of Professor Christopher Goodnow except where otherwise stated in the text or acknowledgements.

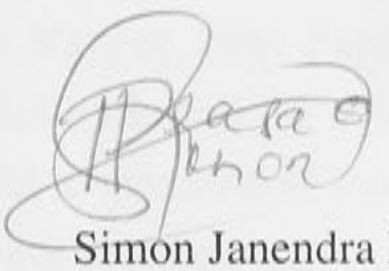

Simon Janendra Prasad

* In my haste to complete this thesis I unfortunately overlooked members of my advisory panel, Drs. Arno Müllbacher and Peter Milburn, whom I would also like to thank for useful discussions.

Acknowledgements

My sincere thanks go to my supervisor, Professor Christopher Goodnow, for his excellent supervision during the course of this study. It has been an honour and a pleasure to have had a mentor of Professor Goodnow's calibre. I have learned much (or so I hope...) from Professor Goodnow's passion and commitment for research and his rigorous and creative mind.

I am especially grateful to Dr. Sarah Townsend, former postdoctoral fellow in the lab, for her invaluable support and advice during the initial stages of my project. Dr. Townsend, along with Drs. Bennett Weintraub and Suzanne Hartley, also former postdoctoral fellows in the lab, helped create a stimulating learning environment.

Thanks also to Dr. Anand Gautam, my Honours supervisor, who introduced me to the phenomenon of dendritic cells and who assisted in acquiring reagents for the establishment of dendritic cell cultures.

Furthermore, I would like to thank Jane Rayner, Pete Papathanasiou, Steve Martin, Lauren Wilson, Christine White and Dr. Julie Blasioli for being supportive and encouraging colleagues in the lab. I am also grateful to members of the Medical Genome Centre for their critical role in the maintenance of mice colonies.

Special thanks go to Geoff Osborne and Sabine Grüninger of the JCSMR FACS Facility, members of JCSMR Photography and Electron Microscopy Unit, and personnel at the Computer Help Desk for their time and assistance.

Finally, I would like to extend my special thanks to my mum and Lucy for their unwavering support and patience during all my endeavours. I especially acknowledge Lucy's inspiring role in the last few weeks as we await the birth of our first child.

Dedicated to Mum, Nani, Lucy and The Little One....

Abstract

Genes outside the Major Histocompatibility Complex (MHC) create a general susceptibility to autoimmunity in non-obese diabetic (NOD) mice. The current study has utilized NOD.H-2^k and control B10.BR (B10.H-2^k) congenic mice to study dendritic cell generation, both in vitro and in vivo, in an attempt to explore cellular processes which might be affected by non-MHC NOD genes.

Initial in vitro results revealed that NOD.H-2^k bone marrow cells cultured in the presence of GM-CSF and IL-4 generated a reduced yield of dendritic cells. This was underpinned by heterogeneous proliferation and elevated levels of apoptosis in NOD.H-2^k cultures. Both of these phenotypes appeared unique to the NOD.H-2^k background as the response to growth factor stimulation of bone marrow cells from other H-2^k congenic strains was comparable to the response of cells from the B10.H-2^k strain. Using allelic variants of Ly5 to distinguish between strain-specific cells, it was determined that B10.H-2^k myeloid precursors in co-culture with NOD.H-2^k precursors develop normally into dendritic cells. This indicated that the inability of NOD.H-2^k myeloid precursors to generate substantial numbers of dendritic cells in vitro was a cell-intrinsic feature of NOD.H-2^k myeloid precursors.

To assess the relative physiological capacity of NOD.H-2^k and B10.H-2^k myeloid precursors to reconstitute irradiated hosts and generate dendritic cells in vivo, mixed bone chimeric mice were constructed. A mixed inoculum comprising a 1:1 mixture of bone marrow cells from B10.H-2^k and NOD.H-2^k mice was used to reconstitute irradiated B10.H-2^k recipients. Reconstitution of recipients was analyzed by flow cytometry, again using allelic variants of Ly5 to distinguish between donor cells. Surprisingly, the myeloid lineage of cells in recipient mice was disproportionately derived from the NOD.H-2^k donor while the lymphoid compartment was even between the two donors. Interestingly, the skewing towards NOD.H-2^k-derived dendritic cells in the spleen was accounted for predominantly by the CD8α^- negative subset, reflecting a similar and unique bias observed in unmanipulated NOD.H-2^k mice.

Overall, findings from this study demonstrate for the first time that non-MHC NOD genes confer on myeloid precursors a cell-intrinsic phenotype which alters dendritic cell generation both in vitro and in vivo. It is conceivable that dysregulation of antigen presenting cell function of dendritic cells may explain the breach of peripheral tolerance mechanisms in NOD mice.

Publications

Prasad, S.J. and Goodnow, C.C. Cell-intrinsic effects of non-MHC NOD genes on dendritic cell generation. *Manuscript in preparation.*

Selected Conference Papers

Prasad, S.J. and Goodnow, C.C.(1999). Cell-Intrinsic Effect of NOD Genes on Dendritic Cells.
Sixth Conference of the Immunology Group of Victoria, Mt. Buffalo, Victoria.

Prasad, S.J. and Goodnow, C.C.(1999) Cell-Intrinsic Effect of NOD Genes on Dendritic Cells.
29th Annual Conference of the Australian Society for Immunology, Dunedin, New Zealand.

Table of Contents

Abbreviations

^{o}C	Degrees Celsius
BrDU	5-bromo-2'-deoxyuridine
CD	Cluster of Differentiation
CHS	Contact Hypersensitivity
cDNA	complementary Deoxyribonucleic acid
cpm	counts per minute
Ci	Curie
cm	centimeter
CTL	Cytotoxic T Lymphocyte
CTLA-4	Cytotoxic T Lymphocyte Antigen-4
DMSO	Dimethylsulfoxide
DNA	Deoxyribonucleic acid
DNase	Deoxyribonuclease
dNTP	Deoxynucleotide triphosphate
EAE	Experimental Autoimmune Encephalomyelitis
EDTA	Ethylenediamine tetra-acetic acid
EBV	Epstein-Barr Virus
FACS	Fluorescence-activated Cell Sorter
FBS	Foetal Bovine Serum
FITC	Fluorescein Isothiocyanate
g	Gravity
g	Gram
G	Gauge
GM-CSF	Granulocyte and Macrophage Colony Stimulating Factor
H2	Major Histocompatibility Complex of mice
HEL	Hen Eggwhite Lysozyme
HEV	High Endothelial Venule
HLA	Human Histocompatibility Leukocyte Antigen
hr	Hour/s
ICAM-1	Intercellular Adhesion Molecule 1
IDDM	Insulin-dependent Diabetes Mellitus
IFN	Interferon
Ig	Immunoglobulin
Ii	Invariant Chain
IL	Interleukin
ip	intraperitoneal
IPC	Interferon Producing Cell
KLH	Keyhole Limpet Hemocyanin
L	Litre/s

LFA-3	Lymphocyte-associated Antigen 3
LPS	Lipopolysaccharide
M	Molar
MIIC	MHC class II Compartment
MC540	Merocyanin 540
MDC	Macrophage-derived Chemokine
MIP	Macrophage Inflammatory Protein
mg	Milligram/s
mL	Milliliters
mM	Millimolar
mRNA	Messenger Ribonucleic Acid
µg	Microgram/s
µm	Micrometre/s
µM	Micromolar
MHC	Major Histicompatibility Complex
MLR	Mixed Leukocyte Reaction
MMR	Macrophage Mannose Receptor
NOD	Non-obese Diabetic
NON	Non-obese non-diabetic
NK Cell	Natural Killer Cell
op	Osteopetrotic
OVA	Ovalbumin
PBS	Phosphate Buffered Saline
PCR	Polymerase Chain Reaction
PE	Phycoerythrin
pH	$-\log_{10}[H^+]$
PI	Propidium Iodide
PVC	Polyvinyl Chloride
RAG	Recombinase Activating Gene
RIP	Rat Insulin Promoter
RPMI	Roswell Park Memorial Institute
RT-PCR	Reverse Transcriptase PCR
SCID	Severe Combined Immunodeficiency
SDS	Sodium Dodecyl Sulphate
SE	Standard Error
TAE	Tris/Acetate/EDTA Buffer
Tris	Tris(hydroxymethyl) aminomethane
UV	Ultra Violet
v/v	Volume/Volume
w/v	Weight/Volume

Chapter 1

General Introduction

1.1 Insulin-dependent Diabetes Mellitus

The Non-obese Diabetic (NOD) mouse is a model for human Insulin-dependent Diabetes Mellitus (IDDM), also known as Type I or autoimmune diabetes (Baxter and Cooke, 1995; Wicker et al, 1995; Tisch and McDevitt, 1996; Vyse and Todd, 1996; Delovitch and Singh, 1997). NOD mice spontaneously develop autoimmune diabetes with pathology remarkably similar to that observed in human patients. Patients with autoimmune diabetes are at constant risk of severe hypoglycemia due to pharmacologic administration of insulin. A large fraction of the patients develop a series of morbid and often fatal complications including renal failure, proliferative retinopathy leading to blindness and neuropathic syndromes due to chronic hyperglycemia. As in humans, susceptibility to autoimmune diabetes in NOD mice is multifactorial and is underpinned by the complex interplay of genetic and environmental factors. Overt disease results from T cell-mediated destruction of insulin-secreting β cells in the pancreatic islets of Langerhans. Genetic mapping in NOD mice has led to the discovery of at least 15 susceptibility loci (termed *Idd*), which include MHC (*Idd1*) and non-MHC-linked (*Idd2-15*) genes. Although the NOD MHC is necessary, it is insufficient to induce diabetes, thus emphasizing the importance of non-MHC NOD genes in diabetes susceptibility.

1.2 Origin of the NOD mouse

The NOD mouse was discovered at the Shionogi Research Laboratories in Japan during the derivation of a spontaneously cataract prone CTS strain (Kikutani and Makino, 1992). The NOD mouse strain originated from Swiss albino stock and was derived from ICR outbred mice. The discovery, in 1974, of a female mouse exhibiting diabetic symptoms without obesity spurred the development of the NOD strain. Selective breeding using the offspring of the female mouse was performed, and the NOD strain was established in 1980. The NOD-related non-obese non-diabetic (NON) strain was also developed at this time. In 1985, breeding pairs of NOD mice obtained from the breeding nucleus maintained at Shionogi were taken to the USA. NOD/Lt, the line derived from these mice, is currently maintained by Dr. E. Leiter at the Jackson Laboratory, Bar Harbor, Maine, USA. Most of the colonies around the world are derived from this colony.

1.3 The Pathology and Natural History of IDDM

Autoimmune diabetes is a biphasic disease characterized by an initial leukocytic infiltration into islets, termed insulitis, followed by overt disease which is precipitated by the destruction of insulin-secreting β cells. The first islet abnormality is manifested by the swelling of blood vessels around the islets. This is accompanied by the coming into prominence of the perivascular connective tissue. These early signs of inflammation trigger the initial infiltrate into islets and elevated numbers of infiltrating leukocytes can be detected in NOD mice as early as 3 weeks of age. This initial infiltrate precedes lymphocytic infiltration and comprises dendritic cells and macrophages (Jansen et al, 1994). At this stage elevated numbers of infiltrating dendritic cells and macrophages accumulate in the periductal areas but remain outside the islet proper. Subsequent lymphocytic infiltration entails direct invasion of islets by infiltrating cells. Diabetes is the final clinical outcome when most of the β cell mass has been destroyed. Insulin production as a result is insufficient to maintain glucose homeostasis, leading to hyperglycemia and its associated clinical consequences. Insulitis is more severe in female NOD mice and is indicative of their relatively increased susceptibility to overt diabetes. In high incidence NOD colonies, overt diabetes occurs at 18-20 weeks of age. The cumulative incidence for diabetes is 80-90% in females compared with 10-40% in males. This pronounced gender bias is not seen in human patients. Environmental factors affecting disease incidence in NOD colonies include diet, viral infection and temperature (Elliot et al, 1988; Oldstone, 1990; Williams et al, 1990; Pozzilli et al, 1993). There is a positive correlation between disease incidence and the level of sanitation in NOD colonies. Germ-free NOD mice have nearly 100% disease incidence. Correspondingly, a North-South gradient of disease incidence is observed in human populations (Karvonen et al, 1993). Inhabitants of Northern Europe are more susceptible to autoimmune diabetes than those resident in the tropics.

1.4 The Role of T cells in IDDM

The effector and cellular mechanisms by which β cells are destroyed remain to be fully elucidated. In a longitudinal study of prediabetic NOD mice, Miyazaki et al (1985) demonstrated, by immunohistochemical analyses, the predominance of T cells in pancreatic islets. Both CD4 and CD8 T cells are the most prominent cells in insulitic lesions of NOD mice although their respective roles in the pathology of autoimmune diabetes remains unclear (Miller et al, 1988). The absence of insulitis and diabetes in athymic NOD nude mice and neonatally thymectomized NOD mice demonstrate that T cells are essential for diabetes induction (Yagi et al,1992). Also, antibody-mediated

depletion of T cells in NOD mice was found to reduce the incidence of diabetes (Koike et al, 1987). Further direct evidence for the implication of T cells in diabetes induction came in studies involving the adoptive transfer of diabetogenic T cells into non-diabetic recipients (Bendelac et al, 1987; Christianson et al, 1993). Prior to the study by Bendelac et al (1987), diabetes induction studies used adoptive transfer of diabetogenic lymphocytes into irradiated, adult and non-diabetic NOD mice. In these studies the complete ablation of endogenous T cells could not be assumed and therefore complicated interpretation of results obtained (Wicker et al, 1986; Miller et al,1988) Therefore, Bendelac et al (1987) developed a neonatal model for diabetes transfer using syngeneic cells from diabetic donors. It was shown that splenocytes from diabetic NOD mice could accelerate the onset of diabetes in recipient neonates. This model was also used to investigate the role of specific subsets of T cells in diabetes induction. By antibody-mediated depletion of appropriate subsets of T cells from splenocytes, it was shown that both CD4 and CD8 T cells were required.

The relative contribution of CD4 and CD8 T cells in diabetes induction was demonstrated in adoptive transfer experiments using the NOD-SCID (severe combined immunodeficiency) mice, which are free of both insulitis and diabetes, as recipients (Christianson et al,1993). This study employed a NOD congenic stock, NOD-NON-Thy1^{a} as donors. As in neonates, the contribution of endogenous T cells in recipients was eliminated and the contribution of allotype-tagged, transferred T cells could be unequivocally established. Use of NOD-SCID as recipients also bypassed the need for irradiation. It was shown in this model that splenic lymphocytes from diabetic NOD-NON-Thy1^{a} could efficiently transfer diabetes to all unmanipulated NOD-SCID females within 30 days post-transfer. The presence of donor T cells in spleen and pancreas was confirmed by flow cytometry. This study also demonstrated the differential diabetogenic potential of prediabetic versus diabetic CD4 T cells versus CD8 T cells. Whereas CD4 T cells from diabetic mice efficiently induce diabetes in NOD-SCID recipients, CD8 T cells from diabetic mice were incapable of inducing diabetes. However, both CD4 and CD8 T cells from prediabetic donors were required to transfer diabetes to NOD-SCID recipients.

That CD4 T cells alone were capable of initiating diabetes was demonstrated by Haskins and McDuffie (1990). This study showed that an accelerated onset of diabetes could be observed by injecting young, unmanipulated NOD mice (2-3 weeks of age) with in vitro primed islet reactive CD4 T cell clones derived from NOD mice. Prior to transfer the clones were activated for 3-4 days by restimulation with antigen and antigen presenting cells, and then expanded for 3-4 days in the presence of Interleukin (IL)-2 alone. It was concluded from this study that primed CD4 T cells were sufficient to initiate diabetes. However, these results do not rule out a role for CD8 T cells. Further evidence

that CD4 T cells alone may be the effectors of β cell destruction came in a study by Wang et al (1991). It was demonstrated in this study that destruction of transplanted syngeneic islets by spontaneously diabetic NOD mice is CD4 T cell-dependent. A subsequent study by Wong et al (1996) showed that an islet reactive CD8 T cell clone can transfer the rapid onset of diabetes in both irradiated NOD and unmanipulated NOD-SCID mice. This disease transfer was shown to occur independent of CD4 T cells but required prior stimulation of the CD8 clones in the presence of the costimulatory molecule, B7.

Evidence supporting the need for CD8 T cells in the initiation of autoimmune diabetes has also come from the development of a NOD mouse strain lacking the expression of β2-microglobulin (β2-m) (Katz et al,1993a; Wicker et al,1994a; Serreze et al,1994). Disruption of β2-m results in almost total lack of cell surface MHC Class I expression and therefore CD8 T cells (Gosgrove et al,1991; Koller et al,1989; Zijlstra et al,1989). Introduction of the β2-m mutation on the NOD background by selective backcrossing (4-8 generations) confers NOD mice resistant to both insulitis and diabetes for more than 7 months of age. In light of the evidence to date, there is a consensus that both CD4 and CD8 T cells are required as effectors for diabetes induction.

1.4.1 T helper (T_h) Subsets in Autoimmune Diabetes

As in the case of the relative role of T cell subsets in autoimmune diabetes, data obtained to date regarding the functional role of T_h subsets remains conflicting. CD4 T helper cells may be subdivided into distinct subsets, T_h1 and T_h2, on the basis of their cytokine profiles (Mosmann et al, 1986). These subsets exert reciprocal down-regulatory effects mediated by their respective cytokines. The signature cytokines of T_h1 cells include IL-2, Interferon (IFN)-γ and Tumor necrosis factor (TNF)-α, which promote cellular immunity. On the other hand, the signature cytokines of T_h2 cells include IL-4 and IL-10, which promote humoral immunity.

Evidence for the immunopathology of autoimmune diabetes to be considered in the context of the $T_h1/2$ paradigm is provided by a number of studies using NOD mice. It has been demonstrated that administration of cytokines or monoclonal antibody treatment that promote T_h1 or T_h2 CD4 T cells exercerbate and prevent diabetes, respectively (Trembleau et al, 1995; Rapoport et al, 1993). In vivo administration of recombinant IL-4 to prediabetic NOD mice was shown to prevent diabetes. Biweekly intraperitoneal injections of 50ng of IL-4 into 6 week old NOD mice showed cumulative diabetes incidence of <10% (1/12) by 20 weeks of age, compared with 75% (9/12) disease incidence in untreated controls. Similarly, a previous study showed that administration of

anti-IFNγ monoclonal antibody could prevent the onset of cyclophosphamide-induced diabetes (Debray-Sachs et al, 1991). Biweekly intraperitoneal injections of 2mg of anti-IFNγ monoclonal antibody into 8 week old female NOD showed cyclophosphamide-induced diabetes incidence at 70% (7/10), compared with 85% (11/13) disease incidence in untreated controls, followed for 40 days. Prevention of diabetes is also observed by the in vivo administration of recombinant human (rhu) IL-10 into NOD mice (Pennline et al, 1994). Groups of 9-10 week old NOD mice received daily subcutaneous injections of rhuIL-10 (1μg) or control protein, and were followed for at least 15 weeks thereafter. At 15 weeks post-treatment, the cumulative incidence of diabetes in the treated group was 25% (5/20) compared with 85% (17/20) in the control group.

Conversely, administration of IL-12 into young, prediabetic NOD mice accelerates the onset of diabetes (Trembleau et al, 1995). IL-12 is a key cytokine which promotes T_h1 type response both in vitro (Manetti et al, 1993; Hsieh et al, 1993) and in vivo (Afonso et al, 1994). In studying the role of IL-12 in autoimmune diabetes Trembleau et al (1995) used prediabetic, 8-10 week old female NOD mice which received daily intraperitoneal injections of 0.3μg IL-12 for the first 7 days, followed by injections of 0.15μg IL-12 for the next 24 days. All (10/10) treated mice developed diabetes 4 weeks post-treatment, compared with 1/10 for untreated controls. Furthermore, this study tested IFNγ and IL-4 production by islet-infiltrating CD4 T cells, following IL-12 administration. In vitro stimulation of purified CD4 T cells with anti-T cell receptor monoclonal antibody showed that CD4 T cells from NOD mice injected with IL-12 produced 4-fold higher amounts of IFNγ than from untreated controls. In contrast, IL-4 production was decreased in pancreas-infiltrating CD4 T cells from IL-12 treated as compared with control NOD mice.

Similarly, islet-specific TNFα expression (Green et al, 1998) or administration of TNFα into NOD female neonates accelerates the onset of diabetes (Yang et al, 1994). Correspondingly, neonatal neutralization of TNFα using anti-TNFα monoclonal antibody rendered almost complete protection to NOD mice, as seen by the absence of insulitis in treated mice. However, TNFα neutralization initiated in 4 week old NOD mice merely delayed the onset of diabetes, suggesting that TNFα has a critical role in the early development of islet autoimmunity by influencing lymphocyte recruitment.

Evidence for a T_h1-mediated immunopathology in autoimmune diabetes is also provided by studying the ratio of signature cytokine transcripts in leukocyte-infiltrating islets using quantitative RT-PCR (Fox and Danska, 1997). Fox and Danska (1997) have shown that a high ratio of IFNγ/IL-4 expression can be observed in the islet-infiltrated T cells of 4-6 week old NOD mice. This ratio appears to be predictive of both the onset of

destructive insulitis and high incidence of diabetes in female NOD mice. In contrast, a high reciprocal ratio is detected in the islet-infiltrated T cells of male NOD mice. The predominance of IL-4 in male NOD mice is predictive of the onset of non-destructive insulitis and low incidence of diabetes.

1.4.2 Costimulation and T_h Subsets in NOD Mice

Activation of T cells requires at least two signals. Firstly, antigen specific signal is transmitted through the T cell receptor, which recognizes antigenic peptides in the context of MHC molecules on the surface of antigen presenting cells. Secondly, costimulatory signals are delivered by antigen presenting cell-expressed B7.1 (CD80) and B7.2 (CD86) by engaging their receptor, CD28, on T cells (Linsley and Ledbetter, 1993; June et al, 1994). Costimulatory signals mediated through CD28 appear to be critical in maintaining T cell responses. In an attempt to study the role of CD28-mediated costimulation in autoimmune diabetes, Lenschow et al (1996) introduced a CD28 null mutation or a transgene encoding the cytotoxic T lymphocyte antigen (CTLA)-4 fused to immunoglobulin (CTLA-4-Ig, a CD28 antagonist) onto the NOD background by backcrossing. Contrary to expectation, both the CD28-deficient NOD mice and NOD mice carrying the CTLA-4Ig transgene displayed a more rapid and severe onset of diabetes compared with control littermates. Further analysis of these mice revealed that disruption of CD28/B7 interactions resulted in the generation of T_h1 type cytokines in favor of T_h2 cytokines.

1.4.3 The Role of TGFβ in IDDM

Protection from autoimmune diabetes can also be achieved by islet-specific transforming growth factor (TGF)β1 transgene expression (King et al, 1998). TGFβ1 belongs to the regulatory T_h3 group of cytokines and has been shown to inhibit cell growth and inflammation (Gray et al, 1994; Sitnicka et al, 1996; Strober et al, 1997). Evidence supporting the anti-inflammatory role of TGFβ1 has come from the TGFβ1-deficient ($TGF\beta1^{-/-}$) mice. These mice develop mutiple-organ inflammatory disease which is lethal by 3-5 weeks of age (Shull et al, 1992). Besides its anti-inflammatory role, TGFβ1 appears to be capable of active immunosuppression in models of oral tolerance (Strober et al, 1997; Weiner, 1997). Furthermore, TGFβ1 appears to have a reciprocal relationship with IFNγ in regulating mucosal inflammation and autoreactive T cells in situ (Strober et al, 1997). However, the mechanism by which TGFβ1 engages in its reciprocal relationship with IFNγ is unknown. Taking into account the overall effects of TGFβ1, King et al (1998) postulated that TGFβ1 may also prevent autoimmune diabetes. As expected, female NOD mice expressing islet-specific TGFβ1 have 30%

diabetes incidence compared with 75% in non-transgenic littermates. In vitro stimulation of T cells from NOD mice expressing islet-TGFβ1 reveals a preference of these T cells for macrophages over B cells as antigen presenting cells. Furthermore, in vitro stimulation of T cells from islet TGFβ1 expressing NOD mice results in the polarization of islet-specific responses towards a T_h2 type phenotype.

To view the pathology of autoimmune diabetes exclusively in the context of the $T_h1/2$ paradigm is an oversimplification as cytokines are pleiotropic and regulate several phenomena besides T_h subsets. Evidence which negates the conventional role of the $T_h1/2$ subsets in autoimmune diabetes is provided in a number of studies. NOD mice deficient in the prototypical T_h1 cytokine, IFNγ, develop diabetes with delayed onset but with similar incidence to that observed in wild type NOD mice (Hultgren et al, 1996). Conversely, NOD mice deficient in the IFNγ receptor α chain showed a marked reduction in insulitis and were completely protected from spontaneous and cyclophosphamide-induced diabetes (Wang et al, 1997). Protection from diabetes in IFNγ receptor α chain deficient NOD mice did not correlate with global imbalances in the $T_h1/2$ cell ratio. Instead, resistance to diabetes in these mice reflected potential defects in antigen presenting cell or in the islet β cell targets or both.

Experiments using transgenic mice expressing IL-10 in islets and their offspring from backcrosses to NOD mice have demonstrated that pancreatic IL-10 did not inhibit but, instead, accelerated autoimmune diabetes (Lee et al, 1994; Wogensen et al, 1994; Moritani et al,1994). It came as a surprise that localized production of IL-10 accelerated the onset and increased the prevalence of diabetes. More that 90% of islet-IL-10 NOD mice developed diabetes at 5-10 weeks of age, when none of the non-transgenic littermates had disease. Further contradictory evidence against the $T_h1/2$ paradigm comes from adoptive transfer experiments using islet-reactive T_h clones. Katz et al (1995) employed the BDC2.5 T cell receptor transgenic mouse to generate CD4 T cells with identical T cell receptor specificity but different effector phenotypes. The T cell receptor transgenic BDC2.5 CD4 T cells are specific for unknown islet antigen and restricted by the NOD MHC (Katz et al, 1993b). Naive CD4 T cells can differentiate into T_h1 or T_h2, depending on the cytokine milieu present at the time of initial activation (Swain, 1994). T_h1 or T_h2 effectors can be generated in vitro in the presence of appropriate cytokines. Effectors thus generated when transferred into mice remain stable for months. Katz et al (1995) found that transferred T_h1-like cells (95% purity) actively promoted diabetes in neonatal NOD recipients. In contrast, T_h2-like cells infiltrated the islets but did not induce disease. Surprisingly, T_h2-like cells when co-transferred with T_h1-like cells did not

confer diabetes resistance to recipient mice. A similar study involving islet-reactive CD4 T cell clones, isolated from the spleen of unprimed NOD mice, was carried out by Akhtar et al (1995). It was shown that a single injection of T_h1 effectors, as determined by cytokine secretion profile in vitro, inhibited adoptive transfer of diabetes into unmanipulated, non-diabetic female NOD mice for the entire 12 month observation period. Most recently, it has been demonstrated that diabetes develops equivalently in NOD mice deficient in IL-12 expression and in normal NOD controls (Trembleau et al, 1999). IL-12, therefore, is dispensable for diabetes development in NOD mice.

1.5 Humoral Response and Autoantigens in Type 1 Diabetes

Although many autoimmune diseases are characterized by the presence of autoantibodies, a direct role for autoantibodies in the pathological process of diabetes remains controversial. Autoantibodies against several islet autoantigens, including insulin (Palmer et al, 1983), glutamic acid decarboxylase 65 (GAD65) (Baekkeskov et al, 1982; Baekkeshov, 1990), and IA-2 (a tyrosine phosphatase) (Hawkes et al, 1996) are detectable in the sera of humans with IDDM for several years prior to the onset of overt diabetes. The presence of antibodies against these antigens can predict subsequent development of diabetes in prediabetic relatives with a sensitivity of >80% (Hagopian et al, 1993 a and b; Verge et al, 1998). In contrast to humans, autoantibodies to putative antigens in the NOD mouse have been difficult to detect (Myers et al, 1998; Mackay et al, 1996).

1.5.1 Insulin and GAD as Autoantigens

The two most studied autoantigens in autoimmune diabetes are insulin and its precursors and the enzyme GAD. Insulin is expressed in copious quantities in the islets. Expression of insulin, however, is not restricted to islets as it has recently been shown that there are thymic cells that express peripheral antigens, such as insulin and GAD, in humans (Vafiadis et al, 1997; Pugliese et al, 1997; Sospedra et al, 1998) and in rodent models of IDDM (Smith et al, 1997; Heath et al, 1998). Islets within NOD mice have been shown to contain CD4 T cells that recognize insulin (Daniel et al, 1995). These CD4 T cells specifically recognize an insulin-derived peptide consisting of amino acids 9-23 of the β chain of insulin and are capable of adoptively transferring diabetes (Daniel and Wagmann, 1996). An overlapping CD8 T cell epitope, consisting of amino acids 15-23 of the β chain of insulin, has recently been identified (Wong et al, 1999). The insulin β chain is, therefore, an obvious target for both pathogenic CD4 and CD8 T cells in the

NOD mouse. Interestingly, a CD4 T cell clone, with HLA-DR restriction, isolated from a recently diagonosed diabetic patient was demonstrated to be specific for insulin β chain 11-27 (Schloot et al, 1998).

The other major putative autoantigen in humans is GAD. GAD is present in two isoforms, GAD65 and GAD67, which catalyze the biosynthesis of the neurotransmitter γ-aminobutyric acid. GAD is primarily located in neuroendocrine tissues and the distribution of the two isoforms differs between humans and the NOD mouse. GAD65 is predominant in the pancreas of humans. In contrast, GAD67 is more abundant in the islets of mice (Kim et al, 1993; Petersen et al, 1993). The physiological function of GAD in the islets remains to be determined. CD4 T cell reactivity to GAD (Zekzer et al, 1998) has been detected in young NOD mouse, ahead of detectable reactivity to any other antigens (Kaufman et al, 1993; Tisch et al, 1993). It has subsequently been demonstrated that diabetes in NOD mice can be prevented by administration of GAD in various ways (Tian et al, 1996a and b). To date no CD8 T cells reactive to GAD have been isolated from NOD mice but they have been found in humans (Panina-Bordignon et al, 1995).

T cell reactivity in IDDM patients can be detected to a region of GAD homologous to the Coxsackie B P2-C viral protein (Atkinson et al, 1994). The fact that Coxsackie B viral infections have been implicated in cases of IDDM has led to the hypothesis that the phenomenon of molecular mimicry may contribute towards diabetes development. It has been demonstrated in the BDC2.5 T cell receptor transgenic mouse model of diabetes (Katz et al, 1993b), where T cells are specific for an unknown islet antigen (Bergman and Haskins, 1994), that infection with Coxsackie B4 virus accelerated the onset of diabetes (Horwitz et al, 1998). Since no T cell response to the virus was observed, it was implied that the acceleration in diabetes was due to inflammation and bystander activation and not molecular mimicry.

Most recent evidence implicating GAD as a key autoantigen in NOD mice has been provided in a study by Yoon et al (1999). This study employed a transgenic model in which expression of both isoforms of GAD were prevented using an antisense construct under the rat insulin promotor (RIP). In the transgenic line with the greatest apparent reduction of both isoforms in the islets, insulitis and diabetes were abolished. Cells from this transgenic line were unable to transfer diabetes. Conversely, diabetic splenocytes were unable to adoptively transfer disease into this transgenic line. The mechanism for diabetes suppression in this model, however, remains to be elucidated.

Besides insulin and GAD, ICA512 (IA-2) (Christie et al, 1994; Hawkes et al, 1996; Solimena et al, 1996) and Heat Shock Protein (HSP)60 are two other putative autoantigens. Although ICA512 is important in the prediction of type 1 diabetes in

humans, its importance in NOD mice remains unclear. Inspite of antibodies against HSP60 being detected in the NOD mouse, corresponding antibodies in humans are as yet undiscovered.

To address the role of B cells in autoimmune pathology in the NOD mouse, Serreze et al (1996) produced a stock of NOD mice deficient in B lymphocytes. This was accomplished by the congenic transfer of an immunoglobulin (Ig)μ gene functionally disrupted by homologous recombination. NOD.Igμ$^{-/-}$ mice are resistant to diabetes and this resistance can not be overcome by infusions of immunoglobulin from diabetic NOD donors (Serreze et al, 1998). However, susceptibility to diabetes was restored in NOD.Igμ$^{-/-}$ mice reconstituted with syngeneic bone marrow admixed with NOD B lymphocytes. A direct role for B cells in the pathology of autoimmune diabetes remains unclarified as a previous report (Yang et al, 1997) contradicts the finding of Serreze et al by demonstrating that a proportion of NOD.Igμ$^{-/-}$ mice (29%) develop diabetes.

1.6 The Genetic Basis of Autoimmune Diabetes

Besides being a model for human IDDM, the NOD mouse also serves as a model for studying complex polygenic diseases since 15-20 different loci are linked to disease development (Wicker et al, 1995; Baxter amd Cook, 1995; Vyse and Todd, 1996). Loci contributing to diabetes susceptibility are termed *Idd*. The first susceptibility locus recognized is linked to the MHC and is termed *Idd1*. Studies with MHC congenic strains of mice have demonstrated that the NOD MHC is necessary but insufficient to induce diabetes. This observation indicates the need for epistatic interaction between MHC and non-MHC NOD genes for diabetes development. Current evidence suggests that the genotype of the MHC on the NOD background determines target tissue for autoimmune destruction, while non-MHC NOD genes appear to confer overall susceptibility to autoimmunity.

1.6.1 The MHC

Genetic analyses undertaken in human populations and in NOD mice have implicated the MHC as a strong predisposing factor to autoimmune diabetes (Thorsby, 1993; Hattori et al, 1986). In human patients, MHC-associated diabetes susceptibility and resistance are predominantly, but not exclusively, determined by polymorphisms at the HLA-DQ β locus (Todd et al, 1987). Similarly, susceptibility and resistance to IDDM in the NOD mouse are also linked to the MHC (H-2 in mice). The diabetes prone NOD mice are homozygous for a unique H-2 haplotype, H-2g^{7}.

1.6.2 MHC class II

The demonstration that particular MHC Class II molecules have positive, neutral or negative association with human autoimmune diabetes has prompted intense investigation and speculation on the NOD MHC (Nepom, 1990a and b; Sheehy, 1992). Consequently, the NOD MHC class II allele has received a lot of attention. The unique NOD H-2^{g7} carries a non-productive I-Eα chain due to a deletion mutation in its promoter region (Acha-Orbea and McDevitt, 1987). The I-Aα chain is identical to that in the H-2^{d} haplotype but the I-Aβ chain is novel and shares an intriguing similarity with diabetes-associated DQβ chains (Todd et al, 1987). Most murine I-Aβ chains (counterpart of human DQβ chain) carry histidine and aspartic acid at positions 56 and 57, which are replaced in NOD by proline and serine, respectively (Hattori et al, 1986; Acha-Orbea, 1987). In humans, presence of aspartic acid in DQβ alleles is associated with resistance to diabetes, while presence of alanine, serine or valine is associated with susceptibility to diabetes. The crystal structure of HLA-DR1 reveals the formation of a salt-bridge between aspartic acid at position 57 and arginine at position 76 of the α chain (Brown et al, 1993). This observation supports the hypothesis that the β chain residue 57 influences peptide binding of MHC class II molecules. Indeed, Carrasco-Merin et al (1996) have presented evidence suggesting that I-A^{g7} is relatively unstable and binds some peptides poorly.

Introduction of transgenic non-NOD MHC I-A or I-E into the NOD background reduces or prevents insulitis and diabetes (Lund et al, 1990; Slattery et al, 1990; Singer et al, 1996; Pilstrom and Bohme, 1997). Results from such studies are, however, difficult to interpret due to possible secondary effects of transgene introduction. These effects may arise as result of the site of transgene integration or the copy number of the transgene. Furthermore, introduction of I-A^{g7} itself as a transgene into the NOD background is protective (Wherret et al, 1997). Interestingly, it has recently been postulated that unpaired or poorly paired I-Aβ chains adversely affect B cell viability (Labrecque et al, 1999). Unpaired or poorly paired I-Aβ chains result from transgenic overexpression of I-Aβ, exceeding the available pool of I-Aα or invariant chain (chaperone involved in MHC class II biosynthesis) and triggering cell toxicity aspect of the unfolded protein stress response.

The actual number and location of MHC-linked diabetogenic gene/s remains to be elucidated. The recombination frequency within the MHC region is low or MHC-linked genes are in linkage disequilibrium, making it difficult to fine map a gene by standard linkage analysis in breeding studies using inbred strains. Hattori et al (1999) introduced a

recombinational hotspot from the B10.A mouse into the region between the MHC class I K and class II A of the NOD mouse to dissect the MHC region. Replacement of the NOD region between MHC class I K and class II A with the same region in B10.A mice prevented the development of diabetes. Thus, in addition to MHC class II genes, there is at least 1 other diabetogenic gene linked to the MHC.

1.6.3 The NOD MHC (*Idd1*) is Diabetogenic

In outcross-backcross studies of NOD with diabetes-resistant strains C3H (Hattori et al, 1986) and NON (non-obese non-diabetic strain which is closely related to NOD) (Prochazka et al, 1987), diabetic progeny were homozygous for the NOD MHC, indicating the presence of MHC-linked recessive susceptibility gene/s. However, Wicker et al (1987, 1989), using the B10 strain as outcross partner, also identified rare diabetic MHC heterozygotes that had only one dose of the NOD MHC. The B10 strain was used in this latter study since it is diabetes-resistant and, as observed in NOD, does not express I-E MHC class II (Mathis, 1983). The use of B10 eliminated the possibility of diabetes-resistance conferred by I-E when C3H and NON strains are used as outcross partners. These initial mapping studies established the link between autoimmune diabetes and the NOD MHC, which appeared dominant but with low penetrance.

1.6.4 Analysis of MHC Congenic Strains

The effects of a single *Idd* locus can be studied by constructing *Idd* congenic strains. A number of *Idd1* congenic strains have been developed by introgressing the MHC from a non-diabetic strain onto the NOD background, and vice versa (Wicker et al, 1992; Prochazka et al, 1989). Congenic strains are identical at the locus of interest but genetically disparate in all other regions. Construction of a congenic strain begins by outcrossing two strains, one provides the genetic background and the other the locus to be introgressed. Progeny from this initial outcross are then repeatedly backcrossed to the strain providing the genetic background. Introduction of MHC from a disease-resistant strain onto the NOD background renders diabetes resistance to NOD mice. However, the reciprocal congenic does not confer diabetes susceptibility to disease-resistant strains. Neither of the two MHC congenic strains, NOD.H-2^b in which the MHC was derived from the B10 strain and the NOD.H-2^b from the B6 strain, develop insulitis or diabetes (Wicker et al, 1992; Wicker et al, 1995). In reciprocal MHC congenics, the NOD MHC expressed on the B10 or B6 genetic backgrounds does not confer insulitis or diabetes to these resistant strains (Wicker et al, 1995).

The construction of NOD.H-2 congenic strains have also underscored the contribution of non-MHC NOD genes towards autoimmune pathology. NOD.H-2^k or h4 and NOD.H-2^b congenic strains get neither insulitis nor diabetes but are autoimmune prone with different target tissue specificities (Podolin et al, 1993; Robinson et al, 1997). The NOD.H-2^k or h4 congenic mice get autoimmune thyroiditis while the NOD.H-2^b congenic mice get autoimmune sialitis. These studies suggest that on the NOD background, the genotype of the MHC determines target tissue for autoimmune destruction, while non-MHC NOD genes confer an overall susceptibility to autoimmunity.

1.6.5 Genetic Mapping of non-MHC *Idd* in NOD Mice

The availability of substantial pedigrees of both diabetic and non-diabetic progeny, generated by the crossing of NOD with disease-resistant strains, and the demonstration of microsatellite (short dinucleotide repeats, $>10^5$ per genome) polymorphism between inbred strains of mice (Love et al, 1990) have facilitated mapping of diabetes susceptibility loci in NOD mice (Todd et al, 1991).

Screening the NOD mouse for non-MHC susceptibility loci is accomplished by first crossing NOD mice with a disease-resistant MHC congenic strain (B10.H-$2g^7$). The F1 hybrids are then backcrossed to NOD and the incidence of diabetes assessed in the backcross progeny. Non-MHC susceptibility loci are then mapped by analysing the associations of microsatellites with disease. Polymerase chain reaction (PCR) amplification of microsatellites allows easy scoring of allelic variants on the basis of size differences (Hearne et al, 1992). To detect susceptibility loci, diabetic progeny from the backcross are typed at polymorphic loci, and the number of homozygotes and heterozygotes is assessed. No linkage to disease will result in equal numbers of homozygote and heterozygote individuals to be observed. An excess of homozygotes in the diabetic population indicates the presence of a NOD susceptibility locus. Excess of heterozygotes in the diabetic population indicates either the presence of a dominant susceptibility allele from the non-diabetic strain or the presence of recessive protective NOD allele. Such a mapping strategy has been employed to identify the majority of non-MHC loci conferring susceptibility to autoimmune diabetes to NOD mice (Todd et al, 1991; Prochazka et al, 1987; Ghosh et al, 1993).

The contribution of non-MHC NOD genes to diabetes becomes apparent when NOD mice are outcrossed to B10 or non-obese non-diabetic (NON) genetic backgrounds. The NON strain is related to the NOD strain but, as the name suggests, is resistant to diabetes (Kikutani and Makino, 1992). The contribution of the B10 versus NON genetic

backgrounds to diabetes is illustrated when (NOD x B10.H-2^{g7}) F1 and (NOD x NON.H-2^{g7}) F1 are analyzed for diabetes incidence (Wicker et al, 1995). All of the (NOD x B10.H-2^{g7}) F1 remain diabetes-free. In contrast, a significant percentage of (NOD x NON.H-2^{g7}) F1 develop insulitis (7/30, 23%) and diabetes (3/80, 4%). These differential diabetogenic potentials between B10 and NON genetic backgrounds reflect differences in alleles carried at the non-MHC-linked loci.

Further evidence implicating non-MHC NOD genes in diabetes induction comes from the study of congenic NOD mice carrying resistance alleles at two *Idd* loci (Wicker et al, 1994b). Wicker et al (1994b) developed NOD congenic strains which express the B10 or B6 alleles at *Idd3* and/or *Idd10*. Analysis of diabetes incidence in these strains demonstrate that non-NOD alleles at *Idd3* and *Idd10* individually provide partial protection to diabetes. However, epistatic interaction between resistance alleles at both *Idd3* and *Idd10* on the NOD background results in virtually complete protection from diabetes.

The *Idd3* locus overlaps between autoimmune diabetes in the NOD mouse and the mouse experimental autoimmune encephalomyelitis (EAE) model for human multiple sclerosis, suggesting the possible presence of genes common to both these diseases (Vyse and Todd, 1996). A recent study investigated whether this overlap was due to a shared "autoimmunity gene" or merely random grouping of 2 unrelated genes (Encinas et al, 1999). In addition to becoming spontaneously diabetic, NOD mice can also develop EAE. The latter can be induced by immunization with peptide antigens derived from the EAE autoantigen, myelin (Bernard et al, 1997). In EAE induction studies using NOD congenic lines carrying B6-derived regions encompassing increasingly smaller congenic intervals of the *Idd3* locus, Encinas et al (1999) demonstrate that an EAE resistance gene colocalizes with a diabetes resistance gene in a genetic interval less than 0.15 cM. This interval contains the IL-2 gene known to be polymorphic between NOD and B6 mice (Ghosh et al, 1993; Denny et al, 1997). IL-2 is a possible candidate gene for autoimmune diabetes and EAE susceptibility because of its role in T cell development and differentiation (Denny et al, 1997). IL-2 is essential for the maintenance of tolerance as IL-2$^{-/-}$ mice are prone to severe autoimmunity (Sadlack et al, 1995).

1.6.6 Concluding Remarks

Overall, advances in mapping susceptibility loci in NOD mice, along with the creation of congenic strains with increasingly narrower intervals, will facilitate identification and understanding the function of *Idd* genes. It is hoped that the study of NOD mice will provide insights into the genetics and pathophysiology of Type 1 diabetes in humans. Elucidation of disease-linked molecular and biochemical pathways in NOD mice will encourage development of protocols for advance diagnosis, cure or subsequent therapeutic intervention.

1.7 Dendritic Cells

Dendritic cells form a specialized system of antigen presenting cells which are critical in initiating and modulating primary T cell-mediated immune responses (Steinman, 1991; Cella et al, 1997; Hart, 1997; Banchereau and Steinman, 1998). Dendritic cells derive their name from their unusual dendritic morphology characterized by irregular cell shape and numerous cytoplasmic processes which are either dendritic (spiny) or sheet-like. Besides their obvious function in dendritic cell migration and in providing a large surface area, cytoplasmic processes have also been speculated to be involved in antigen capture and direct interaction with T cells. Dendritic cells constitutively express high levels of cell surface Major Histocompatibility Complex (MHC) molecules and possess potent accessory function for the stimulation of naive T cells.

Interest in the physiological function of dendritic cells has stimulated research which has led to the elucidation of their origin and definition of their general characteristics. Dendritic cells are myeloid-derived and are present in trace quantities in most tissue where they act as mobile sentinels of the immune system by constantly sampling the extracellular milieu for antigen. When viewed in situ, such as in skin, airways or lymphoid organs, dendritic cells appear stellate. Dendritic cells inhabit discrete anatomic regions of lymphoid and non-lymphoid organs and are interconnected by their migratory nature. Peripheral or tissue dendritic cells share characteristic structure, phenotype and function. They are considered to be phenotypically and functionally immature. Immature dendritic cells are characterized by their ability to acquire and process antigen and subsequently migrate, via blood or afferent lymph, to draining lymph node. Peptide epitopes generated as a result of antigen processing are displayed in the context of cell surface MHC molecules for recognition by the naive T cells in the draining lymph node. The process of antigen encounter, migration and interaction with T cells triggers maturation of dendritic cells. Maturation of dendritic cells entails the up-regulation of their immunostimulatory capacity at the expense of their ability to acquire and process complex antigen.

Most recently, research has also uncovered phenotypic heterogeneity among dendritic cells resident in secondary lymphoid tissue, with potential functional specialization within subsets present. Overall, dendritic cells play a pivotal role in both innate and adaptive immunity, and provide a nexus between the two arms of immunity. Besides acting as sentinels against pathogens invading tissue, dendritic cells also appear to be important in the initiation and maintenance of autoimmune responses against peripheral tissue. Consistent with the latter, there is now emerging evidence that dendritic cells may be critical in the induction of peripheral tolerance mechanisms.

* It was subsequently demonstrated that Transforming Growth Factor (TGF)-β is a crucial factor in the cytokine cocktail required for Langerhans cell development (Strobl et al, 1996).

1.7.1 Origin and Differentiation of Dendritic Cells

As with all other Leukocyte Common Antigen (CD45) positive cells, dendritic cells originate from hematopoietic stem cells and their progenitors in the bone marrow. Dendritic cells were discovered in mice by Steinman and Cohn (1973, 1974). Dendritic cells were shown to be of myeloid origin during their initial in vivo characterization (Steinman et al, 1974). This was demonstrated in allogeneic bone marrow chimeric mice. Parental strain mice when irradiated and reconstituted with bone marrow cells from F1 hybrid mice developed splenic dendritic cells, as determined by morphological criteria, expressing donor MHC on their cell surface. A similar study demonstrated that epidermal dendritic cells (Langerhans cells) were also of myeloid origin (Frelinger et al, 1979). An early study with human bone marrow also shed light on the origin of dendritic cells (Goordyal and Isaacson,1985). This initial study with human bone marrow cells demonstrated immunohistochemically that bone marrow colonies generated in methyl cellulose medium, supplemented with placental conditioned medium as source of growth factors, contained both macrophages and Langerhans cells.

The availability of recombinant growth factors enabled investigation of the effects of specific growth factors on hematopoietic precursors. Further evidence for a common precursor for dendritic cells and myeloid cells arose from in vitro culture of myeloid precursors stimulated with Granulocyte and Macrophage Colony Stimulating Factor (GM-CSF). In mice, dendritic cells precursors are present in both bone marrow and blood, and generate dendritic cells, granulocytes and macrophages in response to GM-CSF stimulation (Inaba et al, 1992 a,b; Inaba et al, 1993a). In humans, $CD34^+$ precursors isolated from bone marrow, cord and peripheral blood, generate dendritic cells in response to stimulation with GM-CSF and other growth factors (Young et al, 1995; Reid et al, 1992; Strunk et al, 1996; Caux et al, 1992). In particular, the combination of GM-CSF and TNFα synergize to generate Langerhans cells from $CD34^+$ cord blood precursors (Caux et al, 1992). Dendritic cells also develop from $CD14^+$ human peripheral blood monocytes cultured in the presence of GM-CSF and IL-4 (Sallusto and Lanzavecchia, 1994). Dendritic cells generated under these culture conditions have the characteristics of immature dendritic cells and can be induced to mature by inflammatory stimuli provided by TNFα, IL-1, Lipopolysaccharide (LPS) and anti-CD40 monoclonal antibody. The immature dendritic cells generated from monocyte precursors still retain the Macrophage Colony Stimulating Factor (M-CSF) receptor which is down-regulated following the induction of maturation. The emerging paradigm thus is that pluripotent precursors, of myeloid origin, may develop into dendritic cells, macrophages or granulocytes, depending on the external stimuli.

As mentioned above, human monocytes can be induced to develop into dendritic cells when cultured in the presence of GM-CSF and IL-4 (Sallusto and Lanzavecchia, 1994). However, whether physiological stimuli triggered the development of monocytes into dendritic cells in vivo remained unclear until recently. Initial in vitro evidence provided by Randolph et al (1998) demonstrated that human monocytes differentiate into dendritic cells in an in vitro model of transendothelial trafficking without the addition of exogenous cytokines. In this model, monocytes, transiently resident in the subendothelial matrix, efficiently developed into dendritic cells in response to phagocytic stimulus. The nascent dendritic cells migrated across the endothelium in the ablumenal-to-lumenal direction, a migratory path that parallels the migration of dendritic cells from the periphery into the lumen of an afferent lymphatic vessel. Importantly, monocytes that remained in the subendothelial matrix differentiated into macrophages. This data support the concept that monocytes can develop into dendritic cells under physiological conditions. Indeed evidence indicating that monocytes can serve as precursors for dendritic cells in vivo has come from a recent study (Randolph et al, 1999). This study employs murine models to demonstrate that monocytes become lymph node dendritic cells in vivo following administration of fluorescent latex beads. Inflammatory monocytes phagocytosed subcutaneously administered beads and mainly differentiated into tissue resident macrophages. However, a significant minority of monocytes, bearing beads, migrated to the draining lymph node, acquired dendritic cell markers and became resident in the paracortical regions of the lymph node. Furthermore, the transport of beads to draining lymph node was markedly reduced in the monocyte-deficient osteopetrotic (op) mouse (Wiktor-Jedrzejczak et al, 1991) although monocyte-independent dendritic cell populations were intact in the op mouse (Witmer-Pack et al, 1993). This suggests that monocytes serve as precursors for a subset of dendritic cells initiating in peripheral tissue. Overall, the study by Randolph et al (1999) provide important evidence regarding the mysterious ontogenic relationship of dendritic cells with monocytes and macrophages.

1.8 General Features of Dendritic Cells

The generally accepted current model of dendritic cell development assigns dichotomy of function on dendritic cells, dependent on the stage of their maturation. The phenotype and function of dendritic cells are intimately-linked with whether they are immature or mature as will be outlined next.

1.8.1 Immature Dendritic cells and Antigen Handling

Immature tissue dendritic cells are characterized by their optimal ability to actively acquire and process antigen, and their inabilty to stimulate naive T cells. Numerous features of immature dendritic cells enable them to fulfil their sentinel role in peripheral tissue. Firstly, they can capture particulate and microbial antigen by phagocytosis (Inaba et al, 1993b; Moll et al, 1993; Reis et al, 1993; Svensson et al, 1997). In vitro generated immature dendritic cells when pulsed with bacteria can elicit potent immune responses both in vitro and in vivo (Svensson et al, 1997). Interestingly, dendritic cells, but not macrophages, may acquire antigen from apoptotic cells in vitro and induce MHC class I-restricted cytotoxic T lymphocytes (CTLs) (Albert et al, 1998). This could be a mechanism by which dendritic cells acquire antigens from tumours, transplants, infected cells, or even endogenous tissue, for stimulation or tolerization of CTLs. Secondly, immature dendritic cells form large pinocytic vesicles in which extracellular fluid and solutes are sampled for antigen, in a process termed macropinocytosis (Sallusto et al, 1995). Contents of a macropinosome may then be delivered to specialized late-endosomal structures known as MHC Class II compartments (MIIC) (Pierre et al, 1997). MIIC are enriched for MHC class II molecules and other molecules which facilitate antigen processing and subsequent loading of peptides generated onto MHC molecules. Although immature dendritic cells are active in the biosynthesis of MHC class II molecules and in peptide loading, the assembled MHC class II-peptide complexes are mostly targeted to endosomal compartments and only transiently to the cell surface (Pierre et al, 1997). Thirdly, immature dendritic cells express receptors mediating adsorptive endocytosis. These include C-type lectin receptors like macrophage mannose receptor (MMR) (Sallusto et al 1995) and DEC-205 (Jiang et al, 1995). Furthermore, immature dendritic cells also express Fcγ and Fcε receptors (Sallusto and Lanzavecchia, 1994; Maurer et al, 1995). The combination of macropinocytosis and receptor-mediated antigen uptake enable efficient presentation of minute quantities of antigen. Another distinct feature of immature dendritic cells is the profile of chemokine receptors they express (Sallusto et al, 1998; Sallusto et al, 1999). Immature dendritic cells express receptors for chemokines secreted at inflammatory sites, namely, CCR1, CCR2, CCR5 and CXCR1. Encounter with antigen, however, dramatically alters the fate of an immature dendritic cell.

1.8.2 Migration and Maturation

A critical feature of dendritic cells is their capacity to migrate. Migration enables dendritic cells to fulfill their normal immunosurveillance of incoming antigens in tissue and their subsequent rendezvous with T cells in secondary lymphoid tissue. The rate of dendritic cell movement between blood and tissue and tissue and secondary lymphoid organs under normal conditions is likely to be low. Insights into the phagocytic activity and mobilization of dendritic cells in vivo has been demonstrated in a comprehensive study by Matsuno et al (1996). This study tracks particle-laden rat dendritic cells following the intravenous administration of particulate tracers. The majority of particle-laden cells in lymph were identified as dendritic cells on the basis of standard cell surface markers and in vitro functional capacity. Particle-laden dendritic cells were first detected in the liver and in the spleen 1 hr after injection. Particle-laden cells accumulated in the paracortical regions of celiac nodes 18 hr after particle injection. This study implicates liver dendritic cells in initiating immune responses to systemic antigen. Furthermore, BrDU (5-bromo-2'-deoxyuridine) feeding of the rats revealed that most of the particle-laden dendritic cells were recently produced by the terminal division of precursor cells.

The rate of dendritic cell movement is substantially increased during an inflammatory response to meet increased need for antigen presentation. Extravasation of dendritic cells from the blood stream requires dendritic cells to initially tether to the endothelium. Extravasation of leukocytes is mediated by selectins that bind to specific carbohydrates on the cell surface (Springer, 1994). Recently it has been demonstrated that blood dendritic cells express ligands for P- and E-selectin, which are expressed at low levels on endothelial cells and up-regulated during an inflammatory response (Robert et al, 1999). Also demonstrated was that dendritic cells preferentially extravasate at sites of inflammation. This novel finding suggests that blood dendritic cells are perpetually on standby to respond to inflammatory stimuli.

Although constitutive immigration of blood dendritic cells occurs to replenish tissue dendritic cells and for normal immunosurveillance purposes, emigration of dendritic cells from tissue may be induced during inflammatory responses. Correspondingly, dendritic cells are rapidly mobilized into airway epithelia following inhalation of virus or bacteria (McWilliam et al, 1994). This was demonstrated in a study which aimed to detect dendritic cell response after challenge of the airways with live infectious organisms (both viral and bacterial pathogens) to which mice had not previously been exposed, and an inert protein antigen (Ovalbumin, OVA) to which mice were presensitized by parenteral immunization. The common feature of all these challenge

regimes was the transient waves of dendritic cells which were recruited into the epithelium during the early phase of cellular inflammatory response. The transient recruitment of intraepithelial dendritic cells corresponded to a 2-3-fold increase in dendritic cell numbers. Coincident with the inflammatory response was the substantial increase in the number of dendritic cells in draining lymph node (McWilliam et al, 1996). This increase was attributable to the arrival of antigen-loaded dendritic cells from inflamed tissue as well as the recruitment of circulating dendritic cell precursors from blood (Robert et al, 1999).

The skin is a favored model to study emigration of dendritic cells from the periphery to secondary lymphoid tissue. It is well documented that exposure of skin to contact sensitizer (such as fluorescein isothiocyanate, FITC) induces migration of contact sensitizer-loaded Langerhans cells to draining lymph node, within 24hr, to become interdigitating dendritic cells in the paracortical regions of draining lymph node. A recent study has elegantly reiterated previous findings of dendritic cell migration induced by contact sensitizers (Knight et al, 1985; Macatonia et al, 1986; Austyn et al, 1988), by histological analysis of the localization of FITC-positive Langerhans cells in the T cell zone of draining lymph node (Tang and Cyster, 1999). Furthermore, intradermal injection of murine IL-1β or TNFα into mouse skin leads to a reduction in numbers of Langerhans cells (Cumberbatch and Kimber, 1992; Roake et al, 1995). Both of these cytokines are elicited during exposure to contact allergens.

The intimate relationship between in vivo migration and maturation of dendritic cells has been shown in a study using systemic administration of LPS to mice (de Smedt et al, 1996). LPS treatment of mice induces the migration of most splenic dendritic cells from the marginal zone to T cell areas within 4-6 hr. This movement entails a maturation process as characterized by the down-regulation of antigen processing capacity and up-regulation of immunostimulatory properties. Maturation involves increased cell surface expression of MHC class II and the costimulatory B7 molecules. The loss of antigen processing capacity of LPS-treated dendritic cells was assessed by the inability of freshly isolated treated dendritic cells to present protein antigen in vitro. Furthermore, systemic administration of LPS causes a massive egress of dendritic cells from non-lymphoid tissue such as skin, heart, kidney and intestine (Roake et al, 1995).

Numerous changes occur during the maturation of dendritic cells. In some instances antigenic stimulus may be sufficient to induce maturation of dendritic cells. Dendritic cells down-regulate their capacity to acquire and process soluble native antigen. In vitro observations have shown that loss of antigen processing capacity correlates with loss of acidic organelles involved in antigen processing (Stossel et al, 1990).

[*] Maturation involves a marked up-regulation of receptors for chemokines expressed in secondary lymphoid tissue with concomitant down-regulation of receptors for inflammatory cytokines.

Furthermore, ceramide, induced during maturation, can limit the ability of dendritic cells to capture antigen (Sallusto et al, 1996). Maturation involves the transformation of MIIC to non-lysosomal vesicles which discharge their MHC-peptide complexes to the cell surface while down-regulating synthesis of new MHC class II molecules (Cella et al, 1997; Pierre et al, 1997). Maturation also entails a ten-fold increase in the half-life of MHC class II molecules on the cell surface of mature dendritic cells. Cell surface expression of MHC class II molecules is controlled by the developmental regulation of the MHC class II-associated invariant chain (Ii) proteolysis (Pierre and Mellman, 1998). Invariant chain cleavage in MIIC is mediated by endosomal proteases called cathepsins. In immature dendritic cells, inefficient Ii cleavage due to reduced cathepsin S activity leads to MHC class II-Ii complexes being transported to MIIC. In contrast, mature dendritic cells possess efficient cathepsin S activity leading to elevated levels MHC class II molecules being targeted to the cell surface. This differential trafficking of MHC class II molecules is due to the reduced expression of the cathepsin S inhibitor, cystatin c, in mature dendritic cells.

Mature dendritic cells secrete chemokines and up-regulate adhesion molecules to recruit, cluster and activate T cells. Mature dendritic cells show increased expression of costimulatory molecules including CD40, CD80 (B7.1) and CD86 (B7.2) (Sallusto et al, 1995; Caux et al, 1994a and Inaba et al, 1994). Dendritic cells also undergo a rapid and coordinated switch in chemokine receptor expression during maturation. Maturation involves a marked up-regulation of receptors for chemokines expressed in secondary lymphoid tissue with concomitant loss of receptors for inflammatory chemokines. For instance, mature dendritic cells up-regulate CCR7 and acquire responsiveness to EBI1 ligand chemokine (ELC) and MIP-3 β, a chemokine secreted by lymphoid tissue (Dieu et al, 1998; Sallusto et al, 1998). The signal transduction pathways that regulate dendritic cell maturation, however, remain to be fully elucidated. A recent study has employed LPS stimulation of a growth factor-dependent primary dendritic cell-line to illustrate that dendritic cell survival and maturation are regulated by distinct signalling pathways (Rescigno et al, 1998). It was shown in this study that mitogen activated protein (MAP) kinase inhibitors induced apoptosis in the dendritic cell line, but left the NFκB-mediated maturation signals unaffected. This evidence suggests that survival and maturation of dendritic cells are regulated by the MAP kinase and NFκB signal transduction pathways, respectively.

1.9 Dendritic Cell and T Cell Interaction

The potent T cell stimulating capacity of mature dendritic cells has been documented extensively in early studies. Mature dendritic cells elicit T cell-mediated immunity in the presence of antigens, alloantigens and superantigens. Activation of naive and unprimed T cells by dendritic cells has been demonstrated in studies carried out both in vitro and in vivo (Steinman et al, 1997). Only a few dendritic cells, in comparison to macrophages and B cells, are required to evoke potent T cell responses. In mixed leukocyte reactions (MLR), the in vitro model for graft rejection, as few as 300-1000 dendritic cells can double the proliferative capacity of $5x10^6$ allogeneic responder splenic cells, while $0.3\text{-}1x10^5$ dendritic cells can induce maximal stimulation of 30- to 80-fold (Steinman and Witmer, 1978). Besides priming T cells in response to mismatched MHC, dendritic cells have also been shown to efficiently activate T cells in response to superantigens, antigens derived from infectious agents and tumours (Bhardwaj et al, 1993; Inaba et al, 1993b; Paglia et al, 1996; Mayardomo et al, 1995). Dendritic cells pulsed with minute quantities of superantigen are significantly more efficient than macrophages or B cells in stimulating naive primary T cells in vitro (Bhardwaj et al, 1993). This potency in antigen presenting cell function in response to low dose antigen is attributable to both the delivery of CD28- and CD4-mediated costimulatory signals during antigen presentation. A similar in vitro study using naive transgenic T cells, I-E^k -restricted and specific for a peptide of cytochrome c, as responders has also verified the efficacy of dendritic cells as antigen presenting cells. Fewer dendritic cells, compared to macrophages and activated B cells, were required to stimulate transgenic T cells in the presence of a constant amount of cytochrome c peptide antigen (Croft et al, 1992).

The initial physical interaction between antigen-loaded dendritic cells and specific T cells was for the first time directly visualized in vivo by Ingulli et al (1997). Ingulli et al (1997) used confocal microscopy to track the in vivo location of fluorescent dye-labelled dendritic cells and naive CD4 T cells specific for an OVA-peptide and I-A^d -restricted, after adoptive transfer into syngeneic recipients. This study elegantly demonstrates that dendritic cells pulsed in vitro with OVA peptide home to the paracortical regions of lymph node and form large clusters of specific T cells.

Chemokines play an important role in dendritic cell-T cell interaction. Two recent studies have identified dendritic cell chemokines that preferentially attract naive or mature T cells, respectively (Adema et al, 1997; Tang and Cyster, 1999). The first study reported the identification and characterization of a C-C chemokine (DC-CK1) that is specifically expressed by human dendritic cells at high levels in germinal centres and T cell areas of secondary lymphoid tissue. DC-CK1 is a potent chemoattractant for naive T

* TRANCE/RANKL (TNF-related Activation-induced cytokine/receptor activator of NF-κB ligand)

TRANCE/RANKL

cells as shown in in vitro chemotaxis assays. The previously mentioned second study uses a murine model to illustrate that FITC-sensitized Langerhans cells upregulate macrophage-derived chemokine (MDC) during migration into draining node dendritic cells. This study employs a combination of light microscopy and in situ hybridization to generate images showing that FITC positive dendritic cells in draining lymph node upregulate MDC RNA. Furthermore, this study demonstrates that MDC is preferentially chemotactic for activated T cells.

Recent data on dendritic cell-T cell interaction is strongly suggestive of the nature of interaction being mutual. What has become evident is that T cells may further enhance the T cell stimulatory capacity of dendritic cells. Evidence supporting this phenomenon is provided by the effects of CD40 ligation on dendritic cells. Ligation of CD40 has been shown to increase dendritic cell viability (Caux et al, 1994b; Ludewig et al, 1995) and maturation (Sallusto and Lanzavecchia, 1994). Furthermore, CD40 ligation is a potent inducer of IL-12 secretion by dendritic cells. Dendritic cells secrete high levels of IL-12 in response to CD40-ligation in vitro (Koch et al, 1996; Cella et al, 1996). The secreted IL-12, in turn, would favor the generation of T helper 1 (T_h1) type response (Macatonia et al, 1995). Dendritic cell survival is also promoted by the newly described TRANCE/RANK (TNF-related Activation-induced cytokine/receptor activator of NF-κB) receptor (Anderson et al, 1997; Wong et al, 1997) on dendritic cells. The TRANCE/RANK receptor is ligated by the TNF family of proteins expressed by activated and memory T cells. The converse scenario would be the suppression of dendritic cells by T cell-secreted factors. Indeed, there are studies which show that IL-10 induces apoptosis in dendritic cells (Ludewig et al, 1995) and downregulates their immunostimulatory capacity (Caux et al, 1994c) as well as their IL-12 production (Koch et al, 1996).

Most recently, definitive and direct evidence for the influence of T cells on dendritic cells has come from a study using T cell-deficient mice (Shreedhar et al, 1999). This study employed the induction of contact hypersensitivity (CHS) responses to haptens as an integrative model to examine different aspects of dendritic cell function in vivo. Results obtained during the course of this study support the concept that acquisition of full functional capacity by dendritic cells is a T cell -dependent phenomenon. Evidence for this concept is provided by the presence of markedly fewer Langerhans cells and draining lymph node dendritic cells in T cell-deficient SCID and RAG mutant mice. This dendritic cell deficiency, however, was overcome by reconstitution of mutant mice with purified normal T cells. Reconstitution with normal T cells also induced partial maturation of mainly immunophenotypically immature dendritic cells seen in T cell deficient mice. Furthermore, reconstitution of T cells restored the ability of hapten-bearing dendritic cells

* In addition to CD40/CD40L interaction for the induction of CTL responses, there is also an important role for CD27-CD70 interactions between dendritic cells and CTLs (Stuhler et al, 1999). Human CTLs, on interaction with dendritic cells, have been shown to upregulate CD70 molecules for subsequent costimulation of T_h and dendritic cells.

from SCID mice to efficiently initiate a CHS response when adoptively transferred into naive, syngeneic immunocompetent recipients. These results suggest that T cells are critical for normal dendritic cell maturation and function in vivo.

Another manifestation of dendritic cell-T cell interaction is the recently proposed role of dendritic cells to "license" CTLs to kill virus-infected targets. Data from three separate studies suggests a dynamic three cell interaction which incorporates sequential interaction of dendritic cells and helper T cells, followed by the interaction between dendritic cells and killer T cells (Ridge et al, 1998; Bennett et al, 1998; Schoenberger et al, 1998). An initial, CD40-dependent, interaction between dendritic cells and T helper cells takes place. The T helper cell, in turn, 'conditons' the dendritic cell to a state where it can now directly co-stimulate killer T cells. The initial CD40-dependent can be bypassed by viral infection of dendritic cells. *

1.10 Heterogeneity of Dendritic Cells in Lymphoid Tissue

Recent advances in the characterization of dendritic cells in lymphoid tissue have revealed phenotypic differences among lymphoid tissue dendritic cell subsets (Vremec et al, 1992; Vremec and Shortman, 1997; Leenen et al, 1998). This phenotypic difference correlates with discrete microanatomical locations occupied by specific subsets of dendritic cells in the mouse spleen (Pulendran et al, 1997). Currently there are no reliable criteria for delineating dendritic cell subsets. In mouse spleen, however, CD8α (Vremec et al, 1992) and DEC-205 (Kraal et al, 1986) have been used to distinguish between dendritic cells resident in marginal and T cell zones (Pulendran et al, 1997).

The expression of the CD8α homodimer on dendritic cells was first demonstrated by Vremec et al (1992). Both splenic and thymic dendritic cells were shown to express cell surface CD8α and contain CD8α mRNA. Although thymic dendritic cells express both CD8α and β chains, the α chain is present in relative excess. Splenic dendritic cells express only the α chain of CD8. As yet there is no evidence supporting a functional role for cell surface CD8α on dendritic cells.

An important reagent in the study of lymphoid tissue dendritic cells subsets is the monoclonal antibody against DEC-205 (formerly known as NLDC-145). The DEC-205 monoclonal antibody was raised by immunizing rats with mouse lymphoid stromal tissue and then selecting for hybridomas that stained T cell areas in tissue sections (Kraal et al, 1986). The monoclonal antibody stained dendritic profiles in T cell zones and primarily stained Dendritic cells and Epithelial Cells in the thymic cortex. Molecular and functional

* A third subset of splenic dendritic cells expressing CD4 on the cell surface has also been recently described (Vremec et al, 2000).

characterization of the receptor for DEC-205 have shown it to be an intergral membrane protein, with molecular weight of 205 kDa, containing multi-lectin domains, homologous to the macrophage mannose receptor which are able to bind carbohydrates and mediate endocytosis (Jiang et al, 1995). Indeed, it has been shown that DEC-205 is an endocytic receptor which can internalize antigen and direct it to specialized antigen processing compartments.

The detection of cell surface CD8α on dendritic cells and the availability of the DEC-205 monoclonal antibody have provided insights into the heterogeneity of dendritic cells in lymphoid tissue (Pulendran et al, 1997). In mouse spleen, two subsets of dendritic cells have been show in anatomically distinct locations. A minor subset of dendritic cells, so-called interdigitating dendritic cells, is situated in the white pulp T cell zone (the inner periarteriolar sheath). The majority of dendritic cells in the spleen is found at the marginal zone and splenic red pulp. Flow cytometric analyses of splenic dendritic cells have shown the presence of two distinct dendritic cell subsets: one of which expresses both DEC-205 and CD8α on the cell surface, and the other expresses neither of these molecules. A further difference between these subsets includes the differential cell surface expression of the myeloid antigen, CD11b, on the subset negative for both CD8α and DEC205. The presence or absence of CD11b on splenic dendritic cell subsets has encouraged the reference of each subset as the putative myeloid-related and lymphoid-related dendritic cells, respectively (Vremec and Shortman, 1997). In contrast to CD8α expression, CD11b expression is upregulated during culture so both subsets acquire equivalent levels of expression between subsets. Similarly, DEC205 is upregulated during culture so both subsets become positive, although the difference in levels of expression is maintained. Therefore, CD8α and DEC205 remain as reliable markers for the putative lymphoid-related dendritic cell subset in the spleen. Immunohistochemical data shows that DEC-205 stains only the interdigitating dendritic cells. On the basis of these observations, interdigitating dendritic cells are the most likely candidates for being the $CD8\alpha^+$ subset of dendritic cells.

Molecular evidence for the presence of $CD8\alpha^-$ and $^+$ dendritic cell subsets has recently come from a study with the RelB deficient ($RelB^{-/-}$) mice (Wu et al, 1998). The transcription factor RelB is a member of the NFκB/Rel family. Expression of RelB mRNA is restricted to lymphoid tissue and in interdigitating dendritic cells (Carrasco et al, 1993). $RelB^{-/-}$ mice lack both thymic and splenic dendritic cells and show impaired antigen presenting cell function and cellular immunity, despite the presence of normal numbers of Langerhans cells (Burkly et al, 1995). These mice have a perturbed thymic architecture. Furthermore, these mice exhibited multi-focal inflammation and myeloid hyperplasia. It is now apparent that the absence of thymic dendritic cells may be a

*Similarly, Pulendran et al (1997) also demonstrated that the CD8α^+ dendritic cells were the highest producers of IL-12 in response to stimulation with a cocktail of *staphylococcus aureus* enterotoxin, GM-CSF and IFNγ.

secondary phenomenon underpinned by systemic inflammation and disrupted thymic architecture. Wu et al (1998) generated bone marrow chimeric mice by reconstituting normal mice with $RelB^{-/-}$ bone marrow. Analysis of chimeric mice showed that similar numbers of thymic dendritic cells were produced by the RelB mutant and normal bone marrow cells. However, almost all $RelB^{-/-}$ bone marrow-derived splenic dendritic cells were $CD8\alpha^+$ and DEC-205^+. This represented a 10-fold reduction in $CD8\alpha^-$ dendritic cells, whereas normal bone marrow-derived splenic dendritic cells constituted almost a 1:1 ratio of $CD8\alpha^+$ to $CD8\alpha^-$ dendritic cells. Thus, the marked reduction in $CD8\alpha^-$ splenic dendritic cells is a direct consequence of a stem cell-intrinsic effect of the RelB mutation. Furthermore, RelB appears to selectively regulate the $CD8\alpha^-$ subset of dendritic cells.

1.10.1 Functional Specialization within Dendritic Cell Subsets?

Preliminary in vitro data has led to the suggestion that $CD8\alpha^+$ dendritic cells may possess regulatory/tolerogenic function while their $CD8\alpha^-$ counterparts perform pro-immunity functions (Süss and Shortman, 1996; Kronin et al, 1996). It has been demonstrated that $CD8\alpha^+$ dendritic cells are less efficient in inducing proliferation of purified allogeneic CD4 T cells compared to $CD8\alpha^-$ dendritic cells (Süss and Shortman, 1996). More dead cells were observed in $CD8\alpha^+$ dendritic cell MLR cultures than in $CD8\alpha^-$ dendritic cell MLR cultures. The mechanisms for reduced cell viability in $CD8\alpha^+$ dendritic cell MLR cultures remain to be elucidated. A similar regulatory role of $CD8\alpha^+$ dendritic cells was also observed in MLR cultures containing purified allogeneic CD8 T cells (Kronin et al, 1996). Again, the proliferative capacity of CD8 T cells stimulated with $CD8\alpha^+$ dendritic cells was relatively reduced. This reduced proliferation of CD8 T cells correlated with relatively reduced IL-2 secretion in the MLR cultures. It was concluded from this study that $CD8\alpha^+$ dendritic cells regulate CD8 T cell proliferation by limiting their IL-2 production.

There is also initial in vivo evidence demonstrating differential capacity of the two dendritic cell subsets to secrete IL-12 (Sousa et al, 1997). This study shows that in response to microbial stimulation in vivo, majority of IL-12 secreting dendritic cells in the spleen are $CD8\alpha^+$, as determined by flow cytometry. IL-12 secretion in this model is rapid and independent of CD40 ligand. *

More recently, a number of studies have attempted to demonstrate delineation of function between the two dendritic cell subsets both in vitro (Ohteki et al, 1999) and in vivo (Pulendran et al, 1999; Maldonado-Lopez et al, 1999, Smith and Fazekas de St. Groth, 1999). Results obtained by Ohteki et al (1999) show that IL-12 impacts

differentially on the two dendritic cell subsets in vitro. Correspondingly, CD8α$^+$ dendritic cells secrete approximately 5-fold higher level of IFNγ than do CD8α$^-$ dendritic cells, when both subsets are sorted and cultured in the presence of IL-12. This results suggest that IL-12 secreted by CD8α$^+$ dendritic cells acts in autocrine manner for IFNγ production and subsequent generation of a T_h1-type response. In vivo results reported by Pulendran et al (1999), Maldonado-Lopez et al (1999) and Smith and Fazekas de St. Groth (1999) seem to contradict the regulatory role assigned on the CD8α$^+$ dendritic cells on the basis of the previously described in vitro evidence (Süss and Shortman, 1996). Overall, these studies present data which suggest that both dendritic cell subsets can prime antigen specific T cells with similar kinetics and magnitude in vivo. However, each dendritic cell subset appears to provoke distinct T_h responses in vivo (Pulendran et al, 1999; Maldonado-Lopez, 1999). While the CD8α$^+$ dendritic cells promote an IL-12-mediated T_h1 type response, the CD8α$^-$ dendritic cells appear to promote a T_h2 type of response. To date functional specialization within dendritic cell subsets remains controversial and obscure.

1.11 Dendritic Cells as Link between Innate and Adaptive Immunity

Two recent studies have identified dendritic cell precursors in human blood as the principal producers of IFNα (Siegal et al, 1999; Cella et al, 1999). IFNα is among the key mediators of innate immunity and can be induced in response to various inflammatory stimuli, including viral and bacterial infections. IFNα acts by inhibiting viral replication, activating NK cells and macrophages, increasing MHC class I expression , and providing survival signals to lymphocytes. Both groups isolated a rare blood leukocyte on the basis of cell surface HLA-DR and CD4 expression, and absence of lineage markers. These cells were found to secrete up to 1000 times more IFNα than the same number of bulk blood cells, in response to viral stimulation in vitro. These Interferon Producing Cells (IPCs) differentiate to mature dendritic cells when cultured with IL-3 and CD40 ligand. IPCs are able to induce IL-4 secretion by T cells, hence promoting a T_h2 type response. A T_h2 type response mediated by IPCs is thought to serve as a negative feedback mechanism which downregulates immune responses during viral infections (Payvandi et al, 1998). IPCs, detected immunohistochemically on the basis of distinct cell surface markers, are undetectable in normal lymph nodes but can be detected in close proximity to high endothelial venules (HEVs) in inflamed lymph nodes. This location, along with the expression of CD62 (P-selectin) ligand and CXCR3 (inflammatory chemokine receptor), suggests that IPCs enter lymph nodes from blood via HEVs during inflammatory responses.

1.12 Dendritic Cells in Autoimmune Diabetes

Evidence from a number of studies seem to suggest that part of the predisposition to autoimmune diabetes may be manifested at the level of hematopoietic precursors which give rise to antigen presenting cells. Engraftment NOD bone marrow cells can transfer diabetes-susceptibility to disease-resistant strains (Serreze et al, 1988; Wicker et al, 1988). Thus, bone marrow cells expressing NOD susceptibility genes are essential for diabetes induction. In vitro stimulation of hematopoietic precursors derived from both human prediabetics and NOD mice show impaired responses to GM-CSF and other myeloid growth factors (Jansen et al, 1995; Takahashi et al, 1998; Serreze et al, 1993a and b; Langmuir et al, 1993). Furthermore, dendritic cells constitute the initial infiltrate into the islets of NOD mice (Jansen et al, 1994). Interestingly, it has recently been shown that repeated priming with dendritic cells, bearing an epitope expressed on target tissue, can induce the development of secondary lymphoid-like structures in the target tissue, ultimately leading to tissue destruction (Ludewig et al, 1998).

That NOD bone marrow cells were essential for diabetes induction was demonstrated in bone marrow chimeric mice. F1 hybrid mice generated by crossing NOD with diabetes-resistant strain are resistant to diabetes. However, F1 hybrids become susceptible to diabetes when irradiated and reconstituted with NOD bone marrow cells. Whether majority of reconstituted F1 hybrids get insulitis or diabetes depends on the genotype of the disease-resistant strain. Majority of irradiated (NOD x B10.H-$2g^7$)F1 that are reconstituted with NOD bone marrow cells develop insulitis and some become diabetic (Wicker et al, 1988). Majority of (NOD x NON.H-$2g^7$)F1 hybrids similary treated develop diabetes (Serreze et al, 1988). Since the NON strain shares more alleles with NOD than does the B10 strain, these results imply that NOD alleles also act within the radio-resistant (predominantly non-hematopoietic) cells.

Defects in dendritic cells generated in vitro from precursors isolated from Type I diabetic and prediabetic patients have been reported (Jansen et al, 1995; Takahashi et al, 1998). Dendritic cells generated from monocyte precursors isolated from the blood of diabetics show a reduced ability to cluster and to stimulate autologous and allogeneic T cells, compared with dendritic cells from healthy controls. Similarly, monocyte-derived precursors from the blood of prediabetics respond suboptimally in response to stimulation with GM-CSF and IL-4. In contrast to controls matched for age, sex and MHC genotype, precursors from prediabetics generate fewer dendritic cells which appeared to be phenotypically and functionally distinct. Dendritic cells generated from prediabetics expressed lower levels of cell surface costimulatory molecules and were relatively inefficient in stimulating autologous T cells.

As in humans, hematopoietic deficiencies have also been detected in the NOD mouse (Serreze et al, 1993a and b; Langmuir et al, 1993). NOD bone marrow cells generated fewer colonies than Balb/c bone marrow cells, in response to stimulation with myeloid growth factors. The myeloid growth factors used include GM-CSF, IL-3 and IL-5 (Langmuir et al, 1993). This phenotype, however, was not replicated in vivo as NOD myeloid precursors formed similar number of spleen colonies when injected into irradiated syngeneic recipients, compared with precursors from Balb/c mice. In another study, it was shown that colony stimulating factor 1 (CSF-1) and IFNγ stimulation of NOD bone marrow cells resulted in abnormal macrophage development and maturation (Serreze et al, 1993a). Macrophages from disease-resistant strains secreted higher levels of LPS-stimulated IL-1 compared with macrophages generated from NOD bone marrow cells. It was also shown in this study that majority of the disease-resistant (NODxNON.H-$2g^7$) F1 hybrid mice when irradiated and reconstituted with NOD bone marrow cells developed diabetes. No recipients reconstituted with of a 1:1 mixture of NOD and NON.H-$2g^7$ bone marrow cells developed diabetes, however. Impaired maturation of NOD macrophages may therefore be of pathogenic significance in NOD mice.

Elevated numbers of dendritic cells and macrophages constitute the initial infiltrate into the islets of NOD mice. This occurs as early as 3 weeks of age in both male and female NOD mice and precedes lymphocytic infiltration into islets (Jansen et al, 1994). It has recently been shown that this initial arrival of dendritic cells and macrophages into islets coincides with them being the primary producers of the proinflammatory cytokine, TNFα, in the islets, as determined by double immunofluorescence analysis (Dahlen et al, 1998). Thus, early dendritic cell and macrophage infiltration and TNFα secretion in islets may be crucial in the initiation and development of diabetes.

Important evidence for the role of dendritic cells in autoimmune response against peripheral tissue came in a study by Ludewig et al (1998). This study employs transgenic mice which target the expression of the lymphocytic choriomeningitis virus glycoprotein (LCMV-GP) to pancreatic β cells by using the rat insulin promoter (RIP). RIP-GP mice do not spontaneously develop diabetes. However, when infected with LCMV, these mice develop an acute form of non-lethal diabetes (Ohashi et al, 1991; Oldstone et al, 1991). The study by Ludewig et al (1998) investigates the role of dendritic cells in the initiation and maintenance of autoimmune diabetes, by repeatedly priming RIP-GP mice with dendritic cells constitutively expressing the immunodominant CTL epitope of LCMV-GP. This regime of repeated CTL activation by dendritic cells results in severe and destructive mononuclear cell infiltration into islets. A conspicous feature of this process was the formation of islet-associated secondary lymphoid-like structures, observed in other

autoimmune syndromes, including Hashimoto's thyroiditis (Iwatani et al, 1993) and rheumatoid arthritis (Randen et al, 1995). Thus, repeated priming by dendritic cells bearing peripheral antigen can induce formation of de novo lymphoid structures in target peripheral tissue and provoke tissue autoimmunity.

1.13 Project Objective

It is now evident that diabetogenic loci outside the MHC create an overall susceptibility to autoimmunity in the NOD mouse (Wicker, 1997). Against the NOD autoimmune-prone background, alleles within the MHC determine the target tissue for autoimmune destruction. Autoimmune pathology may be directed against salivary or thyroid glands or the pancreas depending on the genotype of the MHC on the NOD background.

This thesis analyzes the effects of non-MHC diabetogenic loci on the cell biology and function of dendritic cells. There are several key reasons for focusing on this facet of immunity. First, bone marrow cells, carrying diabetogenic loci, are essential for diabetes induction in NOD mice (Wicker et al, 1988; Serreze et al, 1988), and dendritic cells and macrophages constitute the initial infiltrate into islets of young NOD mice (Jansen et al, 1994). The advent of these antigen presenting cells, prior to lymphocytic infiltration, is coincident with the secretion of the proinflammatory cytokine, TNFα, by these antigen presenting cells (Dahlen et, 1998). Importantly, it is has been demonstrated that repeated priming of mice with dendritic cells bearing islet-expressing epitope leads to severe and rapid onset of diabetes (Ludewig et al, 1998). Such an immunization regime transforms the pancreas into lymph node-like structures, a phenomenon observed in other autoimmune pathologies (Iwatani et al, 1993; Randel et al, 1995). Overall, these data suggest that dendritic cells may be of critical importance in the initiation and maintenance of autoimmune responses against peripheral tissue.

The current project utilized B10.BR and NOD.H-2^k congenic mice to investigate dendritic cell generation, both in vitro and in vivo, in an attempt to explore cellular processes which may be affected by diabetogenic loci outside the MHC. It is conceivable that dysregulation of antigen presenting cell function of dendritic cells, mediated by non-MHC NOD genes, may explain the breach of peripheral tolerance mechanisms in NOD mice.

Chapter 2

Materials and Methods

2.1 Commonly Used Reagents (Chemicals, Buffers and Media)

Commonly used reagents, along with their sources, are listed in Appendix A1.

2.2 Mice

Inbred B10.BR, NOD.H-2^k, Balb/c, mice expressing the 3A9 transgenic T cell receptor on the B10.BR background, CBA/H and AKR mice were housed under specific pathogen free conditions in microisolator cages in the Medical Genome Centre or the Animal Services Unit at the JCSMR. Balb.H-2^k mice were purchased from the Animal Resources Centre, Perth, Australia. Mice used in this project were 8-16 weeks of age and where necessary matched for age and sex.

2.3 Cell Culture Conditions

Mammalian cell lines and primary cell cultures were maintained in RPMI 1640 culture medium (JCSMR; GibcoBRL, Life Technologies, Grand Island, NY, USA) supplemented with 10% (v/v) heat inactivated foetal bovine serum (FBS) (Trace Biosciences, NSW, Australia), 0.05mM β-mercaptoethanol (GibcoBRL), 2mM L-Glutamine (GibcoBRL), 10mM HEPES (Sigma Chemical Co., MO, USA) and antibiotics (100U/mL penicillin, 100μg/mL streptomycin; GibcoBRL). In this thesis, the terms 'medium' or 'RPMI' refer to the 10% (v/v) FBS/RPMI described here, unless otherwise stated.

Cell cultures were maintained at 37°C in a 5% carbon dioxide atmosphere in an automated incubator (model 3194: Forma Scientific, OH, USA) with humidity provided by a solution 0.025% (w/v) benzalkonium chloride in sterile double distilled water. Incubators were disinfected routinely with 70% (v/v) ethanol or with a solution of the viricidal disinfectant, Virkon (Antec International, Suffolk, UK) prepared according to the manufacturer's specifications.

Centrifugation of cells for the purposes of washing was performed in polypropylene, gamma-irradiated Falcon conical tubes (Becton and Dickinson Labware,

Franklin Lakes, NJ, USA) at 200*g* for 4-6 minutes at 4°C. For washing, cells were pelleted by centrifugation and resuspended in required volume of fresh medium. Viable cell numbers were determined by the exclusion of cells positive for the vital dye, trypan blue (0.4% w/v; Sigma Chemicals Co.), as observed on a haemocytometer under a light microscope.

2.4 Cell Lines

All cell lines used during the course of this project are listed in the table below, together with details of their source and functional purpose.

Table 2.1

Cell Line	Comments	Source	Reference
3DO.54.8	I-A^d-restricted, OVA323-339-specific T cell hybridoma	Marrack[a]	Shimonkevitz et al (1983)
A20	EBV-transformed B lymphoblastoid cell line	McDevitt[b]	Kim et al (1979)
HT-2	IL-2 and IL-4-dependent T cell line used in bioassays	McDevitt	Watson (1979)
GK1.5	B cell hybridoma for obtaining anti-CD4 antibody	Gautam[c]	Dialynas et al (1983)
RA3.3A1	B cell hybridoma used for obtaining B220 antibody	Hodgkin[d]	Coffman and Weissman (1981)
Sf9	Insect cell line used for infection with recombinant baculovirus encoding growth factors	Hapel[e]	Gruenwald and Heitz (1993)

a Gift from Prof. P. Marrack, National Jewish Hospital and Research Centre, CO, USA.

b Supplied by Prof. H.O. McDevitt, Stanford University, CA, USA.

c. Supplied by Dr. A.M. Gautam, M&E Biotech, Copenhagen, Denmark

d. Supplied by Dr. P.D. Hodgkin, Centenary Institute, Sydney, NSW, Australia

e. Supplied by Dr. A.H. Hapel, John Curtin School of Medical Research, ANU, Canberra.

The A20 B cell line and the 3DO T cell hybridoma were maintained at 37°C (5% CO_2) in appropriate sized Nunc tissue culture flasks (Nunc™ Brand Products, Nalge Nunc International, Denmark) containing RPMI 1640 medium supplemented with 10% FBS. Cultures were fed when medium became acidic, as indicated by a change of medium colour to yellow, or when cells in culture became confluent. This was done by removing required volume of cultured cells and adding back required amount of fresh medium. RA3.3A9 and GK1.5 B cell hyridoma cells were propagated in large Nunc tissue culture flasks (800mL volume) until almost all cells underwent apoptosis. Culture supernatants were harvested and centrifuged (800*g* for 10 minute at 4°C) to eliminate cellular debris. Supernatants were microfiltered, using a 0.2 micron filter (Millex®-GP, Millipore Corporation, MA, USA), and stored at 4°C. HT-2 cells were maintained in culture medium including 50 units per mL recombinant murine IL-2 (gift from Prof. Christopher Parish, JCSMR). Protocols employed for maintenance of *Spodoptera frugiperda* (Sf9) insect cells are described in section 2.6.4.

2.5 Monoclonal Antibodies

All monoclonal antibodies, directed against murine cell surface molecules, used during the course of this project are listed in the table below, along with their isotype, specificity and source.

Table 2.2

Antibody	Isotype	Specificity	Source	Reference
10-3.6.2 -FITC	mIgG2a	I-A$\beta^{f,k,r,s,u,g7}$	McDevitt[1]	Landais et al (1986)
3E2	AHIgG	CD54 (ICAM-1)	Müllbacher	Scheynius et al (1993)
14-4.4S-FITC	mIgG2a	I-E$\alpha^{d,k,p,r,u}$	McDevitt	Ozato et al (1980)
34-1-2S	mIgG2a	anti-H-2 K^dD^d	Müllbacher[2]	Ozato et al (1982)
31M	rIgM	anti-CD8	Finch[3] via Müllbacher	Ceredig et al (1989)

Table 2.2 - cont

Antibody	Isotype	Specificity	Source	Reference
B7.1	rIgG2a	CD80	Müllbacher	Razi-Wolf et al (1992)
B220 (RA3-6B2) -FITC or -PE	rIgG2a	CD45	Goodnow[4] Caltag[5]	Coffman and Weissmann (1981)
CD69-biotin	AHIgG	CD69	Pharmingen[6]	Yokoyama et al (1988)
GK1.5-FITC or -PE	rIgG2a	CD4	Caltag	Dialynas et al (1983)
$Ly5^a$ (AS20.1) -FITC or -PE or -Biotin	mIgG2a	CD45a	Goodnow	Shen et al (1986)
$Ly5^b$ (104) -FITC or -Biotin	mIgG2a	CD45b	Pharmingen	Shen et al (1986)
Mac1-FITC	rIgG2b	CD11b	Caltag	Springer et al (1979)
N418-Biotin or -FITC	AHIgG	CD11c	Townsend[8] Prasad[9]	Metlay et al (1990)
OX6-FITC or -PE	mIgG1	$I\text{-}A^{f,k,r,s,u,g7}$	Pharmingen	Fukumoto (1982)
Thy1.2-FITC	rIgG2a	CD90.2	Pharmingen	Gunter et al (1984)
Vβ8.2-FITC (MR5-2)	mIgG2a	Vβ8.2 T cell receptor	Pharmingen	Kanagawa O. (1988)

1. Supplied by Prof. H.O. McDevitt, Stanford University, CA, USA.
2. Supplied by Dr. A. Müllbacher, JCSMR, ANU, Canberra.
3. Dr. Frank W. Finch, University of Chicago, IL, USA.
4. Supplied by Prof. C.C. Goodnow, JCSMR, ANU, Canberra.
5. Caltag, Burlingame, CA, USA.
6. Pharmingen, San Diego, CA, USA.
7. Gift from Prof. P. Marrack, National Jewish Hospital and Research Centre, CO, USA.
8. Supplied by Dr. S. Townsend, University of British Columbia, Vancouver, B.C., Canada.
9. Antibody purified from the N418 hybridoma (supplied by Dr. Hapel, JCSMR) and conjugated to FITC during my Honours year (1995)

Abbreviations in Table 2.2

AH	Armenian Hamster
FITC	Fluorescein Isothiocyante
Ig	Immunoglobulin
m	murine
PE	Phycoerythrin
r	rat

2.5.1 Secondary Staining Reagents

Table 2.3

Reagent	Purpose	Source
Goat Anti-mouse IgG-FITC	2^o with 34-1.2S	Pierce, Rockford, IL, USA
Rabbit Anti-Hamster IgG-FITC	2^o with 3E2	Pierce
Goat Anti-rat IgG-FITC	2^o with B7.1	Caltag
Streptavidin-Phycoerythrin* (SA-PE)		Caltag
Streptavidin-Cy Chrome™* (SA-TC)		Pharmingen

* Secondary (2^o) reagents used with biotinylated antibodies

2.6 In Vitro Culture of Dendritic Cells

2.6.1 Harvesting Bone Marrow Cells

The protocol employed for culturing dendritic cells in vitro was adapted from Inaba et al (1992a). Mice providing bone marrow were euthanized by cervical dislocation in a tissue culture hood. All subsequent steps were carried out aseptically. The skin from each hind leg was peeled from the bottom of the foot to the top. Excess muscle from legs were removed by using scissors while holding end of bones with forceps. The legs were then severed at the pelvic joints and just above and below the knee. This was followed by cutting off the feet. A 3mL syringe (Becton Dickinson Medical (S) Pte Ltd, Singapore) with a 25G needle (Terumo Medical Corporation, Elkton, MD, USA) attached was filled with 2-5 mL sterile RPMI. The needle was inserted into bone marrow cavity of femur or tibia. Bone marrow was flushed out into a petri dish until bone cavity appeared white. The bone marrow suspension was passed through a nylon mesh cell strainer (70µm, Falcon®, Becton and Dickinson Labware) to remove small pieces of bone and debris. The filtered suspension, containing bone marrow cells from one mouse, was collected into a sterile 50mL polypropylene Falcon conical tube (Falcon®Blue Max, Becton and Dickinson Labware) and counted on a heamocytometer under light microscopy. The nuclear staining White Blood Cell Counting Dye (see Appendix 2.3h) was used to distinguish between leukocytes and erythrocytes during counting. Routinely, there were approximately $5x10^7$ leukocytes from the hind limbs of one mouse. The suspension was centrifuged at 200*g* (Beckman CPKR Centrifuge: Beckman Instruments, Palo Alto, CA , USA) for 5 minutes at room temperature and the supernatant was discarded. The pellet was resuspended in a 900µL cocktail of monoclonal antibodies to be described below.

2.6.2 Complement-mediated Lysis of Lymphocytes

Cedarlane Low-Tox® -M Rabbit complement (Accurate Chemical &Scientific Corp, NY, USA) was reconstituted in 1mL ice-cold double distilled water. 100µL aliquots were frozen at -20°C. 1 in 10 dilution of complement was used for lysis. A 900µL volume antibody cocktail comprising optimal doses of the following monoclonal antibodies was made: 1 in 2.5 anti-B220 neat (RA3.3A9 supernatant), 1 in 5 of anti-CD4 (GK1.5 supernatant) and anti-CD8 (31M supernatant provided by Dr. Müllbacher, JCSMR). Approximately $5x10^7$ bone marrow leukocytes were resuspended in the above antibody cocktail in 50mL polypropylene Falcon conical tubes and incubated for 30-40 minutes at 4°C. The antibody-labelled suspension was diluted to 10 mL and washed by centrifuging at 200*g* for 5 minutes at room temperature to remove excess antibody. The

pellet was resuspended in 1mL medium containing 100µL complement and incubated at 37°C for 30-45 minutes. The lysed sample was washed twice as previously described and resuspended in 5mL medium.

2.6.3 Separation of Mononuclear Cells

The above 5mL suspension was layered onto 5ml Ficoll gradient (Ficoll-Paque™ PLUS, Amersham Pharmacia Biotech, Uppsala, Sweden) in a 15mL Falcon polypropylene conical tube (Falcon®Blue Max Jnr). The tube was centrifuged at 500*g* for 20 minutes at room temperature. Interface cells were gently removed with a sterile Pasteur pipette. A maximum of 1-2 mL volume of interface cells was harvested. Interface cells were diluted in 20mL medium and washed twice by centrifugation at 4°C firstly at 500*g* and then at 200*g*. Cells were then resuspended in growth factor-supplemented medium as described next.

2.6.4 Growth Factors for Dendritic Cell Culture

Recombinant baculovirus-encoding murine (m) GM-CSF and mIL-4 were obtained from Dr A. Hapel and Prof I. Young, respectively. The baculovirus expression system for the production of growth factors used baculovirus carrying lethal deletions of some essential components of the virus genome (BaculoGold™ system, Pharmingen). The lethal deletions were rescued by a complementing polyhedrin-based transfer plasmid vector encoding either mGM-CSF or mIL-4 under the polyhedrin promotor. Sf9 insect cells were co-transfected with the BaculoGold™ virus (linearized viral DNA) and the growth factor-encoding transfer plasmid. After several days, recombinant virus which arise as a result of homologous recombination between the plasmid and the viral DNA are selected in a plaque assay. Recombinant virus was used to infect Sf9 insect cells. Infected insect cells secreted particular growth factor into culture medium. Expression of growth factors were analyzed in bioassays to be described below. The process of growth factor production is summarized in the schematic illustrated in Figure 2.1.

Sf9 insect cells at a density of $1x10^7$ cells per mL insect cell medium (Sf-900 II SFM GibcoBRL) supplemented with 10% FBS was obtained from Dr. Hapel's laboratory and cultured in 30mL culture volume in tightly capped 800mL Nunc tissue culture flasks. Cultures were fed every 2-3 days by removing all medium from culture flask and adding equal volumes of fresh insect cell medium. Prior to infection with recombinant baculovirus semi-confluent monolayer of Sf9 cells in culture were gradually adapted to serum free insect cell medium. This was done by initially feeding cultures with

Figure 2.1.
Schematic illustrating production of growth factors using recombinant baculovirus expression system

See text for details.

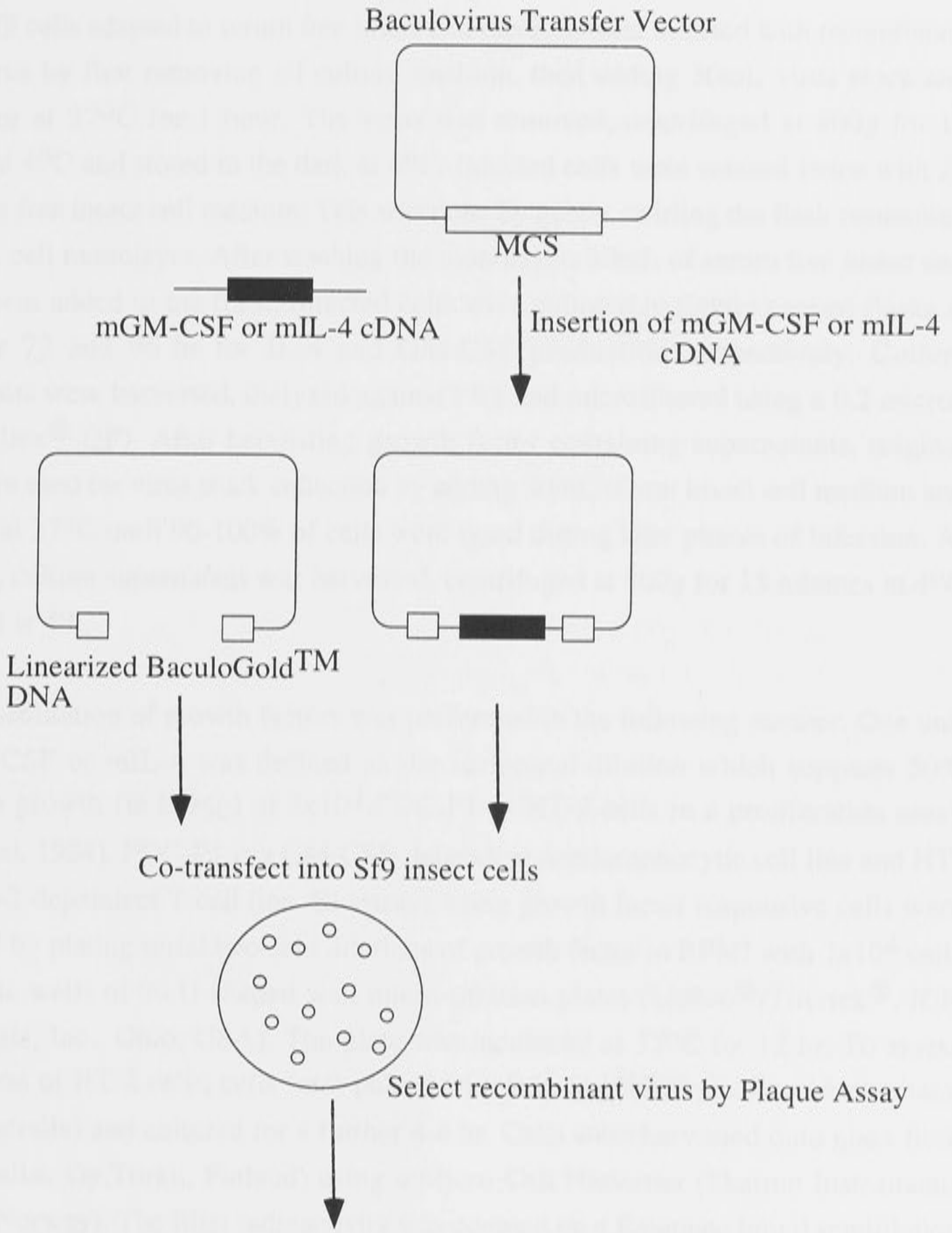

Key: MCS - Multiple Cloning Site

equal volumes of serum and serum free insect cell medium, followed 2-3 days later by feeding with only serum free insect cell medium. Serum free insect cell medium enables Sf9 cells to form adherent monolayers, making them suitable for infection.

Sf9 cells adapted to serum free insect cell medium were infected with recombinant baculovirus by first removing all culture medium, then adding 30mL virus stock and incubating at 27°C for 1 hour. The virus was removed, centrifuged at 800*g* for 10 minutes at 4°C and stored in the dark at 4°C. Infected cells were washed twice with 20 mL serum free insect cell medium. This was done by gently swirling the flask containing the insect cell monolayer. After washing the monolayer, 30mL of serum free insect cell medium was added to the flask. Infected cells were cultured in tightly capped flasks at 27°C for 72 and 96 hr for IL-4 and GM-CSF production, respectively. Culture supernatants were harvested, dialyzed against PBS and microfiltered using a 0.2 micron filter (Millex®-GP). After harvesting growth factor containing supernatants, original flasks were used for virus stock collection by adding 30mL serum insect cell medium and culturing at 27°C until 90-100% of cells were lysed during later phases of infection. At this point, culture supernatant was harvested, centrifuged at 800*g* for 15 minutes at 4°C and stored at 4°C.

Quantitation of growth factors was performed in the following manner. One unit of mGM-CSF or mIL-4 was defined as the reciprocal dilution which supports 50% maximum growth (ie ED_{50}) of $2x10^4$ FDC-P1 or HT-2 cells in a proliferation assay (Hapel et al, 1984). FDC-P1 is a GM-CSF-dependent myelomonocytic cell line and HT-2 is an IL-2-dependent T cell line. Bioassays using growth factor responsive cells were performed by plating serial two-fold dilutions of growth factor in RPMI with $2x10^4$ cells in triplicate wells of 96 U-shaped well micro-titration plates (Linbro®/Titertek®, ICN Biomedicals, Inc., Ohio, USA). The plate was incubated at 37°C for 12 hr. To assess proliferation of HT-2 cells, cells were pulsed with 0.5µCi [^{3}H]Thymidine (Amersham, NSW, Australia) and cultured for a further 4-6 hr. Cells were harvested onto glass fibre filters (Wallac Oy,Turku, Finland) using a Micro Cell Harvester (Skatron Instruments AS, Lier, Norway). The filter radioactivity was counted on a Betaplate liquid scintillation counter (model 1205; Wallac Oy, Turku, Finland). [^{3}H]Thymidine incorporation data was recorded as counts per minute (cpm).

2.6.5 Culture of Myeloid Precursors

$1x10^6$ lymphocyte-depleted bone marrow leukocytes, resuspended in 1mL medium suppplemented with 800 U/mL mGM-CSF and 200 U/mL mIL-4 were dispensed into individual wells of 24 well Linbro plates (Linbro®/Titertek®), as described previously (Inaba et al, 1992a). Cultures were fed on days 2 and 4 by gently swirling plate and aspirating 50% of the medium, and adding back equal amount of fresh growth factor-supplemented medium. Loosely adherent cell clusters were harvested on day 5 and then on day 7, pelleted by centrifugation (200*g*), resuspended in fresh growth factor-supplemented medium, and subcultured onto fresh plates, keeping the number of wells constant throughout the culture. The dose of growth factors in culture was halved from day 5 onwards. On day 8 of culture, loosely adherent or floating cells were harvested, washed twice, and used as required.

2.7 Transmission Electron Microscopy (TEM)

$1x10^6$ cells from bone marrow cultures on day 8 were harvested and resuspended in 1mL RPMI, and supplied to the JCSMR Electron Microscopy Unit for routine TEM. For TEM, cells were fixed in 2% glutaraldehyde in 0.1M cacodylate buffer (pH 7.4). Cells were post-fixed in 1% osmium tetroxide in 0.1M cacodylate buffer (pH 7.4), dehydrated and dried in a critical point drying apparatus. This was followed by embedding cells in Spurr's resin. Thin sections of 80nm were cut on a Reichert Ultracut E and stained with lead citrate. Sections were viewed in a Hitachi H7000 electron microscope.

2.8 Fluorescence Activated Cell Sorter (FACS) Analysis - Cell Staining, Data Acquisition and Analysis

Flow cytometry experiments were conducted using the standard Argon laser FACScan Cytometer (Becton Dickinson, San Jose, CA, USA) with standard filter configuration. In all experiments Forward Scatter (FSC) was used as the threshold parameter. Data acquisition and analysis were carried using the CELLQuest™ software package (version 3.1, ©1994-1997, Becton Dickinson). The number of cells acquired varied from $5x10^3$ to $1x10^5$ depending on the requirements of the assay. Generally, 0.5-$1x10^4$ events were acquired during analysis of red blood cell-depleted blood leukocytes, splenocytes and thymocytes. 0.5-$1x10^5$ events were acquired during the analysis of

cultured or primary dendritic cells. Furthermore, appropriate gating of events during acquisition or subsequent analysis will be shown in representative FACS plots.

2.8.1 Staining Cells for Flow Cytomery

All reagents used in flow cytometry experiments were diluted in a PBS-based FACS buffer (see Appendix A2.1a) containing 2% (v/v) FBS and 0.01% (v/v) sodium azide. The FACS buffer was always stored in the dark at 4^{o}C. Prior to staining, red blood cells from primary tissue suspensions were depleted by Tris-ammonium chloride (see Appendix A2.1d)-mediated lysis, washed twice and resuspended at the required concentration in FACS buffer. Cells resuspended in FACS buffer were dispensed into 96 U-shaped microwell plates (Linbro®/Titertek®) at a concentration of 0.5-1x10^{6} cells per well. Primary and secondary staining reagents used are shown in Tables 2.2 and 2.3, respectively. Cells were stained with appropriately diluted primary reagents in 25µL stain volume in the dark for 20 minutes at 4^{o}C. This primary incubation was followed by 2 large volume washes. This was done by first adding 175µL FACS buffer to each well, then centrifuging the plate for 10 seconds at 800*g* at 4^{o}C in a benchtop centrifuge (Labofuge 400R; Heraeus Instruments, N.J.,USA). The plate was flicked with a firm wrist to eliminate supernatant. The plate was gently tapped on the sides to resuspend pellet in residual supernatant. This preceding wash procedure was then repeated. Appropriately diluted secondary reagents where necessary were added and cells incubated in the same way as during the primary incubation. Cells were washed twice as after the primary incubation and resuspended in 100µL FACS buffer or FACS fix buffer (containing 0.1% paraformaldehyde, see Appendix A2.1b). 4x10^{3} absolute counting beads (polystyrene fluorospheres, Flow-Count™, Coulter Corporation, Miami, Florida, USA) per 100µL buffer were included in the FACS or FACS fix buffer when absolute quantitation of cells was necessary. Resuspended stained cells were transferred to 1.2 mL polypropylene cluster tubes (Costar Corporation, Cambridge, MA, USA) and taken for acquisition.

Optimal concentrations of primary and secondary reagents were pre-determined in titration assays by staining red blood cell-depleted splenocytes with two-fold serial dilutions of reagents.

2.9 Whole Blood Stains

Staining of whole blood for flow cytometry differed from the protocol outlined above and, therefore, will be described next.

2.9.1 Harvesting Blood

Cages of mice to be bled were placed under a heat lamp for 3-4 minutes to induce vasodilation. Individual mice were immobilized in a standard conical restrainer and bled by inserting a 26G needle into the lateral tail vein. Then needle was withdrawn and the resulting drops of blood collected with a heparinized hematocrit capillary tube (Hirschmann Laborgerate, Germany). Blood in the capillary tube was blown out into 100µL Alsevers (JCSMR stock, Appendix A2.3a) in a 96 U-shaped microwell plates (Linbro®/Titertek®) The capillary tube was swirled in the well to mix blood and Alsevers. Alternatively, mice were sacrificed in presence of carbon dioxide and blood was collected from the chest cavity using a plastic Pasteur pipette. The blood/Alsevers mixture could be kept at room temperature for up to 2 hours prior to processing to be described section 2.9.3. Collected blood was not diluted in Alsevers when staining whole blood was necessary.

2.9.2 Staining Whole Blood

Required antibody cocktails were prepared by first preincubating primary antibodies with appropriate secondary reagents in FACS buffer at 4°C for time required to bleed mice. Where required other directly-conjugated primary antibodies were subsequently added to the cocktail. 2µL of whole blood was stained at 4°C for 20 minutes with appropriate antibodies in a total 25µL stain volume. Each well was then diluted with 175µl RPMI containing $4x10^3$ counting beads per 100µL RPMI. Stained blood samples were then transferred to cluster tubes and taken immediately for acquisition. Samples were acquired at a slow flow rate until 400 beads were acquired.

2.9.3 Processing Blood

The plate containing the blood/Alsevers solution was centrifuged at 800*g* for 10 seconds at room temperature. The supernatant in each well was aspirated using a multi-channel pipette. 200µL of Tris ammonium chloride was then added to each well and the pellet resuspended by pipetting up and down 5 times. The plate was incubated at room

temperature for 10 minutes. The plate was centrifuged again and the supernatant aspirated as before. The preceding procedure of Tris ammonium chloride addition, pellet resuspension, incubation, centrifugation and supernatant aspiration was repeated. Finally the cells were resuspended in FACS buffer, washed once and stained as before.

2.9.4 Absolute Quantitation of Blood Leukocytes

Whole and processed blood were analyzed in parallel in order to determine the frequency of rare blood leukocytes. This was done by comparing the frequency of rare leukocytes, monocytes in this study, relative to B cells. B cells, being the most numerous in whole blood, are readily detectable and countable on the flow cytometer. As mentioned above, counting beads were added to whole blood samples for the quantitation B cells. Firstly, the relative proportions of B cells and monocytes in processed (red blood cell-depleted) blood were determined as fractions of total leukocytes. Absolute numbers of monocytes were determined by multiplying the absolute number of B cells in whole blood by the ratio of the relative proportions of monocytes to B cells in the same sample of processed blood leukocytes.

2.10 Screening for the Presence of T cell receptor Transgene

Mice were screened for the presence of T cell receptor (TCR) transgene expression by ear punch PCR reactions as described by Chen and Evans (1990).

2.10.1 Collecting Ear Punches

Mice were individually ear marked with ear punch using the dominant hand while appropriately holding mice with the other hand. The last punch-hole was saved in labelled 500µL eppendorf tubes (Eppendorf-Netherlor-Hinz-GmbH, Hamburg, Germany). The working area and fingers were kept clean between mice. The punch and forceps used were carefully rinsed and dried between mice. This was to minimize carry-over DNA from one mouse to another, which can give false positives especially with high copy-number transgenic mice.

2.10.2 Processing Ear Punches

Processing of ear punches was carried out in a clean working area using Gilson pipettes designated for this purpose. 20µL ear-punch digestion mix was added to each tube containing an ear punch. The digestion mix included the following ingredients:

50 mM Tris pH8.0
2mM NaCl
10 mM EDTA
1% (v/v)SDS
1mg/mL Proteinase K

The digestion mix was made in advance, autoclaved and store at room temperature. All tubes containing ear punches were warmed in a heat block to 55°C for 20 minutes. This was followed by vortexing each tube to dislodge and break up the partly digested ear punch. The tubes were warmed again to 55°C for a further 20 minutes. 180µL of triple distilled water was added to each tube. The tubes were capped tightly and placed in a heat block set at 100°C for 5 minutes to inactivate Proteinase K and to melt DNA strands. The tubes were cooled and required volumes of the digest was used in a PCR reaction immediately or stored at -20°C for later use.

2.10.3 Polymerase Chain Reaction (PCR)

The primers used to amplify the 3A9 T cell receptor transgene and for the positive control endogenous product (I-E^k α chain) are shown below.

Primers

(1) 3A9 T cell receptor transgene
5' Primer: GCAGTCACCCAAAGCCCAAG
3' Primer: CCCCAGCTCACCTAACACTG

(2) I-E^k α chain
5' Primer: AGTCTTCCCAGCCTTCACACTCAGAGGTAC
3' Primer: CATAGCCCCAAATGTCTGACCTCTGGAGAG

PCR Reaction mix

Amplification of the transgenic T cell receptor was carried out under conditions previously optimized in the laboratory. Amplification of the transgene generates a 371 base pair long fragment for the transgene versus a 264 base pair product for the endogenous Vβ 8.2 gene segment. Shown below are the ingredients and volumes used in the 50μL PCR reaction mix.

Reagent	Volume (μL)
10x PCR Buffer	5
40 mM dNTPs	1
Control Primers	
5'	1
3'	1
TCR Primers	
5'	1
3'	1
Triton X 100 (10% stock)	0.5
DNA Polymerase	0.25
Template DNA	1
Triple distilled water	38.25
	50

The PCR reaction was conducted using a Corbett Research FTS-960 Thermal Cycler. Non-specific amplification was monitored by the inclusion of negative controls containing all ingredients except template. PCR efficiency was monitored by the inclusion of positive control primers to the I-E^k α chain known amplify a product different in size to target product. The program for amplification was outlined below:

Temperature	**Time**	**Number of Cycles**
94°C	2 minutes	1
94°C	15 seconds	1
60°C	30 seconds	1
72°C	45 seconds	35
4°C	1 minute	HOLD

At the end of the cycle, 5-10% of the reaction was removed and electrophoresed on a 1% agarose gel, containing 0.5μg/mL ethidium bromide. Presence of PCR products were visualized by UV transillumination. Standard DNA markers (GibcoBRL) were also run in parallel.

2.11 CFSE Labelling of Leukocytes

Whole spleen and lymph node cells or lymphocyte-depleted bone marrow cells were labelled with 5-(and 6-) carboxyfluorescein succinimidyl ester (CFSE; Molecular Probes, Oregon, USA) in a modified manner to what was described by Lyons and Parish (1994). Briefly, cells were washed once by centrifuging at 200*g* for 4-5 minutes at room temperature. Cells at a density of 0.5-1x10^7 cells per mL RPMI containing 1.25µM CFSE were incubated for 7 minutes at room temperature. The labelling was stopped by adding excess cold RPMI. The cells were washed 3 times in cold RPMI, counted and resuspended at required density in RPMI.

2.12 Antigens

Protein and peptide antigens used in antigen presentation assays are listed below.

Chicken Egg Albumin (Ovalbumin, OVA) - Sigma Chemical Co.
OVA323-339 peptide - synthesized at the Biomolecular Resources Facility, JCSMR.
Hen Eggwhite Lysozyme (HEL) - Sigma Chemical Co.
HEL46-61 peptide - synthesized at the Protein and Nucleic Acid Facility, Stanford University, Palo Alto, CA, USA

Antigen stocks were made by dissolving each antigen in sterile RPMI. Suspensions were microfiltered and stored at -20^{o}C.

2.13 Antigen Presentation Assay using a T Cell Hybridoma

Two different T cell assays were employed during the course of this project. The first has been previously described (Shimonkevitz, 1983) and was used as part of the functional analyses of dendritic cells generated in vitro from myeloid precursors isolated from Balb/c mice. The ability of day 8 Balb/c bone marrow-derived dendritic cells to present protein (Ovalbumin) and peptide antigen (OVA323-339) was compared against an EBV-transformed, Balb/c-derived B cell line (A20). Essentially, antigen presentation to the T cell hybridoma, 3DO, (I-A^d-resricted and OVA323-339-specific) was assessed using an IL-2 bioassay. The 3DO T cell hybridoma has previously been shown to secrete IL-2 in response to ovalbumin presented by the I-A^d-expressing A20 cells (Shimonkevitz et al, 1983). The assay was performed in a polystyrene 96 well flat-bottom microtitre

plate (Nunc, Roskilde, Denmark). Antigen presenting cells and T cell hybridoma cells were washed twice and resuspended in RPMI at required densities. $5x10^3$ dendritic cells or $2.5x10^4$ A20 cells (unfixed) were cocultured in triplicate wells with $2.5x10^4$ T cell hybridoma cells, in the presence of two-fold serial dilutions of OVA or OVA 323-339. The total culture volume in each well was 200µL. Negative control wells contained no antigen. Plates were incubated at 37°C for 18-24 hr. 150µL supernatant was harvested into fresh 96 well plates and frozen for 30 minutes at -70°C to lyse all viable cells.

T cell response was measured by assaying culture supernatant for IL-2 activity. This was done by using a secondary culture of the IL-2-dependent cell line, HT-2 (Watson, 1979), in 96 well flat-bottom plates. HT-2 cells were washed 3-4 times to remove residual IL-2 from culture and resuspended in RPMI at 10^5 cells per mL. 50µL of this suspension was added to an equal volume of the primary culture supernatant. Positive control wells included RPMI (10% FBS) supplemented with 50U/mL recombinant murine IL-2. The plate was incubated at 37°C for 12 hr. As before, proliferation of HT-2 cells was assessed by pulsing cells with 0.5µCi [^{3}H]Thymidine and cultured for a further 4-6 hr. Cells were harvested onto glass fibre filters using a Micro Cell Harvester. The filter radioactivity was counted on a Betaplate liquid scintillation counter. [^{3}H]Thymidine incorporation data was recorded as cpm.

2.14 Antigen Presentation Assay using Transgenic T Cells

A second in vitro T cell assay, to be described below, was specifically designed to allow the frequency of responding T cells to be visualized and quantitated. The assay was designed to determine any functional difference between control B10.BR-derived dendritic cells and test NOD.H-2^k-derived dendritic cells to activate specific T cells and induce their proliferation. Cultured day 8 bone marrow cells, derived from either strain, were harvested and transferred to 15mL polypropylene Falcon conical tubes. Cells were washed twice in RPMI by centrifugation and used as source of dendritic cells. To synchronize T cell activation and limit antigen delivery, cultured dendritic cells were pulsed with required doses of antigen. For this purpose, 1-5 x 10^6 cultured bone marrow cells were resuspended in almost 15mL RPMI, containing appropriate doses of HEL or HEL46-61, and incubated at 37°C for 2hr. The cells were washed twice in RPMI to eliminate unbound antigen. Two-fold serial dilutions of pulsed antigen presenting cells were co-cultured in triplicate wells with $3x10^5$ spleen and lymph node leukocytes from the 3A9 T cell receptor transgenic mice on the B10.BR background, as source of transgenic CD4 T cells (Ho et al, 1994). Each well contained a total volume of 200µL

RPMI, consisting of spleen and lymph node cells prelabelled with CFSE as previously described (2.11). Negative control wells contained the highest number of unpulsed antigen presenting cells. The plates were incubated at 37°C from 14hr to 5 days. Prior to plating, the presence of the 3A9 T cell receptor transgene was reconfirmed by flow cytometry using the anti-clonotypic monoclonal antibody, Vβ8.2.

After 15 hr of incubation, CD4 T cell activation was analyzed by flow cytometry using the early activation marker, CD69. Proliferation of CD4 T cells on days 3 and 5 was also analyzed by flow cytometry using CFSE dilution. Following cell staining, cells were resuspended in FACS or FACS fix buffer containing $4x10^3$ absolute counting beads per 100μL buffer. The presence of known concentration of counting beads in each sample enabled the absolute quantitation of responding CD4 T cells.

2.15 In Vitro Proliferation and Apoptosis Assay

A flow cytometry-based proliferation and apoptosis assay was designed to gain insight into the nature of the response of myeloid precursors, following growth factor stimulation, early in culture. Bone marrow cells were harvested from B10.BR and NOD.H-2^k mice and processed as previously described. Prior to culturing in the presence of growth factors, lymphocyte-depleted bone marrow cells were labelled with CFSE. The levels of proliferation and apoptosis on Days 1, 2 and 3 of culture were analyzed by flow cytometry. Apoptotic cells were detected by staining with merocyanin 540 (MC540; Sigma Chemical Co.), a lipophilic dye, which intercalates loosely-packed lipids (McEvoy et al, 1988; Mower, Jnr. et al, 1994; Frey, 1997) exposed on the membrane of apoptotic cells. Staining of cells with the appropriate concentration of MC540 was like the usual antibody staining of cells except cells were incubated at 4°C in the dark for a duration of 4 minutes. As with staining using other reagents, MC540 stained cells were washed twice, resuspended in 100μL FACS buffer and taken for acquisition on the flow cytometer. Again, addition of beads in the FACS buffer allowed quantitation of cell populations of interest.

2.16 Enrichment for Splenic and Thymic Dendritic Cells

The protocol to enrich for splenic and thymic dendritic cells was adapted from Vremec and Shortman (1997). One spleen or thymus from relevant mice was cut into small fragments and suspended in 10mL RPMI containing 1mg/mL Collagenase A

(Boehringer Mannheim GmBH, Mannheim, Germany) and 0.02mg/mL DNase (Boehringer Mannheim). The mixture was digested with intermittent agitation for 25 minutes at 22°C. Dendritic cell-T cell complexes were disrupted by the addition of 200µL of 0.5M EDTA (pH 7.2) and the digest agitated for a further 5 minutes. The digest was passed through a cell strainer to remove undigested stromal material. Cells were recovered from the digest by centrifugation at 200*g* for 5 minutes at room temperature. Cells were resuspended in 5mL RPMI. The cell suspension was layered onto 14.5% (w/v) metrizamide (Nycomed Pharma, Oslo, Norway) gradient (See Appendix A2.3f), contained in a 15mL Falcon conical polypropylene tube, and centrifuged at 800*g* for 10 minutes at room temperature. Low density interface cells were harvested and washed twice. The dendritic cell-enriched low density cells were stained with appropriate antibodies and analyzed by flow cytometry.

2.17 Bone Marrow Reconstitution Assays

2.17.1 Irradiation of Recipients

Three 8-12 week old B10.BR or NOD.H-2^k male or female mice were placed in a sterile cylindrical canister 10cm diameter x 20cm long containing tissue paper for nestling into and absorbing urine. These canisters are made of opaque PVC and have two screw-capped ends. The ends are mesh-filtered and provide good ventilation and protect contained mice from external infection. The canisters were secured horizontally inside a Taconic shipping box and taken by car to the CSIRO Division of Entomology Cesium source irradiator. Each canister was placed in the irradiator and a programmable timer was used to deliver precisely 5 Gray. The mice were held in the canisters for 3 hr in a quiet and cool place before a second dose of 5 Gray was delivered. The mice were then returned to microisolator cages in the Medical Genome Centre.

2.17.2 Reconstitution

Total bone marrow cells from donor female B10.BR and NOD.H-2^k mice (8-12 weeks of age) were aseptically harvested as described before (2.6.1). Bone marrow cells were washed twice and resuspended at $1x10^7$ leukocytes per mL RPMI. 200µL of this inoculum ($2x10^6$ leukocytes) was injected via the lateral tail vein into each irradiated mouse immobilized in standard conical restraint. Control groups of recipient mice received either B10.BR or NOD.H-2^k bone marrow cells alone while the test group of mice received an inoculum comprising a 1:1 mixture of B10.BR and NOD.H-2^k bone marrow cells. Reconstituted mice were given drinking containing Polymyxin B ($8.5x10^5$

U/mL; Sigma Chemicals Co.) and Neomycin (1.1 mg/mL; Sigma Chemicals Co) ad libitum for the duration of reconstitution.

2.17.3 Assessment of Reconstitution

Recipient mice were screened for the level of chimerism 5 weeks post-reconstitution. This was done by flow cytometric analysis of peripheral blood leukocytes. Mice were micro-bled through the lateral tail vein as described previously (2.9.1). Distinguishing B10.BR-derived cells from NOD.H-2^k -derived cells in recipient mice was made possible by the allelic variants of CD45 (Ly5) expressed between the strains (McClive et al, 1994). NOD.H-2^k-derived cells express $Ly5^a$ while B10.BR-derived cells express $Ly5^b$. Antibodies against B cells, T cells and monocytes, in combination with anti-$Ly5^a$ monoclonal antibody were used to assess the level of reconstitution in blood of recipient mice. Further analysis of recipient mice was performed 10-12 weeks post-reconstitution by flow cytometric determination of the origin of splenic and thymic dendritic cells. Enrichment for splenic and thymic dendritic cells was achieved as previously described (2.16).

Chapter 3

Generation and Characterization of Bone Marrow-Derived Dendritic Cells

3.1 Introduction

Paucity of dendritic cells in tissue and tedious protocols for their isolation have until recently limited the comprehensive cellular, biochemical and molecular analyses of dendritic cells. However, the discovery that specific growth factor stimulation of hematopoietic precursors in liquid culture systems resulted in the generation of sizeable numbers of dendritic cells has facilitated these analyses (Witmer-Pack et al, 1987; Heufler et al, 1988; Scheicher et al, 1992; Inaba et al, 1992a and b; Caux et al, 1992; Sallusto and Lanzavecchia, 1994). The first liquid culture system developed to generate substantial numbers of dendritic cells involved the use of precursors from mouse blood in cultures supplemented with GM-CSF (Inaba et al, 1992b). Typical dendritic cells were released from loosely-attached, proliferating cell aggregates during the course of culture. Dendritic cells from such cultures were readily identified on the basis of their distinct shape, ultrastructure and repertoire of cell surface markers. Dendritic cells generated in liquid cultures, in response to GM-CSF stimulation, expressed high levels of cell surface MHC class II molecules and were potent stimulants of mixed leukocyte reactions. Dendritic cells thus generated enabled analyses of their distinct morphology, phenotype and function. This liquid culture system was extended to the culture of MHC class II negative precursors from the bone marrow (Inaba et al, 1992a). As with precursors from blood, myeloid precursors were stimulated with GM-CSF. GM-CSF stimulation of myeloid precursors resulted in three distinct types of myeloid cells: granulocytes, macrophages and dendritic cells. Enrichment of dendritic cells in culture was carried out by removing non-adherent granulocytes during feeding of cultures, while macrophages remained firmly adherent.

A similar culture system was subsequently established for precursors isolated from human blood (Sallusto and Lanzavecchia, 1994). Besides GM-CSF, the culture was supplemented with IL-4. The presence of IL-4 in culture is thought to enhance viability of precursors during culture and also favors the development of precursors towards dendritic cells over that of macrophages (Strunk et al, 1996). In contrast to the murine culture system of generating dendritic cells, cultured human dendritic cells could be induced to mature by addition into culture of TNFα (Sallusto and Lanzavecchia, 1994).

The establishment of liquid cultures of hematopoietic precursors, supplemented with GM-CSF and IL-4, provides an efficient source of dendritic cells and facilitates investigation of these critical antigen presenting cells.

3.2 Objective:

The initial objective of this project was to establish an in vitro bone marrow culture system to generate dendritic cells, to be used for morphological, immunophenotypic and functional analyses. As reported in the literature, bone marrow cultures were supplemented with GM-CSF and IL-4. The availability of recombinant baculovirus encoding murine GM-CSF and murine IL-4 within the JCSMR ensured sufficient supplies of critical growth factors required during the course of this study. A further objective for this part of the study was to use the in vitro generated dendritic cells to develop a flow cytometric-based functional assay. Specifically, it was aimed that the assay would allow the frequency of responding T cells to be visualized and quantitated when antigen is presented by dendritic cells .

3.3 Morphological Analysis of In Vitro Generated Dendritic Cells

Bone marrow cells from the hind limbs of Balb/c mice were aseptically harvested and depleted of lymphocytes by complement-mediated lysis as previously described (Inaba et al, 1992a). The monoclonal antibodies used to delplete B and T lymphocytes included: RA3.3A9 (anti-B220), GK1.5 (anti-CD4) and 31M (anti-CD8). Further information regarding isotype and source of the monoclonal antibodies used and detailed protocols for lymphocyte depletion are described in sections 2.5 and 2.6.2 of the Methods Chapter, respectively. Viable mononuclear cells were enriched on a Ficoll gradient, washed in RPMI twice by centrifugation, and the pellet resuspended in RPMI supplemented with 800U/mL GM-CSF and 200U/mL IL-4. Cells were plated at a density of $1x10^6$ cells per mL growth factor supplemented medium per well in 24 well Linbro tissue culture plates. Details of how the growth factors were derived and quantitated are described in section 2.6.4. Cultures were fed on days 2 and 4 by gently swirling plates and removing half the medium in each well and adding fresh growth factor-supplemented medium. Feeding served the additional purpose of removing non-adherent granulocytes that are also generated during culture.

Observation by inverted light microscopy during the course of culture revealed the presence of numerous clusters of proliferating cells attached to a monolayer of adherent cells as of day 3 of culture (Figure 3.1a). The size and number of these clusters expanded between days 3 and 5 of culture. The loosely-adherent clusters were dislodged by gentle pipetting and replated onto fresh plates, in the presence of medium supplemented with

Figure 3.1

Phase contrast micrographs depicting the development of dendritic cells in liquid cultures of lymphocyte-depleted murine bone marrow cells supplemented with GM-CSF and IL-4.

(a) High-power view of proliferating cell clusters attached to a monolayer of adherent cells on day 3 of culture (250x magnification). Cells with dendrites can be seen at the periphery of clusters.

(b) High-power view (250x magnification) of individual cells with dendrites as seen on day 8 of culture when clusters were harvested and subcultured onto fresh plates.

Figure 3.1

(a)

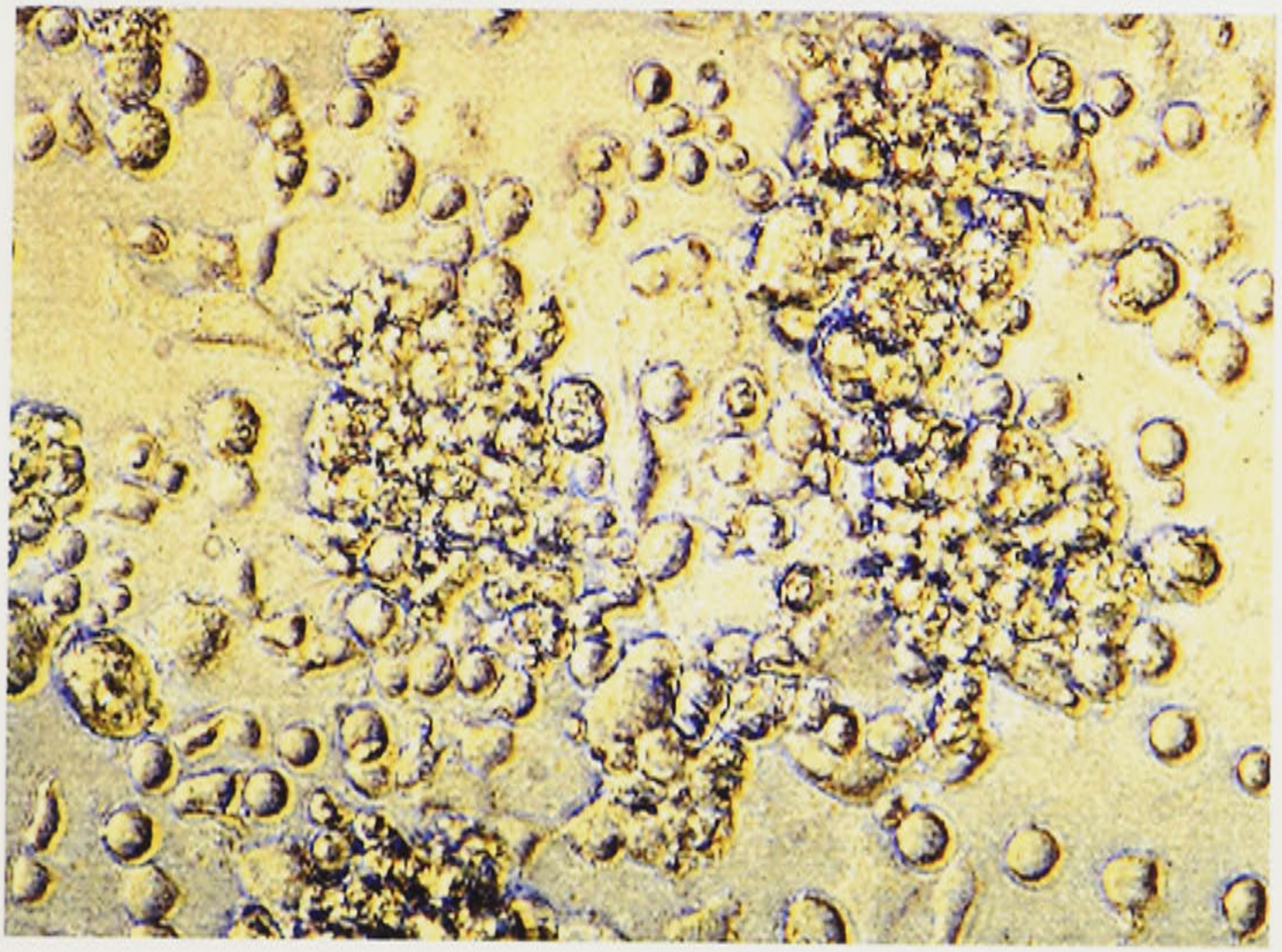

(b)

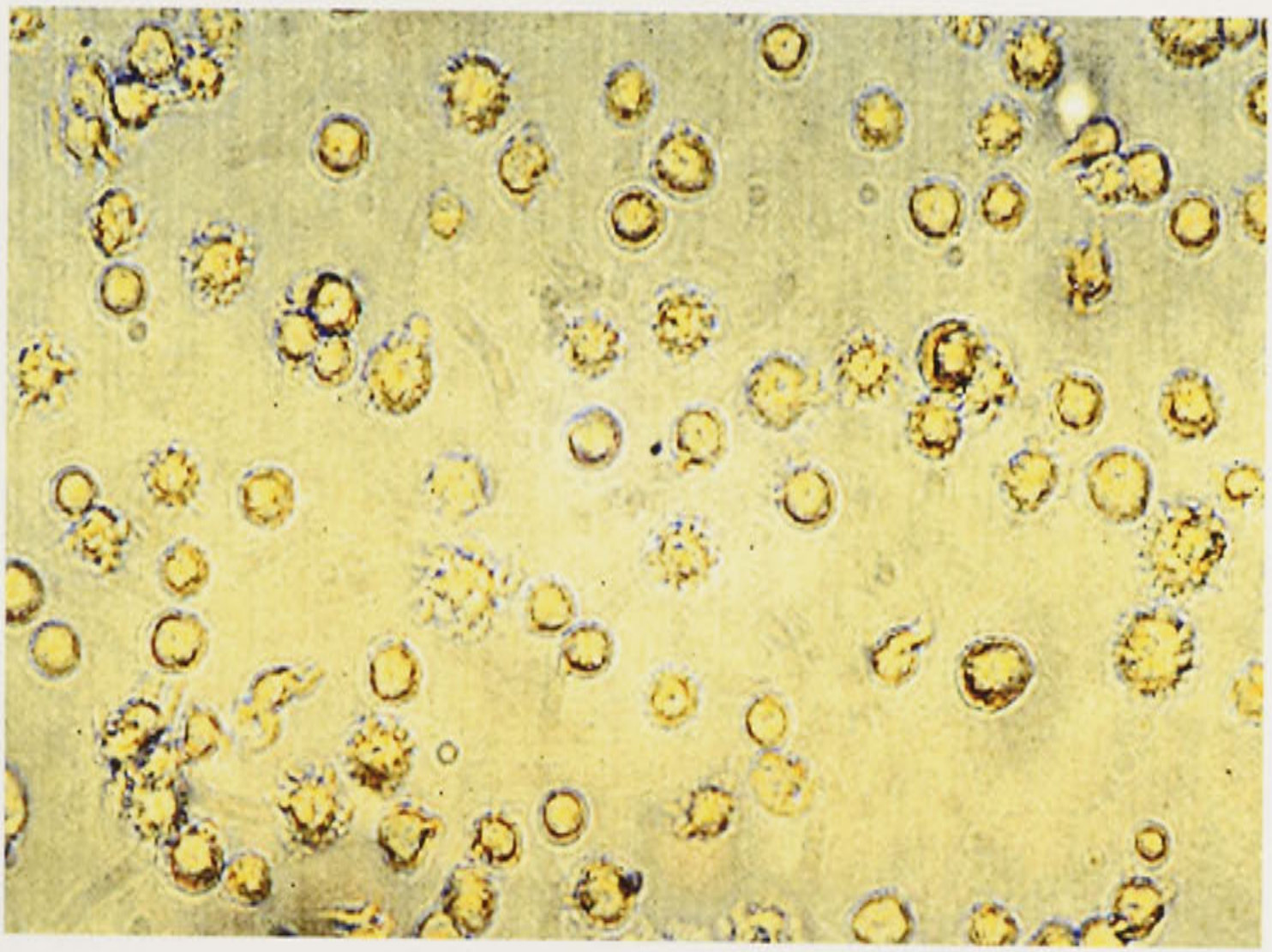

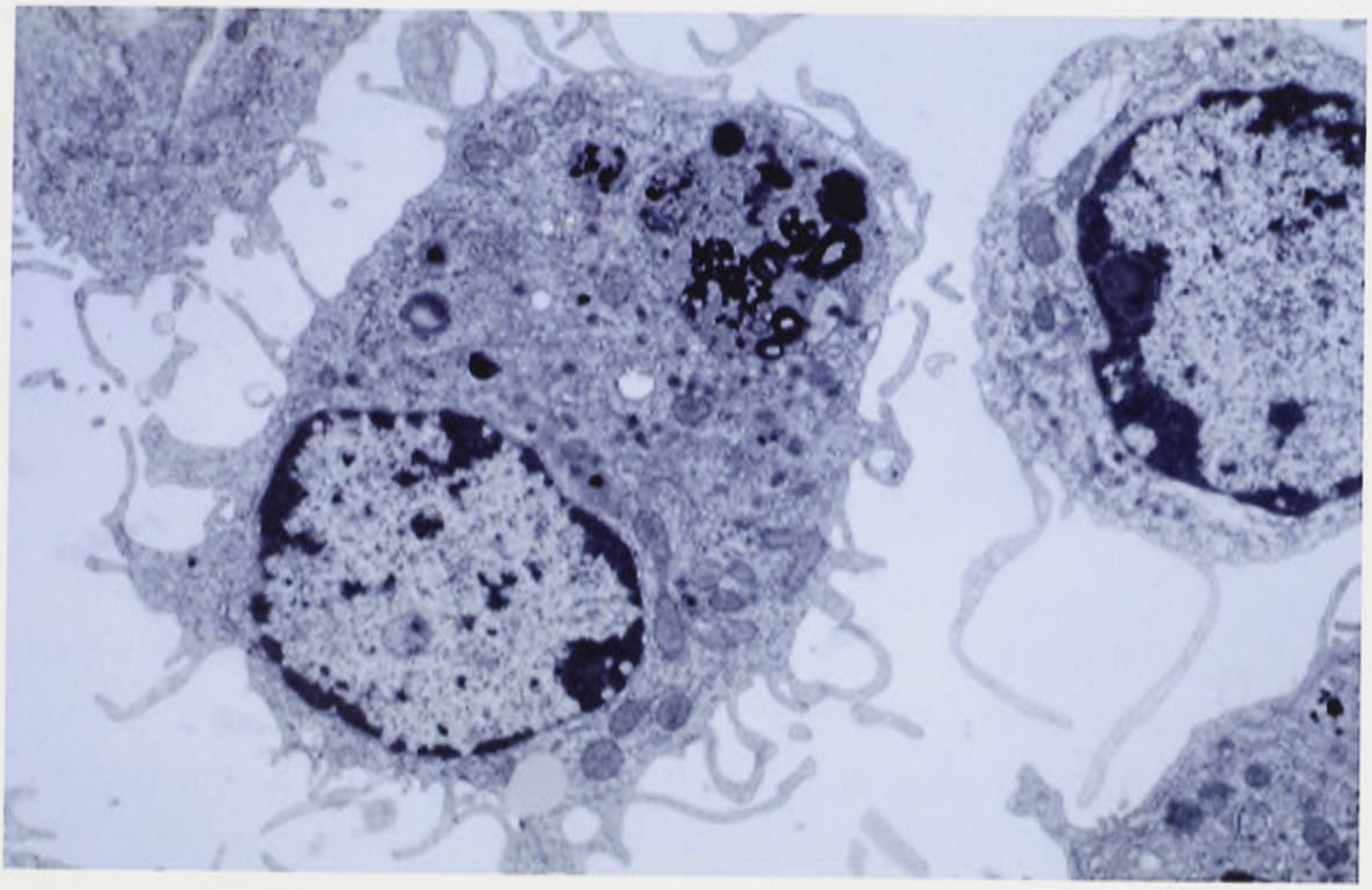

Figure 3.2

Transmission electron micrograph of dendritic cells on day 8 of culture

Numerous cytoplasmic processes or dendrites are seen. The absence of numerous electron dense granules in the cytoplasm suggests the absence of lysosomal or phagocytic structures.

Scale bar represents 5μm. 7500x magnification.

reduced concentrations of growth factors. Cultured cells were subcultured in this manner on days 5 and 7. This process of subculturing enriched for dendritic cells by eliminating adherent macrophages. Optimal yields of dendritic cells were obtained on day 8, as individual cells with typical dendritic cell morphology were released from the clusters (Fig.3.1b). Numerous large cells with cytoplasmic processes, or dendrites, were observed floating in culture on day 8. Ultrastructural analysis by Transmission Electron Microscopy (see section 2.7 for details) of day 8 dendritic cells clearly revealed the presence of dendrites and a large irregularly-shaped nucleus (Figure 3.2). The cells were generally 10-20 μm in diameter, excluding dendrites. The cytoplasm contained many mitochondria but few electron dense granules representing lysosomal compartments involved in antigen processing.

3.4 Immunophenotypic Analysis of Day 8 Dendritic Cells

Cells on day 8 of culture were harvested and analyzed for the cell surface expression of a panel of standard dendritic cell markers by single-colour flow cytometry. Cells were stained (as described in section 2.8) with fluorescent-tagged or unconjugated primary monoclonal antibodies (section 2.5) specific for CD11c (N418), MHC class I (34-1-2S) and class II (10.3.6) molecules, B7-1 and ICAM-1 (3E2). Appropriate fluorescent secondary reagents (section 2.5.1) were used where required. Unlabelled cells or cells incubated with appropriate secondary reagents were used as controls for directly conjugated or unconjugated antibodies, respectively. The N418 monoclonal antibody is used as a specific marker for murine dendritic cells (Metlay et al, 1990). In a typical culture, >80% of cells on day 8 displayed classic dendritic cell morphology. Flow cytometric analysis of these cells for standard dendritic cell surface markers confirmed the morphological observations described earlier. As shown in Figure 3.3, most of the cells on day 8 of culture stained positive for N418. Correspondingly, these cells expressed high levels of MHC class I and class II molecules. Furthermore, most of these cells were found to express the costimulatory molecule, B7.1, and the adhesion molecule, ICAM-1. Inspite of the lack of isotype specific controls for staining antibodies, the above cell surface marker expression pattern mirrors that previously reported for both murine and human dendritic cells (Inaba et al, 1992a; Sallusto and Lanzavecchia, 1994).

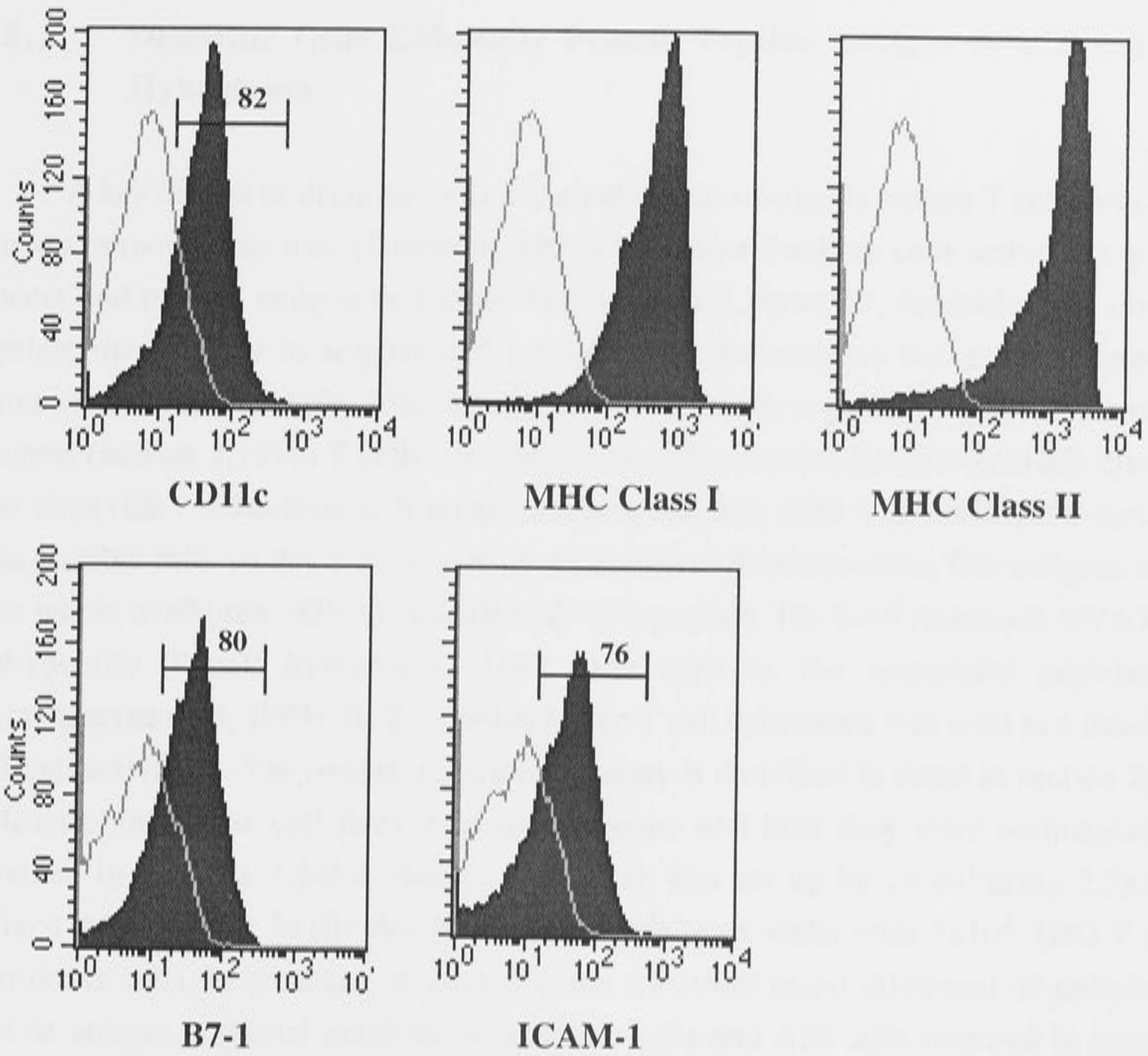

Figure 3.3

Cell surface phenotype of dendritic cells on day 8 of culture.

Cells harvested on day 8 of a typical culture were stained for a selected panel of monoclonal antibodies specific for markers on mature dendritic cells and analyzed by single-colour flow cytometry. Shaded histograms represent the relative fluorescence of the marker shown. Unshaded histograms represent either unstained controls or appropriate secondary antibody control. Dead cells were eliminated from analysis by propidium iodide exclusion. Bars over histograms indicate percentage of viable cells positive for the particular marker shown.

* It appears that dendritic cells are 5-fold more efficient in presenting OVA323-339 to T cell hybridoma cells than unfixed A20 cells since 5 times as many A20 cells were required to induce comparable levels of IL-2 secretion (Figure 3.4a). However, this conclusion needs to be validated by titrating the dose of antigen presenting cells with a fixed dose of peptide.

3.5 Functional Analyses of Dendritic Cells

3.5.1 Dendritic Cells Efficiently Present Peptide Antigen to a T cell Hybridoma

A key feature of dendritic cells is their ability to efficiently initiate T cell-mediated primary immune responses (Steinman, 1991). Immature dendritic cells actively acquire, process and present antigen to T cells. On maturation, however, dendritic cells down-regulate their ability to acquire and process complex antigens but acquire a potent immunostimulatory capacity. The capacity of dendritic cells to present peptide and protein antigens (section 2.12) to T cells was compared with a murine (Balb/c-derived) Epstein Barr virus (EBV)-transformed B lymphoblastoid cell line, A20. Cultured Balb/c-derived bone marrow cells on day 8 were used as the source of dendritic cells. The antigens used were whole ovalbumin (OVA) and OVA323-339 peptide. The I-A^d restricted, OVA323-339-specific T cell hybridoma, 3DO, was used as the responder population (Shimonkevitz et al, 1983). IL-2 secretion by the T cell hybridoma was used as a measure of T cell activation. The antigen presentation assay is described in detail in section 2.13. A description of the cell lines used in this assay and how they were maintained is provided in sections 2.3-2.4. Briefly, the assay was set up by co-culturing $2.5x10^4$ unfixed A20 cells or $5x10^3$ dendritic cells in triplicate wells with $3x10^4$ 3DO T cell hybridoma cells, in presence of graded doses (two-fold serial dilutions) of protein or peptide antigen. Optimal numbers of dendritic cells and A20 cells required to present OVA and OVA323-339 were determined elsewhere (Prasad S., Honours Thesis, 1995).

Both dendritic cells and A20 cells stimulated the 3DO T cell hybridoma cells in an antigen dose-dependent manner. It is evident from Figure 3.4a that dendritic cells are 5-fold more efficient in presenting OVA323-339 to T cell hybridoma cells than unfixed A20 cells since 5 times as many A20 cells were required to induce comparable levels of IL-2 secretion*. In contrast, dendritic cells appeared relatively less efficient in presenting whole ovalbumin (Fig.3.4b). Whereas A20 cells presented both OVA and OVA323-339 equally well, the capacity of dendritic cells to present OVA was markedly reduced in response to the entire range of OVA concentrations where T cell response was detectable. This is consistent with the conclusion that mature dendritic cells are inefficient at acquiring native proteins and processing them into peptides (Sallusto and Lanzavecchia, 1994).

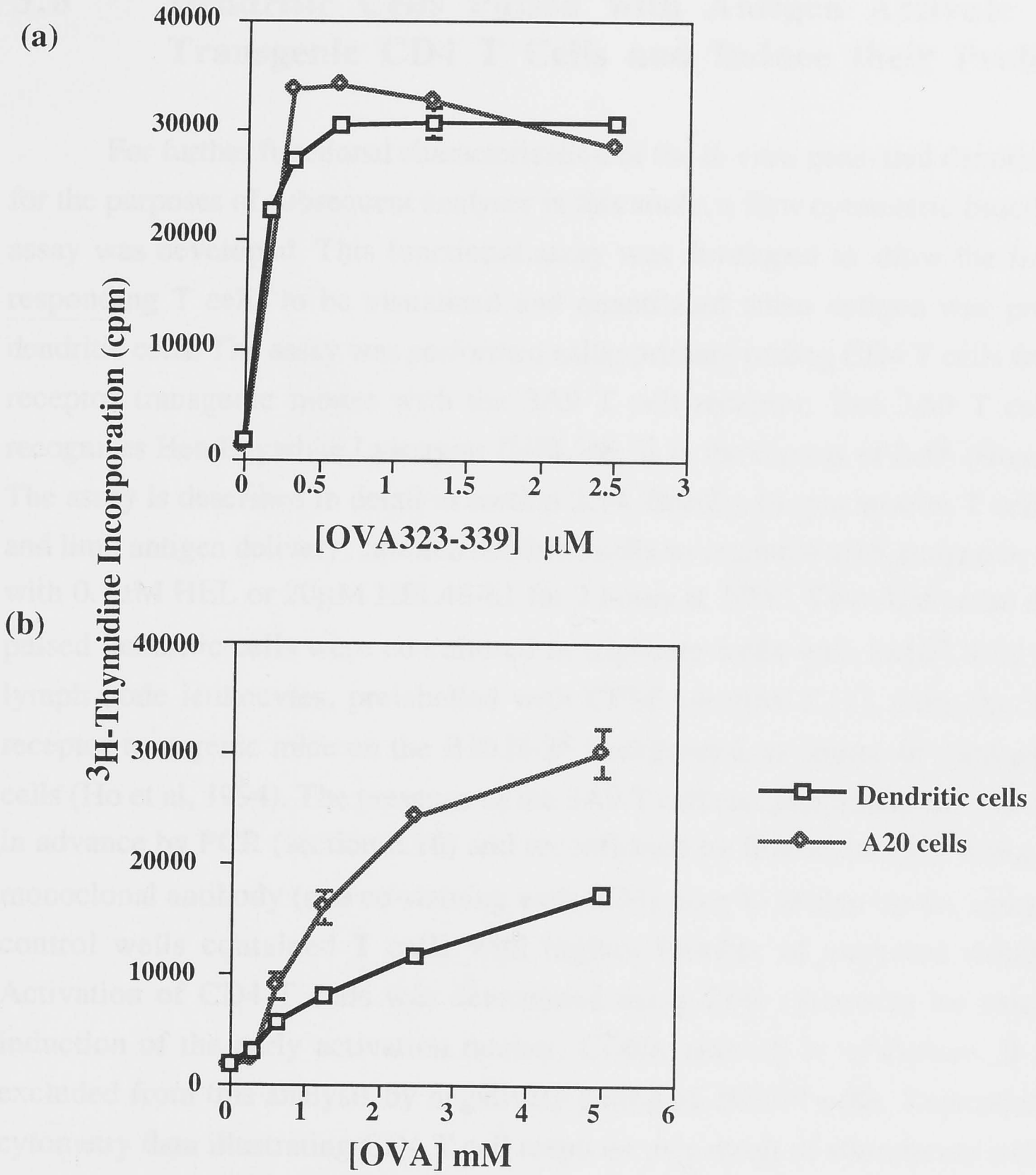

Figure 3.4

Cultured dendritic cells efficiently present peptide antigen to a T cell hybridoma.

Five thousand Balb/c -derived dendritic cells or $2.5x10^4$ unfixed A20 cells were co-cultured in triplicate wells with $3x10^4$ I-A^d-restricted, OVA323-339-specific 3DO T cell hybridoma cells, in the presence of shown concentrations of OVA323-339 (a) or OVA (b). IL-2 secretion by activated T cells was measured in culture supernatants by the proliferation of the IL-2-dependent cell line, HT-2 (y-axis of both plots). Data is presented as mean of triplicate wells +- SE.

3.6 Dendritic Cells Pulsed with Antigen Activate Primary Transgenic CD4 T Cells and Induce their Proliferation

For further functional characterization of the in vitro generated dendritic cells and for the purposes of subsequent analyses in this study, a flow cytometric-based functional assay was developed. This functional assay was developed to allow the frequency of responding T cells to be visualized and quantitated when antigen was presented by dendritic cells. The assay was performed using primary resting CD4 T cells from a T cell receptor transgenic mouse with the 3A9 T cell receptor. The 3A9 T cell receptor recognizes Hen Eggwhite Lysozyme (HEL)46-61 in the context of I-A^k (Ho et al, 1994). The assay is described in detail in section 2.14. Briefly, to synchronize T cell activation and limit antigen delivery, cultured dendritic cells were pulsed with antigen by incubating with 0.1μM HEL or 20μM HEL46-61 for 2 hours at 37°C. Two-fold serial dilutions of pulsed dendritic cells were co-cultured in triplicate wells with $3x10^5$ total spleen and lymph node leukocytes, prelabelled with CFSE (section 2.11), from the 3A9 T cell receptor transgenic mice on the B10.H-2^k background, as source of transgenic CD4 T cells (Ho et al, 1994). The presence of the 3A9 T cell receptor transgene was determined in advance by PCR (section 2.10) and reconfirmed by flow cytometry using the Vβ8.2 monoclonal antibody (and co-staining with CD4) prior to setting up the assay. Negative control wells contained T cells with highest number of unpulsed dendritic cells. Activation of CD4 T cells was determined using flow cytometry by measuring the induction of the early activation marker, CD69, after 15 hr of culture. B cells were excluded from this analysis by negatively gating on $B220^+$ cells. Representative flow cytometry data illustrating CD4 T cell response as a result of stimulation with dendritic cells pulsed with 20μM HEL46-61 is depicted in Figure 3.5a. In the absence of antigen, no induction of CD69 was observed on CD4 T cells (Fig.3.5a, left panel). In contrast, dendritic cells pulsed with 20μM HEL46-61 induced the expression of CD69 on >80% of CD4 T cells (Fig. 3.5a, right panel). Graphical representation of the results obtained during this functional assay is shown in Fig.3.5b. A clear titration curve of CD69 induction is seen in response to graded doses of dendritic cells pulsed with HEL46-61, with $>1x10^3$ dendritic cells per well inducing maximal CD69 expression. Dendritic cells pulsed with HEL, however, exhibited a reduced capacity to induce CD69 on CD4 T cells. Just over 25% of T cells express CD69 in response to the highest dose of dendritic cells pulsed with HEL. This reduced capacity of dendritic cells to present whole protein antigens mirrors the pattern already observed in the previous assay in which dendritic cells inefficiently presented OVA to 3DO T cell hybridoma cells. This reduced capacity of dendritic cells to present native HEL protein may be attributable to either their inability to process complex protein antigens or to the suboptimal (non-saturating) concentration of HEL used in the assay.

* **Fig. 3.5**

Note: A role for B cells, present in culture, in antigen presentation would require HEL46-61 loaded onto dendritic cells to be shed or transferred to the B cells. Dendritic cells pulsed with HEL46-61 and cocultured with transgenic B cells specific for HEL were unable to induce CD69 expression on the B cells (Townsend and Goodnow, 1998).

HEL used in this assay was purchased from Sigma and prepared by 3x crystallization, followed by dialysis and lyophilization (~95% purity). High concentration stock solutions were prepared, aliquoted and stored at -20^{o}C. Stock solutions were thawed for single use only.

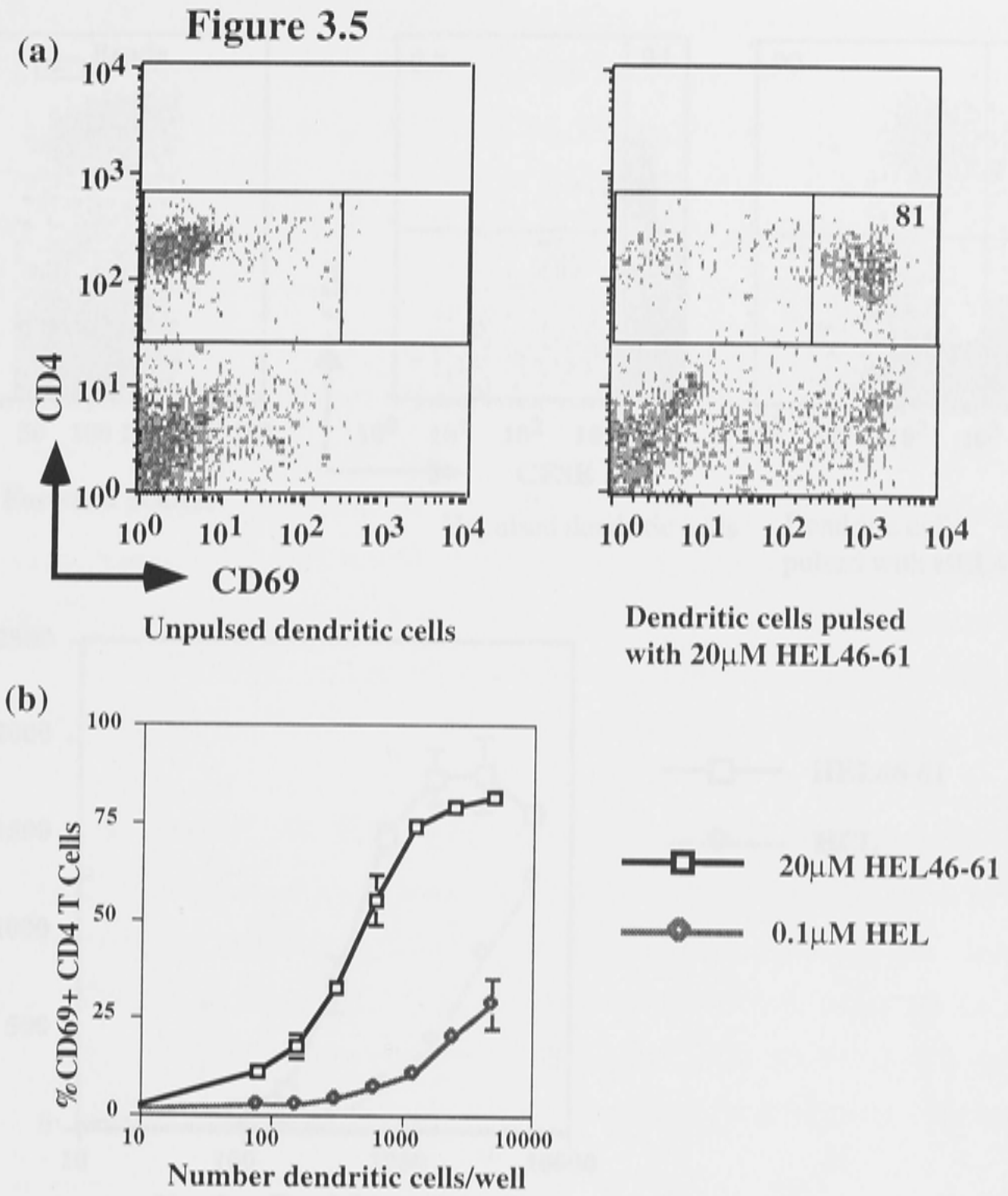

Figure 3.5
Cultured dendritic cells induce CD69 expression on a primary transgenic CD4 T cell.
Day 8 dendritic cells were initially pulsed with 20mM HEL46-61 or 0.1mM HEL by incubating dendritic cells with relevant antigen for 2 hr at 37°C. Pulsed dendritic cells were washed, serially diluted and cocultured in triplicate wells of 96 microwell plates in the presence of $3x10^5$ total spleen and lymph node leukocytes from mice carrying the 3A9 T cell receptor transgene on the B10.H-2^k background. Spleen and lymph node leukocytes were pre-labelled with CFSE. T cell activation was measured by flow cytometry using the early activation marker, CD69, after 15 hr of incubation. Specific activation of CD4 T cells was determined by co-staining cells with anti-CD4 monoclonal antibody (GK1.5). The level of CD4 T cell proliferation was similarly determined by measuring CFSE dilution after 72 hr of culture.
(a) Representative FACS data illustrating CD4 T cell activation in response to stimulation with unpulsed dendritic cells (left panel) or dendritic cells pulsed with 20mM HEL46-61 (right panel). B cells were excluded from this analysis by negatively gating on B220+ cells.
(b) Dose response of CD4 T cell activation in response to stimulation with HEL46-61 or HEL pulsed dendritic cells.

*

#

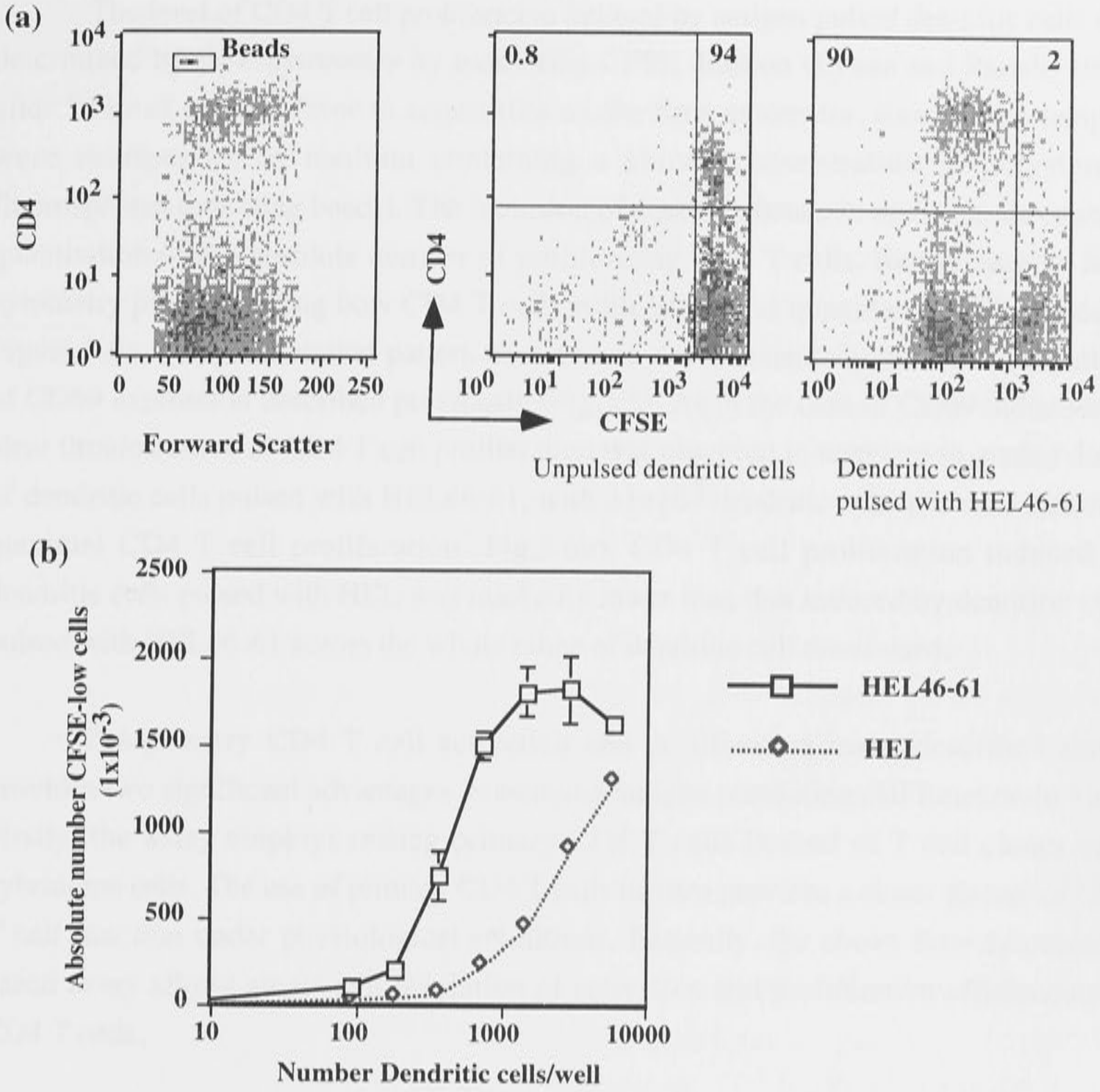

Figure 3.6

Cultured dendritic cells induce proliferation of a primary transgenic CD4 T cell.

(a) Representative FACS plots illustrating CD4 T cell proliferation in response to stimulation with unpulsed dendritic cells or dendritic cells pulsed with 20μM HEL46-61. The inclusion of counting beads enabled absolute quantitation of responding CD4 T cells (rectangular region in top panel). Numbers in quadrants represent percent CD4 T cells in that quadrant.

(b) Dose response of CD4 T cell proliferation in response to stimulation with HEL46-61 or HEL pulsed dendritic cells. Dose response data is presented as mean of triplicate wells +- SE. Note: CD69 induction and CFSE dilution are also observed in CD4 negative cells. These are mainly CD4 and CD8 double negative T cells, arising from transgene induced anomaly in thymic selection, that are exported to the periphery.

The level of CD4 T cell proliferation induced by antigen-pulsed dendritic cells was determined by flow cytometry by measuring CFSE dilution (Lyons and Parish, 1994) after 72 hr of culture. Prior to acquisition on the flow cytometer, stained cell samples were resuspended in medium containing a known concentration of polystyrene fluorospheres (counting beads). The inclusion of counting beads in each sample enabled quantitation of the absolute number of proliferating CD4 T cells. Representative flow cytometry plots depicting how CD4 T cell proliferation was quantitated is illustrated in Figure 3.6a. The proliferation pattern observed on day 3 essentially mirrored the pattern of CD69 expression described previously (Fig.3.5). As in the case of CD69 induction, a clear titration curve of CD4 T cell proliferation was observed in response to graded doses of dendritic cells pulsed with HEL46-61, with $\geq 1 \times 10^3$ dendritic cells per well inducing maximal CD4 T cell proliferation (Fig.3.6b). CD4 T cell proliferation induced by dendritic cells pulsed with HEL was markedly lower than that induced by dendritic cells pulsed with HEL46-61 across the whole range of dendritic cell doses used.

The primary CD4 T cell activation and proliferation assay described above provides two significant advantages in assaying antigen presenting cell function in vitro. Firstly, the assay employs resting primary CD4 T cells instead of T cell clones or T hybridoma cells. The use of primary CD4 T cells in vitro provides a closer picture of CD4 T cell function under physiological conditions. Secondly, the above flow cytometric-based assay allows single cell resolution of activation and proliferative efficiencies of CD4 T cells.

3.7 Discussion

The liquid culture system of generating dendritic cells, pioneered by Inaba et al (1992a), was adapted and successfully established and utilized during the course of this study. The availability of such culture systems has facilitated extensive characterization of dendritic cells by bypassing the use of tedious purification protocols required to isolate this trace cell type residing in most tissue. The discovery that GM-CSF stimulation of hematopoietic precursors in vitro resulted in the generation of dendritic cells has been a major advance in the study of dendritic cell biology. In vitro generated dendritic cells have enabled extensive cellular, biochemical and molecular characterization of this unique cell type.

The liquid culture system employed lymphocyte-depleted bone marrow cells as precursors of dendritic cells. Myeloid precursors stimulated with GM-CSF and IL-4 followed a course of development as described previously (Inaba et al, 1992a, Sallusto

and Lanzavecchia, 1994). This culture system consistently generated approximately 1.5-2x10^6 dendritic cells per 2 donor mice, with >80% purity, after 8 days of culture. This yield of dendritic cells is low compared to that reported by Inaba et al (1992a) who generated 5x10^6 dendritic cells per mouse at 60% purity. Most recently, an advanced method for generating large quantities of highly pure dendritic cells from mouse bone marrow cells has been described (Lutz et al, 1999). The advanced method incorporates a number of modifications in the protocol established by Inaba et al (1992a). These modifications include: (i) avoidance of antibody-mediated depletion of lineage positive cells in the bone marrow to circumvent precursor loss, (ii) reduction in the density of cells plated, (iii) lengthening the culture period to 10-12 days, and (iv) reduction of the GM-CSF dose from day 8 or 10 onwards to minimize granulocyte contamination.

Microscopic analysis showed that individual dendritic cells were released from loosely-adherent, proliferating clusters. Ultrastructural analysis of these cells suggested the presence of primarily mature dendritic cells. This was indicated by the absence of numerous cytoplasmic electron dense granules representing lysosomal compartments involved in the generation of peptide epitopes by processing of complex protein antigens. Analysis of a panel of cell surface markers characteristic of dendritic cells substantiated this observation as almost all of day 8 cells uniformly expressed high levels of MHC class I and class II molecules. Furthermore, most of these cells expressed the costimulatory molecule, B7.1, and the adhesion molecule, ICAM-1. Thus, as known for mature dendritic cells in vivo, cultured dendritic cells were appropriately-equipped to efficiently activate T cells (Banchereau and Steinman, 1998). The expression of high levels of MHC molecules allows presentation of more T cell determinants, while adhesion molecules serve to cluster T cells. Costimulatory molecules expressed on dendritic cells may reduce the threshold for T cell activation or qualitatively regulate the nature of a T cell response.

Functional analysis of day 8 dendritic cells provided further evidence supporting the presence of mainly mature dendritic cells. These cells efficiently presented peptide antigens to T cells but were found to be relatively inefficient in presenting whole protein antigens. Two antigen presentation assays with distinct antigens and responder T cells were employed in this study. Firstly, dendritic cells were less efficient in inducing IL-2 secretion by the 3DO T cell hybridoma in response to OVA, compared with control A20 cell lines. However, dendritic cells presented the already processed OVA323-339 more efficiently than A20 cells. Secondly, dendritic cells pulsed with HEL appeared less efficient in inducing CD69 expression on primary, transgenic CD4 T cells. In contrast, equivalent numbers of dendritic cells pulsed with HEL46-61 were able to induce maximal CD69 expression. The apparent inability of dendritic cells to present HEL could be due to

the suboptimal (non-saturating) concentration of HEL used and not solely due to the down-regulated antigen processing capacity of mature dendritic cells. Coincident with their ability to induce maximal CD69 expression, dendritic cells pulsed with HEL46-61 efficiently induced proliferation of antigen specific primary CD4 T cells. Taken together, these results indicated that dendritic cells generated in the liquid culture system utilized in this study, produced mainly mature dendritic cells. This state of maturation was reflected in morphological, phenotypic and functional analyses. The failure to efficiently process and present protein antigens suggested that these dendritic cells had down-regulated their antigen processing capacity. Unlike in the human dendritic cell culture system, the trigger for maturation in the murine dendritic cell culture system remains to be identified. It is possible that factors derived from foetal calf serum or baculovirus-derived growth factors may be responsible for dendritic cell maturation in this culture system. Furthermore, the physical stress involved in subculturing cells is also thought to contribute towards dendritic cell maturation.

Biochemical events underlying the process of dendritic cell maturation have recently been studied in both cultured human and murine dendritic cells (Cella et al, 1997; Pierre et al, 1997). Key findings in both systems include the demonstration that immature dendritic cells are active in the biosynthesis of MHC class II molecules and peptide loading. Newly synthesized MHC class II molecules are mainly targeted to lysosomal compartments and MHC class II-peptide complexes are only transiently expressed on the cell surface as they are rapidly removed and degraded. The process of maturation entails a 10-fold increase in cell surface half life of MHC class II molecules, with newly synthesized MHC class II molecules mainly targeted to the cell membrane. The increased half life of cell surface MHC class II molecules is critical as it allows sufficient time for the antigenic cargo of dendritic cells to be scanned by T cells.

As previously mentioned, factors inducing maturation in cultured human dendritic cells are known and include TNFα and CD40 ligand (Sallusto and Lanzavecchia, 1994). Remarkably, stimulation of human dendritic cells for 24 hour with TNFα or CD40L results in two- to three-fold increase in cell surface MHC class II, ICAM-1, LFA-3, CD40 and B7. The functional consequences of these changes entailed enhanced T cell stimulatory capacity and a reduced ability to present protein antigen. These observations suggest that under physiological conditions dendritic cell maturation may be induced by inflammatory stimuli or interaction with T cells. Consistent with this, it has also been shown that systemic administration of LPS into mice induces the maturation and redistribution of marginal zone dendritic cells in the spleen to the T cell zone (De Smedt et al, 1996).

* However, GM-CSF transduced tumor cells have been shown to elevate dendritic cell numbers in vivo (Hanada et al, 1996).

Although substantial numbers of dendritic cells can be generated in in vitro cultures by stimulating myeloid precursors in the presence of GM-CSF, it is unlikely that a similar sequence of developmental events occur in the bone marrow or blood, both of which have been the source of precursors for culture (Inaba et al, 1992a and b). Mature dendritic cells are detectable neither in bone marrow nor in blood. Inaba et al (1992a) suggest that immature dendritic cell progeny are exported from the bone marrow into the circulation from where the progeny are able to populate tissue. In contrast to the in vitro capacity of GM-CSF to generate dendritic cells, GM-CSF or GM-CSF and IL-4 treatment of mice did not result in significant increase in dendritic cell numbers in vivo (Maraskovsky et al, 1996). To date only the hematopoietic growth factor Flt-3 ligand (Lyman et al, 1993) is known to stimulate excess dendritic cell production in vivo. It had been previously shown that in vivo administration of Flt-3 ligand dramatically increased the number of hematopoietic progenitors in the bone marrow, blood and spleen, resulting in elevated levels of myelopoiesis and lymphopoiesis (Brasel et al, 1995; Brasel et al, 1996). Maraskovsky et al (1996) have demonstrated that treatment of mice with Flt-3 ligand results in substantial increase in the number of functionally mature dendritic cells in vivo. In Flt-3 ligand-treated mice, absolute number of MHC class II^+ and $CD11c^+$ cells was increased 17-fold in the spleen, 4-fold in the inguinal and axillary nodes and 6-fold in the peripheral blood. These results, however, must be interpreted taking into account that Flt-3 ligand treated spleens are 2-3 fold larger than control spleens, and splenic architecture appears disrupted (Pulendran et al, 1997).

Dendritic cells generated in vitro provide a source of potential vehicles for cellular-based immunotherapy. The availability of substantial number of dendritic cells has made it possible to test dendritic cell-based immunization regimes, especially with the intention of eliciting CTL responses against tumor antigens (Young and Inaba, 1996). Numerous studies in experimental animal models have demonstrated the feasibility of such an approach. Immunization of mice with dendritic cells pulsed with synthetic peptides (Mayordomo et al, 1995; Celluzzi et al, 1996), eluted peptides from tumor cell lines (Zitvogel et al, 1996) and intact soluble proteins (Paglia et al, 1996) induce protective CTL responses against tumors. In vitro generated dendritic cells pulsed with tumor antigens and injected into animal tumor models have been shown to elicit anti-tumor immune responses, resulting in protection against tumors and reduction of established tumors (Specht et al, 1997; Song et al, 1997; Schuler and Steinman, 1997). Various modes of using dendritic cells as vehicles for tumor antigens are possible and are curently being investigated. Viral vectors, naked and plasmid DNA, RNA, liposomes with nucleic acids of proteins, tumor lysates, apoptotic cells and peptides could also be delivered via dendritic cells.

Chapter 4

Functional and Developmental Analyses of Dendritic Cells Generated from B10.BR and NOD.H-2^k Congenic Strains

4.1 Introduction

Autoimmune diabetes is a complex polygenic disease. Genetic susceptibility to autoimmune diabetes is conferred by susceptibility loci within and outside the MHC in the NOD mouse model. It has now become clear that non-MHC diabetogenic loci create an overall susceptibility to autoimmunity in the NOD mouse (Wicker, 1997). Against the autoimmune prone NOD background, alleles within the MHC appear to determine the target tissue for autoimmune destruction. Autoimmune pathology may be directed against the pancreas, thyroid or salivary glands, depending on the genotype of the MHC on the NOD background. A simplified summary of NOD genetics and how target tissues for autoimmune destruction may be altered, depending on the genotype of the MHC, is illustrated in Figure 4.1.

Several lines of evidence suggest that part of the genetic predisposition to autoimmune diabetes resides in hematopoietic stem cells which give rise to antigen presenting cells. In radiation chimeric mice, bone marrow-derived cells from NOD mice can reconstitute diabetes susceptibility in disease-resistant strains (Serreze et al, 1988; Wicker et al, 1988). It is not known whether this susceptibility resides in lymphocytes or antigen presenting cells. Myeloid-derived dendritic cells and macrophages have been shown to constitute the initial infiltrate into pancreatic islets of prediabetic young NOD mice, prior to infiltration by lymphocytes (Jansen et al, 1994). Furthermore, dendritic cells and macrophages have been demonstrated to be the initial and principal producers of TNFα in pancreatic islets (Dahlen et al, 1998). TNFα has been shown to have a critical role in the initial stages of islet autoimmunity (Green et al, 1998; Yang et al, 1994). Given that dendritic cells have a well established role in promoting T cell responses in processes like rejection of tissue grafts in vivo (Lafferty et al, 1983) and generation of T helper 1 type responses in vitro (O'Garra and Murphy, 1994), a role for dendritic cells in mediating tissue-specific autoimmunity is possible. Interestingly, a recent study has demonstrated that repeated priming with dendritic cells, bearing a self antigen that is transgenically expressed in the pancreatic islets, results in severe and rapid onset of diabetes. A striking feature of the pathology induced by the repeated priming with dendritic cells is the formation of secondary lymphoid-like structures in the islets, ultimately leading to tissue destruction (Ludewig et al, 1998).

Figure 4.1

The genotype of the MHC, on the NOD background, determines target tissue for autoimmune destruction while non-MHC NOD genes confer overall susceptibility to tissue-specific autoimmunity.

Studies in NOD.H-2 congenic strains underscore the differential roles of MHC and non-MHC genes in tissue autoimmunity. Firstly, the NOD MHC (H-2^{g7}) is essential but insufficient to induce diabetes. This is demonstrated by the absence of diabetes in the NOD.H-2^{k} and converse B10.H-2^{g7} congenic strains. Secondly, the genotype of the MHC, on the autoimmune-prone NOD background, determines target tissue for autoimmune destruction. This is demonstrated by the presence of tissue autoimmunity against altered targets in NOD.H-$2^{h4\ or\ k}$ and NOD.H-2^{b} congenic strains. The presence of H-$2^{h4\ or\ k}$ or H-2^{b} on the NOD background renders NOD mice susceptible to autoimmune thyroiditis or sialitis, respectively. Altogether, these observations implicate non-MHC NOD genes in creating an overall susceptibility to tissue-specific autoimmunity.

Figure 4.1. Simplified Summary of NOD Mouse Genetics

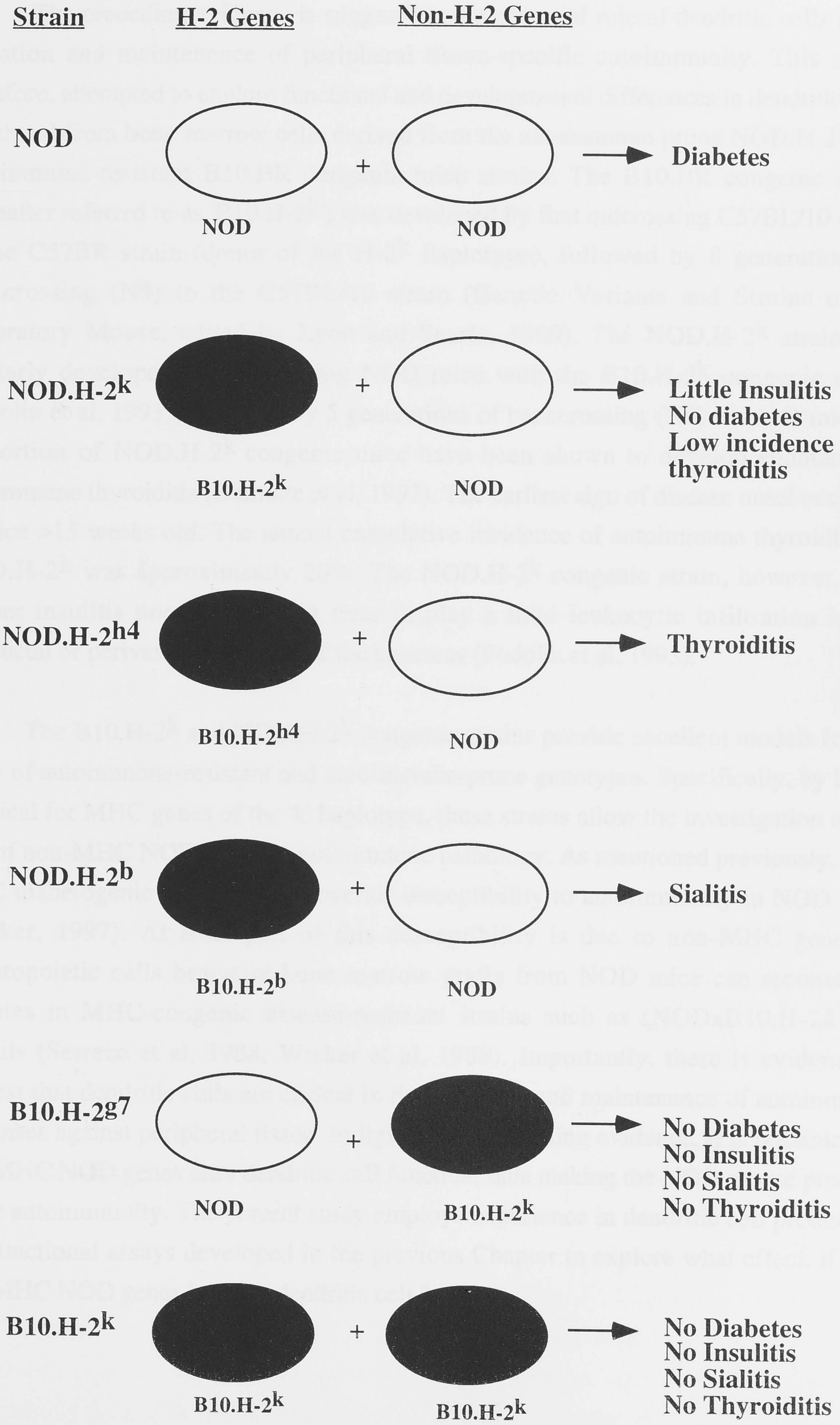

4.2 Objective:

The preceding evidence is suggestive of a potential role of dendritic cells in the initiation and maintenance of peripheral tissue-specific autoimmunity. This study, therefore, attempted to explore functional and developmental differences in dendritic cells generated from bone marrow cells derived from the autoimmune prone NOD.H-2^k and autoimmune-resistant B10.BR congenic mice strains. The B10.BR congenic strain (hereafter referred to as 'B10.H-2^k') was developed by first outcrossing C57BL/10 strain to the C57BR strain (donor of the H-2^k haplotype), followed by 8 generations of backcrossing (N9) to the C57BL/10 strain (Genetic Variants and Strains of the Laboratory Mouse, edited by Lyon and Searle, 1990). The NOD.H-2^k strain was similarly developed by outcrossing NOD mice with the B10.H-2^k congenic strain (Podolin et al, 1993), followed by 5 generations of backcrossing (N6) to NOD mice. A proportion of NOD.H-2^k congenic mice have been shown to develop spontaneous autoimmune thyroiditis (Damotte et al, 1997). The earliest sign of disease onset occurred in mice >15 weeks old. The annual cumulative incidence of autoimmune thyroiditis in NOD.H-2^k was approximately 20%. The NOD.H-2^k congenic strain, however, gets neither insulitis nor diabetes but does display a mild leukocytic infiltration in the periductal or perivascular regions of the pancreas (Podolin et al, 1993).

The B10.H-2^k and NOD.H-2^k congenic strains provide excellent models for the study of autoimmune-resistant and autoimmune-prone genotypes. Specifically, by being identical for MHC genes of the 'k' haplotype, these strains allow the investigation of the role of non-MHC NOD genes in autoimmune pathology. As mentioned previously, non-MHC diabetogenic loci create an overall susceptibility to autoimmunity in NOD mice (Wicker, 1997). At least part of this susceptibility is due to non-MHC genes in hematopoietic cells beacause bone marrow grafts from NOD mice can reconstitute diabetes in MHC-congenic disease-resistant strains such as (NODxB10.H-$2g^7$)F1 hybrids (Serreze et al, 1988; Wicker et al, 1988). Importantly, there is evidence to suggest that dendritic cells are critical in the initiation and maintenance of autoimmune responses against peripheral tissue. In light of the preceding evidence, it is possible that non-MHC NOD genes alter dendritic cell function, thus making the NOD mouse prone to tissue autoimmunity. The current study employs experience in dendritic cell production and functional assays developed in the previous Chapter to explore what effect, if any, non-MHC NOD genes have on dendritic cell function.

4.3 Functional Analyses of Cultured Bone Marrow Cells

Bone marrow cell cultures to generate dendritic cells and antigen presentation-T cell activation assays developed in the previous Chapter were used to test the hypothesis that non-MHC diabetes susceptibility genes from NOD mice act by altering dendritic cell function. An in vitro flow cytometric-based functional assay, developed in the previous Chapter and described in detail in section 2.14, was used to determine the ability of cultured bone marrow cells, derived from B10.H-2^k and NOD.H-2^k mice, to activate CD4 T cells and induce their proliferation. The design of this assay enables single cell resolution of activation and proliferation efficiencies of responding T cells. The assay was performed by harvesting cells, cultured in the presence of GM-CSF and IL-4, on day 8 of culture and using them as antigen presenting cells. These antigen presenting cells were pulsed with 0.2μM or 2μM or 20μM HEL46-61 or 0.1μM HEL, washed by centrifugation, serially diluted and co-cultured in triplicate wells with CFSE-labelled lymph node and spleen leukocytes ($3x10^5$ per well) from mice carrying the 3A9 T cell receptor transgene on the B10.H-2^k background. The 3A9 T cell receptor transgenic CD4 T cells are I-A^k -restricted and specific for HEL46-61 (Ho et al, 1994). Activation of responder CD4 T cells was determined using flow cytometry by measuring the induction of the early activation marker, CD69, after 15 hr of culture. Proliferation of CD4 T cells was determined by measuring the level of CFSE dilution on days 3 and 5 of culture. Absolute cell numbers of proliferating CD4 T cells were determined by the inclusion of counting beads to each sample prior to acquisition on the flow cytometer.

The activation of CD4 T cells was determined by flow cytometry by measuring the induction of the early activation marker, CD69 (Figure 4.2). Representative FACS plots illustrating the induction of CD69 expression on CD4 T cells by B10.H-2^k or NOD.H-2^k myeloid antigen presenting cells is shown in Fig.4.2a. It was evident from Fig.4.2b that there was no apparent difference in the ability of antigen presenting cells, derived from B10.H-2^k or NOD.H-2^k strains, to induce CD69 expression on CD4 T cells, under the various conditions employed during the course of this analysis. Maximal CD69 induction was observed when antigen presenting cells ($6x10^3$ per well) were pulsed with 20μM HEL46-61. In this instance, the highest number of antigen presenting cells induced CD69 expression on 80% of CD4 T cells.

The level of CD4 T cell proliferation on days 3 and 5 of culture, as measured by CFSE dilution, is shown in Figure 4.3. Graphical representations of the level of CD4 T cell proliferation on days 3 and 5 of culture are depicted in Fig.4.3a-b. A reproducible difference in the proliferation responses of CD4 T cells, induced by B10.H-2^k or

Figure 4.2

T cell activation by B10.H-2^k versus NOD.H-2^k myeloid cells.

Bone marrow cells obtained from B10.H-2^k and NOD.H-2^k mice, depleted of lymphocytes and cultured in the presence of GM-CSF and IL-4 to generate dendritic cells. Cultured cells were harvested after 8 days, washed by centrifugation and pulsed with shown doses of HEL46-61 peptide or native HEL protein. Antigen pulsed cells were washed again to eliminate unbound antigen. Shown numbers of pulsed, viable bone marrow cells were added to triplicate wells and co-cultured with $3x10^5$ CFSE-labelled spleen and lymph node leukocytes from mice expressing the 3A9 T cell receptor transgene on the B10.H-2^k background. Expression of the early activation marker, CD69, on CD4 T cells was measured by flow cytometry after 15 hr of culture.

(a) Representative FACS plots showing CD4 T cell activation in response to stimulation with antigen-pulsed or unpulsed $6x10^3$ myeloid cells. Numbers in quadrants represent percentage CD4 T cells expressing CD69.

(b) Mean percent CD69 positive CD4 T cells +/- SE in triplicate wells is shown as a function of the input number of viable antigen-pulsed myeloid cells. Data is representative of three independent experiments.

Figure 4.2

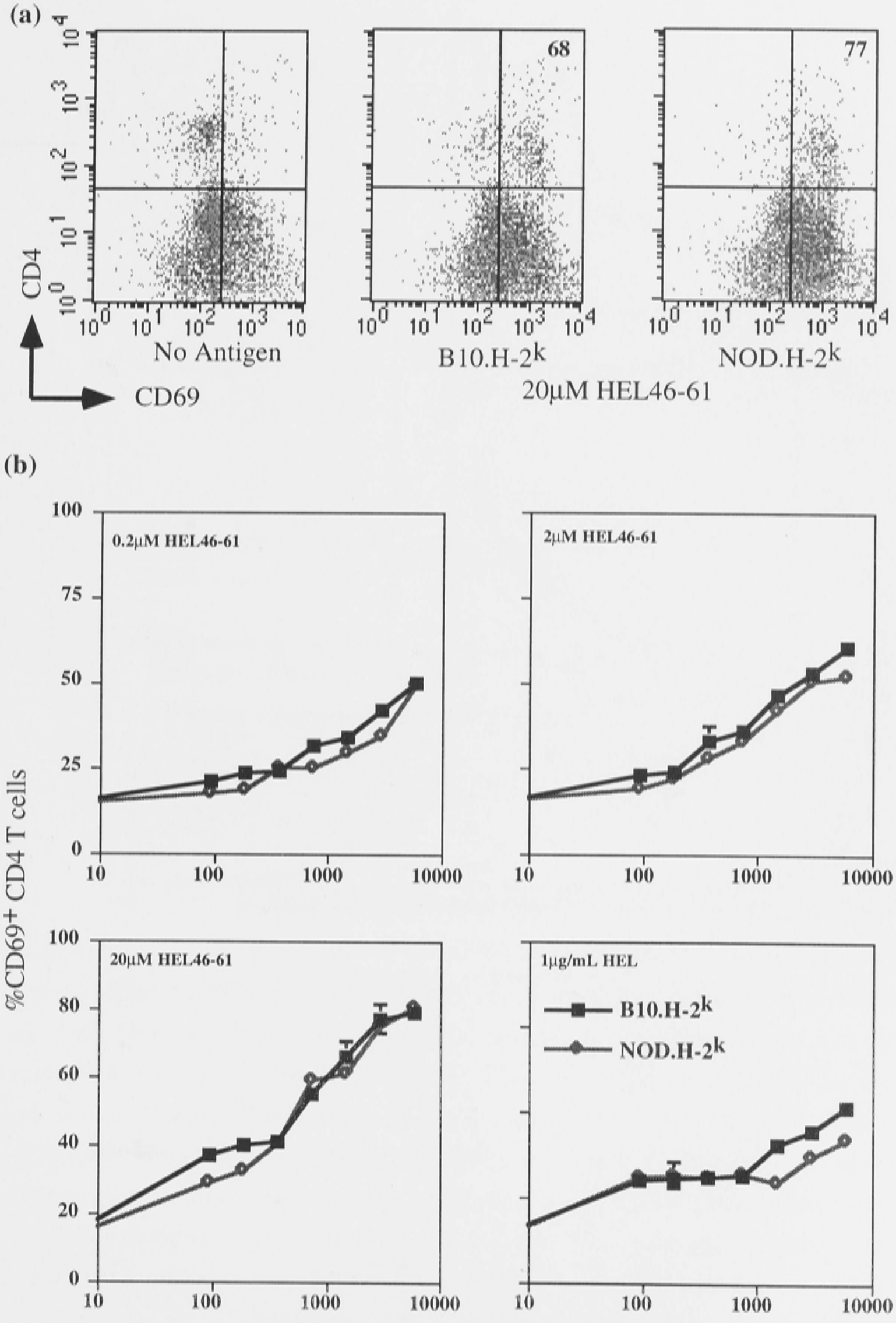
(a)
CD4
CD69
No Antigen
68
77
B10.H-2k
NOD.H-2k
20μM HEL46-61
(b)
0.2μM HEL46-61
2μM HEL46-61
20μM HEL46-61
1μg/mL HEL
B10.H-2k
NOD.H-2k
%CD69+ CD4 T cells
Number viable bone marrow cells/well

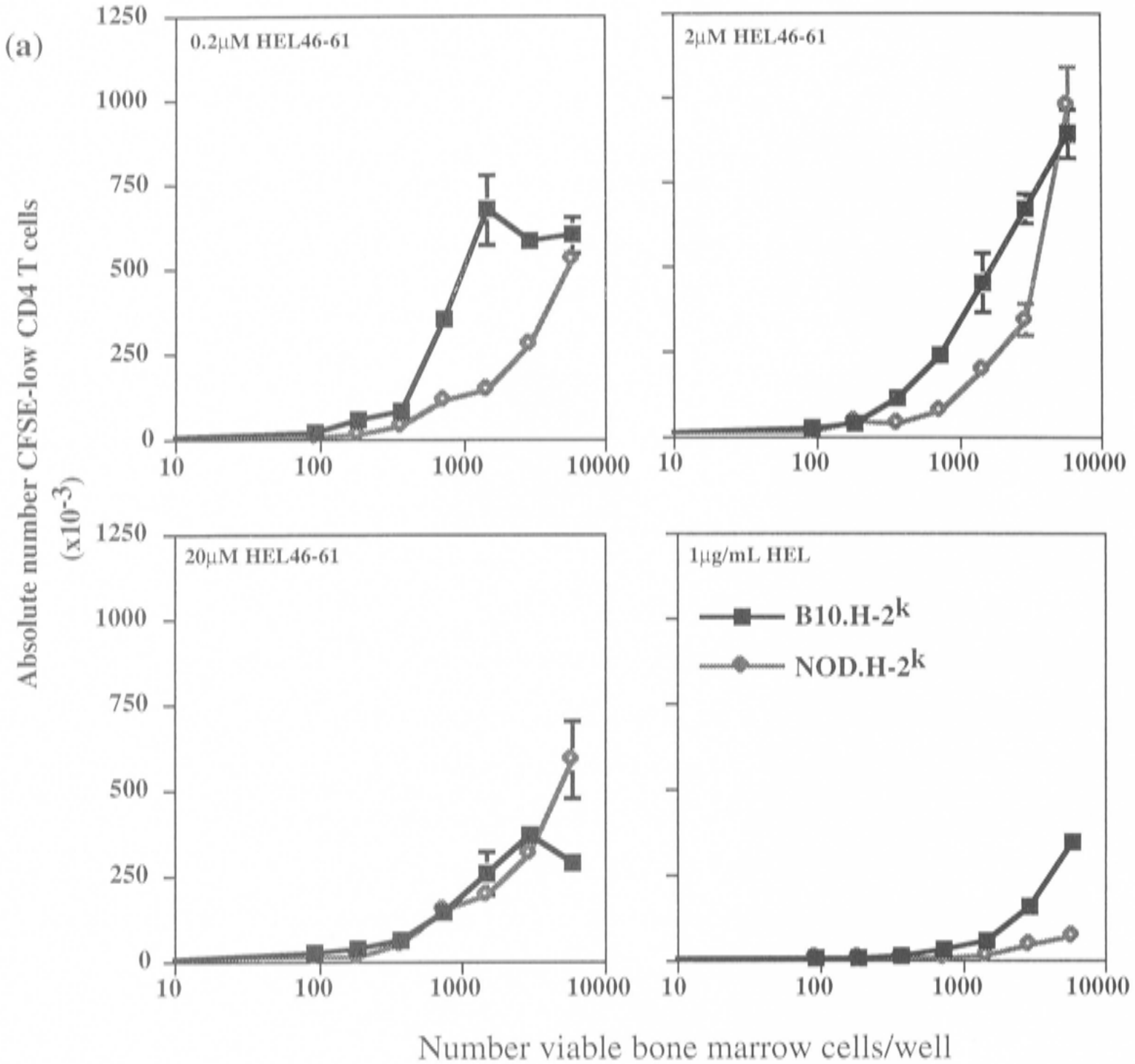

Figure 4.3

Proliferation of CD4 T cells measured by CFSE dilution

Bone marrow cells from B10.H2^k or NOD-H2^k cultures were harvested on day 8, pulsed with antigen and co-cultured in triplicate wells with CFSE-labelled lymph node and spleen leukocytes from the 3A9 T cell receptor transgenic mice as described in Fig.4.2. Proliferation of CD4 T cells on days 3 (4.3a) and 5 (4.3b) was analyzed by measuring CFSE dilution using flow cytometry. Quantitation of the absolute number of CFSE-positive CD4 T cells was carried out by including known concentration of Coulter Counting beads in samples prior to acquisition. Mean number proliferated (CFSE-low) CD4 T cells +/- SE in triplicate wells is shown as a function of the input number of viable antigen-pulsed cells. Data presented is representative of three independent experiments.

Fig. 4.3

Note: Total viable cells were not normalized for dendritic cell number.

Figure 4.3

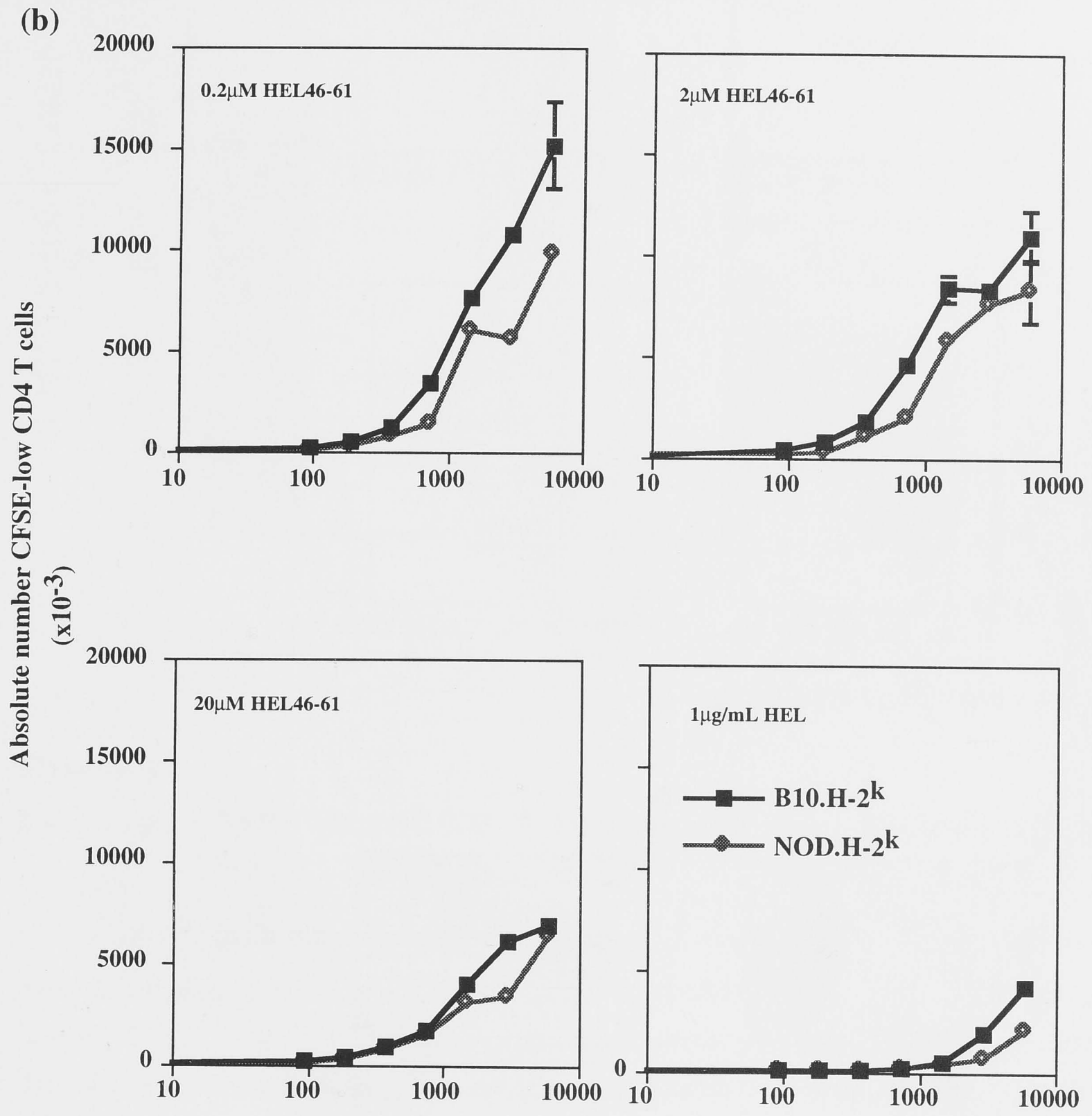
(b)
Absolute number CFSE-low CD4 T cells (x10-3)
0.2μM HEL46-61
2μM HEL46-61
20μM HEL46-61
1μg/mL HEL
B10.H-2k
NOD.H-2k
20000
15000
10000
5000
0
10
100
1000
10000
Number viable bone marrow cells/well

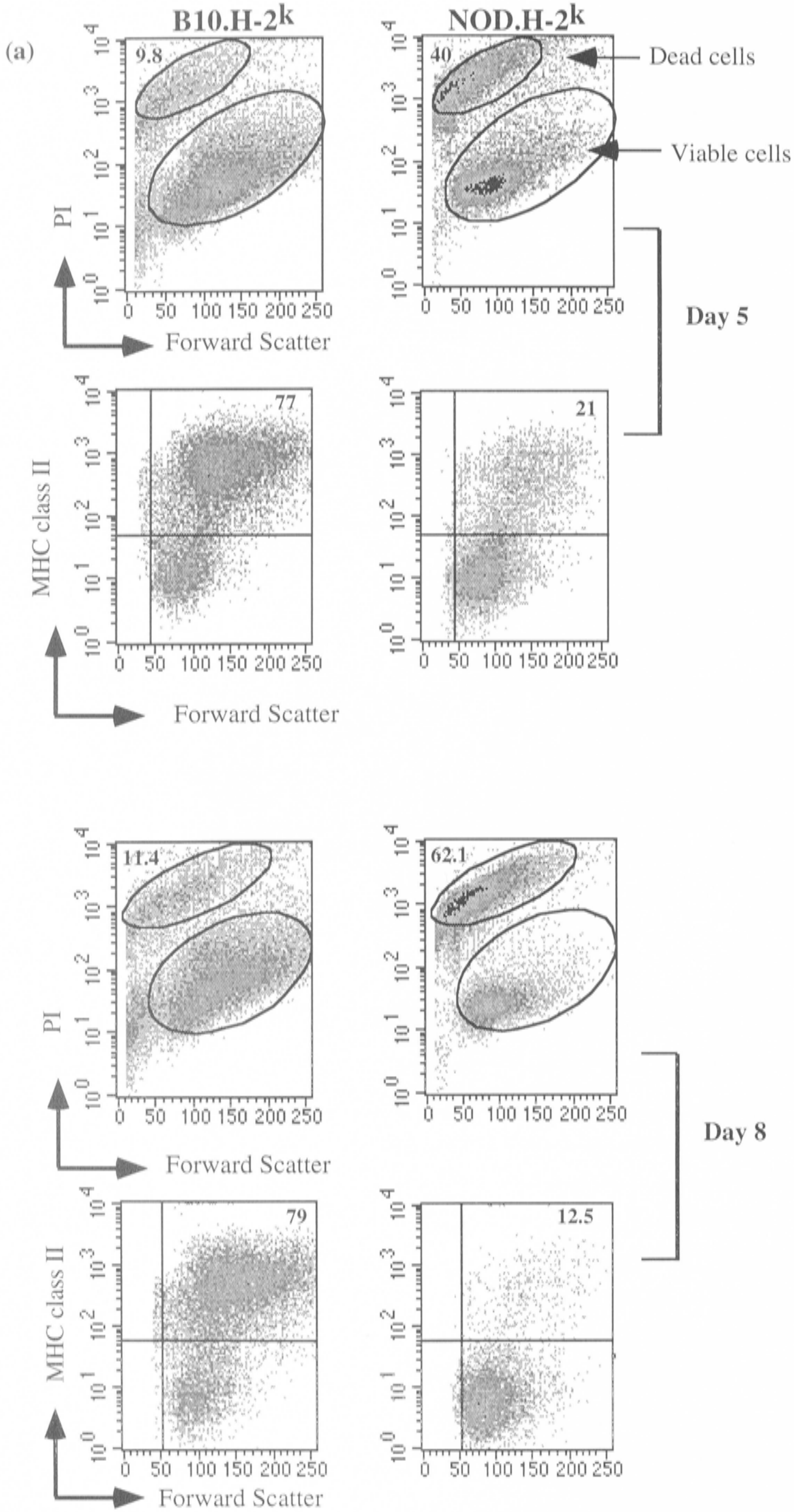
(a)
B10.H-2k
NOD.H-2k
9.8
40
Dead cells
Viable cells
PI
Forward Scatter
Day 5
77
21
MHC class II
Forward Scatter
11.4
62.1
Day 8
79
12.5
MHC class II
Forward Scatter

Figure 4.4

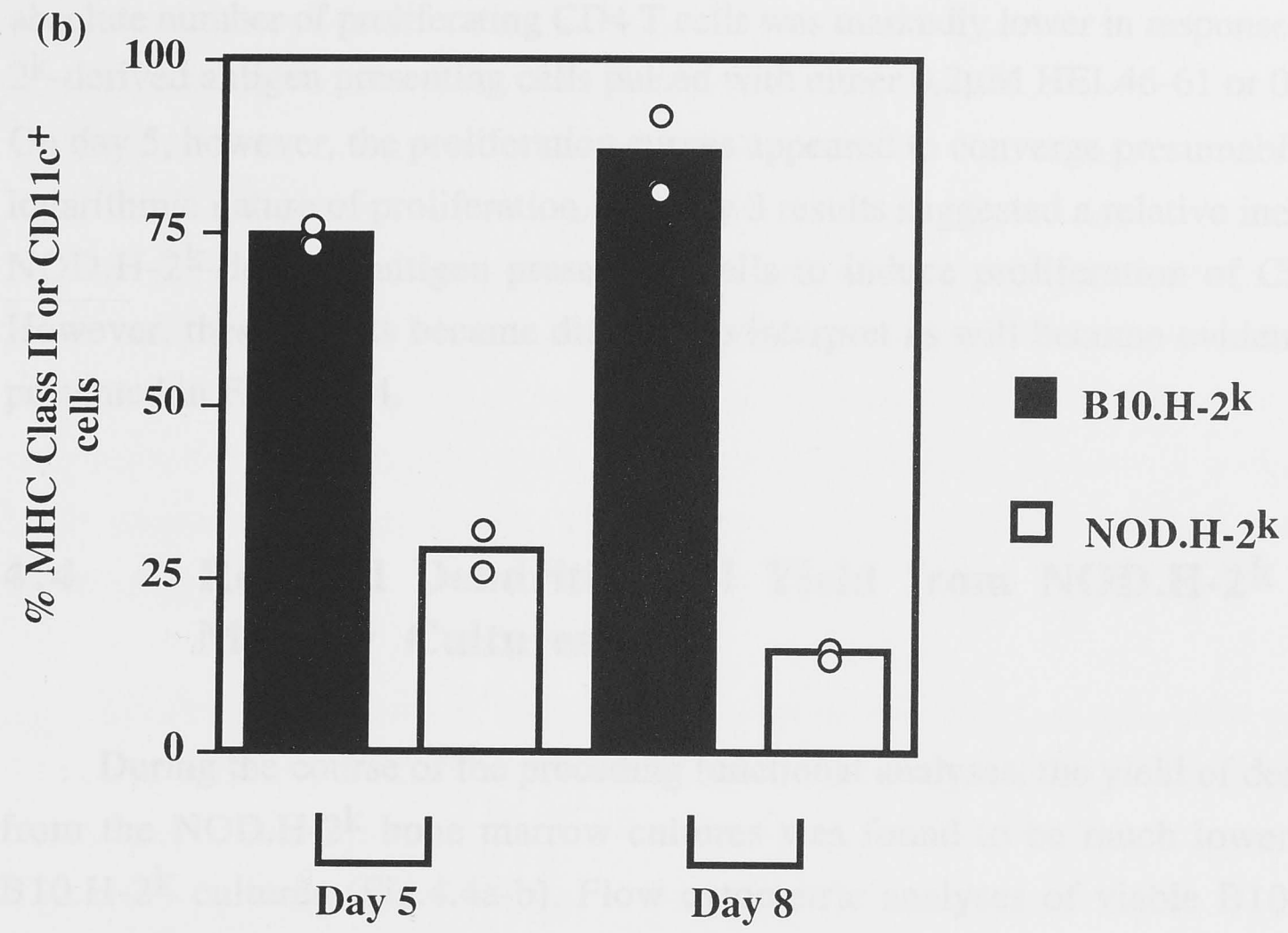

Figure 4.4

Bone marrow cells from NOD.H-2^k mice generate fewer dendritic cells in culture.

The yield of viable dendritic cells from B10.H-2^k and NOD.H-2^k bone marrow cultures on days 5 and 8 was determined by flow cytometry using anti-MHC class II (10.3.6) or anti-CD11c (N418) monoclonal antibody. Dead cells and cellular debris were eliminated from analysis by propidium iodide (PI) exclusion and appropriate forward and side scatter gating.

(a) Representative FACS plots illustrating low yield of dendritic cells from NOD.H-2^k cultures on days 5 and 8. Numbers near elliptical regions represent percentage total cells in that region. Numbers near quadrants represent percentage viable cells in that quadrant. MHC class II profiles represent viable cells only, using gates shown.

(b) The yield of viable dendritic cells from individual mice is shown by circles, and columns represent mean values. Data is representative of 5 separate experiments.

NOD.H-2^k myeloid-derived antigen presenting cells, was observed on day 3 when antigen presenting cells were pulsed with either 0.2μM HEL46-61 or 0.1μM HEL. The absolute number of proliferating CD4 T cells was markedly lower in response to NOD.H-2^k-derived antigen presenting cells pulsed with either 0.2μM HEL46-61 or 0.1μM HEL. On day 5, however, the proliferation curves appeared to converge presumably due to the logarithmic nature of proliferation. The day 3 results suggested a relative inefficiency of NOD.H-2^k-derived antigen presenting cells to induce proliferation of CD4 T cells. However, these results became difficult to interpret as will become evident from data presented in Figure 4.4.

4.4 Reduced Dendritic Cell Yield from NOD.H-2^k Bone Marrow Cultures

During the course of the preceding functional analyses, the yield of dendritic cells from the NOD.H-2^k bone marrow cultures was found to be much lower than from B10.H-2^k cultures (Fig.4.4a-b). Flow cytometric analyses of viable B10.H-2^k- and NOD.H-2^k-derived bone marrow cells on day 5 of culture for the cell surface expression of the N418 marker (CD11c) or MHC class II molecules revealed that dendritic cells constituted 75% of the cells in B10.H-2^k cultures, compared with 30% in NOD.H-2^k cultures. Similary, dendritic cells constituted >80% cells in B10.H-2^k cultures on day 8, compared to only 15% in the NOD.H-2^k cultures. Concomitant with the reduced number of dendritic cells, NOD.H-2^k cultures contained a greater proportion of dead cells, as measured by propidium iodide staining. B10.H-2^k cultures contained 9.8% and 11.4% dead cells on days 5 and 8, respectively. In contrast, NOD.H-2^k cultures contained 40% and 62.1% dead cells on days 5 and 8, respectively.The previously observed inefficiency of NOD.H-2^k-derived antigen presenting cells to induce proliferation of CD4 T cells may thus be accounted for by a relative deficiency in dendritic cell numbers in NOD.H-2^k-derived antigen presenting cell population.

4.5 Reduced Dendritic Cell Yield is a Cell-Intrinsic Feature of NOD.H-2^k Myeloid Precursors

The reduced yield of dendritic cells from NOD.H-2^k cultures prompted the question of whether or not this phenotype was cell-intrinsic to NOD.H-2^k myeloid precursors. It was conceivable that NOD.H-2^k myeloid cells in culture secreted factors which could inhibit the survival, proliferation and differentiation of NOD.H-2^k myeloid precursors in an autocrine manner in vitro. If this were the case, paracrine effects on B10.H-2^k

myeloid precursors in co-culture would be likely. Alternatively, NOD.H-2^k myeloid precursors may possess a genetic predisposition, underpinned by non-MHC NOD genes, to generate fewer dendritic cells in vitro. To resolve this issue, B10.H-2^k and NOD.H-2^k bone marrow cells were co-cultured at a 1:1 ratio and the cells generated from this culture analyzed by flow cytometry on days 5 and 8 of culture. The experimental design of this assay is illustrated in Figure 4.5. The allelic variants of the cell surface marker Ly5 (CD45 or Leukocyte Common Antigen) expressed between B10.H-2^k and NOD.H-2^k mice (McClive et al, 1994) enabled flow cytometric analysis of strain specific cells in co-culture. Cell surface Ly5 is expressed by all nucleated hematopoietic cells and readily detectable by flow cytometry using Ly5 monoclonal antibodies. Cells from the B10.H-2^k strain express the 'b' allotype of Ly5 whereas cells from the NOD.H-2^k strain express the 'a' allotype.

On day 5 of co-culture, MHC class II positive and negative cells were gated (Figure 4.6a) and analyzed for Ly5 allotype expression. The majority (>70%) of MHC class II expressing cells present on day 5 of culture were B10.H-2^k-derived ie. $Ly5^b$ positive (Fig.4.6b). By contrast, MHC class II negative cells in the same co-culture were equally derived from either strain (Fig.4.6c). On day 8 of culture, the bias of MHC class II positive cells towards B10.H-2^k origin was more extreme than observed on day 5 (Fig.4.6d). As on day 5 of culture, MHC class II negative cells in the same culture on day 8 were equally derived from either strain (Fig.4.6e). Since B10.H-2^k myeloid precursors appeared to develop in co-culture like they would alone, it was concluded that the reduced capacity of NOD.H-2^k myeloid precursors to generate dendritic cells in in vitro cultures was a cell-intrinsic feature of NOD.H-2^k myeloid precursors. This data is the first demonstration of a cell-intrinsic phenotype of NOD.H-2^k myeloid precursors which affects dendritic cell generation in vitro.

4.6 Heterogeneous Proliferation and Elevated Levels of Apoptosis in NOD.H-2^k Bone Marrow Cultures

A number of possibilities could account for the reduced yield of dendritic cells from NOD.H-2^k bone marrow cultures. These include reduced proliferation, increased levels of apoptosis, inability to differentiate, or a combination of these factors attributable to NOD.H-2^k myeloid precursors. In order to distinguish between these possibilities and to unravel the mechanisms contributing towards the reduced dendritic cell yield from NOD.H-2^k bone marrow cultures, a flow cytometric-based in vitro proliferation and apoptosis assay (described in detail in section 2.15) was designed to monitor the fate of bone marrow cells during the early days of culture. Bone marrow cells from either strain

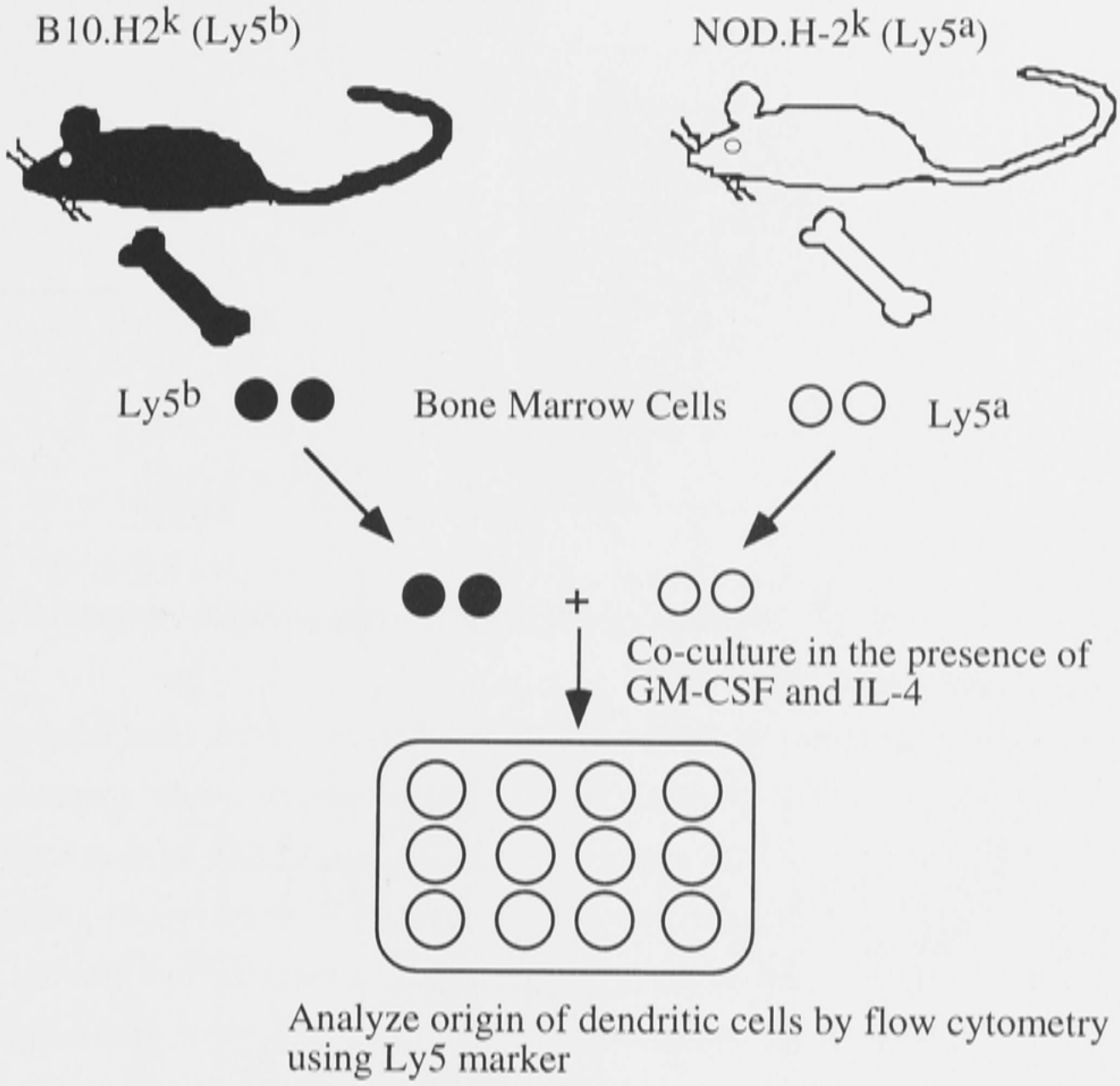

Figure 4.5

Experimental design for mixed bone marrow cell cultures.

In order to determine whether or not the reduced yield of dendritic cells from NOD.H-2^k bone marrow cells was a cell-intrinsic feature of NOD.H-2^k myeloid precursors, bone marrow cells from B10.H-2^k and NOD.H-2^k were admixed and cultured in the presence of GM-CSF and IL-4. Bone marrow cells were aseptically harvested from the hind limbs of B10.H-2^k or NOD.H-2^k mice and depleted of lymphocytes by complement-mediated lysis. A 1:1 mixture ($1x10^6$ leukocytes in total) of lymphocyte-depleted bone marrow leukocytes from both strains were cultured in 1mL growth factor-supplemented RPMI. The relative production of dendritic cells in culture from each precursor pool was determined on days 5 and 8 by flow cytometry using the cell surface-expressed allelic variants of Ly5 to distinguish between dendritic cells derived from the two strains. All nucleated hematopoietic cells from the B10.H-2^k strain express the'b' allotype of Ly5, while NOD.H-2^k cells express the 'a' allotype.

Figure 4.6

Restricted ability of NOD.H-2^k myeloid precursors to generate dendritic cells in vitro is a cell-intrinsic phenotype.

Bone marrow cultures to generate dendritic cells were established as before, except input cells comprised a 1:1 mixture of $1x10^6$ total lymphocyte-depleted bone marrow leukocytes from B10.H-2^k and NOD.H-2^k mice. The relative production of dendritic cells from each precursor pool was determined on days 5 and 8 by flow cytometry using allelic variants of Ly5 to distinguish between dendritic cells derived from the two strains.

(a) Dendritic cells (I-A^k -positive) and other cells (I-A^k -negative) were gated and analyzed for $Ly5^a$ (NOD.H-2^k -specific) and $Ly5^b$ (B10.H-2^k -specific) expression.

(b) Relative proportions of dendritic cells from $Ly5^a$ (NOD.H-2^k) and $Ly5^b$ (B10.H-2^k) origin at day 5.

(c) Relative proportions of other cells from $Ly5^a$ (NOD.H-2^k) and $Ly5^b$ (B10.H-2^k) origin at day 5.

(d) and (e). Comparable analysis of the relative proportions of $Ly5^a$ and $Ly5^b$ cells at day 8 of culture. Numbers in rectangular regions or quadrants represent percentage of total or MHC class II^+ or $^-$ cells in that region or quadrant, respectively. Data is representative of three independent experiments.

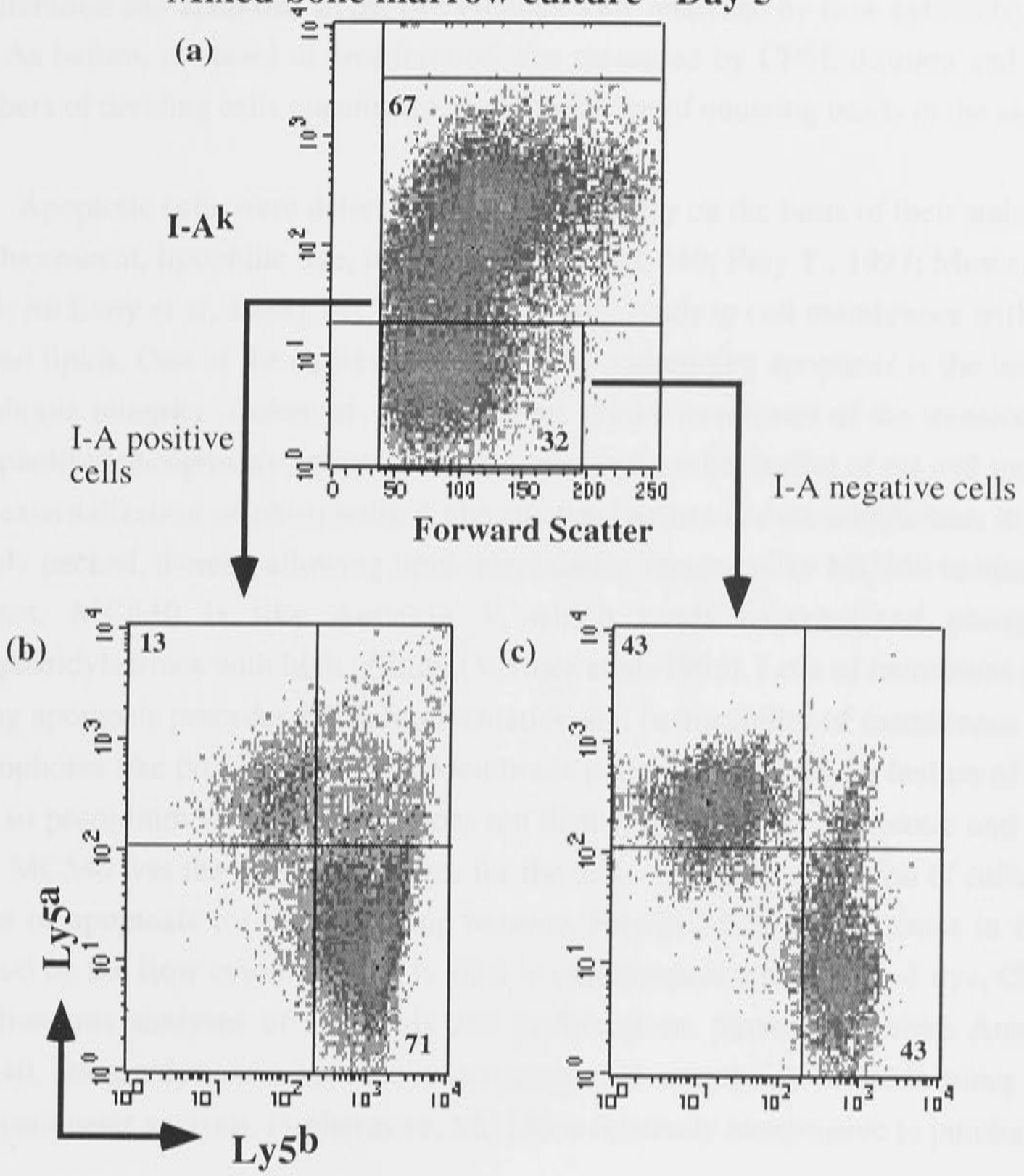
Mixed bone marrow culture - Day 5
(a)
I-A^k
67
32
I-A positive cells
I-A negative cells
Forward Scatter
0
50
100
150
200
250
(b)
13
71
(c)
43
43
Ly5^a
Ly5^b
Mixed bone marrow culture - Day 8
I-A positive cells
I-A negative cells
(d)
3.5
16.6
78
(e)
46.3
3
44

Figure 4.6

were prelabelled with CFSE and cultured in the presence of GM-CSF and IL-4. Proliferation and apoptosis in the two cultures were analyzed by flow cytometry on days 1-3. As before, the level of proliferation was measured by CFSE dilution and absolute numbers of dividing cells quantitated by the inclusion of counting beads in the assay.

Apoptotic cells were detected by flow cytometry on the basis of their staining with the fluorescent, lipophilic dye, merocyanin 540 (MC540; Frey T., 1997; Mower Jr et al, 1994; McEvoy et al, 1988). MC540 preferentially binds to cell membranes with loosely packed lipids. One of the earliest events in cells undergoing apoptosis is the loss of cell membrane integrity (Cohen et al, 1992). This occurs as a result of the translocation of phospholipid phosphatidylserines from the inner to the outer leaflet of the cell membrane. The externalization of phospholipid phosphatidylserines causes membranes to become loosely packed, thereby allowing lipid-intercalating reagents like MC540 to bind. In this respect, MC540 is like Annexin V which binds externalized phospholipid phosphatidylserines with high affinity (Vermes et al, 1995). Loss of membrane integrity during apoptosis precedes DNA fragmentation and permeability of membranes to DNA fluorophores like propidium iodide. Membrane permeability is also a feature of necrotic cells so propidium iodide staining does not distinguish between apoptotic and necrotic cells. MC540 was the reagent of choice for the flow cytometric detection of cells in early stages of apoptosis for the following reasons. Firstly, MC540 fluoresces in the FL-2 channel on the flow cytometer and is ideal in combination with the FL-1 dye, CFSE, for simultaneous analyses of apoptosis and proliferation. Secondly, unlike Annexin V, MC540, being a dye, does not require conjugation to appropriate fluorochromes for such multiparameter analysis. Furthermore, MC540 is relatively inexpensive to purchase.

Results from the above assay are presented in Figure 4.7. Representative flow cytometry data depicting how cell proliferation was determined are shown in histogram plots (Fig.4.7a). Myeloid precursors in B10.H-2^k cultures proliferated uniformly and generated a discrete population of cells that had undergone similar numbers of cell division (indicated by unimodal CFSE-low peak) on day 3 (Left panel). By contrast, NOD.H-2^k myeloid precursors proliferated heterogeneously (Right panel). Aberrant proliferation in NOD.H-2^k cultures was characterized by the presence of cells that had undergone variable numbers of cell division (indicated by the presence of sequential CFSE-low peaks), absent from B10.H-2^k cultures. Quantitation of the absolute number of proliferating cells is shown in Fig.4.7b. The absolute number of viable cells that had divided in the B10.H-2^k bone marrow culture doubled between days 2 and 3, but remained relatively stable in the NOD.H-2^k culture during this period.

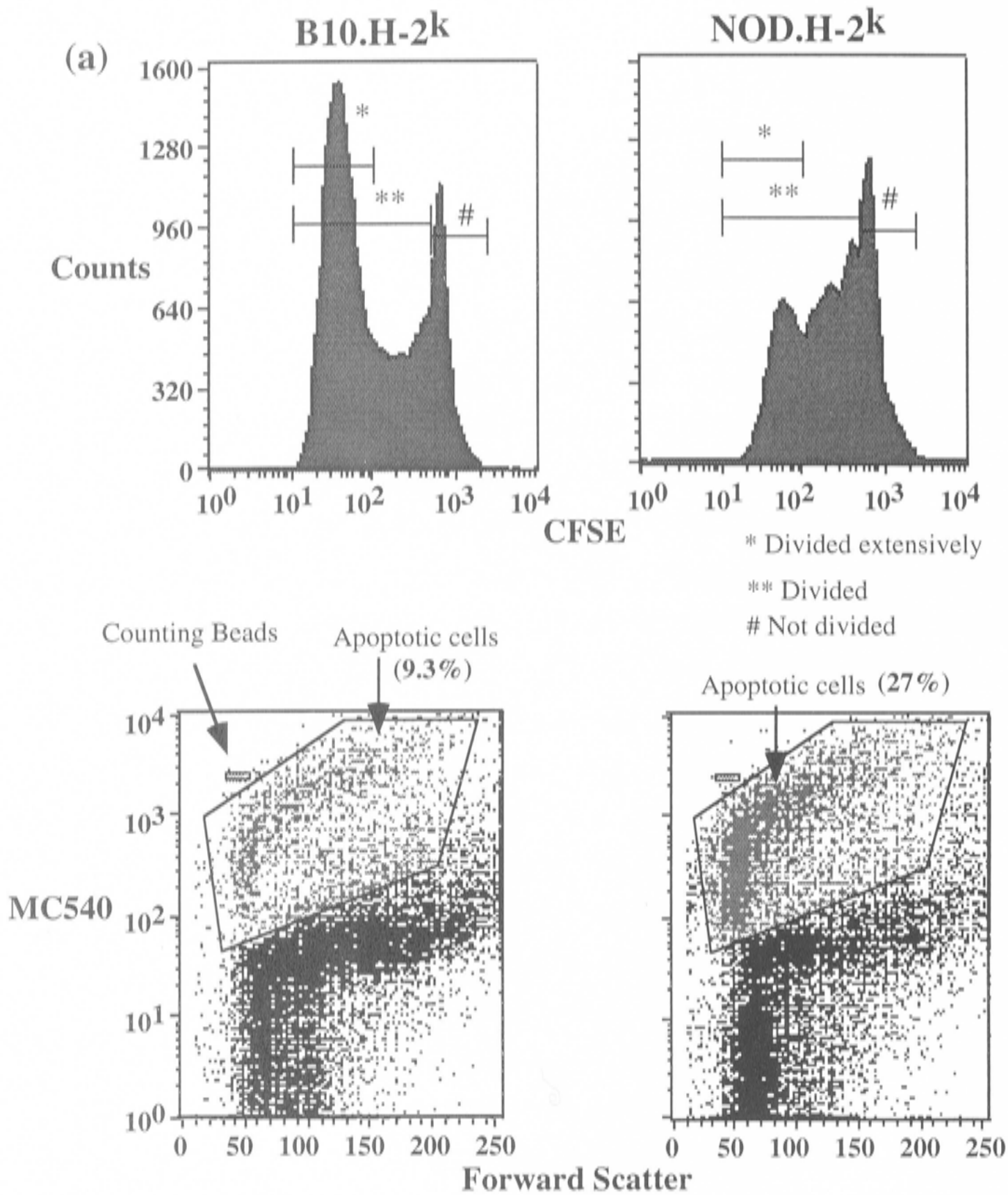

Figure 4.7

Heterogeneous proliferation and elevated levels of apoptosis and in NOD.H-2^k bone marrow cultures.

Bone marrow cultures to generate dendritic cells were established as before, except input cells were labelled with CFSE.

(a) Cultures were analyzed on day 3 for proliferating (CFSE-low) and apoptotic cells (MC540$^+$) by 2-colour flow cytometry.

(b) Proliferation on days 1-3 as revealed by CFSE dilution in each of the cultures.

(c) Apoptotic cells on days 1-3 were detected by MC540 positivity. Both relative and absolute numbers of MC540$^+$ cells are shown. Data presented in (b) and (c) is representative of three independent experiments. Circles represent actual value from bone marrow cultures derived from single mouse, and columns depict mean values.

Figure 4.7 (b)

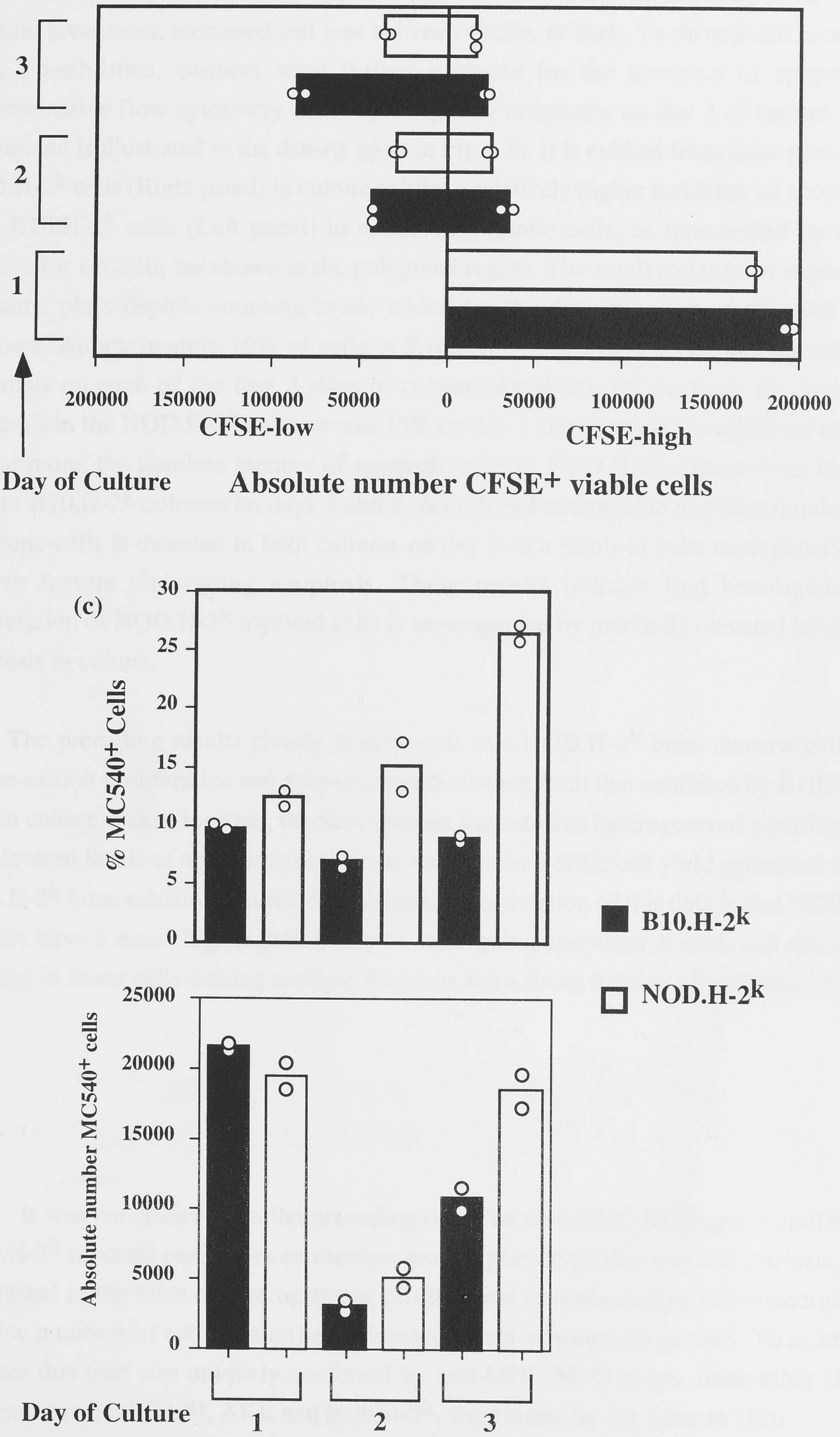
3
2
1
200000
150000
100000
50000
0
50000
100000
150000
200000
CFSE-low
CFSE-high
Day of Culture
Absolute number CFSE+ viable cells
(c)
% MC540+ Cells
30
25
20
15
10
5
0
B10.H-2k
NOD.H-2k
Absolute number MC540+ cells
25000
20000
15000
10000
5000
0
Day of Culture
1
2
3

* Alternatively, NOD-H.2^{k} myeloid precursors may have an inherent inability to make multiple successive divisions, in addition to or independent of any tendency towards apoptosis.

The aberrant proliferation observed in NOD.H-2^k bone marrow cultures may be attributable to either the variable rates of entry into successive divisions by NOD.H-2^k myeloid precursors, increased cell loss between cycles, or both. To distinguish between these possibilities, cultures were further screened for the presence of apoptosis. Representative flow cytometry data depicting how apoptosis, on day 3 of culture, was determined is illustrated in the density plots in Fig.4.7a. It is evident from these plots that NOD.H-2^k cells (Right panel) in culture exhibit a relatively higher incidence of apoptosis than B10.H-2^k cells (Left panel) in culture. Apoptotic cells, as represented by cells positive for MC540, are shown in the polygonal region. The small rectangular region on the same plots depicts counting beads added for the determination of absolute cell numbers. Approximately 10% of cells in B10.H-2^k bone marrow cultures underwent apoptosis on each of the first 3 days of culture (Fig.4.7c). By contrast, the level of apoptosis in the NOD.H-2^k cultures was 13% on day 1 and increased to >25% on day 3. Furthermore, the absolute number of apoptotic cells in NOD.H-2^k cultures was higher than in B10.H-2^k cultures on days 2 and 3. A high and comparable absolute number of apoptotic cells is detected in both cultures on day 1 as a result of cells unresponsive to growth factors undergoing apoptosis. These results indicate that heterogeneous proliferation of NOD.H-2^k myeloid cells is accompanied by markedly elevated levels of apoptosis in culture.

The preceding results clearly demonstrate that NOD.H-2^k bone marrow cells in culture exhibit proliferative and apoptotic trends distinct from that exhibited by B10.H-2^k cells in culture. Taken together, the above results indicate that heterogeneous proliferation and elevated levels of apoptosis underpin the reduced dendritic cell yield generated from NOD.H-2^k bone marrow cultures. The simplest interpretation of this data is that NOD.H-2^k cells have a much higher probability of undergoing apoptosis at each cell division, resulting in fewer cells making multiple divisions and a rising fraction of apoptotic cells. *

4.7 Heterogeneous Proliferation is Unique to NOD.H-2^k Bone Marrow Cells in Culture

It was concluded from the preceding data that non-MHC NOD genes confer on NOD.H-2^k myeloid precursors an aberrant growth phenotype that was cell-intrinsic and manifested in the form of heterogeneous proliferation (as indicated by cells undergoing variable numbers of cell division) and elevated levels of apoptosis in vitro. To examine whether this trait was uniquely conferred by non-MHC NOD genes, three other H-2^k congenic strains, CBA/H, AKR and Balb.H-2^k, were tested by the same in vitro

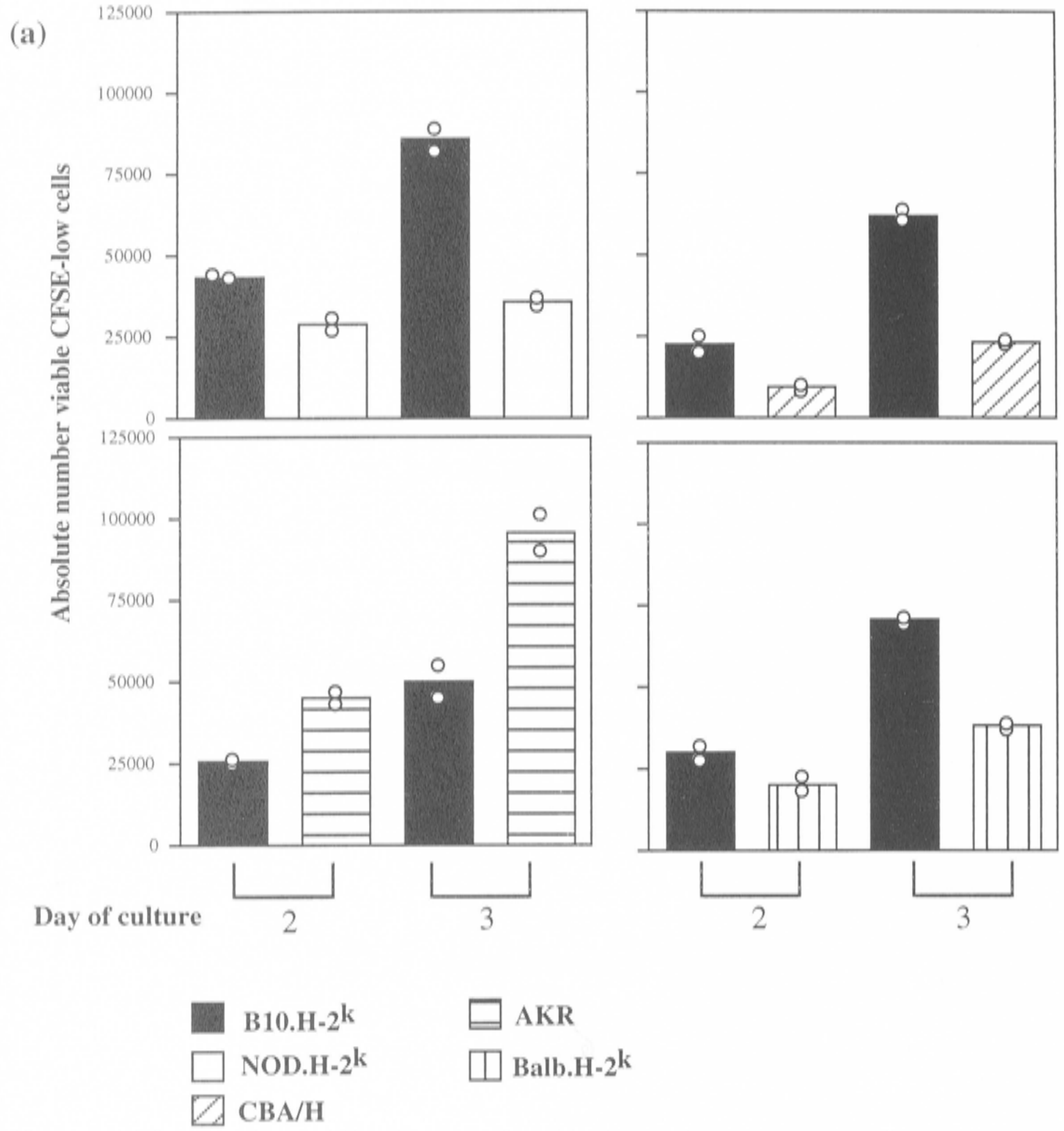

Figure 4.8

Heterogeneous proliferation and elevated levels of apoptosis is unique to NOD.H-2^k bone marrow cultures.

Bone marrow from the H-2^k congenic strains, CBA/H, AKR and Balb.H-2^k, were tested by the in vitro proliferation and apoptosis assay described in Fig.4.7. Bone marrow cultures from each of these strains were compared with parallel cultures from the B10.H-2^k strain.

(a) Proliferation on days 2-3 as revealed by CFSE dilution in each of the cultures.

(b) Representative proliferation profiles of selected strains.

(c) Apoptotic cells on days 2-3 were detected by MC540 positivity. Circles represent value from bone marrow cultures derived from single mice, and columns depict mean values.

Figure 4.8

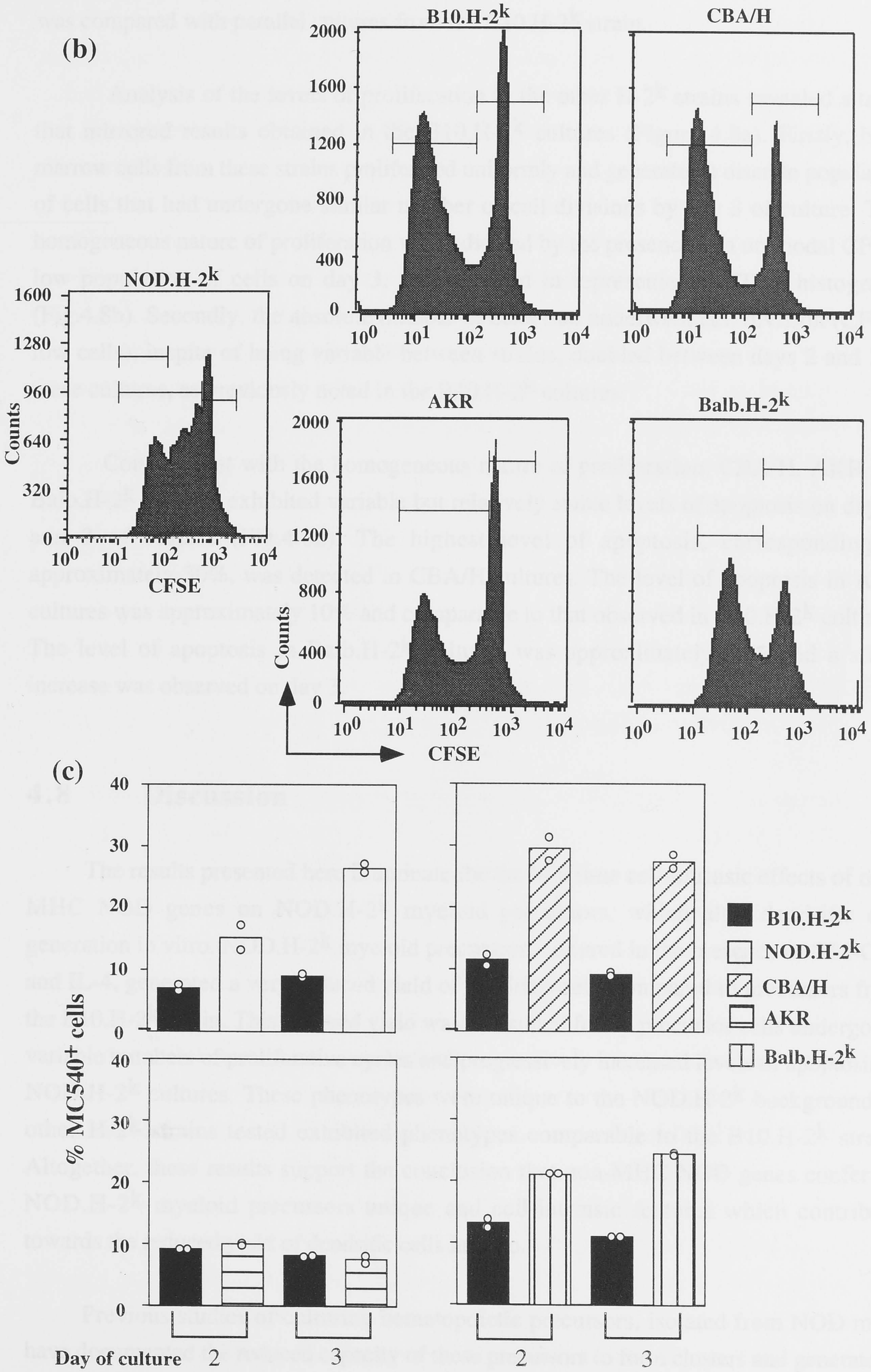
(b)
B10.H-2k
CBA/H
NOD.H-2k
AKR
Balb.H-2k
Counts
CFSE
(c)
% MC540+ cells
Day of culture
2
3
B10.H-2k
NOD.H-2k
CBA/H
AKR
Balb.H-2k

proliferation and apoptosis assay. Bone marrow cultures from each of these H-2^k strains was compared with parallel cultures from the B10.H-2^k strain.

Analysis of the levels of proliferation in the other H-2^k strains revealed a trend that mirrored results obtained in the B10.H-2^k cultures (Figure 4.8a). Firstly, bone marrow cells from these strains proliferated uniformly and generated a discrete population of cells that had undergone similar number of cell divisions by day 3 of culture. This homogeneous nature of proliferation was indicated by the presence of a unimodal CFSE-low population of cells on day 3, as illustrated in representative CFSE histograms (Fig.4.8b). Secondly, the absolute number of cells that underwent cell division (CFSE-low cells), inspite of being variable between strains, doubled between days 2 and 3 in these cultures, as previously noted in the B10.H-2^k cultures.

Concomitant with the homogeneous nature of proliferation, CBA/H, AKR and Balb.H-2^k cultures exhibited variable but relatively stable levels of apoptosis on days 2 and 3 of culture (Fig.4.8c). The highest level of apoptosis, corresponding to approximately 30%, was detected in CBA/H cultures. The level of apoptosis in AKR cultures was approximately 10% and comparable to that observed in B10.H-2^k cultures. The level of apoptosis in Balb.H-2^k cultures was approximately 20% and a slight increase was observed on day 3.

4.8 Discussion

The results presented here illuminate for the first time cell-intrinsic effects of non-MHC NOD genes on NOD.H-2^k myeloid precursors, which alter dendritic cell generation in vitro. NOD.H-2^k myeloid precursors, cultured in the presence of GM-CSF and IL-4, generated a very reduced yield of dendritic cells compared to precursors from the B10.H-2^k strain. This reduced yield was accounted for by precursor cells undergoing variable numbers of proliferative cycles and progressively increased levels of apoptosis in NOD.H-2^k cultures. These phenotypes were unique to the NOD.H-2^k background as other H-2^k strains tested exhibited phenotypes comparable to the B10.H-2^k strain. Altogether, these results support the conclusion that non-MHC NOD genes confer on NOD.H-2^k myeloid precursors unique and cell-intrinsic features which contribute towards the reduced yield of dendritic cells in vitro.

Previous studies of culturing hematopoietic precursors, isolated from NOD mice have documented the reduced capacity of these precursors to form clusters and generate

antigen presenting cells, including dendritic cells (Serreze et al, 1993a and b; Langmuir et al, 1993; Morel et al, 1999). NOD bone marrow cells generated fewer colonies in vitro than Balb/c bone marrow cells, in response to stimulation with myeloid growth factors including GM-CSF, IL-3 and IL-5 (Langmuir et al, 1993). This phenotype, however, could not be replicated in vivo as NOD myeloid precursors generated comparable number of colonies in the spleen when injected into irradiated syngeneic recipients, compared with precursors from control Balb/c mice. In a related study, it was shown that CSF-1 and IFNγ stimulation of NOD bone marrow cells resulted in abnormal macrophage development and maturation (Serreze et al, 1993a and b). Macrophages generated in vitro from disease-resistant strains secreted higher levels of LPS-stimulated IL-1 compared with macrophages generated from NOD bone marrow cells. Most recently, Morel et al (1999) have demonstrated that NOD-derived bone marrow cells, cultured in the presence of GM-CSF and IL-4, generate a lower yield of dendritic cells than diabetes-resistant B10.H-2^k bone marrow cells. Data generated in this study from the culture of B10.H-2^k- and NOD.H-2^k-derived bone marrow cells confirm the evidence provided by the preceding reports. Furthermore, the proliferation and apoptosis assay employed to analyze B10.H-2^k and NOD.H-2^k bone marrow cultures provide an important extension of previous findings by revealing mechanisms responsible for the reduced yield of dendritic cells from NOD.H-2^k bone marrow cultures. Significantly, results described here demonstrate for the first time that the reduced yield of dendritic cells from NOD.H-2^k cultures is a phenotype cell-intrinsic to NOD.H-2^k myeloid precursors.

One mechanistic hypothesis to explain the observed outcomes during the culture of NOD.H-2^k myeloid precursors would be impaired signalling transduced by GM-CSF. Since GM-CSF, IL-3 and IL-5 share a common β chain of the GM-CSF receptor (Miyajima et al, 1993), it is possible that the β common chain itself, and components proximally and/or distally involved, may be responsible for the in vitro phenotypes of NOD.H-2^k myeloid precursors. Thus, the β common chain signal transduction pathway merits investigation in the context of autoimmune diabetes in NOD mice. It is conceivable that NOD.H-2^k hematopoietic precursors transduce an exaggerated initial proliferative signal which in vitro is not matched by complementary survival/differentiation signal/s. This issue will be discussed in detail in the General Discussion (Chapter 6).

As mentioned previously, several possibilities could explain the reduced yield of dendritic cells from NOD.H-2^k bone marrow cultures. These possibilities include reduced proliferation, increased levels of apoptosis, inability to differentiate, or a combination of these factors attributable to NOD.H-2^k myeloid precursors. The in vitro proliferation and apoptosis assay utilized in the analysis of bone marrow cultures

facilitated the resolution between the various possibilities. It was evident from bone marrow cultures that NOD.H-2^k myeloid precursors underwent variable number of cell divisions (heterogeneous proliferation). In addition to the heterogeneous nature of proliferation, NOD.H-2^k bone marrow cultures exhibited a progressive increase in the fraction of apoptotic cells during the course of culture. This reduces the number of NOD.H-2^k precursors entering successive proliferative cycles. By contrast, myeloid precursors in B10.H-2^k cultures divided uniformly and underwent similar number of proliferative cycles. B10.H-2^k bone marrow cultures also exhibited a constant, relatively low fraction of apoptotic cells during the course of culture. Taken together, the simplest interpretation of these results is that heterogeneous proliferation is due to a much higher fraction of cells dying during each cell division, thus dramatically reducing the yield of dendritic cells from NOD.H-2^k bone marrow cultures.

The proliferation and apoptosis response of NOD.H-2^k myeloid precursors, stimulated with GM-CSF and IL-4, was found to be uniquely conferred by non-MHC NOD genes. This finding potentially implicates myeloid-derived antigen presenting cells, especially dendritic cells, in the pathology of autoimmune diabetes. Consistent with the findings from this study of NOD.H-2^k mice and studies conducted using the NOD mouse, in vitro hematopoietic growth defects have also been reported in human diabetics and prediabetics (Jansen et al, 1995; Takahashi et al, 1998). Dendritic cells generated from monocyte precursors isolated from blood of diabetics showed a reduced ability to cluster and to stimulate autologous and allogeneic T cells, compared to dendritic cells generated from healthy controls. Similarly, monocyte-derived precursors from the blood of prediabetics responded suboptimally in response to stimulation with GM-CSF and IL-4 (Takahashi et al, 1998). In contrast to controls matched for age, sex and MHC genotype, precursors from prediabetics generated fewer dendritic cells which appeared phenotypically and functionally compromised. These dendritic cells expressed lower levels of costimulatory molecules on the cell surface and were relatively inefficient in stimulating autologous T cells. Overall, findings from the current study and studies in NOD mice and in human diabetics or prediabetics, suggest a potential dysregulation in the antigen presenting cell population, especially in dendritic cell function, which coexist with the onset and maintenance of autoimmune diabetes.

Chapter 5

In Vivo Analysis of NOD.H-2^k-derived Dendritic Cells

5.1 Introduction

In vitro results described in the previous Results Chapter clearly demonstrated unique and cell-intrinsic effects of non-MHC NOD genes on NOD.H-2^k myeloid precursors. These effects were manifested in the form of elevated levels of apoptosis and fewer cells entering successive divisions and variable rates of division (heterogeneous proliferation), and consequent reduced dendritic cell yield, when NOD.H-2^k myeloid precursors were cultured in the presence of GM-CSF and IL-4. By contrast, control B10.H-2^k myeloid precursors exhibited a basal level of apoptosis and proliferated homogeneously: growth factor responsive cells underwent a relatively uniform number of divisions and at a uniform rate, generating a greater yield of dendritic cells.

Given the reduced capacity of NOD.H-2^k myeloid precursors to generate dendritic cells in vitro, an expected in vivo correlate would be a deficiency in dendritic cell numbers in the NOD.H-2^k mouse. However, since both GM-CSF and the β common chain of the GM-CSF receptor are dispensable for dendritic cell production in vivo (Vremec et al, 1997), the possibility of alternate physiological phenotypes, besides numerical deficiency of dendritic cells in NOD.H-2^k mice, could not be discounted. There are precedents for growth factor redundancy in the development of lymphoid and myeloid cells under physiological conditions. These have been demonstrated in specific ligand and/or receptor deficient mice. For example, in vitro studies show that stem cell factor (SCF) synergizes with IL-7 to induce the proliferation and differentiation of B cell precursors (McNiece et al, 1991; Hirayama et al, 1992; Yasunaga et al, 1995). However, c-kit (receptor for SCF) is dispensable for the in vivo production of B cells since foetal liver cells from c-kit-deficient mice can reconstitute immature and mature B cells in B and T cell-deficient RAG2-deficient mice (Takeda et al, 1997). Similarly, it has previously been reported that IL-3 can augment SCF-dependent mast cell development in vitro (Tsuji et al, 1991). In vivo results from IL-3-deficient mice again contradict in vitro findings by showing that IL-3 is not essential for the generation of mast cells or basophils under physiological conditions (Lantz et al, 1998).

The overall objective for this part of the study was, therefore, to extend the study of dendritic cells to a physiological context. Given the reduced capacity of NOD.H-2^k myeloid precursors to generate dendritic cells in vitro, the initial objective of this part of the study was to quantitate the absolute numbers of primary splenic and thymic dendritic cells in B10.H-2^k and NOD.H-2^k mice. The second objective for this part of the study was to determine the relative physiological capacity of B10.H-2^k and NOD.H-2^k myeloid precursors to reconstitute an irradiated host and generate dendritic cells in vivo.

5.2 Presence of a Putative 'Immature' Dendritic Cell Population in Spleen and Thymus of NOD.H-2^k Mice

A possible in vivo correlate of the reduced capacity of NOD.H-2^k myeloid precursors to generate dendritic cells in vitro was a numerical deficiency of dendritic cells in the NOD.H-2^k mouse. In order to investigate this possibility, enumeration of B10.H-2^k or NOD.H-2^k splenic and thymic dendritic cells in vivo was performed by flow cytometric analyses of dendritic cells enriched from tissue. Since dendritic cells constitute only a trace population in tissue and are firmly attached to tissue stroma, splenic and thymic dendritic cells were released into single cell suspension by collagenase digestion of tissue and subsequently enriched by collecting low density cells after centrifugation on a metrizamide gradient (Vremec and Shortman, 1997). Dendritic cell-enriched low density cells were stained with N418 (anti-CD11c) and anti-MHC class II monoclonal antibodies and analyzed by flow cytometry. As before, inclusion of counting beads in the assay enabled absolute quantitation of tissue-derived dendritic cells. Each dendritic cell quantitation experiment was performed by pair-wise analysis of B10.H-2^k and NOD.H-2^k spleen and thymus. Mice were matched for age and sex for this analysis.

What became obvious during the initial attempts to quantitate dendritic cells in vivo, was a consistent difference in the cell surface expression of MHC class II molecules on both splenic and thymic dendritic cells from the B10.H-2^k and NOD.H-2^k strains. Most splenic dendritic cells from B10.H-2^k mice expressed high levels of MHC class II molecules (Figure 5.1a). Splenic dendritic cells from B10.H-2^k mice were represented mainly by a subset expressing high levels of cell surface MHC class II molecules. In contrast, dendritic cells from the spleen of NOD.H-2^k mice were also represented by a sizeable population of MHC class II-low expressing dendritic cells. Furthermore, thymic dendritic cells from NOD.H-2^k mice comprised predominantly dendritic cells expressing low levels of MHC class II molecules. The presence of dendritic cells expressing intermediate and low levels of MHC class II molecules in the spleen and thymus, respectively, of NOD.H-2^k mice becomes clearer when the relative proportions of

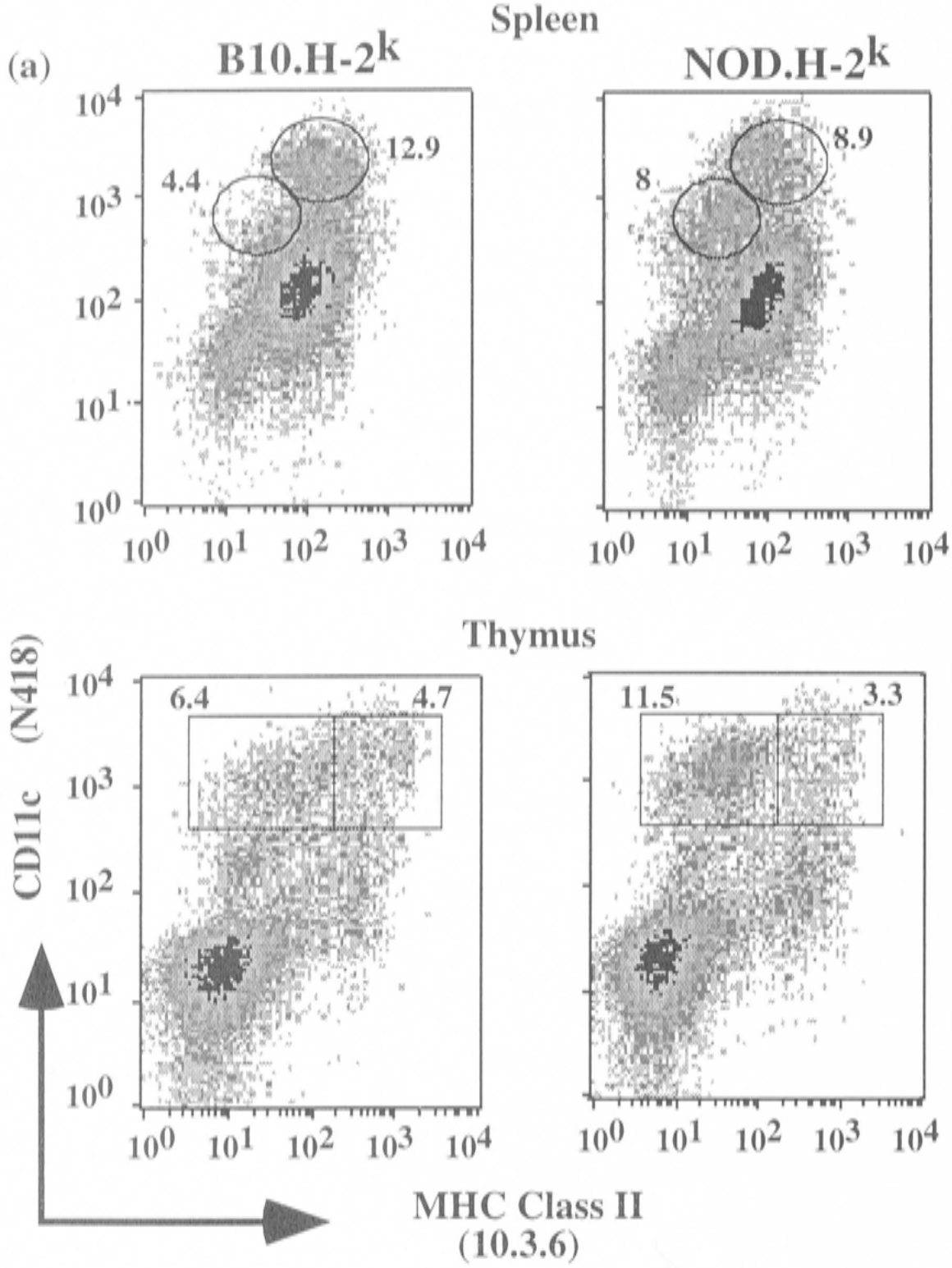

Figure 5.1

Heterogeneity in cell surface MHC class II expression on splenic and thymic dendritic cells from NOD.H-2^k mice.

Dendritic cells from B10.H-2^k or NOD.H-2^k spleen and thymus were obtained by collagenase digestion, followed by enrichment of dendritic cell-containing low density cells on metrizamide gradients. Low density cells were stained with anti-MHC class II (10.3.6) and anti-CD11c (N418) monoclonal antibodies and analyzed by 2-colour flow cytometry. Dendritic cells were gated on the basis of high forward scatter (relative size), CD11c and MHC class II expression and quantitated against known concentration of counting beads included in the assay.
(a) Representative FACS plots of spleen cells (top panels) or thymic cells (bottom panels) are shown. Numbers beside regions represent percentage of large, low density cells in that region.

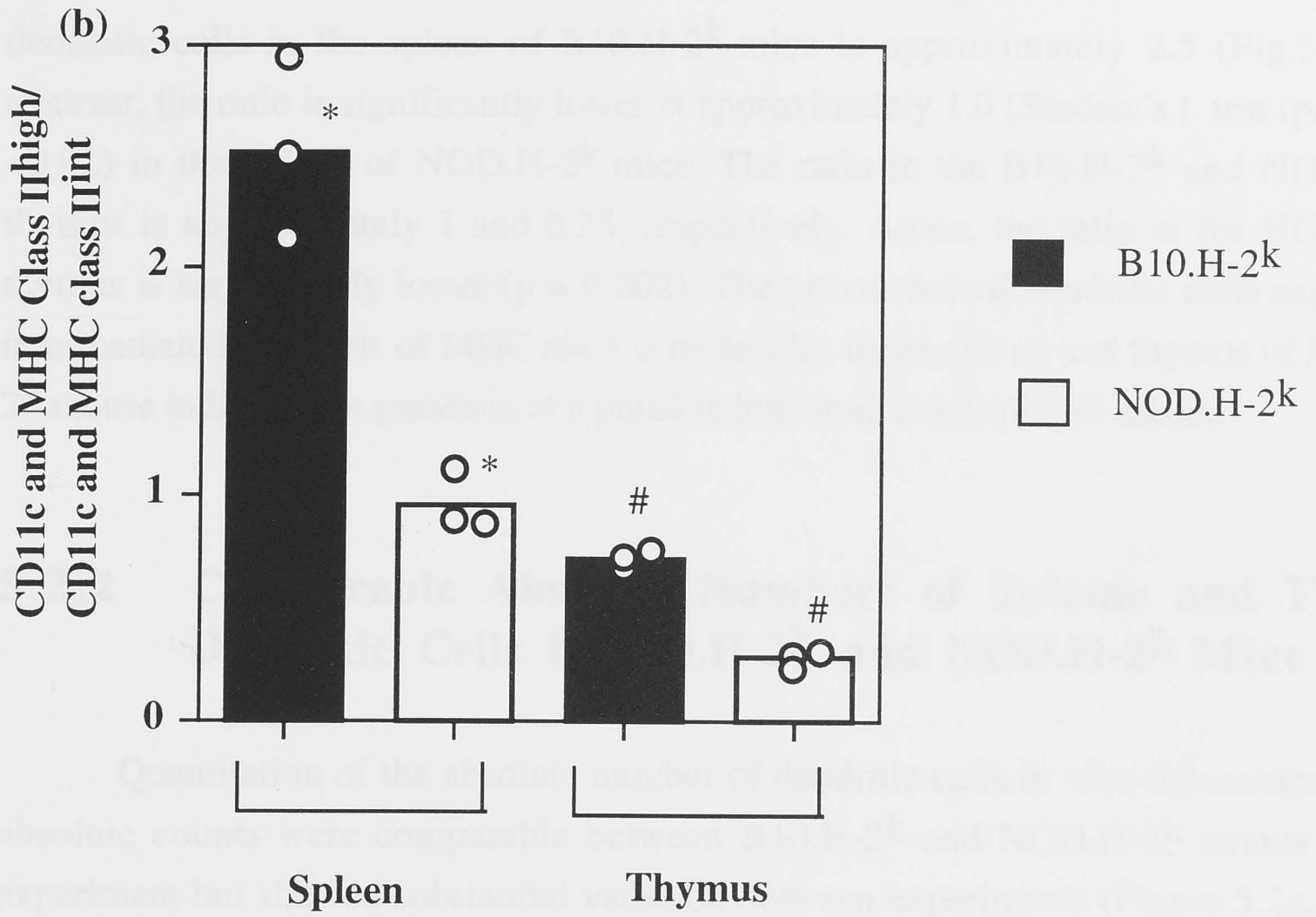

Figure 5.1

Heterogeneity in cell surface MHC class II expression on splenic and thymic dendritic cells from NOD.H-2^k mice.

(b) The ratio of MHC class II-high to MHC class II-intermediate dendritic cells in the spleen and thymus of B10.H-2^k and NOD.H-2^k mice. Columns show mean ratios, circles represent ratio from individual mice. Data is compiled from three separate experiments involving pair-wise analysis of B10.H-2^k and NOD.H-2^k mice. The difference in splenic or thymic ratios between strains were tested for statistical significance using the Student's *t* test (paired).

* p = 0.016, # p = 0.002

dendritic cells expressing high and intermediate/low levels of MHC class II molecules in each strain are considered. The ratio of MHC class II-high to intermediate expressing dendritic cells in the spleen of B10.H-2^k mice is approximately 2.5 (Fig.5.1b). In contrast, the ratio is significantly lower at approximately 1.0 (Student's *t* test (paired), $p < 0.02$) in the spleen of NOD.H-2^k mice. The ratio in the B10.H-2^k and NOD.H-2^k thymus is approximately 1 and 0.25, respectively. Again, the ratio in the NOD.H-2^k thymus is significantly lower ($p = 0.002$). The prevalence of dendritic cells expressing intermediate/low levels of MHC class II molecules in the spleen and thymus of NOD.H-2^k mouse indicates the presence of a putative immature dendritic cell subset.

5.2.2 Comparable Absolute Numbers of Splenic and Thymic Dendritic Cells in B10.H-2^k and NOD.H-2^k Mice

Quantitation of the absolute number of dendritic cells in vivo demonstrated that absolute counts were comparable between B10.H-2^k and NOD.H-2^k strains in each experiment but showed substantial variation between experiments (Figure 5.2a,b). This variation between experiments may be attributed to the intervening manipulations required before the eventual dendritic cell count. Due to this variation, absolute count data is also presented as a ratio of the absolute number of B10.H-2^k splenic or thymic dendritic cells to the absolute number of NOD.H-2^k splenic or thymic dendritic cells from each experiment. It is clear from this analysis that the ratio is approximately 1 in both the spleen and the thymus, indicating that similar absolute numbers of splenic or thymic dendritic cells are present in B10.H-2^k and NOD.H-2^k mice. Since the absolute number of splenic and thymic dendritic cells are comparable in both strains, this data suggests that NOD.H-2^k mice contain a larger pool of immature dendritic cells, or a smaller pool of mature dendritic cells.

5.3 Skewing of the Myeloid Lineage of Cells towards NOD.H-2^k Origin in Mixed Bone Marrow Chimeric Mice

To determine the in vivo potential of NOD.H-2^k hematopoietic stem cells and their progenitors, bone marrow reconstitution studies were performed. Mixed bone marrow chimeric mice were constructed by transferring into irradiated B10.H-2^k recipients an inoculum of total bone marrow cells from B10.H-2^k and/or NOD.H-2^k mice. There are important advantages with this experimental approach. Significantly, mixed bone

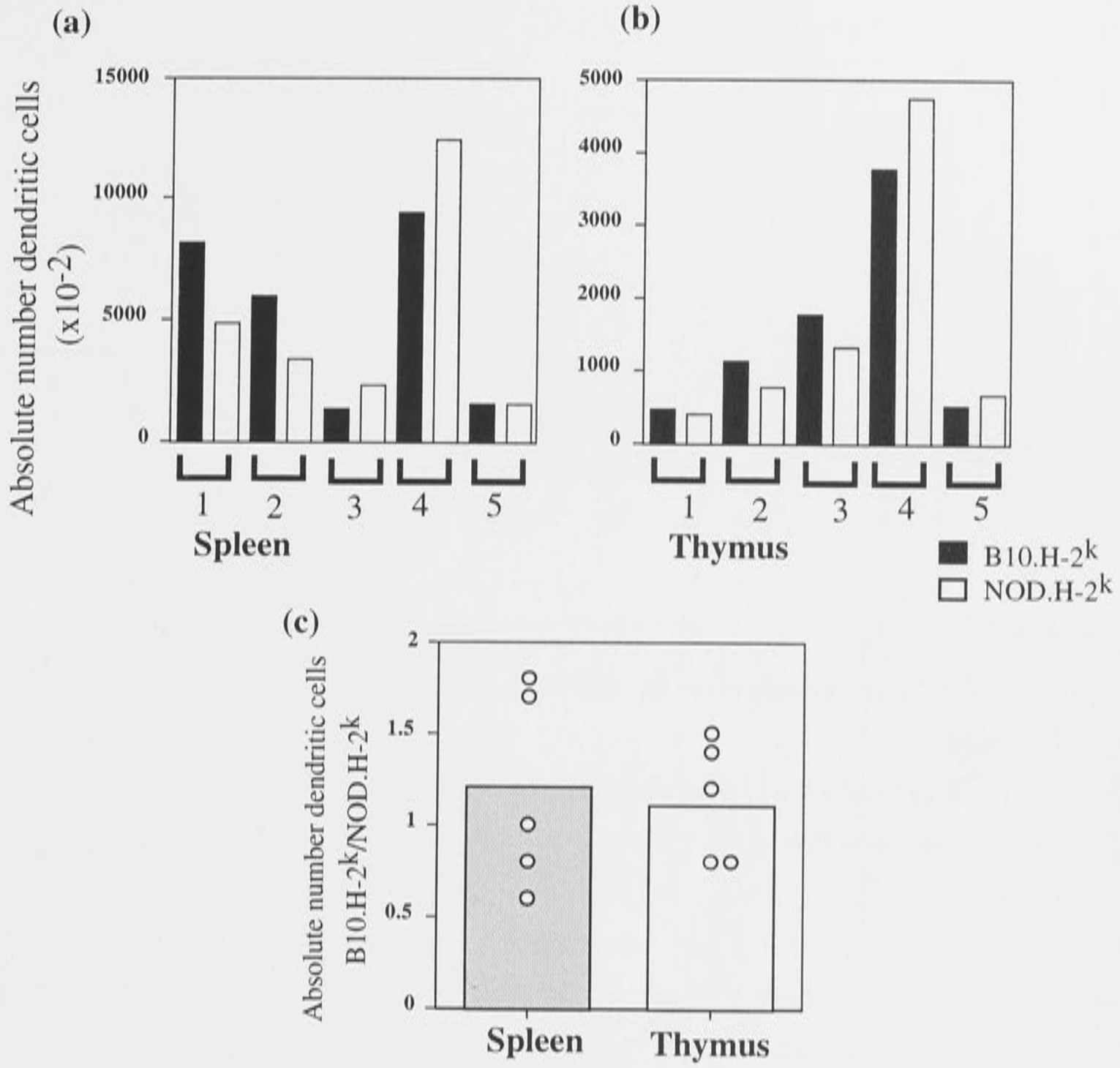

Figure 5.2

Comparable numbers of splenic and thymic dendritic cells in B10.H-2^k and NOD.H-2^k mice.

Dendritic cells from B10.H-2^k and NOD.H-2^k spleen and thymus were obtained, stained and analyzed as described in Fig.5.1.

a) and b) Absolute numbers of splenic and thymic dendritic cells in B10.H-2^k or NOD.H-2^k mice as quantitated in 5 separate experiments. Columns represent absolute number from individual mice analyzed pair-wise during 5 separate experiments.

c) Data is presented as ratio of the absolute number of splenic or thymic dendritic cells from B10.H-2^k mice to the absolute number of splenic or thymic dendritic cells from NOD.H-2^k mice. Columns represent mean ratio from 5 separate experiments involving pair-wise analysis of B10.H-2^k and NOD.H-2^k mice. Circles represent ratio from individual experiments.

Figure 5.3

The majority of blood monocytes in B/N->B chimeric mice are of NOD.H-2^k origin.

Irradiated B10.H-2^k recipients were reconstituted with B10.H-2^k bone marrow cells (B->B), NOD.H-2^k bone marrow cells (N->B), or with a 1:1 mixture of B10.H-2^k and NOD.H-2^k cells (B/N->B). Recipient mice were analyzed by 3-colour flow cytometry for donor-derived leukocytes in blood 8-12 weeks post-reconstitution. B cells, T cells and monocytes in blood were analyzed by using B220, Thy1 and Mac1 monoclonal antibodies, respectively. As before, $Ly5^a$ was used to distinguish between NOD.H-2^k- and B10.H-2^k-derived cells. Representative FACS plots illustrate the relative reconstitution of myeloid and lymphoid lineages in red blood cell-depleted blood leukocytes in recipient mice. Numbers in quadrants represent percentage of leukocytes in that quadrant.

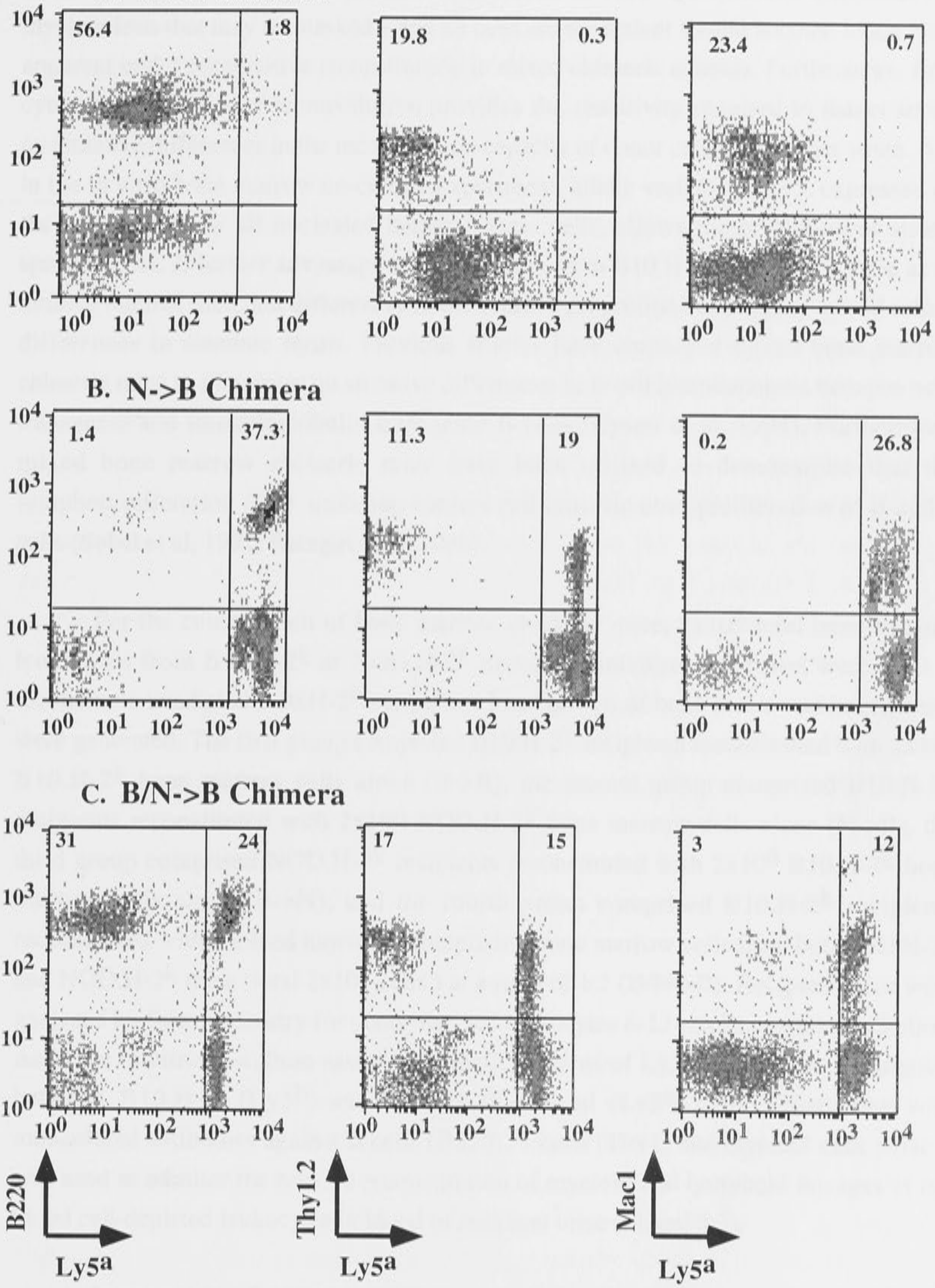

Figure 5.3
The majority of monocytes in B/N->B mixed bone marrow chimeric mice are of NOD.H-2^k origin.

marrow reconstitution studies should elucidate in vivo correlates of the cell-autonomous traits of NOD.H-2^k myeloid precursors observed in vitro. Quantitative differences in myelopoiesis that may be masked when all cells are equivalent should become much more apparent under competitive reconstitution in mixed chimeric animals. Furthermore, flow cytometric analysis of reconstitution provides the sensitivity required to detect subtle quantitative differences in the reconstitution capacity of donor cells from either strain. As in the in vitro bone marrow co-culture experiment, allelic variants of Ly5, expressed on the cell surface by all nucleated hematopoietic cells, allows the resolution of strain-specific cells. A further advantage is that progeny from B10.H-2^k precursors serve as an internal control such that differences in the relative proportions of progeny would reflect differences in absolute terms. Previous studies have employed mixed bone marrow chimeric mice to illuminate quantitative differences in B cell lymphopoiesis between non-transgenic and immunoglobulin transgenic B cells (Cyster et al, 1994). Furthermore, mixed bone marrow chimeric mice have been utilized to demonstrate that the lymphoproliferation *(lpr)* mutation confers cell intrinsic over-proliferation of B and T cells (Sobel et al, 1991; Katagiri et al, 1988).

For the construction of bone marrow chimeric mice, $2x10^6$ total bone marrow leukocytes from B10.H-2^k or NOD.H-2^k mice, or a mixture of the two, were used to reconstitute irradiated B10.H-2^k recipients. Four groups of bone marrow chimeric mice were generated. The first group comprised B10.H-2^k recipients reconstituted with $2x10^6$ B10.H-2^k bone marrow cells alone (B->B), the second group comprised B10.H-2^k recipients reconstituted with $2x10^6$ NOD.H-2^k bone marrow cells alone (N->B), the third group comprised NOD.H-2^k recipients reconstituted with $2x10^6$ B10.H-2^k bone marrow cells alone (B->N), and the fourth group comprised B10.H-2^k recipients reconstituted with a mixed inoculum comprising bone marrow cells from both B10.H-2^k and NOD.H-2^k mice (total $2x10^6$ cells) at a ratio of 1:1 (B/N->B). Recipient mice were analyzed by flow cytometry for donor-derived leukocytes 8-12 weeks post-reconstitution. As in the in vitro co-culture assays, the allelic variants of Ly5 were used to distinguish between B10.H-2^k ($Ly5^b$) and NOD.H-2^k-derived ($Ly5^a$) cells. Co-staining with monoclonal antibodies against B cells (B220), T cells (Thy1) and myeloid cells (Mac1) was used to monitor the relative reconstitution of myeloid and lymphoid lineages of red blood cell-depleted leukocytes in blood of recipient mice (Figure 5.3).

In control N->B chimeric mice, almost all B cells and monocytes were NOD.H-2^k-derived($Ly5^{a+}$), confirming efficient ablation of endogenous hematopoietic cells by the radiation regime employed, and efficient reconstitution with NOD.H-2^k bone marrow cells (Fig.5.3b). However, a proportion of host-derived, radio-resistant T cells still persist (Fig.5.3b, middle panel). Memory T cells are well established to be radio-resistant

(Sado et al, 1980). In contrast to B10.H-2^k recipients, efficient ablation of endogenous cells and reconstitution by donor bone marrow cells did not occur in the reciprocal control B->N chimeric mice (Figure 5.4). Almost all cells in this group of chimeric mice were host-derived. Similar resistance of NOD mice to bone marrow engraftment has been described (Kaufman et al, 1997). The B->B control group served as specificity controls for antibody staining for the Ly5 allotypes (Fig.5.3a).

In B/N->B mice receiving the mixed bone marrow inoculum, B and T cells were derived in approximately equal proportions from the two donors (Fig.5.3c). In contrast, the majority of blood monocytes (Mac1^+) were of NOD.H-2^k origin (Fig.5.3c, right panel). Like monocytes in blood, splenic and thymic dendritic cells in B/N->B group of mice were disproportionately of NOD.H-2^k origin, with NOD.H-2^k-derived dendritic cells constituting 87% total splenic dendritic cells and 82% thymic dendritic cells, respectively (Figure 5.5a-b). As in blood, B and T cells in the spleen and T cells in the thymus of B/N->B were practically even between the two donors (Figure 5.6). Analysis of multiple mixed bone marrow chimeric mice, from two separate experiments, is depicted in Figure 5.7. The mean ratio of NOD.H-2^k to B10.H-2^k leukocytes is approximately 1 for B and T cells in blood and spleen, and for T cells in the thymus. In stark contrast, the ratios for monocytes, thymic dendritic cells and splenic dendritic cells are approximately 4, 3 and 6, respectively. While lymphocytes in blood, spleen and thymus of mixed bone marrow chimeric mice were almost evenly derived from both donors, the myeloid lineage of cells were disproportionately derived from the NOD.H-2^k strain.

The above skewing of the myeloid lineage of cells in mixed bone marrow chimeric mice prompted the question whether this skewing occurred in relative or absolute terms. It was possible that the relative skewing observed was underpinned by an increase in absolute cellularity in the myeloid compartment or reduced cellularity in the lymphoid compartment, or both. To pursue this question, whole blood and red blood cell-depleted (processed) blood leukocytes from bone marrow chimeric mice were stained for B cells, T cells, monocytes and Ly5^a, and analyzed by 3-colour flow cytometry. Coulter counting beads were added to whole blood samples for quantitation of target cell populations. Erythrocytes and platelets were excluded from whole blood analysis by gating on leukocytes on the basis of their forward scatter (relative size) and side scatter (relative granularity, log scale: left panel in top row of Figure 5.8a). Counting beads were similarly gated on the basis of their distinct scatter profiles. Parallel analysis of whole and processed blood enabled absolute quantitation of monocytes which are too infrequent to detect in 2µL whole blood using the flow cytometer. B cells are the most numerous

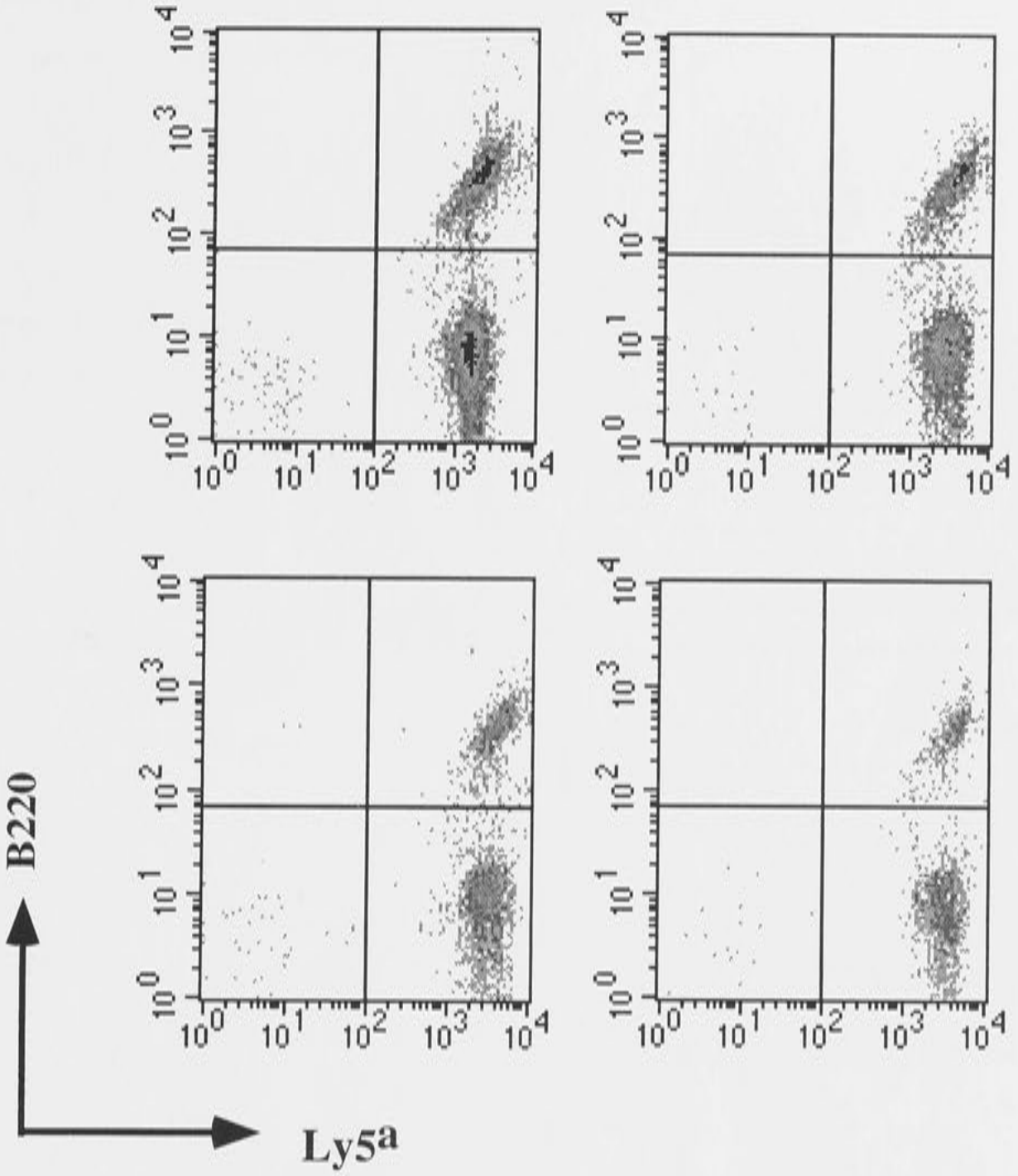

Figure 5.4

NOD.H-2^k recipients are resistant to engraftment.

Bone marrow chimeric mice, using NOD.H-2^k recipients, were constructed and analyzed for B cell reconstitution in blood as described in Fig.5.3. Each panel represents individual NOD.H-2^k recipient.

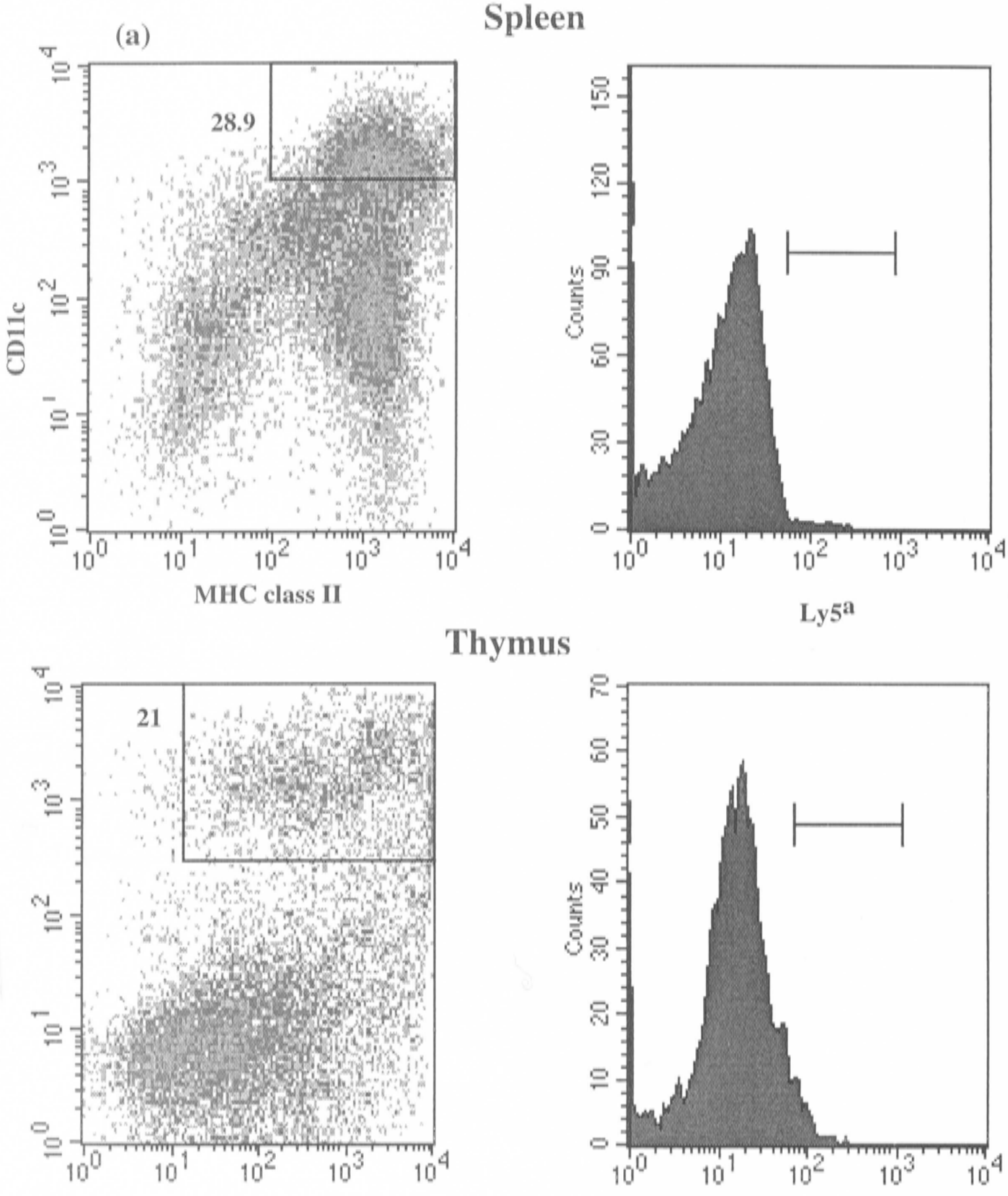

Figure 5.5

Specificity of Ly5^a staining.

(a) Splenic and thymic dendritic cells were obtained from B10.H-2^k mice, stained and analyzed as described in Fig.5.1 except cells were also stained with anti-Ly5^a monoclonal antibody to demonstrate specificity of Ly5^a staining. Splenic and thymic dendritic cells were gated on the basis of high forward scatter (relative size), MHC class II and CD11c expression. Histograms demonstrate control Ly5^a staining of B10.H-2^k dendritic cells. Numbers next to rectangular regions represent percentage dendritic cells in low density, large cells.

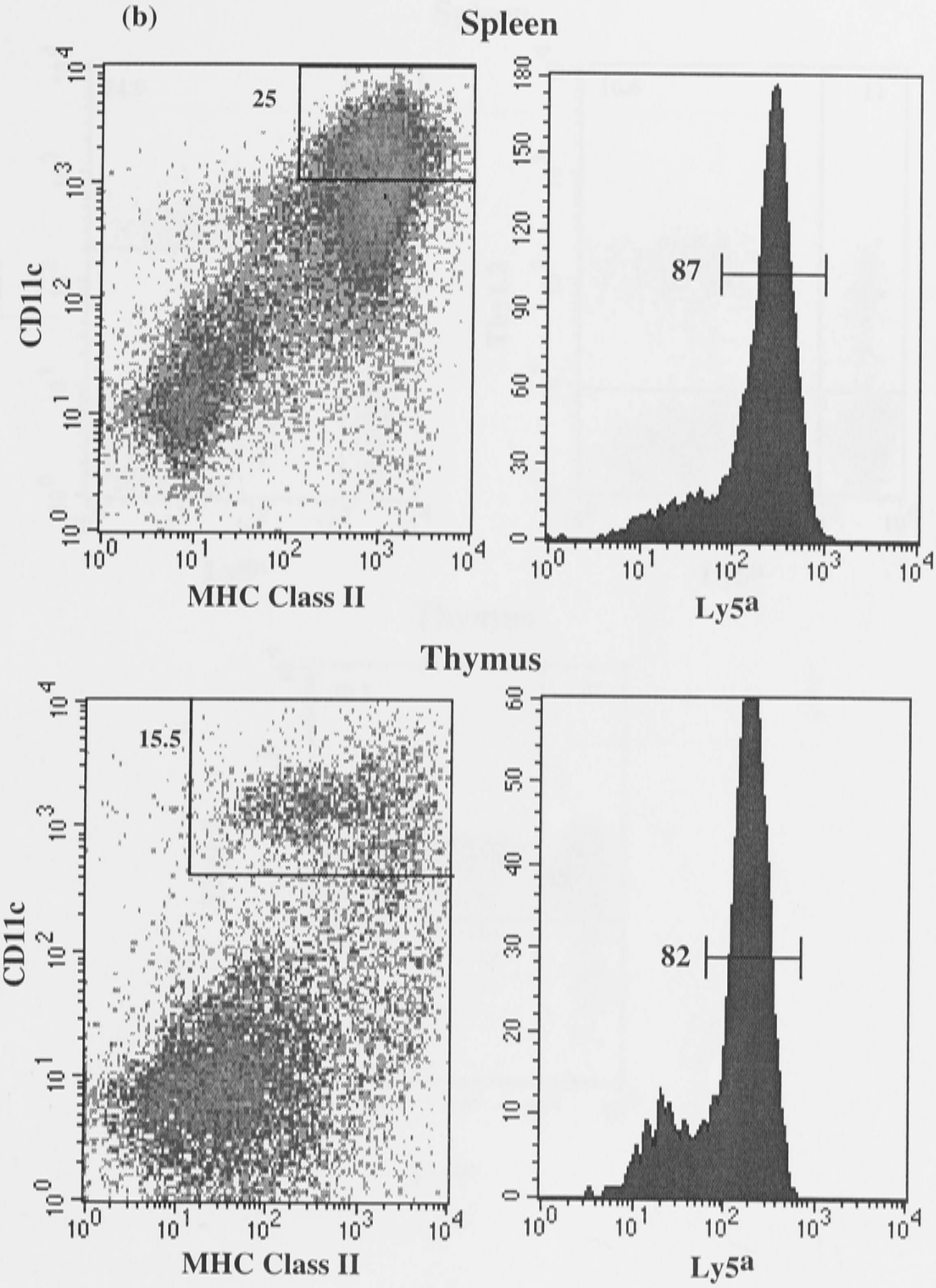

Figure 5.5

The majority of splenic and thymic dendritic cells in B/N->B mixed bone marrow chimeric mice are of NOD.H-2^k origin.

(b) Splenic and thymic dendritic cells in B/N->B mixed bone marrow chimeric mice were analyzed as described in (a). Numbers in histograms represent percentage of dendritic cells that are NOD.H-2^k-derived.

Fig. 5.5

Note: It appears that cells bearing the unique NOD.H-2^k Fc receptor bind SA-TC. Hence, a subset of NOD.H-2^k splenic cells exhibit intermediate fluorescence in the CD11c channel.

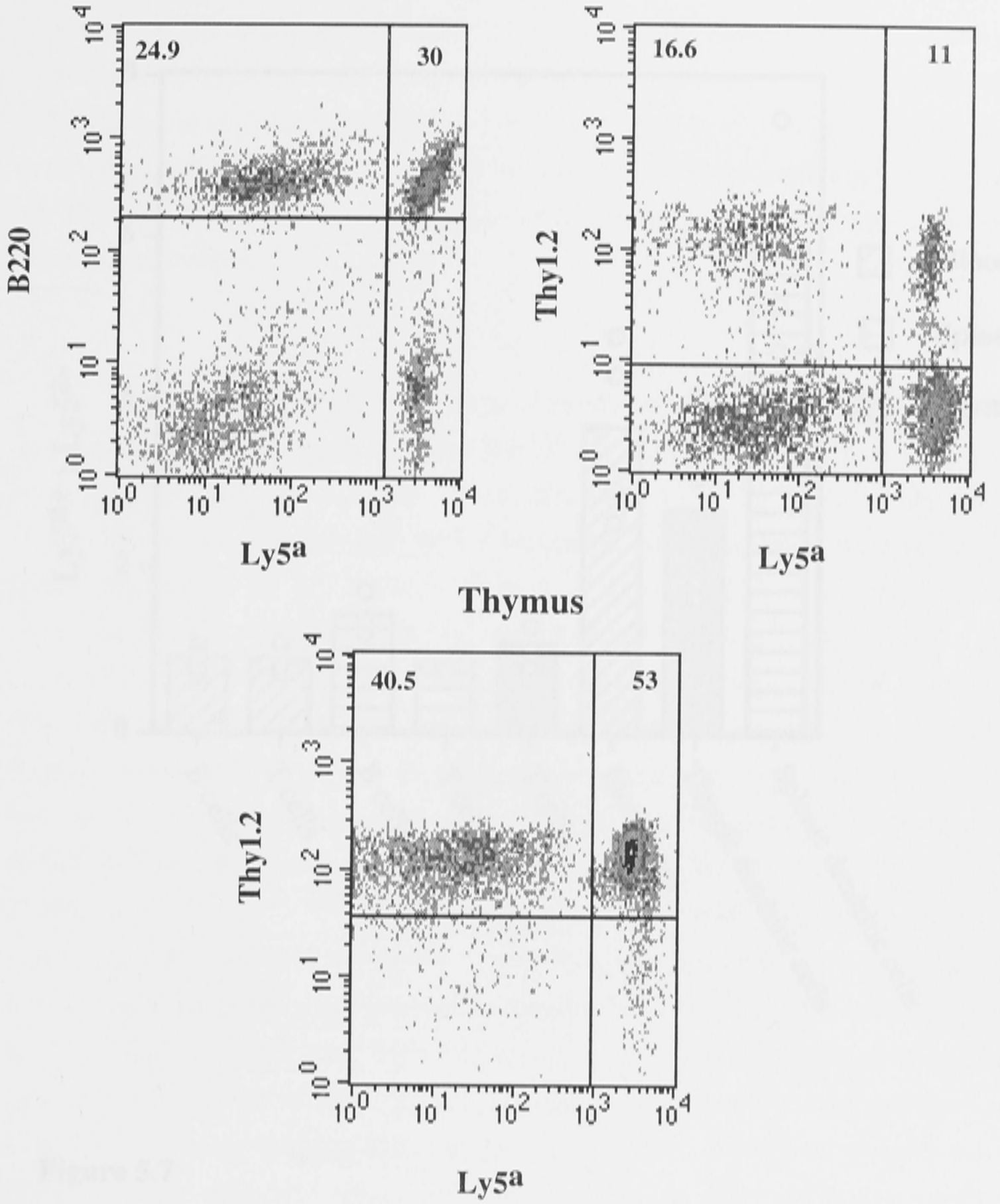

Figure 5.6

B cells and T cells in spleen and T cells in thymus of B/N->B chimeric mice are derived in approximately equal proportions from both donors.

Spleen and thymus harvested from B/N->B chimeric mice 8-12 weeks post-reconstitution were digested with collagenase to obtain single cell suspensions. Cells were stained for B and T cell markers and analyzed by 3-colour flow cytometry. Numbers in quadrants represent the percentage of leukocytes in that quadrant.

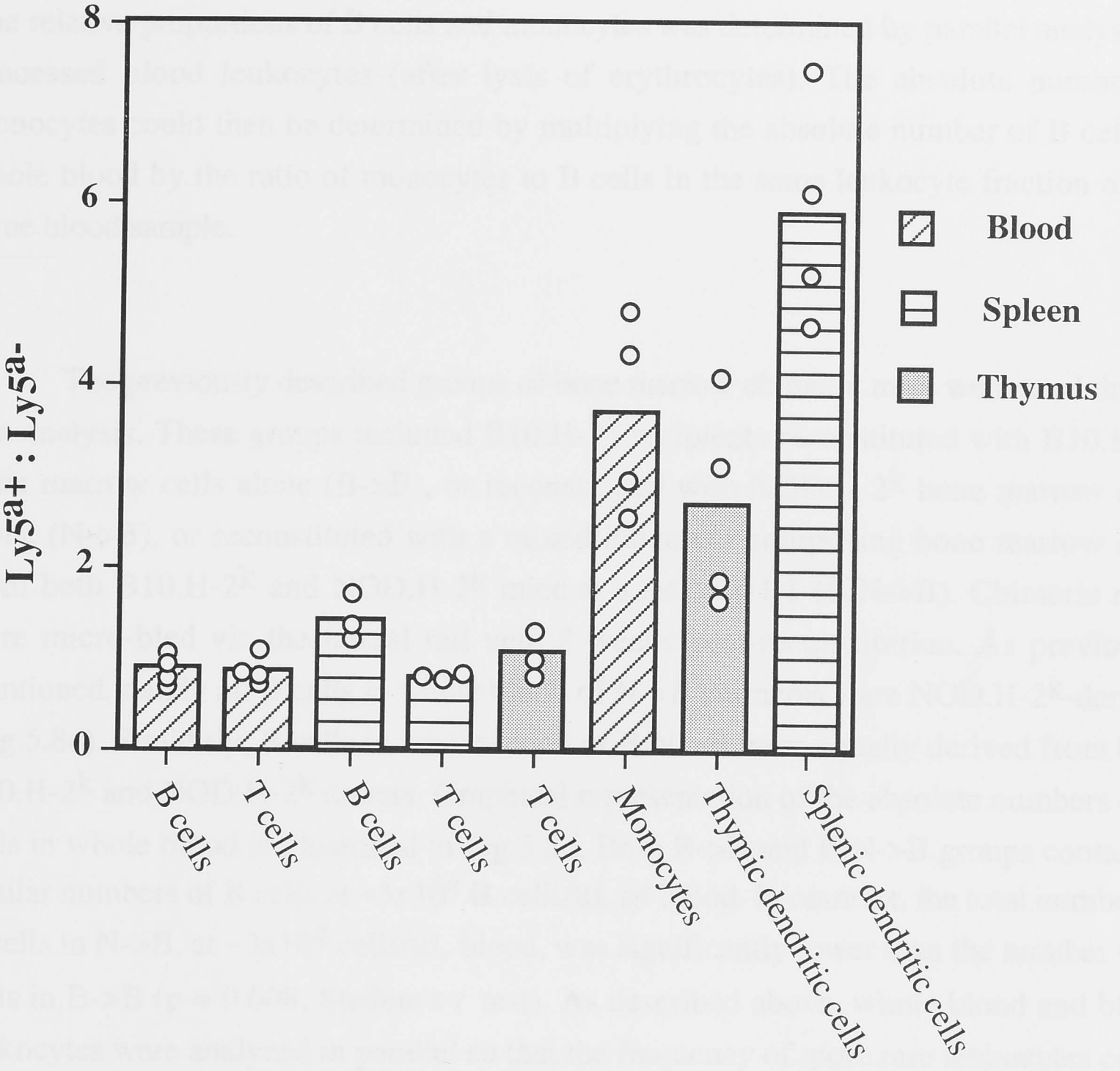

Figure 5.7

Preferential generation of NOD.H-2^k-derived myeloid lineage of cells in B/N->B chimeric mice.

Summary data pooled from two separate bone marrow chimeric experiments showing the $Ly5^{a+}$ to $Ly5^{a-}$ ratio of each of the shown leukocyte population in blood, spleen and thymus of B/N->B mixed bone marrow chimeric mice. Columns represent mean ratios, and circles represent ratio from individual mixed bone marrow chimeric mice.

leukocyte in whole blood and readily detectable and countable with the flow cytometer. The relative proportions of B cells and monocytes was determined by parallel analysis of processed blood leukocytes (after lysis of erythrocytes). The absolute number of monocytes could then be determined by multiplying the absolute number of B cells in whole blood by the ratio of monocytes to B cells in the same leukocyte fraction of the same blood sample.

The previously described groups of bone marrow chimeric mice were used during this analysis. These groups included B10.H-2^k recipients reconstituted with B10.H-2^k bone marrow cells alone (B->B), or reconstituted with NOD.H-2^k bone marrow cells alone (N->B), or reconstituted with a mixed inoculum comprising bone marrow cells from both B10.H-2^k and NOD.H-2^k mice at a ratio of 1:1 (B/N->B). Chimeric mice were micro-bled via the lateral tail vein 8 weeks post-reconstitution. As previously mentioned, nearly all B cells in whole blood of N->B chimeras were NOD.H-2^k-derived (Fig.5.8c). Similarly, B cells in whole blood of B/N->B were equally derived from both B10.H-2^k and NOD.H-2^k donors. Graphical representation of the absolute numbers of B cells in whole blood is illustrated in Fig.5.8d. Both B->B and B/N->B groups contained similar numbers of B cells at ~$5x10^4$ B cells/μL of blood. In contrast, the total number of B cells in N->B, at ~$3x10^4$ cells/μL blood, was significantly lower than the number of B cells in B->B ($p = 0.008$, Student's *t* test). As described above, whole blood and blood leukocytes were analyzed in parallel so that the frequency of more rare leukocytes could be determined by comparing their frequency relative to B cells. Absolute quantitation of monocytes in processed blood leukocytes of the three chimeric mice groups is shown in Fig.5.7e. It is clear that the skewing towards NOD.H-2^k-derived monocytes in mixed bone marrow chimeric mice (B/N->B) occurs in absolute terms, with $2.5x10^4$ monocytes/μL blood being NOD.H-2^k-derived compared with only $5x10^3$ monocytes/μL that were B10.H-2^k-derived. Thus, the skewing towards NOD.H-2^k-derived monocytes in B/N->B mixed chimeric mice is due to both the presence of a higher absolute number of NOD.H-2^k-derived monocytes, and a lower absolute number of B10.H-2^k-derived monocytes. The results obtained from the above analysis are indicative of a preferential generation of NOD.H-2^k-derived monocytes, and by inference the entire myeloid lineage of cells. Furthermore, these results suggest a possible predisposition of NOD.H-2^k myeloid precursors to over-produce myeloid cells at the expense of B cells.

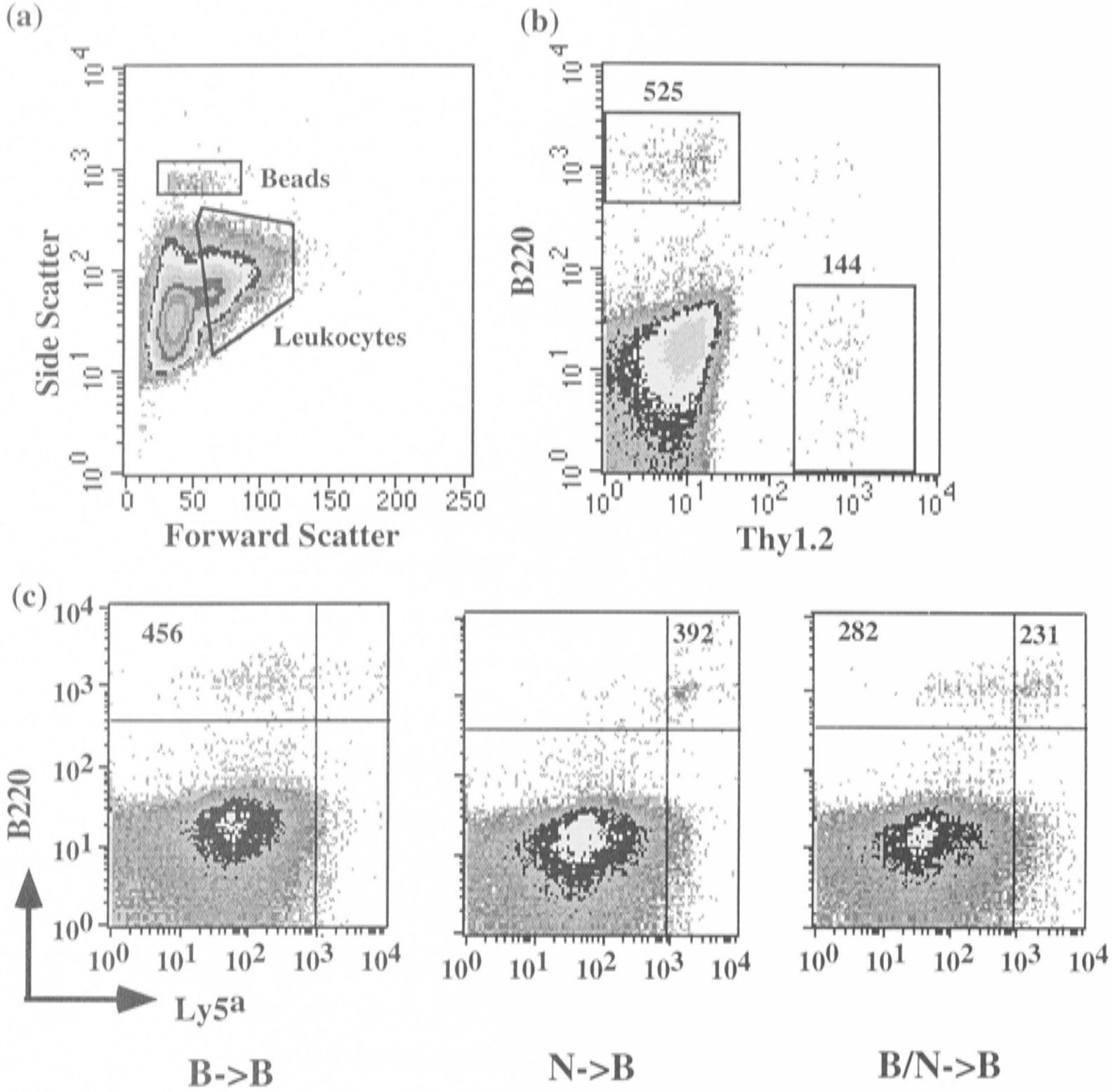

Figure 5.8

Skewing towards NOD.H-2^k-derived monocytes in mixed chimeric mice occurs in absolute terms.

The absolute number of B cells in whole blood of B->B, N->B and B/N->B chimeric mice was determined by staining whole blood in a one-step stain with a 25µL monoclonal antibody cocktail containing antibodies against B cells (B220-PE), T cells (Thy1.2-FITC) and Ly5^a-Biotin (preincubated with SA-TC). Samples were not washed after incubation with stains but were diluted in RPMI containing counting beads and immediately taken for acquisition on the flow cytometer.

(a) Counting beads were enumerated by gating on beads on the basis of their distinct forward and side scatter.

(b) Absolute number of B cells were enumerated on the basis of B220 staining on gated leukocytes.

(c) B cell reconstitution in bone marrow chimeric mice.

Numbers next to regions or in quadrants represent the number of events in that region or quadrant.

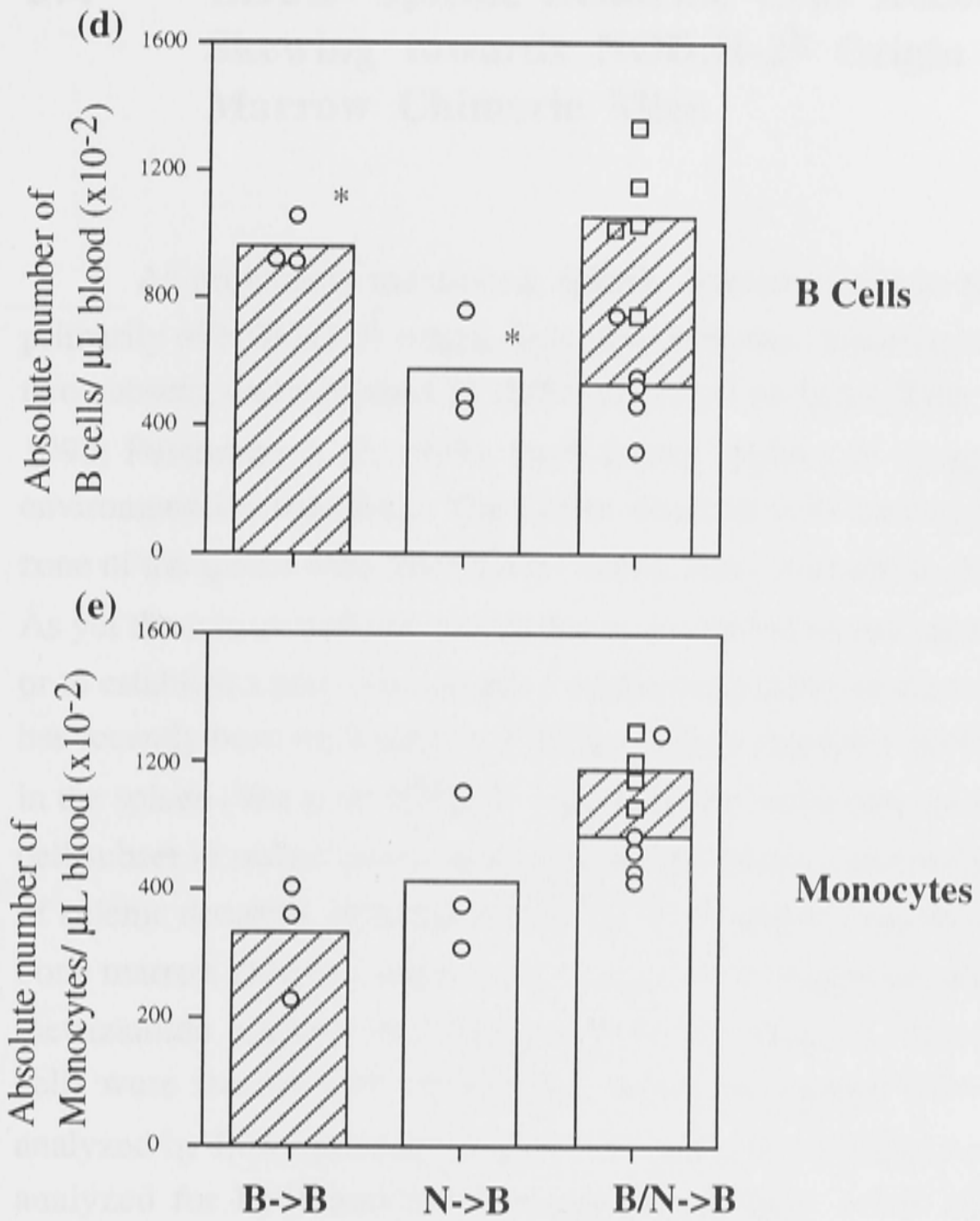

Figure 5.8

(d) The absolute number of B cells in whole blood of chimeric mice as determined in (a). * $p = 0.008$ (Student's *t* test)

(e) The absolute number of monocytes was quantitated by multiplying the ratio of monocytes to B cells in red blood cell-depleted blood leukocytes with absolute number of B cells in the same sample of whole blood. Hatched columns show mean number B10.H-2^k derived leukocytes, while white columns show NOD.H-2^k-derived leukocytes. Circles and squares represent values from blood of individual mice.

5.4 CD8α⁻ Splenic Dendritic Cells Account for the Skewing towards NOD.H-2^k Origin in Mixed Bone Marrow Chimeric Mice

As previously mentioned, splenic dendritic cells in mixed chimeric mice were primarily of NOD.H-2^k origin. Splenic and thymic dendritic cells in the mouse comprise two subsets, distinguished by differential cell surface CD8α expression (Vremec et al, 1992; Pulendran et al, 1997). Each subset appears to occupy distinct microanatomic environments in the spleen. The CD8α$^-$ dendritic cells seem to be resident in the marginal zone of the spleen while the CD8α$^+$ subset seem to reside in the T cell zone of the spleen. As yet there is no definitive evidence to assign functional specialization between subsets or to establish a precursor-progeny relationship between the two subsets. Interestingly, it has recently been reported that RelB selectively regulates the CD8α$^-$ dendritic cell subset in the spleen (Wu et al, 1998). It was, therefore, intriguing to ask which splenic dendritic cell subset in mixed bone marrow chimeric mice accounted for the pronounced skewing of splenic dendritic cells towards NOD.H-2^k origin. Splenic dendritic cells from mixed bone marrow chimeric mice were prepared by collagenase digestion and enrichment on metrizamide gradient as previously described (Fig.5.1). Enriched splenic low density cells were stained with monoclonal antibodies against CD11c, Ly5^a and CD8α, and analyzed by flow cytometry. Large cells positive for CD11c expression were gated and analyzed for Ly5^a and CD8α expression (Figure 5.9a). The over-representation of NOD.H-2^k-derived dendritic cells was primarily within the CD8α$^-$ subset, as the mean ratio of Ly5^{a+} to Ly5^{a-} CD8α$^+$ dendritic cells in mixed bone marrow chimeric mice was 2.6, whereas it was 5.3 in the CD8α$^-$ subset (Fig.5.9b). Thus, the CD8α$^-$ dendritic cell subset in mixed bone marrow chimeric mice was primarily responsible for the over-representation of splenic dendritic cells from the NOD.H-2^k donor. The high ratio of CD8α$^-$ to CD8α$^+$ splenic dendritic cells appeared to be a cell-intrinsic characteristic of the NOD.H-2^k strain since dendritic cells from unmanipulated NOD.H-2^k were 6.5:1 in favor of CD8α$^-$ dendritic cells, whereas dendritic cells from unmanipulated B10.H-2^k mice were more evenly balanced at 1.5:1 (Figure 5.10). The difference between the CD8α$^-$ to CD8α$^+$ splenic dendritic cell ratios from unmanipulated B10.H-2^k and NOD.H-2^k mice is statistically significant ($p = 0.0003$, Student's t test).

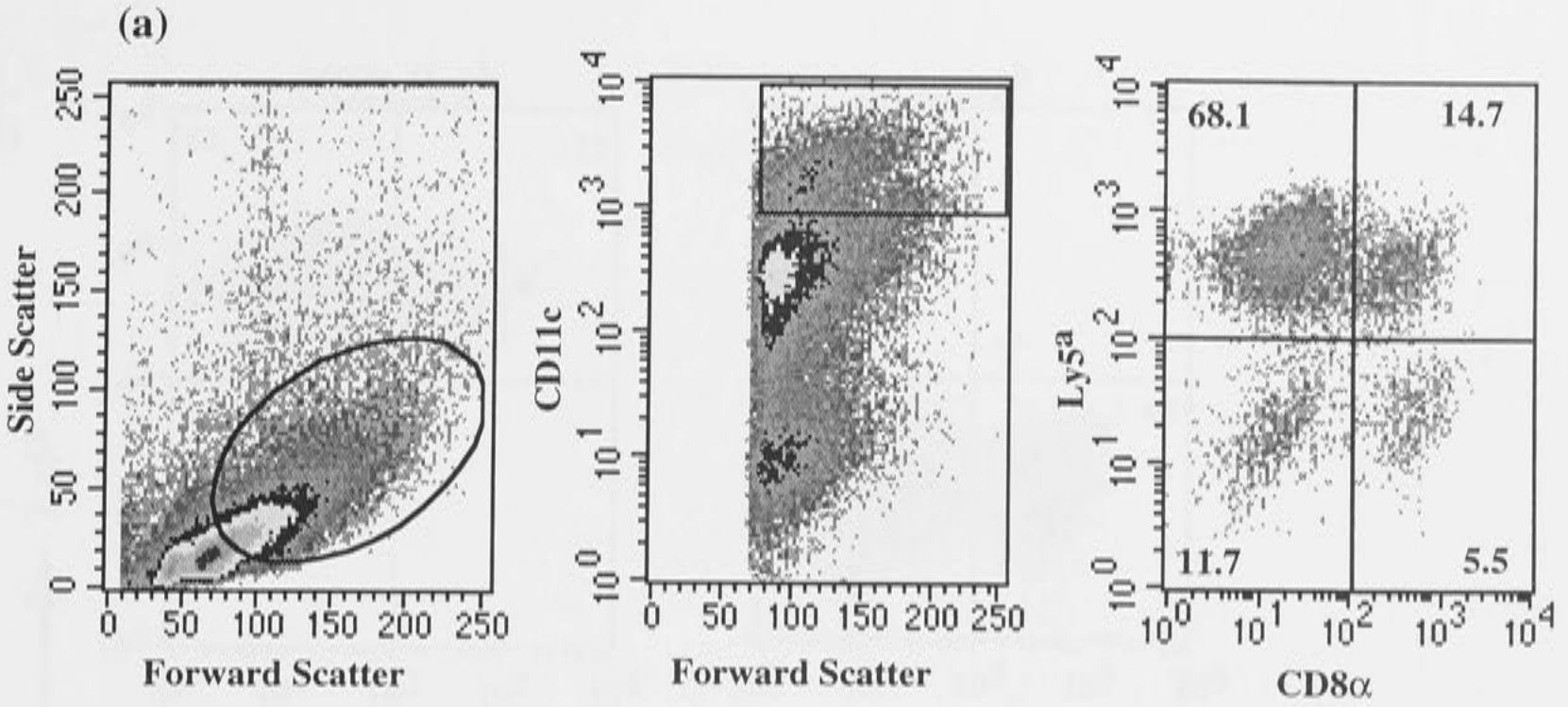

Figure 5.9

Skewing towards NOD.H-2^k-derived splenic dendritic cells in B/N->B is accounted for predominantly by the CD8α^- dendritic cell subset.

Splenic dendritic cells from mixed chimeric mice were obtained, stained and analyzed as described in Fig.5.5.

(a) Representative FACS plots illustrating relative proportions of splenic dendritic cell subsets in B/N->B chimeric mice. Numbers in quadrants represent percentage dendritic cells in that quadrant.

(b) Data is presented as the mean ratio of Ly5^{a+} to Ly5^{a-} dendritic cells (y-axis), against CD8α expression (x-axis). Columns represent mean ratios, and circles represent ratios from individual mice.

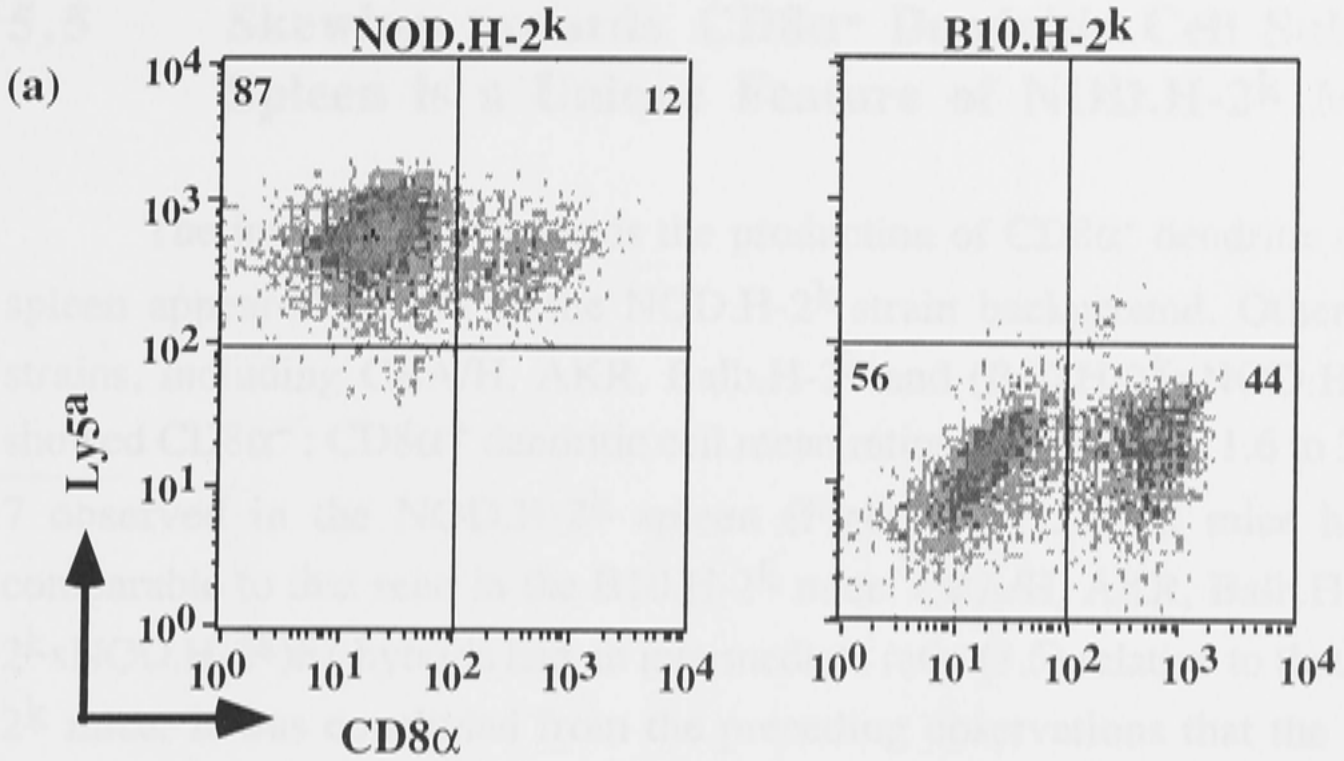

Figure 5.10

The bias towards the CD8α⁻ dendritic cell subset is also observed in unmanipulated NOD.H-2^k mice.

Dendritic cells from spleen of unmanipulated B10.H-2^k and NOD.H-2^k mice were prepared and analyzed for CD11c, Ly5^a and CD8α expression.

(a) Representative FACS plots gated on N418 (CD11c$^+$) cells, illustrating relative proportions of splenic dendritic cell subsets in B10.H-2^k or NOD.H-2^k mice.

(b) Data is presented as the mean ratio of Ly5^{a+} to Ly5^{a-} dendritic cells (y-axis), against CD8α expression (x-axis). For comparison, results from the same analysis using B/N->B mixed bone marrow chimeric mice is shown in the right panel. Columns represent mean ratios, and circles represent ratios from individual mice.
* p = 0.0003, Student's *t* test.

5.5 Skewing towards CD8α⁻ Dendritic Cell Subset in the Spleen is a Unique Feature of NOD.H-2^k Mice

The intrinsic bias towards the production of CD8α⁻ dendritic cell subset in the spleen appeared unique to the NOD.H-2^k strain background. Other H-2^k congenic strains, including CBA/H, AKR, Balb.H-2^k and (B10.H-2^{k}xNOD.H-2^k)F1 hybrids, showed CD8α⁻ : CD8α⁺ dendritic cell mean ratios ranging from 1.6 to 3.5, in contrast to 7 observed in the NOD.H-2^k spleen (Figure 5.11). AKR mice had a ratio (1.6) comparable to that seen in the B10.H-2^k mice. CBA/H, AKR, Balb.H-2^k and (B10.H-2^{k}xNOD.H-2^k)F1 hybrids had an intermediate ratio (3.5) relative to that seen in NOD.H-2^k mice. It was concluded from the preceding observations that the selective bias in mixed bone marrow chimeric mice towards NOD.H-2^k-derived CD8α⁻ dendritic cells was not only a cell-intrinsic but also a unique feature of NOD.H-2^k hematopoietic stem cells as a similar bias is observed in the spleen of unmanipulated NOD.H-2^k mice and not in other H-2^k strains screened. It is interesting that F1 hybrids between B10.H-2^k and NOD.H-2^k have an intermediate CD8α⁻ to CD8α⁺ dendritic cell ratio.

A further question arising from these observations was which splenic dendritic cell subset in NOD.H-2^k mice accounted for the heterogeneity in cell surface MHC class II expression noted earlier (Figure 5.1), and whether this feature was peculiar to the NOD.H-2^k background. Splenic dendritic cells from NOD.H-2^k, B10.H-2^k, AKR, CBA/H, Balb.H-2^k and (B10.H-2^k x NOD.H-2^k)F1 hybrid mice were prepared by collagenase digestion and enrichment on metrizamide gradient as previously described. Enriched splenic low density cells were stained with monoclonal antibodies against CD11c, MHC class II and CD8α, and analyzed by flow cytometry. Large cells positive for CD11c expression were gated and analyzed for MHC class II and CD8α expression (Figure 5.12a). In all the H-2^k congenic strains tested, heterogeneity in cell surface MHC class II expression was only evident in the CD8α⁻ dendritic cell subset (lower left quadrants in all panels). In contrast, the CD8α⁺ dendritic cell subset uniformly expressed high levels of MHC class II molecules in all strains (Upper right quadrant in all panels). The heterogeneity in cell surface MHC class II expression resulted from the presence of CD8α⁻ dendritic cells expressing both high and intermediate/low levels of MHC class II molecules. The largest proportion of dendritic cells expressing intermediate/low levels of MHC class II molecules was observed in the NOD.H-2^k spleen where it constituted 35% of all splenic dendritic cells (Fig.5.12b). The proportion of this subpopulation within the CD8α⁻ dendritic cell subset did not exceed 12.1% in all other H-2^k strains tested. The mean proportions in the other H-2^k strains were 12.1% in B10.H-2^k, 3.5% in AKR, 9.8% in CBA/H, 4.3% in Balb.H-2^k and 8.9% in (B10.H-2^{k}xNOD.H-2^k)F1 hybrids. The fact that F1 hybrids were like the B10.H-2^k parent implies that the NOD.H-2^k trait is

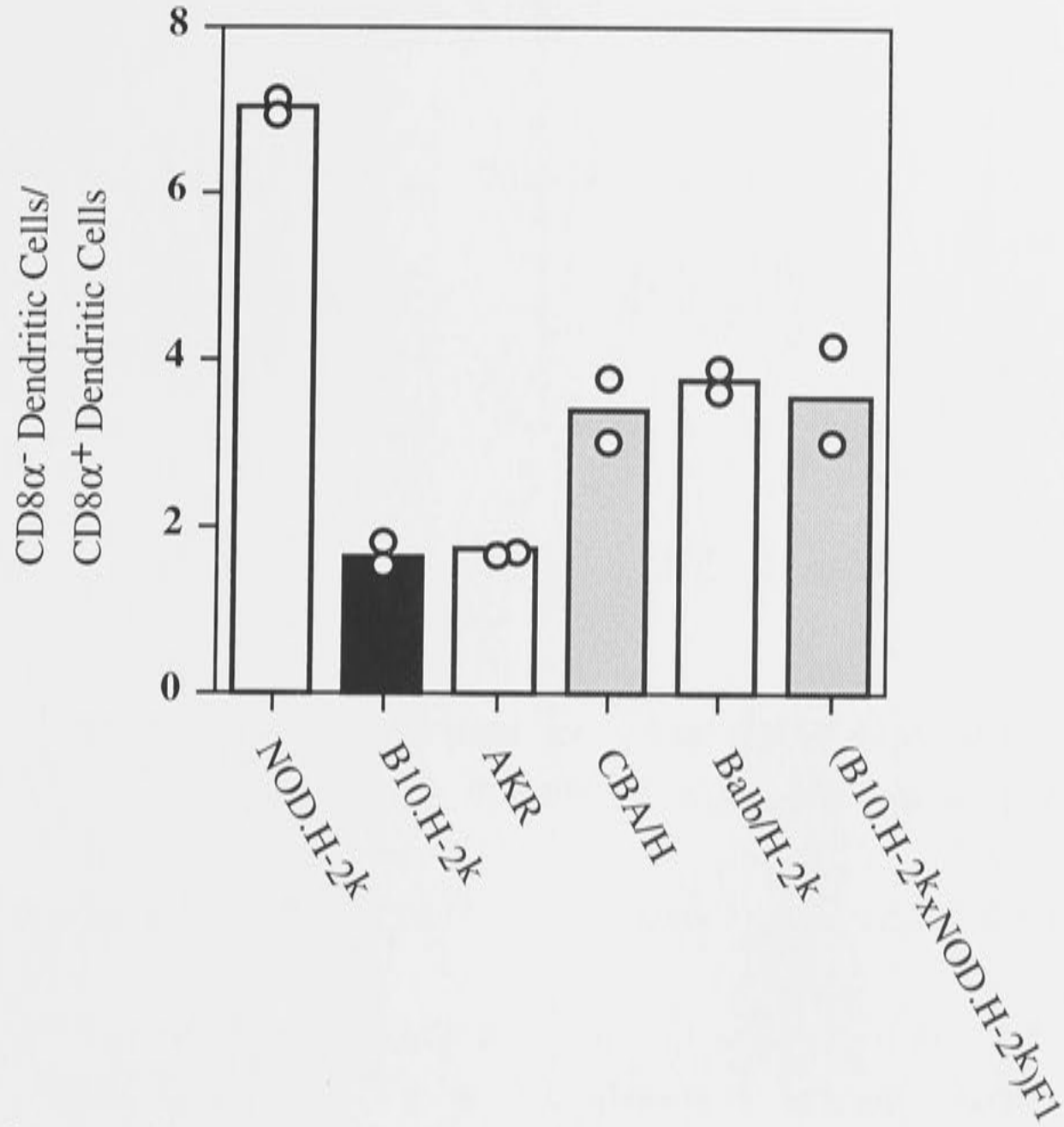

Figure 5.11

Skewing towards the CD8α⁻ dendritic cell subset in the spleen is unique to the NOD.H-2^k background.

Dendritic cells from the spleens of shown H-2^k strains were prepared and analyzed as described in Fig.5.1. except cells were also stained with anti-CD8α monoclonal antibody. Dendritic cells were gated on the basis of high forward scatter (relative size), CD11c and MHC class II positivity and analyzed for CD8α expression. Data is presented as the ratio of CD8α⁻ to CD8α⁺ dendritic cells in the various strains. Columns represent mean ratios, and circles represent ratios from individual mice.

Figure 5.12

Cell surface MHC class II heterogeneity is restricted to the CD8α⁻ dendritic cell subset and is unique to the NOD.H-2^k background.

Dendritic cells from spleens of shown H-2^k congenic strains were prepared and analyzed as previously described.

(a) Representative FACS plots illustrating the presence of CD8α⁻ dendritic cells expressing intermediate and low levels of cell surface MHC class II molecules. Numbers in quadrants represent percentage dendritic cells in that quadrant.

(b) Relative proportions of a putative immature dendritic cell subpopulation within the CD8α⁻ subset in the various H-2^k congenic strains. Columns represent mean proportions, and circles represent proportions from individual mice.

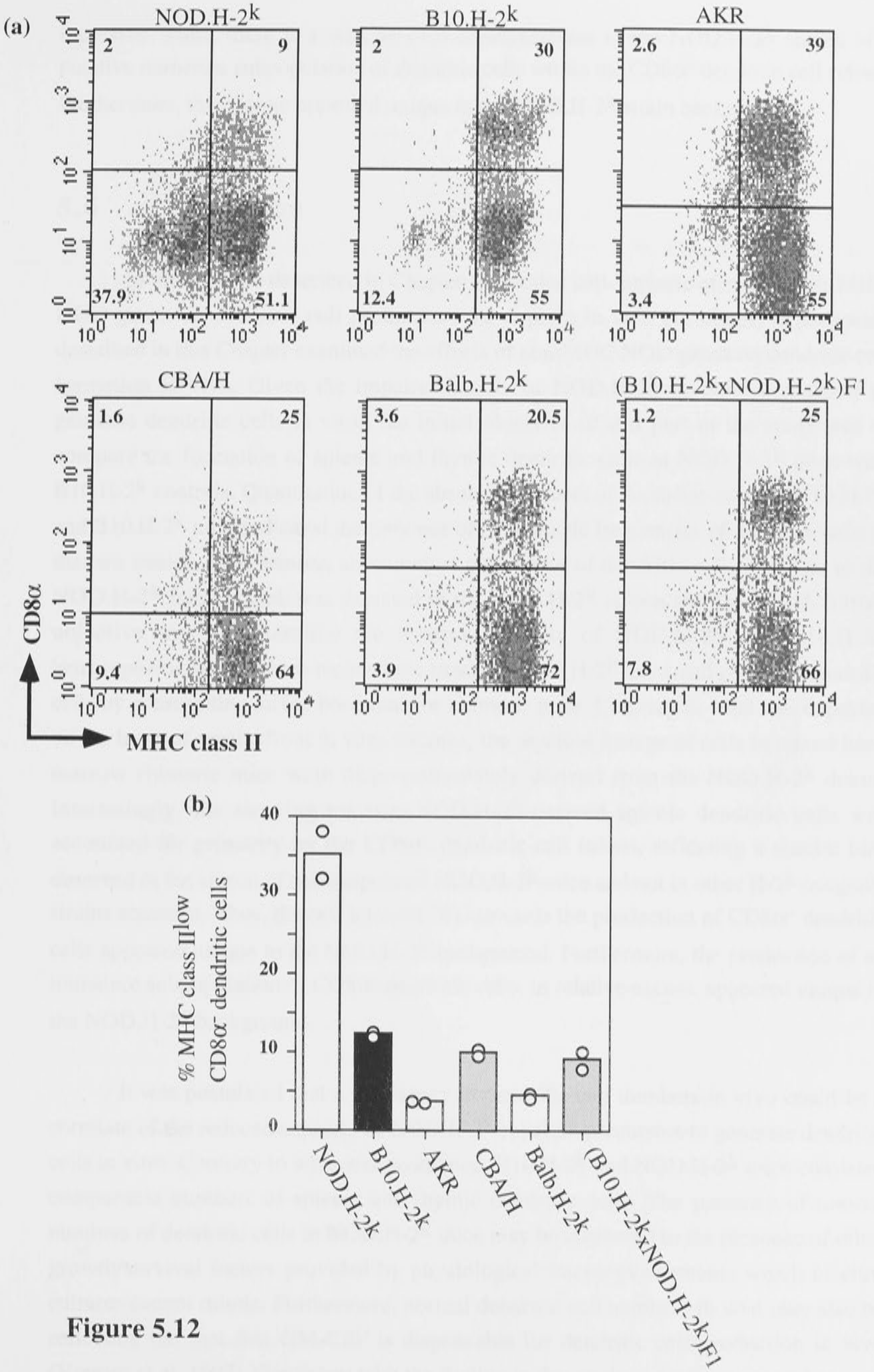
(a)
NOD.H-2k
B10.H-2k
AKR
CBA/H
Balb.H-2k
(B10.H-2kxNOD.H-2k)F1
2
9
37.9
51.1
2
30
12.4
55
2.6
39
3.4
55
1.6
25
9.4
64
3.6
20.5
3.9
72
1.2
25
7.8
66
CD8α
MHC class II
(b)
% MHC class IIlow CD8α- dendritic cells
40
30
20
10
0
NOD.H-2k
B10.H-2k
AKR
CBA/H
Balb.H-2k
(B10.H-2kxNOD.H-2k)F1

Figure 5.12

recessive. Thus, there is a relative over-representation in the NOD.H-2^k spleen of a putative immature subpopulation of dendritic cells within the CD8α^- dendritic cell subset. Furthermore, this feature appeared unique to the NOD.H-2^k strain background.

5.6 Discussion

In vitro results described in Chapter 4 revealed cell-intrinsic effects of non-MHC NOD genes on dendritic cell production. To explore in vivo correlates, experiments described in this Chapter examined the effects of non-MHC NOD genes on dendritic cell formation in vivo. Given the impaired ability of NOD.H-2^k myeloid precursors to generate dendritic cells in vitro, the initial objective of this part of the study was to compare the formation of splenic and thymic dendritic cells in NOD.H-2^k mice with B10.H-2^k controls. Quantitation of the absolute numbers of dendritic cells in NOD.H-2^k and B10.H-2^k mice indicated the presence of comparable frequencies of dendritic cells in the two strains. Furthermore, an immature population of dendritic cells, peculiar to the NOD.H-2^k background, was detected in the NOD.H-2^k spleen and thymus. A further objective was to determine the relative capacity of NOD.H-2^k and B10.H-2^k hematopoietic stem cells to reconstitute irradiated B10.H-2^k hosts and generate dendritic cells by constructing mixed bone marrow chimeric mice. Contrary to what was expected on the basis of results from in vitro cultures, the myeloid lineage of cells in mixed bone marrow chimeric mice were disproportionately derived from the NOD.H-2^k donor. Interestingly, the skewing towards NOD.H-2^k-derived splenic dendritic cells was accounted for primarily by the CD8α^- dendritic cell subset, reflecting a similar bias observed in the spleen of unmanipulated NOD.H-2^k mice and not in other H-2^k congenic strains screened. Thus, the cell intrinsic bias towards the production of CD8α^- dendritic cells appeared unique to the NOD.H-2^k background. Furthermore, the production of an immature subpopulation of CD8α^- dendritic cells, in relative excess, appeared unique to the NOD.H-2^k background.

It was postulated that a deficiency in dendritic cell numbers in vivo could be a correlate of the reduced capacity of NOD.H-2^k myeloid precursors to generate dendritic cells in vitro. Contrary to what was postulated, B10.H-2^k and NOD.H-2^k mice consisted comparable numbers of splenic and thymic dendritic cells. The presence of normal numbers of dendritic cells in NOD.H-2^k mice may be attributed to the presence of other growth/survival factors provided by physiological microenvironments which in vitro cultures cannot mimic. Furthermore, normal dendritic cell numbers in vivo may also be reflecting the fact that GM-CSF is dispensable for dendritic cell production in vivo (Vremec et al, 1997). Consistent with the finding in this study, a previous report has

demonstrated that NOD bone marrow hematopoietic precursors when transferred into irradiated syngeneic recipients form similar number of spleen colonies in vivo as control Balb/c precursors, despite responding suboptimally to in vitro stimulation with GM-CSF, IL-3 and IL-5 (Langmuir et al, 1993).

An expanded population of putatively immature dendritic cells appeared unique to the lymphoid organs of NOD.H-2^k mice, particularly in the thymus. The immature dendritic cell population was characterized by a lower level of cell surface MHC class II expression. These immature dendritic cells were 4-fold more frequent than MHC class II-high expressing dendritic cells in the NOD.H-2^k thymus. In contrast, MHC class II-low and MHC class II-high dendritic cell populations were equally represented in the B10.H-2^k thymus. Evidence suggesting that thymic dendritic cells expressing low levels of cell surface MHC class II molecules were immature came from thymic reconstitution studies (Ardavin et al, 1993). Intrathymic transfer of dendritic cell precursors demonstrated that MHC class II -low and MHC class II-high dendritic cells appeared sequentially, with the former preceding the latter. This observation suggests that the MHC class II-low dendritic cells represents an immature stage in thymic dendritic cell differentiation. Thymic dendritic cells are mainly located in the cortico-medullary border and medulla of the thymus where they are thought to play a key role in negative selection of thymocytes (Ardavin, 1997; Sprent and Webb, 1995). The relative prevalence of MHC class II-intermediate dendritic cells in the NOD.H-2^k thymus could potentially influence a key variable in central (thymic) selection of T cells: MHC-peptide ligand density.

To determine the in vivo differentiation potential of NOD.H-2^k hematopoietic stem cells and their progenitors, mixed bone marrow chimeric mice were constructed by injecting a mixed inoculum of B10.H-2^k and NOD.H-2^k bone marrow cells into irradiated B10.H-2^k recipients. B10.H-2^k mice were chosen as recipients since, as reported for NOD mice (Kaufman et al, 1997), NOD.H-2^k mice were found to be highly resistant to bone marrow engraftment. Results obtained from mixed bone marrow chimeric mice were contrary to that expected on the basis of results from in vitro cultures. The myeloid lineage of cells in mixed bone marrow chimeric mice were predominantly of NOD.H-2^k origin while the lymphoid compartment was even between the two donors. Such a skewing could be explained by the inherent competitive advantage of NOD.H-2^k hematopoietic precursors over B10.H-2^k precursors to generate myeloid cells during reconstitution. Furthermore, NOD.H-2^k hematopoietic precursors may be predisposed to making more myeloid cells at the expense of lymphocytes, as suggested by significantly fewer absolute number of NOD.H-2^k-derived B cells in whole blood of N->B bone marrow chimeric mice. Furthermore, results from bone marrow chimeric mice also

indicated over-production of NOD.H-2^k-derived monocytes in both N->B and B/N->B chimeric mice.

The previously described cell surface MHC class II heterogeneity in splenic and thymic dendritic cells of unmanipulated NOD.H-2^k mice was not detectable in bone marrow chimeric mice. This observation suggests that the cell surface MHC class II heterogeneity in splenic and thymic dendritic cells of NOD.H-2^k mice may be a consequence of microenvironmental influences rather than a cell-intrinsic feature NOD.H-2^k hematopoietic stem cells. Such a possibility can be tested by constructing B->N chimeric mice, provided efficient engraftment occurs in the NOD.H-2^k recipients.

The skewing towards NOD.H-2^k-derived dendritic cells in mixed bone marrow chimeric was most pronounced in the spleen. There were 6-fold more NOD.H-2^k-derived dendritic cells than B10.H-2^k-derived dendritic cells in the spleen of mixed chimeric mice. Interestingly, this skewing towards NOD.H-2^k-derived dendritic cells was accounted for mainly by the CD8α^- subset, reflecting a similar bias observed in unmanipulated NOD-H-2^k mice and not in other H-2^k congenic strains screened. It is worth noting that the (B10.H-2^kxNOD.H-2^k)F1 hybrids showed an intermediate CD8α^- : CD8α^+ dendritic cell ratio, suggesting that the balance between CD8α^+ and CD8α^- subsets in the spleen is a quantitative trait. The presence of the putative immature dendritic cell subpopulation in the NOD.H-2^k spleen was exclusively derived from the CD8α^- dendritic cell subset. The CD8α^+ dendritic cell subset, on the other hand, uniformly expressed high levels of MHC class II molecules in all strains. Taken together, these observations may suggest a potential precursor-progeny relationship between CD8α^- and CD8α^+ dendritic cell subsets. As previously mentioned, the presence of immature splenic dendritic cells was not evident in B/N->B chimeric mice and therefore not a cell-intrinsic feature of NOD.H-2^k hematopoietic stem cells. However, the relative over-representation of immature dendritic cells in NOD.H-2^k spleen appeared unique to the NOD.H-2^k background as immature dendritic cells in the spleen of other H-2^k congenic strains were relatively scarce.

Although the relationship, in terms of origin and function, between the two splenic dendritic cell subsets remains controversial and unresolved, the relative bias towards CD8α^- dendritic cell in the NOD.H-2^k spleen is an interesting cell-intrinsic and unique feature of NOD.H-2^k hematopoietic stem cells. Overall, data from mixed bone marrow chimeric mice demonstrate that non-MHC MHC NOD genes confer on NOD.H-2^k hematopoietic stem cells a cell-intrinsic phenotype which in vivo is manifested by skewing towards the myeloid lineage of cells and the CD8α^- splenic dendritic cell subset.

Chapter 6

Summary and General Discussion

6.1 Introduction

While the NOD MHC is critical in the determination of target tissue for autoimmune destruction, diabetogenic loci outside the MHC confer a general susceptibility to autoimmunity in the NOD mouse. There is sufficient evidence to suggest a role for myeloid-derived antigen presenting cells, especially dendritic cells, in the initiation and maintenance of autoimmune pathology (Jansen et al, 1994; Serreze et al, 1993a and b; Langmuir et al, 1993; Jansen et al, 1995; Takahashi et al, 1998; Ludewig et al, 1998). This study has, therefore, utilized NOD.H-2^k and control B10.H-2^k congenic mice to study dendritic cell generation, both in vitro and in vivo, in an attempt to explore cellular processes which may be affected by non-MHC NOD genes. The results obtained during the course of this study demonstrated for the first time that non-MHC NOD genes conferred on myeloid precursors a cell-intrinsic phenotype which was manifested by:

i) elevated levels of apoptosis and heterogeneous proliferation, resulting in reduced dendritic cell yield during in vitro cultures;
ii) skewing towards the myeloid lineage of cells in vivo; and
iii) selective bias of splenic dendritic cells towards the CD8α^- subset in vivo.

Furthermore, results from the current study demonstrated the prevalence of putatively immature MHC class II-low dendritic cells in NOD.H-2^k mice. The presence of immature dendritic cells was not cell-intrinsic to NOD.H-2^k hematopoietic stem cells but a unique feature of the NOD.H-2^k background. Three key questions arise from the overall results obtained during the course of this study:

A) Why do NOD.H-2^k myeloid precursors respond differently to GM-CSF stimulation in vitro?

B) What is the relationship between the apparently contradictory in vitro and in vivo results?

C) What is the relevance of the overall findings from this study to autoimmune diabetes?

These questions form the basis of the following discussion.

PART A: The Response of NOD.H-2^k Myeloid Precursors In Vitro

6.2 The Uniquely Different Response of NOD.H-2^k Myeloid Precursors to GM-CSF Stimulation In Vitro

Preliminary attempts to generate dendritic cells by culturing myeloid precursors, in the presence of GM-CSF and IL-4, revealed that the yield of dendritic cells from NOD.H-2^k-derived myeloid precursors was dramatically lower than that obtained from precursors isolated from control B10.H-2^k mice. The inability of NOD.H-2^k myeloid precursors to generate control levels of dendritic cells was concluded to be a cell-intrinsic feature of NOD.H-2^k myeloid precursors as B10.H-2^k-derived myeloid precursors developed in co-culture similar to the way they develop in single cultures.

Previous studies have documented hematopoietic deficiencies in in vitro cultures of precursors, isolated from NOD mice and human prediabetic or diabetic patients (Serreze et al, 1993 a and b; Langmuir et al, 1993; Jansen et al, 1995; Takahashi et al, 1998; Morel et al, 1999). Findings from the current study confirm results from previous reports and have been discussed in the context of these reports in the 'Discussion Section' of Chapter 4. Significantly, results from this study provide important extensions of previous findings by demonstrating for the first time that the reduced yield of dendritic cells from NOD.H-2^k cultures is a phenotype cell-intrinsic to NOD.H-2^k myeloid precursors. Furthermore, attempts at dissecting the reduced dendritic cell yield phenotype of NOD.H-2^k-derived myeloid precursors revealed the cellular basis for fewer dendritic cells generated in NOD.H-2^k cultures. While B10.H-2^k cultures exhibited a basal level of apoptosis and homogeneous proliferation, NOD.H-2^k cultures exhibited elevated levels of apoptosis and heterogeneous proliferation during the initial days of culture. Elevated levels of apoptosis and heterogeneous proliferation appeared to be unique features of the NOD.H-2^k background since similarly screened precursors from other H-2^k congenic strains, including CBA/H, AKR and Balb-H-2^k, behaved like precursors from control B10.H-2^k mice. Altogether, these results suggest that non-MHC NOD genes confer on NOD.H-2^k-derived myeloid precursors a cell-intrinsic phenotype which is responsible for the elevated levels of apoptosis and heterogeneous proliferation observed in NOD.H-2^k cultures.

A key question arising from the preceding observations is: what is the molecular basis for the uniquely different mitotic and apoptotic responses of NOD.H-2^k myeloid precursors to GM-CSF stimulation in vitro? A number of potential scenarios could explain the elevated levels of apoptosis and heterogeneous proliferation accounting for the reduced dendritic cell yield from NOD.H-2^k bone marrow cultures. These include proximal, distal or parallel components of signal transduction pathways which determine the fate of a cell by balancing survival and apoptotic cues.

6.2.1 Candidate Molecular Signalling Pathways

GM-CSF, IL-3 and IL-5 are hematopoietic growth factors that are secreted by activated T cells and mast cells (Arai et al, 1990). These cytokines are actively involved in hematopoiesis by modulating proliferation, differentiation, survival and effector functions of cells of the hematopoietic lineages and their progenitors. GM-CSF and IL-3 act on various lineages such as macrophages, granulocytes, erythrocytes, megakaryocytes and hematopoietic progenitors (Metcalf and Nicola, 1992; Gasson, 1991), while IL-5 plays a major role in the development of eosinophils both in humans and in mice (Takatsu, 1988). In both humans and mice the GM-CSF, IL-3 and IL-5 receptor is a heterodimeric complex comprising a cytokine-specific α chain and a shared β common (β_c) chain (Miyajima et al, 1993). In addition to the β_c chain, a unique IL-3-specific β chain is also present in the mouse (Hara et al, 1992). The α chains can bind their ligands with low affinity but the β_c chain does not bind ligand by itself. However, the β_c chain when complexed with an α chain forms a high affinity signalling-competent receptor. It has been previously reported that NOD bone marrow cells display a reduced response to IL-3, IL-5 and GM-CSF (Langmuir et al, 1993). Given this observation, a mechanistic hypothesis to explain the observed elevated levels of apoptosis and heterogeneous proliferation in NOD.H-2^k cultures during this study is a potential defect in the signal transduction mediated by the β_c chain of the GM-CSF receptor.

The role of the human β_c chain in signal transduction has been studied by using a series of cytoplasmic tail truncation mutants (Miyajima et al, 1993). Functional analyses of the deletion mutants was carried out by co-expression of the mutant β_c chain with human GM-CSF receptor α chain in a murine IL-3-dependent cell line, BaF3 (Sakamaki et al, 1992). The cytoplasmic region of the β_c can be subdivided into at least two functionally distinct domains, responsible for transducing mitogenic, survival or negative regulatory signals (Sato et al, 1993). The first and membrane proximal region transduces mitogenic and survival signals by the induction of the proto-oncogene c-myc and activation of DNA replication. The second domain leads to the activation of ras and MAP

(Mitogen-Activated Protein) kinases, with consequent induction of c-fos and c-jun, transcription factors which are involved in cell differentiation. Elimination of amino acid 544 from the membrane proximal region results in a mutant which proliferates in response to GM-CSF stimulation. However, stimulation with GM-CSF is unable to maintain cell viability, causing cells to die by apoptosis while receiving mitogenic signals (Kinoshita et al, 1995). Apoptosis in the mutants was prevented by the ectopic expression of an activated form of ras. Taken together, these results indicate that cell proliferation combines both mitogenic and anti-apoptotic signals. Furthermore, ras plays an important role in the suppression of apoptosis in hematopoietic cells. It is likely that similar mechanisms are operating in the NOD.H-2^k mouse during signal transduction mediated by the β_c chain of the GM-CSF receptor. Such mechanisms could account for the elevated levels of apoptosis and heterogeneous proliferation observed in NOD.H-2^k bone marrow cultures.

An similar scenario has been described in the IL-2-mediated regulation of T cells. IL-2 plays a critical role in the proliferation and survival of T cells (Nelson et al, 1998). In addition, IL-2 plays an opposite role in sensitizing T cells to activation-induced apoptosis (Lenardo, 1991). How IL-2 mediates these opposing outcomes has been recently demonstrated in a study using mutant forms of the IL-2 receptor (Van Parijs et al, 1999b). The IL-2 receptor is a heterotrimeric complex comprising a cytokine binding α chain, and two obligate signalling subunits. The signalling subunits comprise a β chain and a common γ chain which is shared with the IL-4, IL-7, IL-9 and IL-15 receptors (Leonard et al, 1995). Van Parijs et al (1999b) unravelled the molecular basis of the opposing effects of IL-2 by introducing wild type and two mutant forms of the human IL-2 receptor β chain into receptor-deficient murine T cells by retroviral gene transfer. The two mutant forms of the β chain were individually defective in either the Stat-5 (signal transducer and activator of transcription-5) or Akt activation because these molecules were previously implicated in T cell proliferation and survival (Freidmann et al,1996; Ahmed et al, 1997; Brennan et al, 1997; Fujii et al, 1998; Moriggl et al, 1999). Co-transfection with green fluorescent protein (GFP) enabled detection of transfected cells. Results obtained during this study are discussed below.

T cells reconstituted with wild type receptor or receptor deficient in Akt signalling were sensitive to activation-induced death (AICD) when stimulated with anti-CD3 monoclonal antibody. In contrast, T cells reconstituted with receptor deficient in Stat5 signalling were largely resistant to AICD when stimulated with anti-CD3 monoclonal antibody. This reduction in AICD was attributed to reduced Fas (CD95, death receptor belonging to the TNF receptor superfamily) ligand expression in T cells lacking Stat5 activation. The requirement of the two signalling modules was altered in T cell survival.

When stimulated with IL-2, transfectants expressing wild type receptor or receptor deficient in Stat5 signalling remained viable and continued to proliferate. In contrast, transfectants deficient in Akt signalling proliferated for three days then underwent apoptosis. It has previously been shown that IL-2 signalling results in the induction of the anti-apoptotic molecule, Bcl-2 (Adams and Cory , 1998; Chao and Korsmeyer, 1998; Lord et al, 1998). Consistent with this observation, co-transfection of T cells with human Bcl-2 compensated for the lack of Akt signalling. Taken together, these findings support the model that distinct signalling modules within the IL-2 β chain regulate T cell fate by stimulating proliferation or by promoting apoptosis. It is possible that NOD.H-2^k myeloid precursors receive normal mitogenic signals mediated by GM-CSF but are defective in generating sufficient levels of complementary survival signals.

Apoptosis must be averted by inhibiting the function of pro-apoptotic molecules. Such a phenomenon is evident in the cell survival promoted by signalling through phosphatidylinositide-3'-OH kinase (PI-3 kinase) and its downstream target, the serine-threonine kinase Akt (Datta et al, 1999). PI-3 kinase has been shown to be involved in the survival of a number of cell types in response to growth factor stimulation (Datta et al, 1999). Correspondingly, its target Akt has also been shown to be a general mediator of growth factor induced survival in various cell types. Thus, the sequential activation of PI-3 kinase and Akt has become a paradigm for growth factor induced cell survival. In order to elucidate the mechanism by which the PI-3 kinase/Akt pathway promotes cell survival, Datta et al (1997) employed the well-established insulin-like growth factor (IGF)-1 supplemented neuronal culture system. It was previously shown that IGF-1 stimulation specifically activated the PI-3 kinase/Akt pathway in cultured neurons (Dudek et al, 1997). Furthermore, it was shown that IGF-1-mediated induction of the PI-3 kinase/Akt pathway was necessary and sufficient for the survival of neurons in culture. Clues towards the mechanism of Akt action came from the in vitro and in vivo observations that Akt activation triggers the phosphorylation of the pro-apoptotic Bcl-2 family member BAD (Gajewski and Thompson, 1996; Wang et al, 1996; Zha et al, 1996). To test the hypothesis that the IGF-1 induced PI-3 kinase/Akt survival pathway suppressed BAD-mediated apoptosis, neurons were transfected with various derivatives of BAD (Datta et al, 1997). In contrast to neurons transfected with control constructs, the majority of the wild type BAD-transfected neurons underwent apoptosis. Apoptosis in the wild BAD-transfectants was substantially suppressed by treatment with the survival factor, IGF-1. Indeed, by using neurons transfected with mutant forms of BAD, it was demonstrated that IGF-1 promoted PI-3 kinase/Akt-mediated cell survival by site-specific phosphorylation of BAD. This finding was a confirmation of a previous report which demonstrated that IL-3 -mediated survival of a hematopoietic cell line was underpinned by BAD phosphorylation (Zha et al, 1996). Furthermore, it was shown that phosphorylation

of BAD resulted in it being sequestered in the cytosol. This promotes survival by precluding heterodimerization of phosphorylated BAD with anti-apoptotic members of the Bcl-2 family (Adams and Cory, 1998; Chao and Korsmeyer, 1998). Unphosphorylated BAD heterodimerizes with certain anti-apoptotic members of the Bcl-2 family and neutralizes their protective effect. Thus, proximal survival signals may modulate apoptosis by inactivating distal pro-apoptotic molecules.

It is interesting to note that the PI-3 kinase/Akt survival pathway was not required for the survival of a murine mast cell line stimulated with GM-CSF (Scheid et al, 1995). Inhibitors of PI-3 kinase rapidly induced apoptosis in cells incubated in the presence of IL-4 or IL-3. In contrast, cells incubated in the presence of GM-CSF, or to a lesser extent IL-5, could bypass the effects of the inhibitors. These results suggest that alternative survival pathways are activated as a result of GM-CSF stimulation of myeloid cells.

Signals transduced in parallel with growth factor receptor signalling is another possible mechanism by which apoptosis may be induced. Parallel signals may be involved in the downregulation of anti-apoptotic molecules. It has recently been demonstrated that mature lymphocytes express a novel anti-apoptotic protein called cFLIP (Thome et al, 1997). Naive B and T cells express high levels of cFLIP which is downregulated when B and T cells are given a mitogenic or activation stimulus (Irmler et al, 1997; Refaeli et al, 1998). The downregulation of cFLIP in activated lymphocytes correlated with their heightened sensitivity to death receptor-mediated apoptosis. The role of cFLIP in apoptosis was illuminated by expressing cFLIP in primary lymphocytes using a retroviral transfection system (Van Parijs et al, 1999a). It was demonstrated that retrovirus-mediated expression of cFLIP inhibited death receptor induced apoptosis in activated lymphocytes. Interestingly, mice reconstituted with cFLIP expressing bone marrow cells developed B cell-mediated autoimmunity. The autoimmune response was characterized by the presence of anti-DNA autoantibodies and elevated levels of serum immunoglobulins of various isotypes, reminiscent of the autoimmune syndromes observed in *lpr* mice deficient in the death receptor Fas (Cohen and Eisenberg, 1991). Altogether, these results suggest that cFLIP down-regulation renders lymphocytes susceptible to apoptosis and is required to maintain tolerance. Dysregulated downregulation of a survival molecule may be a mechanism that contributes towards elevated levels of apoptosis observed when NOD.H-2^k myeloid precursor are stimulated with GM-CSF in vitro.

Dysregulated mitogenic signals in cultured NOD.H-2^k myeloid precursors could be yet another mechanism which induces apoptosis. The proto-oncogene c-myc has been implicated in the regulation of cell proliferation in several studies (Schmidt, 1999). It is

rapidly induced in quiescent cells given a mitogenic stimulus and is continuously present at an appreciable level throughout the cell cycle in proliferating cells. This suggests that c-myc plays a role in the transition from quiescence to cell proliferation and in the maintenance of proliferation. Conversely, mitogen withdrawal is accompanied by the down-regulation in cells of both c-myc mRNA and protein levels (Dean et al, 1986; Waters et al, 1991), and the entry of cells into growth arrest. The latter observation suggests that c-myc down-regulation is required for cells to enter growth arrest (Waters et al, 1991). Furthermore, c-myc can be a potent inducer of apoptosis when combined with a block in proliferation. Rat-1 fibroblasts constitutively expressing human c-myc, by retroviral gene transfer, undergo apoptosis when deprived of growth factor (Evan et al, 1992). Comparable results were also reported using an IL-3-dependent myeloid cell line (Askew et al, 1991).

PART B: The Link between In Vivo and In Vitro Results

6.3 Skewing of the Myeloid Lineage of cells towards NOD.H-2^k Origin in Mixed Bone Marrow Chimeric Mice (B/N->B)

A potential correlate of the reduced yield of dendritic cells in vitro would be fewer dendritic cells arising from NOD.H-2^k hematopoietic stem cells in vivo. To test the in vivo capacity of NOD.H-2^k hematopoietic stem cells to generate dendritic cells, mixed bone marrow chimeric mice were constructed using irradiated B10.H-2^k recipients. Recipients were reconstituted with an inoculum comprising a 1:1 mixture of bone marrow cells. Again, the allelic variants of Ly5 were used during flow cytometric analysis of donor-derived leukocytes in recipient mice 8-12 weeks post-reconstitution. Contrary to expectation, the myeloid lineage of cells in recipient mice were skewed towards NOD.H-2^k origin, while the lymphoid lineage was practically even between the two donors. Monocytes, thymic dendritic cells and splenic dendritic cells in mixed bone marrow chimeric mice were predominantly NOD.H-2^k-derived. In contrast, total B and T cells in blood and spleen, and total T cells in thymus were derived equally from both donors. The number of monocytes in peripheral whole blood of control N->B chimeric mice appeared to be higher than in the control B->B chimeric mice ($p = 0.084$). Similarly, the number of NOD.H-2^k -derived monocytes in mixed bone marrow chimeric B/N->B mice was significantly higher than the number of monocytes in control B->B chimeric mice ($p = 0.03$). In contrast, the number of B cells in peripheral whole blood of the former group of mice was significantly lower than in the latter group ($p = 0.008$). These results suggest that NOD.H-2^k hematopoietic stems cells may be preferentially generating myeloid cells

over lymphoid cells. Interestingly, a recent study has demonstrated that tissue monocytes, in response to a phagocytic stimulus, migrate to draining lymph node and differentiate into T cell zone dendritic cells in vivo (Randolph et al, 1999). This observation indicates that monocytes can serve as a dendritic cell precursor pool from which lymphoid and peripheral tissue maybe seeded.

6.3.1 Predominance of CD8α⁻ Dendritic Cells in Mixed Bone Marrow Chimeric Mice (B/N->B) and in Unmanipulated NOD.H-2^k Mice

The most pronounced skewing of myeloid cells in B/N->B mixed bone marrow chimeric mice towards NOD.H-2^k origin was seen in the splenic dendritic cell population. Since two dendritic cell subsets (CD8α⁻ and ⁺) form the splenic dendritic cell population, it was interesting to determine which subset was responsible for the skewing towards NOD.H-2^k origin. Interestingly, the skewing towards NOD.H-2^k-derived splenic dendritic cells was accounted for mainly by the CD8α⁻ subset, reflecting a similar bias observed in unmanipulated NOD.H-2^k mice. The CD8α⁻ to CD8α⁺ ratio of splenic dendritic cells in control B10.H-2^k mice was 1.5. In contrast, the same ratio was 6.5 in NOD.H-2^k mice. This bias towards CD8α⁻ dendritic cells in NOD.H-2^k mice appeared unique since other H-2^k strains similarly screened either had an intermediate or B10.H-2^k-like low ratio. Taken together, in vivo results reveal that the cell-intrinsic effects of non-MHC NOD genes on NOD.H-2^k myeloid precursors results in the preferential generation of myeloid cells. Furthermore, non-MHC NOD genes appear to selectively bias splenic dendritic cell population in favor of the CD8α⁻ subset.

6.3.2 Roles of GM-CSF in Myeloid and Dendritic Cell Differentiation

Interestingly, inspite of numerous in vitro studies indicating that GM-CSF is a key cytokine for dendritic cell development, normal numbers of dendritic cells are detected in the lymphoid organs of mice with a null mutation for GM-CSF (Stanley et al, 1994; Dranoff et al, 1994) or β_c chain of the GM-CSF receptor (Robb et al, 1995; Nishinakamura et al, 1995; Vremec et al, 1997). Overall, no hematopoietic defects were observed in these mice. Both these mutants suffer from a lung disease characteristic of the human disease pulmonary alveolar proteinosis (PAP). Mutant mice show markedly reduced alveolar clearance and catabolism of lung surfactant protein, resulting in clogged

* These immature dendritic cells were not detected in B/N->B mixed bone marrow chimeric mice, suggesting that the presence of immature dendritic cells was not a cell-intrinsic feature of NOD.H-2^k hematopoietic stem cells.

It is important to note, however, that the large numbers of CD8α^- mature dendritic cells (MHC class II^{hi}) were produced from NOD.H-2^k precursors in B/N->B chimeras.

air spaces. This pulmonary lesion is thought to be partly due to impaired alveolar macrophage function (Scott et al, 1998). The myeloid growth factor GM-CSF and signalling through the β_c are therefore dispensable for dendritic cell generation and compensatory mechanisms exist in vivo.

The apparent contradiction between in vitro and in vivo results obtained during the course of this finding may be reconciled by taking into account that GM-CSF is redundant for basal level hematopoiesis in vivo but required for hematopoiesis during an immune response. GM-CSF-deficient mice when infected with the facultative intracellular bacterium *Listeria monocytogenes* harbored 50-fold more organisms in their spleen and liver than similarly infected wild-type mice (Zhan et al, 1998). The high bacterium load correlated with a severe depletion of bone marrow hematopoietic cells and a reduced inflammatory response in the peritoneal cavity of GM-CSF-deficient mice. A comparable finding has also been reported in IL-3-deficient mice. Similar to the need for GM-CSF in the generation of dendritic cells in vitro, IL-3 has been shown to augment stem cell factor-dependent mast cell development in vitro (Tsuji et al, 1991; Mayer et al, 1989). Using IL-3-deficient mice, Lantz et al (1998) demonstrate that IL-3 is not essential for the development of mast cells or basophils under physiological conditions. However, when infected with the nematode *Strongyloides venezuelensis,* IL-3-deficient mice show impaired parasite expulsion and mast cell development. Thus, like GM-CSF, IL-3 is redundant for basal hematopoiesis but required during an immune response. Overall, these results suggest that the physiological function of GM-CSF only comes into prominence during an immune response directed against infectious agents or possibly endogenous tissue.

In addition to promoting hematopoiesis under inflammatory conditions, GM-CSF may also be involved in the more subtle processes of myeloid cell differentiation during normal hematopoiesis. As previously mentioned, impaired alveolar macrophage function may be responsible for surfactant accumulation in the lungs of GM-CSF- or β_c-deficient mice (Scott et al, 1998). Findings from the current study show the presence of putative immature dendritic cells, present in relative excess, in the thymus and spleen of NOD.H-2^k mice. These immature dendritic cells expressed intermediate/low levels of cell surface MHC class II molecules. These immature dendritic were not deteced in B/N->B mixed bone marrow chimeric mice, suggesting that the presence of immature dendritic cells was not a cell-intrinsic feature of NOD.H-2^k hematopoietic stem cells.* However, the relative abundance of immature dendritic cells was unique to the NOD.H-2^k background. Furthermore, immature dendritic cells were exclusively contained in the $CD8\alpha^-$ dendritic cell subset.# In contrast, the $CD8\alpha^+$ dendritic cells uniformly expressed high levels of cell surface MHC class II molecules. These results may suggest a potential precursor-progeny

relationship between CD8α⁻ and CD8α⁺ dendritic cell subsets, with the CD8α⁺ dendritic cell representing a terminally differentiated form of dendritic cells. Thus, by exerting its influence on dendritic cell differentiation in vivo, GM-CSF may also determine the balance between dendritic cell subsets.

There are a number of possibilities that could potentially explain the cell-intrinsic bias, mediated by non-MHC NOD genes, towards the CD8α⁻ dendritic cell subset in NOD.H-2^k mice. It is likely that NOD.H-2^k hematopoietic stem cells preferentially commit to the production of myeloid cells in the bone marrow, resulting in more myeloid cells in the periphery as evidenced by results from this study. This bias towards the generation of myeloid cells could be due to impaired negative regulatory signals or too much positive signalling or both for myeloid cell production. Furthermore, enhanced survival and/or proliferation of circulating monocyte precursors in the periphery (Randolph et al, 1999) could account for the relative excess of the CD8α⁻ dendritic cell subset. From the results in this study it is interesting to speculate a possible precursor-progeny relationship between CD8α⁻ and CD8α⁺ dendritic cells, with the CD8α⁺ dendritic cells representing the terminally differentiated subset. Thus, defective differentiation processes, underpinned by impaired GM-CSF signalling, may contribute towards the accumulation of the CD8α⁻ dendritic cell subset. Alternatively, if the CD8α⁺ dendritic cell subset belongs to a distinct lineage, then under-production and reduced survival could explain their relative deficiency. The bias towards myeloid cells could also be coupled to the under-production of B cells, as indicated by results from this study. This could be due to deficiencies in lineage commitment, survival or proliferation of B cell precursors.

It is conceivable that the reduced dendritic cell yield in NOD.H-2^k cultures is a result of NOD.H-2^k myeloid precursors receiving an exaggerated initial proliferative burst which in vitro is not matched by complementary survival and/or differentiation signals. The apparent contradiction between reduced dendritic cell yield observed in NOD.H-2^k cultures and the preferential generation of NOD.H-2^k-derived myeloid lineage of cells in vivo can be reconciled in this context.

6.3.3 Dysregulation in the RelB Pathway as an Alternative Cause for the Bias towards the CD8α⁻ Splenic Dendritic Cell Subset in NOD.H-2^k Mice

While GM-CSF appears not to be essential to form dendritic cells in vivo, another molecular pathway has been identified as being essential. Important molecular evidence supporting functional differences between CD8α⁻ and CD8α⁺ splenic dendritic cells has come from a recent study with the RelB mutant (RelB$^{-/-}$) mice (Wu et al, 1998). The RelB$^{-/-}$ mice have a complex phenotype which include thymic dendritic cell deficiency. Development of lymphoid cells in the mutant mice is unaffected. The in vivo differentiation capacity of RelB$^{-/-}$ stem cells was determined by constructing bone marrow chimeric mice using wild type recipients congenically marked with the Ly5^a allotype to distinguish between host and donor cells. Normal numbers of donor-derived thymic dendritic cells were produced in recipient mice indicating that the absence of thymic dendritic cells in RelB$^{-/-}$ mice may be secondary phenomenon caused by systemic inflammation and disrupted thymic architecture. Interestingly, reconstituted mice displayed a marked reduction in the splenic CD8α⁻ dendritic cell subset compared with the CD8α⁺ dendritic cell subset which was present at control levels. This phenotype was attributed to a consequence of a cell-intrinsic effect of the RelB mutation. RelB, therefore, appears to selectively regulate the CD8α⁻ dendritic cell subset in the spleen. The deficiency of CD8α⁻ dendritic cells in RelB$^{-/-}$ mice is opposite to the expanded pool of these cells in the spleen of unmanipulated NOD.H-2^k mice and in B/N->B mixed bone marrow chimeric mice. It is therefore interesting to consider the possibility that enhancement of signalling pathways connected to RelB may be involved in the dendritic cell imbalance seen in the NOD.H-2^k spleen.

The NFκB family of transcription factors includes p50, p52, p65 (RelA), RelB and c-Rel (Ghosh et al, 1998; May and Ghosh, 1998). Transcriptionally active complexes are formed as a result of dimers formed between family members. In quiescent cells, these complexes are sequestered in the cytoplasm by the inhibitory IκBa and IκBb. IκB molecules mask the nuclear localization signal of NFκB and preclude its nuclear translocation. Signals that induce NFκB activity cause the dissociation and the subsequent degradation of IκB proteins. Degradation of IκB proteins enables NFκB to translocate to the nucleus and induce gene expression.

In addition to its role in the development of CD8α⁻ splenic dendritic cells in mice, in vitro studies suggest that RelB is important in dendritic cell differentiation and functional maturity in both humans and in mice. In humans, RelB mRNA is constitutively expressed by lymphocytes but not by myeloid cells. Upon activation, however, both

myeloid and lymphoid cells up-regulate RelB expression. Immunohistochemical staining of human tissue revealed that RelB is expressed by lymph node but not resting tissue (skin and synovial tissue) dendritic cells (Pettit et al, 1997). In the paracortex, RelB and HLA-DR are co-expressed in interdigitating dendritic cells, with RelB staining localized in the nucleus and HLA-DR staining on the cytoplasmic processes or dendrites. Staining with anti-CD3 monoclonal antibody revealed that $RelB^+$ interdigitating dendritic cells were clustered with $RelB^-$ T cells. Translocation of RelB to the nucleus of in vitro cultured monocyte-derived dendritic cells and activated B cells correlated with these cells acquiring efficient in vitro antigen presenting cell function. Interestingly, a recent study demonstrated that IL-12 acts directly on murine dendritic cells, via a dendritic cell-expressed IL-12 receptor, and induces nuclear translocation of RelB and NFκB p50 (Grohmann et al, 1998). This stimulation resulted in enhanced cell surface MHC class II expression and induction of endogenous IL-12 production.

6.3.4 Functional Specialization within Splenic Dendritic Cell Subsets and its Possible Relevance to Autoimmune Diabetes

Although the existence of splenic dendritic cell subsets is well established, it remains unclear whether these cells represent one cell type in distinct states of differentiation or whether they are distinct cell types performing distinct functions. Preliminary in vitro data has led to the suggestion that $CD8\alpha^+$ may possess regulatory/tolerogenic function while their $CD8\alpha^-$ counterparts perform pro-immunity functions (Süss and Shortman, 1996; Kronin et al, 1996). It has been demonstrated that $CD8\alpha^+$ dendritic cells are less efficient in inducing proliferation of purified allogeneic CD4 T cells compared to $CD8\alpha^-$ dendritic cells (Süss and Shortman, 1996). More dead cells were observed in $CD8\alpha^+$ dendritic cell MLR cultures than in $CD8\alpha^-$ dendritic cell MLR cultures. The mechanisms for reduced cell viability in $CD8\alpha^+$ dendritic cell MLR cultures remain to be elucidated. A similar regulatory role of $CD8\alpha^+$ dendritic cells was also observed in MLR cultures containing purified allogeneic CD8 T cells (Kronin et al, 1996). Again, the proliferative capacity of CD8 T cells stimulated with $CD8\alpha^+$ dendritic cells was relatively reduced. This reduced proliferation of CD8 T cells correlated with relatively reduced IL-2 secretion in the MLR cultures. It was concluded from this study that $CD8\alpha^+$ dendritic cells regulated CD8 T cell proliferation by limiting their IL-2 production.

Further evidence for functional differences between the two dendritic cell subsets was demonstrated in their ability to secrete IL-12 (Sousa et al , 1997). This study showed that in response to microbial stimulation in vivo, the majority of IL-12 secreting dendritic cells in the spleen were CD8α^+, as determined by flow cytometry. IL-12 secretion in this model was rapid and independent of CD40 ligand. Most recently, a number of studies have attempted to demonstrate delineation of function between the two dendritic cell subsets both in vitro (Ohteki et al, 1999) and in vivo (Pulendran et al, 1999; Maldonado-Lopez et al, 1999, Smith and Fazekas de St. Groth, 1999). Ohteki et al (1999) reported that IL-12 impacts differentially on the two dendritic cell subsets in vitro. CD8α^+ dendritic cells secrete approximately 5-fold higher level of IFNγ than do CD8α^- dendritic cells, when both subsets are sorted and cultured in the presence of IL-12. This results suggest that IL-12 secreted by CD8α^+ dendritic cells acts in autocrine manner for IFNγ production and subsequent generation of a T_h1-type response.

In vivo results from reports by Maldonado-Lopez et al (1999), Pulendran et al (1999), and Smith and Fazekas de St. Groth (1999) seem to contradict the the regulatory role of CD8α^+ dendritic cells observed in vitro by Süss and Shortman (1996). Maldonado-Lopez et al (1999) reported that administration into syngeneic recipients of purified CD8α^+ or CD8α^- dendritic cells, loaded ex vivo with antigen, resulted in antigen-specific T cell priming in draining lymph node, as assessed by antigen-dependent proliferation in culture. It is notable that the dendritic cell purification protocol involved overnight culture in GM-CSF of low density spleen cells. It was during this overnight culture that dendritic cells were pulsed with antigen. Analysis of cytokine profiles of draining lymph node cells cultured in vitro revealed that each dendritic cell subset could differentially skew cytokine production towards either a T_h1 or T_h-2-type response. It was shown that CD8α^+ dendritic cells promoted a T_h1-type response while CD8α^- dendritic cells promoted a T_h-2-type response. The capacity of CD8α^+ dendritic cells to mediate a T_h1-type response correlated with its ability to secrete relatively large amounts of IL-12 in response to in vitro stimulation.

Similar findings were reported in the study by Pulendran et al (1999). Pulendran et al (1999) administered Flt-3 ligand into mice to expand dendritic cell numbers in vivo. Flt-3 ligand induces expansion of both the putative myeloid- and lymphoid-related dendritic cell subsets. The ability of these dendritic cell subsets to prime antigen specific transgenic T cells in vivo was investigated in an adoptive transfer model. Detectable numbers of T cell receptor transgenic T cells derived from the DO.11.10/SCID mice were adoptively transferred into syngeneic Balb/c recipients. The DO.11 T cell receptor transgenic mice encode a T cell receptor specific for OVA323-339 and restricted to I-A^d

(Murphy et al, 1990). Dendritic cell subsets, sorted from the spleen of Flt-3 ligand treated mice on the basis of CD11c and CD11b expression, were pulsed with OVA323-339 in vitro and injected into the footpads of mice that had already received DO.11 T cell receptor transgenic T cells. Specific T cell response in draining lymph node was monitored by flow cytometry. Results obtained demonstrated that both dendritic cell subsets could prime antigen specific T cells with similar kinetics and magnitude. However, assessment of cytokine production by antigen specific T cells during in vitro restimulation with antigen revealed that the myeloid-related dendritic cell subset ($CD8\alpha^-$) always induced secretion of much greater levels of IL-10 and IL-4. Both dendritic cell subsets appeared to induce equal levels of IFNγ and IL-2 secretion.

An analogous study, but with different results and interpretations, was reported by Smith and Fazekas de St. Groth (1999). This study employed the adoptive transfer of freshly-purified, moth cytochrome c peptide-pulsed $CD8\alpha^+$ or $^-$ dendritic cells into recipient mice which had been injected with antigen-specific transgenic T cells 2 days earlier. In this model, only donor dendritic cells could present antigen as host antigen presenting cells lacked the MHC corresponding to the restriction of responding T cells. The antigen-specific T cell response in draining lymph node was almost identical regardless of which dendritic cell subset was used as antigen presenting cells. Inspite of this T cell response to both dendritic cell subsets, only the $CD8\alpha^-$ dendritic cells were capable of homing into draining lymph node. This result suggests that differential T_h priming may not result from direct T_h activation by $CD8\alpha^+$ versus $CD8\alpha^-$ dendritic cells. The authors invoke a mechanism of MHC-peptide transfer from $CD8\alpha^+$ to $CD8\alpha^-$ dendritic cells for T cell activation in vivo. Neither of the two preceding studies directly address the physiological function of the $CD8\alpha^+$ dendritic cells resident in T cell zones of secondary lymphoid tissue.

To date functional specialization within dendritic cell subsets remains controversial and obscure. It is, therefore, difficult to postulate the functional relevance, if any, of a bias towards the $CD8\alpha^-$ dendritic cell subset observed in the spleen of NOD.H-2^k mice. If the $CD8\alpha^+$ dendritic cell subset is the major producers of IL-12 in vivo, it is interesting to speculate that a dysregulation in the balance of splenic dendritic cell subsets (relative excess or deficiency of $CD8\alpha^-$ or $^+$ dendritic cells, respectively) could impair the ability of NOD mouse to evoke IL-12-mediated immunosuppressive mechanisms (Falcone and Sarvetnick, 1999). Systemic administration of high doses of IL-12 into NOD mice accelerates diabetes (Trembleau et al, 1995), whereas low doses suppress diabetes development (O' Hara et al, 1996). One possible mechanism by which IL-12 may mediate immunosuppression in the mouse is through the antagonist effect of the IL-12

p40 homodimer [$(p40)_2$] on the biologically-active IL-12 p75 heterodimer (Mattner et al, 1993; Trinchieri G., 1995). Cells secreting the biologically-active IL-12 p75 heterodimer also secrete an excess of monomeric p40 and $(p40)_2$ (D'Andrea et al, 1992; Heinzel et al, 1997). The $(p40)_2$ specifically antagonizes mouse IL-12 (Mattner et al, 1993). As previously mentioned, IL-12 (p40)-deficient NOD mice, although possessing reduced ability to mount T_h1 responses, develop diabetes to the same extent as control NOD mice (Trembleau et al, 1999). Thus, IL-12 is not essential for diabetes development. Interestingly, administration of $(p40)_2$ into young NOD mice results in the reduction of spontaneous and cyclophosphamide-induced diabetes (Trembleau et al, 1997). These findings suggest that IL-12 induced regulatory mechanisms can inhibit diabetes development.

Interestingly, the daily administration of the IL-12-related IL-18 into NOD mice inhibits diabetes development (Rothe et al, 1999). IL-18 is a recently described cytokine which shares biological activities with IL-12 (Takeda et al, 1998). It has recently been shown that cultured dendritic cells from humans and mice and primary dendritic cells from mice secrete functional IL-18 (Stoll et al, 1998). It is conceivable that impaired IL-12/18-mediated immunosuppressive responses could result from an imbalance in dendritic cell subsets.

As previously mentioned, a recent study demonstrated that IL-12 acts directly on murine dendritic cells, via a dendritic cell-expressed IL-12 receptor, and induces nuclear translocation of RelB and NFκB p50 (Grohmann et al, 1998). This stimulation resulted in enhanced cell surface MHC class II expression and induction of endogenous IL-12 production. Significant message for the IL-12 receptor was detected only on the $CD8\alpha^-$ dendritic cell subset. Consistent with this observation, syngeneic $CD8\alpha^-$ dendritic cells pulsed with a poorly immunogenic tumor peptide and exposed to rIL-12 in vitro are able to elicit efficient responses in vivo (Grohmann et al, 1999). Overall, these results indicate that IL-12 modulates dendritic cell phenotype by signalling through RelB. It is interesting to speculate that IL-12, secreted by $CD8\alpha^+$ dendritic cells, could prime the pool of $CD8\alpha^-$ subset present in relative excess in NOD.H-2^k mice, to initiate proimmunity rather than tolerogenic responses.

In light of the preceding evidence and findings from the current study, it is interesting to postulate a role for RelB in the bias towards $CD8\alpha^-$ splenic dendritic cell in NOD.H-2^k mice. Dysregulation of RelB function in NOD.H-2^k mice could occur as a result of impaired negative regulatory signals or excessive positive signals, or both, being transduced. The process of dendritic cell generation from myeloid precursors is delayed when myeloid precursors from the $RelB^{-/-}$ mice are stimulated with GM-CSF (DiMolfetto

et al, 1997). Dysregulated RelB could potentially accelerate the process of dendritic cell generation by making myeloid precursors more responsive to GM-CSF. Consequently, a potential scenario is that the relative excess of one dendritic cell subset may tilt the balance of immune responses in favor of autoimmunity rather than tolerance.

PART C: Relevance to Autoimmune Diabetes

6.4 Causal Link with Autoimmune Diabetes?

The current study demonstrates cell-intrinsic effects of non-MHC NOD genes on dendritic cell generation in vitro and in vivo. Furthermore, a prevalence of immature dendritic cells in NOD.H-2^k mice was unique to the NOD.H-2^k background among a number of H-2^k strains examined. These differences between the autoimmune-resistant B10.H-2^k and the autoimmunity-prone NOD.H-2^k mice, however, do not establish a causal link between these differences and autoimmune diabetes. On the one hand, there are likely to be numerous functional polymorphisms between the strains that are unrelated to diabetes susceptibility. On the other hand, dendritic cells play a key role in immune regulation and hence a good candidate cell type.

Important evidence for the role of dendritic cells in autoimmune response against peripheral tissue came in a study by Ludewig et al (1998). This study employs transgenic mice which express lymphocytic choriomeningitis virus glcoprotein (LCMV-GP) in pancreatic islets using the rat insulin promoter (RIP). RIP-GP mice do not spontaneously develop diabetes. However, when infected with LCMV, these mice develop an acute form of non-lethal diabetes (Ohashi et al, 1991; Oldstone et al, 1991). The Ludewig et al (1998) study investigated the role of dendritic cells in the initiation and maintenance of autoimmune diabetes, by repeatedly priming RIP-GP mice with dendritic cells constitutively expressing the immunodominant cytotoxic T lymphocyte (CTL) epitope of LCMV-GP. This regime of repeated CTL, and quite possibly helper T cell, activation by dendritic cells results in severe and destructive mononuclear infiltration of islets. A notable feature of this process is the formation of islet-associated secondary lymphoid-like structures, observed in other autoimmune syndromes, including Hashimoto's thyroiditis (Iwatani et al, 1993) and rheumatoid arthritis (Randen et al, 1995). Similar secondary lymphoid-like structures are observed in the islets of NOD.H-2^k mice which become diabetic as a result of transgenic expression of HEL in the islets and the 3A9 T cell receptor (Hartley S. and Goodnow C., unpublished observations). Thus, repeated priming by dendritic cells bearing peripheral antigen can induce formation of de novo lymphoid structures and tissue autoimmunity.

Alternatively, the cell-intrinsic and unique features of NOD.H-2^k mice may be unlinked to autoimmune diabetes. There is precedence for such a possibility. Until recently, it was postulated that the chromosome 3 encoded Fc receptor for IgG (FcγRI) was a candidate gene for the induction of autoimmune diabetes (Prins et al, 1993). The NOD *Fcgr I* allele carries mutations resulting in 17 amino acid differences compared with the wild-type B10 allele, and a substantial truncation in the cytoplasmic domain of the receptor. These structural differences in the NOD FcγRI contributed to lower clearance of IgG from the surface of NOD cells than from B10 cells. This functional difference and the localization of *Fcgr I* to the *Idd10* region led to the postulated role of FcγRI in diabetes development. However, congenic mapping of *Idd10* revealed the presence of two linked loci within *Idd10* : *Idd10* and *Idd17* (Podolin et al, 1997). Neither of these intervals contained the *Fcgr I* allele. The *Fcgr I* allele was therefore eliminated as a candidate gene, even though the NOD strain expresses a mutant form of the receptor.

Similarly, the *Slc9a1* (formerly known as *Nhe-1*) gene linked with *Idd11*, located on mouse chromosome 4, was initially proposed to be a candidate gene for diabetes susceptibility (Morahan et al, 1994). The *Slc9a1* gene encodes a Na^+/H^+ exchanger-1 which was found to be genetically and physiologically associated with diabetes susceptibility. The NOD *Slc9a1* allele is distinct from that expressed by diabetes-resistant strains. Furthermore, NOD lymphocytes exhibited higher Na^+/H^+ exchange activity compared with B6 or SJL mice lymphocytes, resulting in NOD lymphocytes having a higher resting intracellular pH. However, a recent study using NOD-*Idd11* congenic strains shows that introduction of the B6-derived *Idd11* chromosomal interval, containing the diabetes-resistant *Slc9a1* allele, onto the NOD background did not confer diabetes protection to the NOD congenic strain (Brodnicki et al, 2000). The *Slc9a1* gene was as a result eliminated as a candidate gene for autoimmune diabetes.

A similar strategy of genetic mapping of loci contributing to the myeloid/dendritic cell abnormalities, detected in this study, would be needed to examine whether these abnormalities are related to autoimmune diabetes. This strategy is outlined in the Future Directions section (6.4.2).

6.4.1 Proposed Model of the Role of Dendritic Cells in Autoimmune Diabetes

In order to consider how the observed myeloid/dendritic cell abnormalities might confer susceptibility to autoimmunity, I have proposed a hypothesis as follows. As yet undefined danger signals emanating from the pancreatic islets will activate resident antigen presenting cells and recruit dendritic cells on immunosurveillance and their precursors from blood. Monocytes provide a ready reservoir of precursors that could differentiate into lymphoid organ or tissue dendritic cells (Randolph et al, 1999). Activated dendritic cells will acquire islet antigen/s and migrate to the draining lymph nodes. Chemokines secreted by dendritic cells recruit lymphocytes to both the islets and the draining lymph nodes, both of which are potential sites for antigen presentation (Kurts et al, 1999). Dysregulated RelB function could contribute towards the exaggerated and continual antigen presenting cell response in the islets by influencing the balance between dendritic cell subsets and IL-12 secretion (See Figure 6.1). The relative deficiency in $CD8\alpha^+$ dendritic cells in NOD.H-2^k mice would result in reduced levels of IL-12 secreted during an immune response. The impact of reduced IL-12 secretion would be two-fold: i) the immunosuppressive effects of IL-12 would be mitigated; and (ii) the ability of bioactive IL-12 to appropriately modulate phenotype/function of the relatively abundant $CD8\alpha^-$ dendritic cell subset would be reduced. The relative excess of $CD8\alpha^-$ dendritic cells would mean the presence of more 'immature' antigen presenting cells. These immature dendritic cell population, present due to dysregulated RelB function, would also amplify immune responses by being hyper-responsive to T cell-secreted factors, like GM-CSF. The combined effect of these features is an unshackled cycle of self-destruction as a seemingly perpetual recruitment of antigen presenting cells and lymphocytes into islets occurs, with the ultimate outcome being the transformation of the pancreas into a lymph node-like structure.

Figure 6.1
Model for the role of dendritic cells in autoimmune diabetes
See text for details.

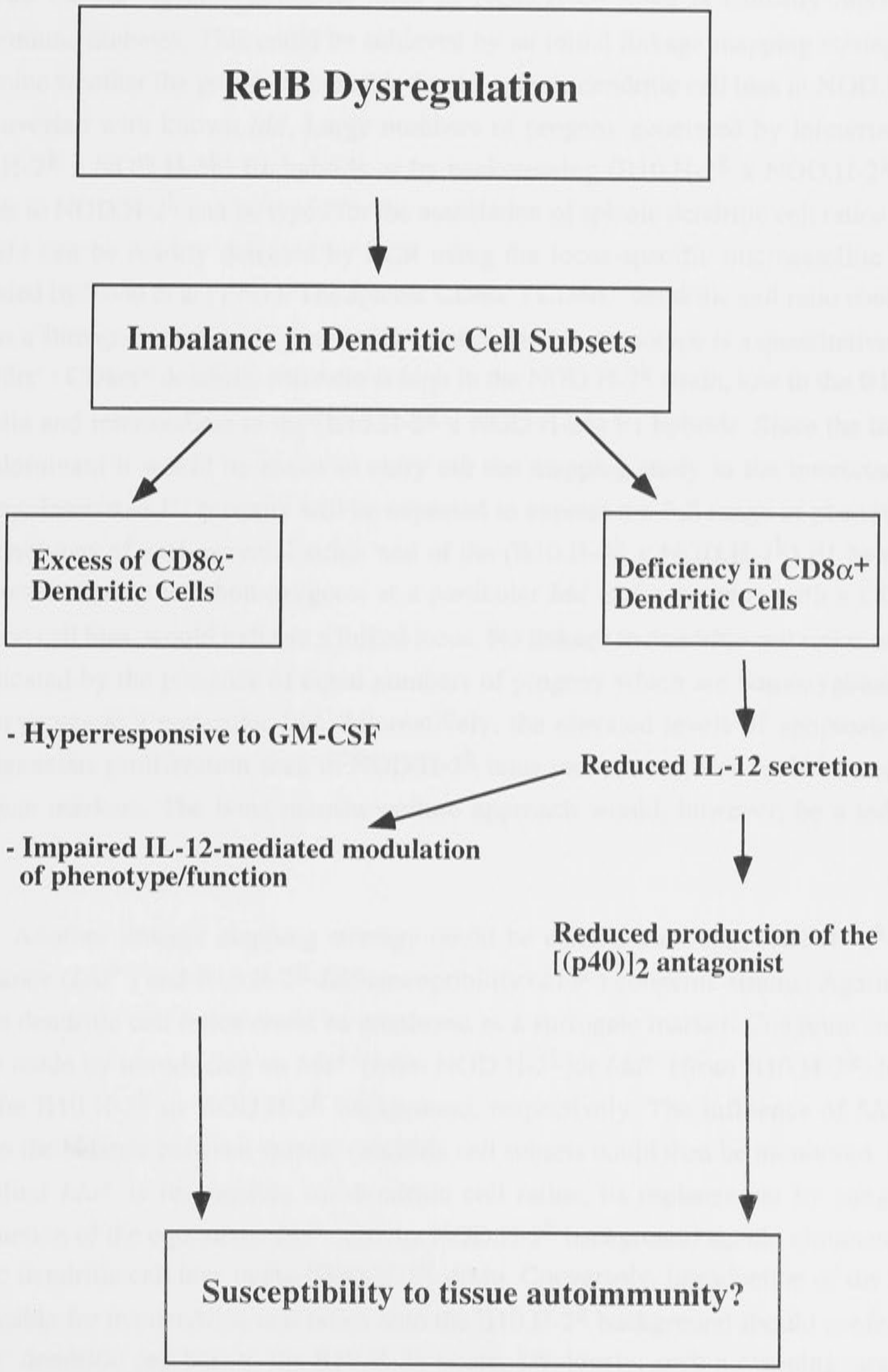

6.4.2 Future Directions

6.4.2.1 Genetic Mapping

The key objective of future experiments would be to establish whether the bias towards CD8α^- splenic dendritic cells in NOD.H-2^k mice is causally-linked to autoimmune diabetes. This could be achieved by an initial linkage mapping strategy to determine whether the gene/s responsible for the splenic dendritic cell bias in NOD.H-2^k mice overlap with known *Idd*. Large numbers of progeny generated by intercrossing (B10.H-2^k x NOD.H-2^k) F1 hybrids or by backcrossing (B10.H-2^k x NOD.H-2^k) F1 hybrids to NOD.H-2^k can be typed for the association of splenic dendritic cell ratios with *Idd*. *Idd* can be readily detected by PCR using the locus-specific microsatellite map generated by Todd et al (1991). The splenic CD8α^- : CD8α^+ dendritic cell ratio could be used as a surrogate marker. As previously mentioned, this phenotype is a quantitative trait as CD8α^- : CD8α^+ dendritic cell ratio is high in the NOD.H-2^k strain, low in the B10.H-2^k strain and intermediate in the (B10.H-2^k x NOD.H-2^k) F1 hybrids. Since the trait is semi-dominant it would be easier to carry out the mapping study in the intercross F2 progeny. Intercross F2 progeny will be expected to express the full range of phenotypes and genotypes of each parental strain and of the (B10.H-2^k x NOD.H-2^k) F1 hybrids. The presence of excess homozygotes at a particular *Idd* in the progeny with a CD8α^- dendritic cell bias, would indicate a linked locus. No linkage to dendritic cell ratios would be indicated by the presence of equal numbers of progeny which are homozygotes and heterozygotes at a particular *Idd*. Alternatively, the elevated levels of apoptosis and heterogeneous proliferation seen in NOD.H-2^k bone marrow cultures could be used as surrogate markers. The bone marrow culture approach would, however, be a tedious one.

Another linkage mapping strategy could be carried out using NOD.H-2^k-*Idd* -resistance (*Idd*^{r}) and B10.H-2^k-*Idd*-susceptibility (*Idd*^{s}) congenic strains. Again, the splenic dendritic cell ratios could be employed as a surrogate marker. Congenic strains can be made by introducing an *Idd*^{s} (from NOD.H-2^k)or *Idd*^{r} (from B10.H-2^k) locus onto the B10.H-2^k or NOD.H-2^k background, respectively. The influence of *Idd*^{s} or *Idd*^{r} on the balance between splenic dendritic cell subsets could then be monitored. If an individual *Idd*^{s} is responsible for dendritic cell ratios, its replacement by congenic introduction of the equivalent *Idd*^{r} onto the NOD.H-2^k background should eliminate the CD8α^- dendritic cell bias in the NOD.H-2^k strain. Conversely, introduction of the *Idd*^{s} responsible for the dendritic cell ratios onto the B10.H-2^k background should confer the CD8α^- dendritic cell bias to the B10.H-2^k strain. Obviously, such a mapping strategy would be extremely useful if a single *Idd* is responsible for the splenic dendritic cell bias.

In the event of an epistatic interaction between *Idd* creating the splenic dendritic cell bias, various permutations of double or multiple *Idd* congenic strains would be required.

6.4.2.2 Bone Marrow Reconstitution Assays to Causally-Link Dendritic Cells with Autoimmune Diabetes Induction

While at least some NOD strain Idd^s alleles have been shown to act within hematopoietic cells, it is not known whether these susceptibility genes act within T cells, B cells, macrophages or dendritic cells. Testing whether Idd^s act on CD8α^- dendritic cells in autoimmune diabetes induction could be done in diabetes transfer assays. In order to determine the role of dendritic cell subsets in the transfer of autoimmune diabetes, irradiated recipient mice expressing model autoantigen in the islet can be reconstituted with a mixture of bone marrow cells from dendritic cell-deficient mice and mice expressing a transgenic T cell receptor specific for the model autoantigen. As positive control group, a mixture of donor bone marrow cells from NOD.H-2^k.SCID mice and B10.H-2^k.SCID mice carrying the 3A9 T cell receptor transgene (B10.H-2^k.SCID.TCR) could be used to reconstitute B10.H-2^k mice expressing islet HEL (iHEL.B10.H-2^k). In the control group, antigen will be presented by myeloid-derived antigen presenting cells from the B10.H-2^k background (See Figure 6.2 for schematic of experiment). The SCID mutation eliminates the role of endogenous and donor B and T (non-transgenic) cells in diabetes induction. The test group would comprise the same recipients reconstituted with a mixture of bone marrow from NOD.H-2^k.SCID mice carrying the RelB mutation (NOD.H-2^k.SCID.RelB$^{-/-}$) and from the B10.H-2^k.SCID.TCR mice. In the test group, antigen will be presented by CD8α^- dendritic cell-deficient myeloid-derived antigen presenting cells from the NOD.H-2^k background. Both groups should then be screened for incidence of diabetes by measuring glucose levels in blood and for islet pathology by immunohistochemistry. The predicted outcome would be a significantly lower incidence of diabetes in the test group compared with that in the control group. However, residual CD8α^- dendritic cells may be sufficient in inducing control levels of diabetes in the test group since the RelB mutation does not completely abrogate the development CD8α^- dendritic cells.

Figure 6.2
Schematic to investigate the role of dendritic cell subsets in autoimmune diabetes.
See text for details.

1) **Control Group** - Myeloid-derived antigen presenting cells from the B10.H-2^k background present antigen

Inoculum bone marrow: 50% NOD.H-2^k.SCID and
50% B10.H-2^k.SCID. TCR

iHEL.B10.H-2^k

2) **Test Group** - CD8α^- dendritic cell-deficient myeloid-derived antigen presenting cells from the NOD.H-2^k background present antigen

Inoculum bone marrow: 50% NOD.H-2^k.SCID.RelB$^{-/-}$ and
50% B10.H-2^k.SCID. TCR

iHEL.B10.H-2^k

Readout: Diabetes, Islet Histology

6.4.3 Concluding Remarks

Overall, the results described herein demonstrate for the first time cell-intrinsic effects of non-MHC NOD genes on hematopoietic stem cells which alter dendritic cell generation, both in vitro and in vivo. These effects were manifested by:

a) elevated levels of apoptosis and heterogeneous proliferation, resulting in reduced dendritic cell yield during in vitro cultures;

b) skewing towards the myeloid lineage of cells in vivo; and

c) selective bias of splenic dendritic cells towards the CD8α^- subset in vivo.

Furthermore, this study demonstrates the prevalence of immature dendritic cells in the NOD.H-2^k strain. This is not a cell-intrinsic feature of NOD.H-2^k hematopoietic stem cells but a unique feature of the NOD.H-2^k strain. Further studies must be aimed at unravelling the genetic basis of these differences, and determining whether contributory gene/s coincide with known *Idd*. Such studies may elucidate molecular/biochemical pathways amenable to therapeutic intervention, genetic or pharmacologic, for the prevention, treatment and cure of Type I diabetes in humans.

Appendices

Appendices

A1 Common Reagents and Suppliers

Reagent	Supplier
Acetic acid (glacial)	BDH Laboratory Supplies, Poole, England
Agarose (Ultrapure)	GibcoBRL
Ammonium chloride	BDH Laboratory Supplies
β-mercaptoethanol	GibcoBRL
CFSE	Molecular Probes
Dimethylsulfoxide (DMSO)	Sigma Chemical Co.
dNTPs	Pharmacia Biotech
Ficoll Paque	Pharmacia Biotech
Ethylenediamine tetra-acetic acid	BDH Laboratory Supplies
Ethidium bromide	Amresco, OH, USA
Foetal bovine serum (FBS)	Trace Biosciences
Glutamine	GibcoBRL
Lysozyme	Sigma Chemical Co.
Magnesium Chloride	BDH Laboratory Supplies
Merocyanin 540	Sigma Chemical Co.
Metrizamide	Nycomed Pharma
Neomycin	Sigma Chemical Co.
Ovalbumin	Sigma Chemical Co.
Polymyxin B	Sigma Chemical Co.
Proteinase K	Sigma Chemical Co.
Paraformaldehyde	BDH Laboratory Supplies
RPMI 1640	JCSMR, GibcoBRL
Sf9-900 insect cell medium	GibcoBRL
Sodium dodecyl sulphate (SDS)	GibcoBRL
Sodium chloride	BDH Laboratory Supplies
Sodium azide	BDH Laboratory Supplies
Taq DNA polymerase	Stratagene USA, CA, USA
Taq DNA polymerase buffer	Stratagene USA
Tris	Boehringer Mannheim
Triton X-100	Sigma Chemical Co.
Trypan blue	Sigma Chemical Co.

A2 Buffers, Media and Stock Solutions

A2.1 Buffers

a) **FACS Buffer**

2% FBS (v/v) and 0.01% sodium azide (v/v) in PBS. Stored at 4°C.

b) **FACS Fix Buffer**

FACS buffer with 0.1% (w/v) paraformaldehyde. Stored at 4°C.

d) **Tris Ammonium Chloride Red Blood Cell Lysis Buffer**

Lysis buffer contains 0.02mM Tris and 0.1M ammonium chloride in PBS.
1.03g Tris and 3.375g ammonium chloride dissolved in 500mL PBS. Adjust pH to 7.2 with concentrated hydrochloric acid. Buffer autoclaved and stored at room temperature.

A2.1.2 DNA Buffers and Gels

a) **TAE DNA Running Buffer**

TAE (1x)
- 40 mM Tris
- 40mM Acetic acid
- 1mM EDTA

b) **DNA Loading Buffer**

- 50% (v/v) glycerol in 10x TAE
- 2mg/mL bromophenol blue

Stored at -20°C.

c) **DNA Gel**

- 1% agarose gel (w/v) in TAE buffer
- 0.5µg/mL ethidium bromide

A2.2 Media

RPMI 1640

For 20 L stock:

208.8g RPMI powder

40g Sodium bicarbonate

Dissolve ingredients in in 20 L double distilled water. Microfilter (0.2µm) and aseptically dispense into sterile Schott bottles.

For cell culture, RPMI 1640 is supplemented with:

- 10% (v/v) heat inactivated (1-4 hr at 57°C) foetal bovine serum
- 0.05mM β-mercaptoethanol
- 2mM L-Glutamine
- 10mM HEPES
- 100U/mL penicillin, 100µg/mL streptomycin.

A2.3 Stock Solutions

a) **Alsevers Solution**

In 1 L stock:

8g sodium citrate

4.2g sodium chloride

20.5g glucose

0.8g citric acid

Dissolve ingredients in 1L distilled water. Adjust pH to 6.1 with 10% citric acid. Autoclave and store at 4°C in 100mL aliquots.

b) **Antibiotics Solution**

Dissolve 8.5×10^5 U/mL Polymyxin B and 1.1 mg/mL Neomycin. Add food color to distinguish from antibiotics-free water. Dispense into 2mL aliquots and store at -20°C. One aliquot used per 550mL water.

c) **CFSE**

5 mM stock made by reconstituting in DMSO. 50µL aliquots stored at -70°C.

d) **Collagenase**

1 mg/mL stock made reconstituting in Hank's buffered saline. 1mL aliquots stored at -20°C.

e) **Merocyanin 540**

1mg/mL stock made by reconstituting in double distilled water. Microfiltered and stored in the dark at 4°C.

f) **Metrizamide**

14.5% (w/v) stock made by dissolving in RPMI 1640 (10% FBS). Microfiltered and dispensed into 5mL aliquots. Stored at -20°C.

g) **Rabbit Complement**

Reconstituted in 1mL ice-cold double distilled water. 100µL aliquots were frozen at -20°C. 1 in 10 dilution of complement was used for lysis.

h) **White Blood Cell Counting Stain**

1.5% v/v acetic acid and 0.01% w/v Gentian Violet in distilled water. Stored at room temperature.

References

References

Acha-Orbea, H., and H. O. McDevitt (1987). The first external domain of the nonobese diabetic mouse class II I-A beta chain is unique. *Proc Natl Acad Sci U S A 84:2435.*

Adams, J. M., and S. Cory (1998). The Bcl-2 protein family: arbiters of cell survival. *Science 281:1322.*

Adema, G. J., F. Hartgers, R. Verstraten, E. de Vries, G. Marland, S. Menon, J. Foster, Y. Xu, P. Nooyen, T. McClanahan, K. B. Bacon, and C. G. Figdor (1997). A dendritic-cell-derived C-C chemokine that preferentially attracts naive T cells. *Nature 387:713.*

Afonso, L. C., T. M. Scharton, L. Q. Vieira, M. Wysocka, G. Trinchieri, and P. Scott (1994). The adjuvant effect of interleukin-12 in a vaccine against Leishmania major. *Science 263:235.*

Ahmed, N. N., H. L. Grimes, A. Bellacosa, T. O. Chan, and P. N. Tsichlis (1997. Transduction of interleukin-2 antiapoptotic and proliferative signals via Akt protein kinase. *Proc Natl Acad Sci U S A 94:3627.*

Akhtar, I., J. P. Gold, L. Y. Pan, J. L. Ferrara, X. D. Yang, J. I. Kim, and K. N. Tan (1995). CD4+ beta islet cell-reactive T cell clones that suppress autoimmune diabetes in nonobese diabetic mice. *J Exp Med 182:87.*

Albert, M. L., B. Sauter, and N. Bhardwaj (1998). Dendritic cells acquire antigen from apoptotic cells and induce class I- restricted CTLs. *Nature 392:86.*

Anderson, D. M., E. Maraskovsky, W. L. Billingsley, W. C. Dougall, M. E. Tometsko, E. R. Roux, M. C. Teepe, R. F. DuBose, D. Cosman, and L. Galibert. 1997. A homologue of the TNF receptor and its ligand enhance T-cell growth and dendritic-cell function. *Nature 390:175.*

Arai, K. I., F. Lee, A. Miyajima, S. Miyatake, N. Arai, and T. Yokota (1990). Cytokines: coordinators of immune and inflammatory responses. *Annu Rev Biochem 59:783.*

Ardavin, C., L. Wu, C. L. Li, and K. Shortman (1993). Thymic dendritic cells and T cells develop simultaneously in the thymus from a common precursor population. *Nature 362:761.*

Ardavin, C. (1997). Thymic dendritic cells. *Immunol Today 18:350.*

Armitage, J. O. (1998). Emerging applications of recombinant human granulocyte-macrophage colony-stimulating factor. *Blood 92:4491.*

Askew, D. S., R. A. Ashmun, B. C. Simmons, and J. L. Cleveland (1991). Constitutive c-myc expression in an IL-3-dependent myeloid cell line suppresses cell cycle arrest and accelerates apoptosis. *Oncogene 6:1915.*

Atkinson, M. A., M. A. Bowman, L. Campbell, B. L. Darrow, D. L. Kaufman, and N. K. Maclaren (1994). Cellular immunity to a determinant common to glutamate decarboxylase and coxsackie virus in insulin-dependent diabetes. *J Clin Invest 94:2125.*

Austyn, J. M., J. W. Kupiec-Weglinski, D. F. Hankins, and P. J. Morris (1988). Migration patterns of dendritic cells in the mouse. Homing to T cell-dependent areas of spleen, and binding within marginal zone. *J Exp Med 167:646.*

Baekkeskov, S., J. H. Nielsen, B. Marner, T. Bilde, J. Ludvigsson, and A. Lernmark (1982). Autoantibodies in newly diagnosed diabetic children immunoprecipitate human pancreatic islet cell proteins. *Nature 298:167.*

Baekkeskov, S., H. J. Aanstoot, S. Christgau, A. Reetz, M. Solimena, M. Cascalho, F. Folli, H. Richter-Olesen, P. DeCamilli, and P. D. Camilli (1990). Identification of the 64K autoantigen in insulin-dependent diabetes as the GABA-synthesizing enzyme glutamic acid decarboxylase [published erratum appears in Nature 1990 Oct 25;347(6295):782]. *Nature 347:151.*

Banchereau, J., and R. M. Steinman (1998). Dendritic cells and the control of immunity. *Nature 392:245.*

Baxter, A. G., and A. Cooke (1995). The genetics of the NOD mouse. *Diabetes Metab Rev 11:315.*

Bendelac, A., C. Carnaud, C. Boitard, and J. F. Bach (1987). Syngeneic transfer of autoimmune diabetes from diabetic NOD mice to healthy neonates. Requirement for both L3T4+ and Lyt-2+ T cells. *J Exp Med 166:823.*

Bennett, S. R., F. R. Carbone, F. Karamalis, R. A. Flavell, J. F. Miller, and W. R. Heath (1998). Help for cytotoxic-T-cell responses is mediated by CD40 signalling. *Nature 393:478.*

Bergman, B., and K. Haskins (1994). Islet-specific T-cell clones from the NOD mouse respond to beta-granule antigen. *Diabetes 43:197.*

Bernard, C. C., T. G. Johns, A. Slavin, M. Ichikawa, C. Ewing, J. Liu, and J. Bettadapura (1997). Myelin oligodendrocyte glycoprotein: a novel candidate autoantigen in multiple sclerosis. *J Mol Med 75:77.*

Bhardwaj, N., J. W. Young, A. J. Nisanian, J. Baggers, and R. M. Steinman (1993). Small amounts of superantigen, when presented on dendritic cells, are sufficient to initiate T cell responses. *J Exp Med 178:633.*

Brasel, K., S. Escobar, R. Anderberg, P. de Vries, H. J. Gruss, and S. D. Lyman (1995). Expression of the flt3 receptor and its ligand on hematopoietic cells. *Leukemia 9:1212.*

Brasel, K., H. J. McKenna, P. J. Morrissey, K. Charrier, A. E. Morris, C. C. Lee, D. E. Williams, and S. D. Lyman (1996). Hematologic effects of flt3 ligand in vivo in mice. *Blood 88:2004.*

Brennan, P., J. W. Babbage, B. M. Burgering, B. Groner, K. Reif, and D. A. Cantrell (1997). Phosphatidylinositol 3-kinase couples the interleukin-2 receptor to the cell cycle regulator E2F. *Immunity 7:679.*

Brodnicki, T. C., P. McClive, S. Couper, and G. Morahan (2000). Localization of Idd11 using NOD congenic mouse strains: elimination of Slc9a1 as a candidate gene. *Immunogenetics 51:37.*

Brown, J. H., T. S. Jardetzky, J. C. Gorga, L. J. Stern, R. G. Urban, J. L. Strominger, and D. C. Wiley (1993). Three-dimensional structure of the human class II histocompatibility antigen HLA-DR1. *Nature 364:33.*

Burkly, L., C. Hession, L. Ogata, C. Reilly, L. A. Marconi, D. Olson, R. Tizard, R. Cate, and D. Lo (1995). Expression of relB is required for the development of thymic medulla and dendritic cells. *Nature 373:531.*

Carrasco, D., R. P. Ryseck, and R. Bravo (1993). Expression of relB transcripts during lymphoid organ development: specific expression in dendritic antigen-presenting cells. *Development 118:1221.*

Carrasco-Marin, E., J. Shimizu, O. Kanagawa, and E. R. Unanue (1996). The class II MHC I-Ag7 molecules from non-obese diabetic mice are poor peptide binders. *J Immunol 156:450.*

Caux, C., C. Dezutter-Dambuyant, D. Schmitt, and J. Banchereau (1992). GM-CSF and TNF-alpha cooperate in the generation of dendritic Langerhans cells. *Nature 360:258.*

Caux, C., B. Vanbervliet, C. Massacrier, M. Azuma, K. Okumura, L. L. Lanier, and J. Banchereau (1994a). B70/B7-2 is identical to CD86 and is the major functional ligand for CD28 expressed on human dendritic cells. *J Exp Med 180:1841.*

Caux, C., C. Massacrier, B. Vanbervliet, B. Dubois, C. Van Kooten, I. Durand, and J. Banchereau (1994b). Activation of human dendritic cells through CD40 cross-linking. *J Exp Med 180:1263.*

Caux, C., C. Massacrier, B. Vanbervliet, C. Barthelemy, Y. J. Liu, and J. Banchereau (1994c). Interleukin 10 inhibits T cell alloreaction induced by human dendritic cells. *Int Immunol 6:1177.*

Cella, M., D. Scheidegger, K. Palmer-Lehmann, P. Lane, A. Lanzavecchia, and G. Alber (1996). Ligation of CD40 on dendritic cells triggers production of high levels of interleukin-12 and enhances T cell stimulatory capacity: T-T help via APC activation. *J Exp Med 184:747.*

Cella, M., F. Sallusto, and A. Lanzavecchia (1997). Origin, maturation and antigen presenting function of dendritic cells. *Curr Opin Immunol 9:10.*

Cella, M., D. Jarrossay, F. Facchetti, O. Alebardi, H. Nakajima, A. Lanzavecchia, and M. Colonna (1999). Plasmacytoid monocytes migrate to inflamed lymph nodes and produce large amounts of type I interferon. *Nat Med 5:919.*

Celluzzi, C. M., J. I. Mayordomo, W. J. Storkus, M. T. Lotze, and L. D. Falo Jr. (1996). Peptide-pulsed dendritic cells induce antigen-specific CTL-mediated protective tumor immunity. *J Exp Med 183:283.*

Ceredig, R., J. Medveczky, and A. Skulimowski (1989). Mouse fetal thymus lobes cultured in IL-2 generate CD3+, TCR-gamma delta-expressing CD4-/CD8+ and CD4-/CD8- cells. *J Immunol 142:3353.*

Chao, D. T., and S. J. Korsmeyer (1998). BCL-2 family: regulators of cell death. *Annu Rev Immunol 16:395.*

Chen, S. Z., and G. A. Evans (1990). A simple screening method for transgenic mice using the polymerase chain reaction. *Biotechniques 8:32.*

Christianson, S. W., L. D. Shultz, and E. H. Leiter (1993). Adoptive transfer of diabetes into immunodeficient NOD-scid/scid mice. Relative contributions of CD4+ and CD8+ T-cells from diabetic versus prediabetic NOD.NON-Thy-1a donors. *Diabetes 42:44.*

Christie, M. R., S. Genovese, D. Cassidy, E. Bosi, T. J. Brown, M. Lai, E. Bonifacio, and G. F. Bottazzo (1994). Antibodies to islet 37k antigen, but not to glutamate decarboxylase, discriminate rapid progression to IDDM in endocrine autoimmunity. *Diabetes 43:1254.*

Coffman, R. L., and I. L. Weissman (1981). B220: a B cell-specific member of th T200 glycoprotein family. *Nature 289:681.*

Cohen, P. L., and R. A. Eisenberg (1991). Lpr and gld: single gene models of systemic autoimmunity and lymphoproliferative disease. *Annu Rev Immunol 9:243.*

Cohen, J. J., R. C. Duke, V. A. Fadok, and K. S. Sellins (1992). Apoptosis and programmed cell death in immunity. *Annu Rev Immunol 10:267.*

Croft, M., D. D. Duncan, and S. L. Swain (1992). Response of naive antigen-specific CD4+ T cells in vitro: characteristics and antigen-presenting cell requirements. *J Exp Med 176:1431.*

Cumberbatch, M., and I. Kimber (1992). Dermal tumour necrosis factor-alpha induces dendritic cell migration to draining lymph nodes, and possibly provides one stimulus for Langerhans' cell migration. *Immunology 75:257.*

Cyster, J. G., S. B. Hartley, and C. C. Goodnow (1994). Competition for follicular niches excludes self-reactive cells from the recirculating B-cell repertoire. *Nature 371:389.*

D'Andrea, A., M. Rengaraju, N. M. Valiante, J. Chehimi, M. Kubin, M. Aste, S. H. Chan, M. Kobayashi, D. Young, E. Nickbarg, and et al. (1992). Production of natural killer cell stimulatory factor (interleukin 12) by peripheral blood mononuclear cells. *J Exp Med 176:1387.*

Dahlen, E., K. Dawe, L. Ohlsson, and G. Hedlund (1998). Dendritic cells and macrophages are the first and major producers of TNF-alpha in pancreatic islets in the nonobese diabetic mouse. *J Immunol 160:3585.*

Damotte, D., E. Colomb, C. Cailleau, N. Brousse, J. Charreire, and C. Carnaud (1997). Analysis of susceptibility of NOD mice to spontaneous and experimentally induced thyroiditis. *Eur J Immunol 27:2854.*

Daniel, D., R. G. Gill, N. Schloot, and D. Wegmann (1995). Epitope specificity, cytokine production profile and diabetogenic activity of insulin-specific T cell clones isolated from NOD mice. *Eur J Immunol 25:1056.*

Daniel, D., and D. R. Wegmann (1996). Protection of nonobese diabetic mice from diabetes by intranasal or subcutaneous administration of insulin peptide B-(9-23). *Proc Natl Acad Sci U S A 93:956.*

Datta, S. R., H. Dudek, X. Tao, S. Masters, H. Fu, Y. Gotoh, and M. E. Greenberg (1997). Akt phosphorylation of BAD couples survival signals to the cell- intrinsic death machinery. *Cell 91:231.*

Datta, S. R., A. Brunet, and M. E. Greenberg (1999). Cellular survival: a play in three Akts. *Genes Dev 13:2905.*

De Smedt, T., B. Pajak, E. Muraille, L. Lespagnard, E. Heinen, P. De Baetselier, J. Urbain, O. Leo, and M. Moser (1996). Regulation of dendritic cell numbers and maturation by lipopolysaccharide in vivo. *J Exp Med 184:1413.*

Dean, M., R. A. Levine, W. Ran, M. S. Kindy, G. E. Sonenshein, and J. Campisi (1986). Regulation of c-myc transcription and mRNA abundance by serum growth factors and cell contact. *J Biol Chem 261:9161.*

Debray-Sachs, M., C. Carnaud, C. Boitard, H. Cohen, I. Gresser, P. Bedossa, and J. F. Bach (1991). Prevention of diabetes in NOD mice treated with antibody to murine IFN gamma. *J Autoimmun 4:237.*

Delovitch, T. L., and B. Singh (1997). The nonobese diabetic mouse as a model of autoimmune diabetes: immune dysregulation gets the NOD [published erratum appears in Immunity 1998 Apr;8(4):531]. *Immunity 7:727.*

Denny, P., C. J. Lord, N. J. Hill, J. V. Goy, E. R. Levy, P. L. Podolin, L. B. Peterson, L. S. Wicker, J. A. Todd, and P. A. Lyons (1997). Mapping of the IDDM locus Idd3 to a 0.35-cM interval containing the interleukin-2 gene. *Diabetes 46:695.*

Dialynas, D. P., Z. S. Quan, K. A. Wall, A. Pierres, J. Quintans, M. R. Loken, M. Pierres, and F. W. Fitch (1983). Characterization of the murine T cell surface molecule, designated L3T4, identified by monoclonal antibody GK1.5: similarity of L3T4 to the human Leu-3/T4 molecule. *J Immunol 131:2445.*

Dieu, M. C., B. Vanbervliet, A. Vicari, J. M. Bridon, E. Oldham, S. Ait-Yahia, F. Briere, A. Zlotnik, S. Lebecque, and C. Caux (1998). Selective recruitment of immature and mature dendritic cells by distinct chemokines expressed in different anatomic sites. *J Exp Med 188:373.*

DiMolfetto, L., C. Reilly, Q. Wei, and D. Lo (1997). Dendritic-like cells from relB mutant mice. *Adv Exp Med Biol 417:47.*

Dranoff, G., A. D. Crawford, M. Sadelain, B. Ream, A. Rashid, R. T. Bronson, G. R. Dickersin, C. J. Bachurski, E. L. Mark, J. A. Whitsett, and et al. (1994). Involvement of granulocyte-macrophage colony-stimulating factor in pulmonary homeostasis. *Science 264:713.*

Dudek, H., S. R. Datta, T. F. Franke, M. J. Birnbaum, R. Yao, G. M. Cooper, R. A. Segal, D. R. Kaplan, and M. E. Greenberg (1997). Regulation of neuronal survival by the serine-threonine protein kinase Akt. *Science 275:661.*

Elliott, R. B., S. N. Reddy, N. J. Bibby, and K. Kida (1988). Dietary prevention of diabetes in the non-obese diabetic mouse. *Diabetologia 31:62.*

Encinas, J. A., L. S. Wicker, L. B. Peterson, A. Mukasa, C. Teuscher, R. Sobel, H. L. Weiner, C. E. Seidman, J. G. Seidman, and V. K. Kuchroo (1999). QTL influencing autoimmune diabetes and encephalomyelitis map to a 0.15-cM region containing Il2. *Nat Genet 21:158.*

Evan, G. I., A. H. Wyllie, C. S. Gilbert, T. D. Littlewood, H. Land, M. Brooks, C. M. Waters, L. Z. Penn, and D. C. Hancock (1992). Induction of apoptosis in fibroblasts by c-myc protein. *Cell 69:119.*

Falcone, M., and N. Sarvetnick (1999). Cytokines that regulate autoimmune responses. *Curr Opin Immunol 11:670.*

Fox, C. J., and J. S. Danska (1997). IL-4 expression at the onset of islet inflammation predicts nondestructive insulitis in nonobese diabetic mice. *J Immunol 158:2414.*

Frelinger, J. G., L. Hood, S. Hill, and J. A. Frelinger (1979). Mouse epidermal Ia molecules have a bone marrow origin. *Nature 282:321.*

Frey, T. (1997). Correlated flow cytometric analysis of terminal events in apoptosis reveals the absence of some changes in some model systems. *Cytometry 28:253.*

Friedmann, M. C., T. S. Migone, S. M. Russell, and W. J. Leonard (1996). Different interleukin 2 receptor beta-chain tyrosines couple to at least two signaling pathways and synergistically mediate interleukin 2- induced proliferation.
Proc Natl Acad Sci U S A 93:2077.

Fujii, H., K. Ogasawara, H. Otsuka, M. Suzuki, K. Yamamura, T. Yokochi, T. Miyazaki, H. Suzuki, T. W. Mak, S. Taki, and T. Taniguchi (1998). Functional dissection of the cytoplasmic subregions of the IL-2 receptor betac chain in primary lymphocyte populations. *Embo J 17:6551.*

Fukumoto, T., W. R. McMaster, and A. F. Williams (1982). Mouse monoclonal antibodies against rat major histocompatibility antigens. Two Ia antigens and expression of Ia and class I antigens in rat thymus. *Eur J Immunol 12:237.*

Gajewski, T. F., and C. B. Thompson (1996). Apoptosis meets signal transduction: elimination of a BAD influence. *Cell 87:589.*

Gasson, J. C. (1991). Molecular physiology of granulocyte-macrophage colony-stimulating factor. *Blood 77:1131.*

Ghosh, S., S. M. Palmer, N. R. Rodrigues, H. J. Cordell, C. M. Hearne, R. J. Cornall, J. B. Prins, P. McShane, G. M. Lathrop, L. B. Peterson, and et al. (1993). Polygenic control of autoimmune diabetes in nonobese diabetic mice. *Nat Genet 4:404.*

Ghosh, S., M. J. May, and E. B. Kopp (1998). NF-kappa B and Rel proteins: evolutionarily conserved mediators of immune responses. *Annu Rev Immunol 16:225.*

Goordyal, P., and P. G. Isaacson (1985). Immunocytochemical characterization of monocyte colonies of human bone marrow: a clue to the origin of Langerhans cells and interdigitating reticulum cells. *J Pathol 146:189.*

Gosgrove, D., D. Gray, A. Dierich, J. Kaufman, M. Lemeur, C. Benoist, and D. Mathis (1991). Mice lacking MHC class II molecules. *Cell 66:1051.*

Gray, J. D., M. Hirokawa, and D. A. Horwitz (1994). The role of transforming growth factor beta in the generation of suppression: an interaction between CD8+ T and NK cells. *J Exp Med 180:1937.*

Green, E. A., E. E. Eynon, and R. A. Flavell (1998). Local expression of TNFalpha in neonatal NOD mice promotes diabetes by enhancing presentation of islet antigens. *Immunity 9:733.*

Grohmann, U., M. L. Belladonna, R. Bianchi, C. Orabona, E. Ayroldi, M. C. Fioretti, and P. Puccetti (1998). IL-12 acts directly on DC to promote nuclear localization of NF-kappaB and primes DC for IL-12 production. *Immunity 9:315.*

Grohmann, U., R. Bianchi, M. L. Belladonna, C. Vacca, S. Silla, E. Ayroldi, M. C. Fioretti, and P. Puccetti (1999). IL-12 acts selectively on CD8 alpha- dendritic cells to enhance presentation of a tumor peptide in vivo. *J Immunol 163:3100.*

Gruenwald, S. and J. Heitz. Baculovirus Expression Vector System: Procedures and Methods Manual (second edition, © 1993 by PharMingen).

Gunter, K. C., T. R. Malek, and E. M. Shevach (1984). T cell-activating properties of an anti-Thy-1 monoclonal antibody. Possible analogy to OKT3/Leu-4.
J Exp Med 159:716.

* K. Hanada, R. Tsunoda and H. Hamada (1996). GM-CSF-induced in vivo expansion of splenic dendritic cells and their strong costimulation activity. *J Leukoc Biol.* 60: 181-90.

Hagopian, W. A., B. Michelsen, A. E. Karlsen, F. Larsen, A. Moody, C. E. Grubin, R. Rowe, J. Petersen, R. McEvoy, and A. Lernmark (1993a). Autoantibodies in IDDM primarily recognize the 65,000-M(r) rather than the 67,000-M(r) isoform of glutamic acid decarboxylase. *Diabetes 42:631.*

Hagopian, W. A., A. E. Karlsen, A. Gottsater, M. Landin-Olsson, C. E. Grubin, G. Sundkvist, J. S. Petersen, E. Boel, T. Dyrberg, and A. Lernmark (1993b). Quantitative assay using recombinant human islet glutamic acid decarboxylase (GAD65) shows that 64K autoantibody positivity at onset predicts diabetes type. *J Clin Invest 91:368.*

Hapel, A. J., H. S. Warren, and D. A. Hume (1984). Different colony-stimulating factors are detected by the "interleukin- 3"-dependent cell lines FDC-Pl and 32D cl-23. *Blood 64:786.*

Hara, T., and A. Miyajima (1992). Two distinct functional high affinity receptors for mouse interleukin-3 (IL-3). *Embo J 11:1875.*

Hart, D. N. (1997). Dendritic cells: unique leukocyte populations which control the primary immune response. *Blood 90:3245.*

Haskins, K., and M. McDuffie (1990). Acceleration of diabetes in young NOD mice with a CD4+ islet-specific T cell clone. *Science 249:1433.*

Hattori, M., J. B. Buse, R. A. Jackson, L. Glimcher, M. E. Dorf, M. Minami, S. Makino, K. Moriwaki, H. Kuzuya, H. Imura, and et al. (1986). The NOD mouse: recessive diabetogenic gene in the major histocompatibility complex. *Science 231:733.*

Hattori, M., E. Yamato, N. Itoh, H. Senpuku, T. Fujisawa, M. Yoshino, M. Fukuda, E. Matsumoto, T. Toyonaga, I. Nakagawa, M. Petruzzelli, A. McMurray, H. Weiner, T. Sagai, K. Moriwaki, T. Shiroishi, R. Maron, and T. Lund (1999). Cutting edge: homologous recombination of the MHC class I K region defines new MHC-linked diabetogenic susceptibility gene(s) in nonobese diabetic mice. *J Immunol 163:1721.*

Hawkes, C. J., C. Wasmeier, M. R. Christie, and J. C. Hutton (1996). Identification of the 37-kDa antigen in IDDM as a tyrosine phosphatase- like protein (phogrin) related to IA-2. *Diabetes 45:1187.*

Hearne, C. M., S. Ghosh, and J. A. Todd (1992). Microsatellites for linkage analysis of genetic traits. *Trends Genet 8:288.*

Heath, V. L., N. C. Moore, S. M. Parnell, and D. W. Mason (1998). Intrathymic expression of genes involved in organ specific autoimmune disease. *J Autoimmun 11:309.*

Heinzel, F. P., A. M. Hujer, F. N. Ahmed, and R. M. Rerko (1997). In vivo production and function of IL-12 p40 homodimers. *J Immunol 158:4381.*

Heufler, C., F. Koch, and G. Schuler (1988). Granulocyte/macrophage colony-stimulating factor and interleukin 1 mediate the maturation of murine epidermal Langerhans cells into potent immunostimulatory dendritic cells. *J Exp Med 167:700.*

Hirayama, F., J. P. Shih, A. Awgulewitsch, G. W. Warr, S. C. Clark, and M. Ogawa (1992). Clonal proliferation of murine lymphohemopoietic progenitors in culture. *Proc Natl Acad Sci U S A 89:5907.*

Ho, W. Y., M. P. Cooke, C. C. Goodnow, and M. M. Davis (1994). Resting and anergic B cells are defective in CD28-dependent costimulation of naive CD4+ T cells. *J Exp Med 179:1539.*

Horwitz, M. S., L. M. Bradley, J. Harbertson, T. Krahl, J. Lee, and N. Sarvetnick (1998). Diabetes induced by Coxsackie virus: initiation by bystander damage and not molecular mimicry. *Nat Med 4:781.*

Hsieh, C. S., S. E. Macatonia, C. S. Tripp, S. F. Wolf, A. O'Garra, and K. M. Murphy (1993). Development of TH1 CD4+ T cells through IL-12 produced by Listeria- induced macrophages. *Science 260:547.*

Hultgren, B., X. Huang, N. Dybdal, and T. A. Stewart (1996). Genetic absence of gamma-interferon delays but does not prevent diabetes in NOD mice. *Diabetes 45:812.*

Inaba, K., M. Inaba, N. Romani, H. Aya, M. Deguchi, S. Ikehara, S. Muramatsu, and R. M. Steinman (1992a). Generation of large numbers of dendritic cells from mouse bone marrow cultures supplemented with granulocyte/macrophage colony-stimulating factor. *J Exp Med 176:1693.*

Inaba, K., R. M. Steinman, M. W. Pack, H. Aya, M. Inaba, T. Sudo, S. Wolpe, and G. Schuler (1992b). Identification of proliferating dendritic cell precursors in mouse blood. *J Exp Med 175:1157.*

Inaba, K., M. Inaba, M. Deguchi, K. Hagi, R. Yasumizu, S. Ikehara, S. Muramatsu, and R. M. Steinman (1993a). Granulocytes, macrophages, and dendritic cells arise from a common major histocompatibility complex class II-negative progenitor in mouse bone marrow. *Proc Natl Acad Sci U S A 90:3038.*

Inaba, K., M. Inaba, M. Naito, and R. M. Steinman (1993b). Dendritic cell progenitors phagocytose particulates, including bacillus Calmette-Guerin organisms, and sensitize mice to mycobacterial antigens in vivo. *J Exp Med 178:479.*

Inaba, K., M. Witmer-Pack, M. Inaba, K. S. Hathcock, H. Sakuta, M. Azuma, H. Yagita, K. Okumura, P. S. Linsley, S. Ikehara, and et al (1994). The tissue distribution of the B7-2 costimulator in mice: abundant expression on dendritic cells in situ and during maturation in vitro. *J Exp Med 180:1849.*

Ingulli, E., A. Mondino, A. Khoruts, and M. K. Jenkins (1997). In vivo detection of dendritic cell antigen presentation to CD4(+) T cells. *J Exp Med 185:2133.*

Irmler, M., M. Thome, M. Hahne, P. Schneider, K. Hofmann, V. Steiner, J. L. Bodmer, M. Schroter, K. Burns, C. Mattmann, D. Rimoldi, L. E. French, and J. Tschopp (1997). Inhibition of death receptor signals by cellular FLIP. *Nature 388:190.*

Iwatani, Y., Y. Hidaka, F. Matsuzuka, K. Kuma, and N. Amino (1993). Intrathyroidal lymphocyte subsets, including unusual CD4+ CD8+ cells and CD3loTCR alpha beta lo/- CD4-CD8- cells, in autoimmune thyroid disease. *Clin Exp Immunol 93:430.*

Jansen, A., F. Homo-Delarche, H. Hooijkaas, P. J. Leenen, M. Dardenne, and H. A. Drexhage (1994). Immunohistochemical characterization of monocytes-macrophages and dendritic cells involved in the initiation of the insulitis and beta- cell destruction in NOD mice. *Diabetes 43:667.*

Jansen, A., M. van Hagen, and H. A. Drexhage (1995). Defective maturation and function of antigen-presenting cells in type 1 diabetes. *Lancet 345:491.*

Jiang, W., W. J. Swiggard, C. Heufler, M. Peng, A. Mirza, R. M. Steinman, and M. C. Nussenzweig (1995). The receptor DEC-205 expressed by dendritic cells and thymic epithelial cells is involved in antigen processing. *Nature 375:151.*

June, C. H., J. A. Bluestone, L. M. Nadler, and C. B. Thompson (1994). The B7 and CD28 receptor families. *Immunol Today 15:321.*

Kanagawa, O. (1988). Antibody-mediated activation of T cell clones as a method for screening hybridomas producing antibodies to the T cell receptor. *J Immunol Methods 110:169.*

Karvonen, M., J. Tuomilehto, I. Libman, and R. LaPorte (1993). A review of the recent epidemiological data on the worldwide incidence of type 1 (insulin-dependent) diabetes mellitus. World Health Organization DIAMOND Project Group [published erratum appears in Diabetologia 1994 Jun;38(6):642]. *Diabetologia 36:883.*

Katagiri, T., P. L. Cohen, and R. A. Eisenberg (1988). The lpr gene causes an intrinsic T cell abnormality that is required for hyperproliferation. *J Exp Med 167:741.*

Katz, J., C. Benoist, and D. Mathis (1993a). Major histocompatibility complex class I molecules are required for the development of insulitis in non-obese diabetic mice. *Eur J Immunol 23:3358.*

Katz, J. D., B. Wang, K. Haskins, C. Benoist, and D. Mathis (1993b). Following a diabetogenic T cell from genesis through pathogenesis. *Cell 74:1089.*

Katz, J. D., C. Benoist, and D. Mathis (1995). T helper cell subsets in insulin-dependent diabetes. *Science 268:1185.*

Kaufman, D. L., M. Clare-Salzler, J. Tian, T. Forsthuber, G. S. Ting, P.Robinson, M. A. Atkinson, E. E. Sercarz, A. J. Tobin, and P. V. Lehmann (1993). Spontaneous loss of T-cell tolerance to glutamic acid decarboxylase in murine insulin-dependent diabetes. *Nature 366:69.*

Kaufman, C. L., H. Li, and S. T. Ildstad (1997). Patterns of hemopoietic reconstitution in nonobese diabetic mice: dichotomy of allogeneic resistance versus competitive advantage of disease-resistant marrow. *J Immunol 158:2435.*

Kikutani, H., and S. Makino (1992). The murine autoimmune diabetes model: NOD and related strains. *Adv Immunol 51:285.*

Kim, K. J., C. Kanellopoulos-Langevin, R. M. Merwin, D. H. Sachs, and R. Asofsky (1979). Establishment and characterization of BALB/c lymphoma lines with B cell properties. *J Immunol 122:549.*

Kim, J., W. Richter, H. J. Aanstoot, Y. Shi, Q. Fu, R. Rajotte, G. Warnock, and S. Baekkeskov (1993). Differential expression of GAD65 and GAD67 in human, rat, and mouse pancreatic islets. *Diabetes 42:1799.*

King, C., J. Davies, R. Mueller, M. S. Lee, T. Krahl, B. Yeung, E. O'Connor, and N. Sarvetnick (1998). TGF-beta1 alters APC preference, polarizing islet antigen responses toward a Th2 phenotype. *Immunity 8:601.*

Kinoshita, T., T. Yokota, K. Arai, and A. Miyajima (1995). Suppression of apoptotic death in hematopoietic cells by signalling through the IL-3/GM-CSF receptors. *Embo J 14:266.*

Knight, S. C., J. Krejci, M. Malkovsky, V. Colizzi, A. Gautam, and G. L. Asherson (1985). The role of dendritic cells in the initiation of immune responses to contact sensitizers. I. In vivo exposure to antigen. *Cell Immunol 94:427.*

Koch, F., U. Stanzl, P. Jennewein, K. Janke, C. Heufler, E. Kampgen, N. Romani, and G. Schuler (1996). High level IL-12 production by murine dendritic cells: upregulation via MHC class II and CD40 molecules and downregulation by IL-4 and IL-10 [published erratum appears in J Exp Med 1996 Oct 1;184(4):following 1590]. *J Exp Med 184:741.*

Koike, T., Y. Itoh, T. Ishii, I. Ito, K. Takabayashi, N. Maruyama, H. Tomioka, and S. Yoshida (1987). Preventive effect of monoclonal anti-L3T4 antibody on development of diabetes in NOD mice. *Diabetes 36:539.*

Koller, B. H., D. E. Geraghty, R. DeMars, L. Duvick, S. S. Rich, and H. T. Orr (1989). Chromosomal organization of the human major histocompatibility complex class I gene family [published erratum appears in J Exp Med 1989 Apr 1;169(4):1517]. *J Exp Med 169:469.*

Kraal, G., M. Breel, M. Janse, and G. Bruin (1986). Langerhans' cells, veiled cells, and interdigitating cells in the mouse recognized by a monoclonal antibody. *J Exp Med 163:981.*

Kronin, V., K. Winkel, G. Suss, A. Kelso, W. Heath, J. Kirberg, H. von Boehmer, and K. Shortman (1996). A subclass of dendritic cells regulates the response of naive CD8 T cells by limiting their IL-2 production. *J Immunol 157:3819.*

Kurts, C., F. R. Carbone, M. F. Krummel, K. M. Koch, J. F. Miller, and W. R. Heath (1999). Signalling through CD30 protects against autoimmune diabetes mediated by CD8 T cells. *Nature 398:341.*

Labrecque, N., L. Madsen, L. Fugger, C. Benoist, and D. Mathis (1999). Toxic MHC class II beta chains. *Immunity 11:515.*

Lafferty, K. J., S. J. Prowse, C. J. Simeonovic, and H. S. Warren (1983). Immunobiology of tissue transplantation: a return to the passenger leukocyte concept. *Annu Rev Immunol 1:143.*

Landais, D., C. Waltzinger, B. N. Beck, A. Staub, D. J. McKean, C. Benoist, and D. Mathis (1986). Functional sites on Ia molecules: a molecular dissection of A alpha immunogenicity. *Cell 47:173.*

Langmuir, P. B., M. M. Bridgett, A. L. Bothwell, and I. N. Crispe (1993). Bone marrow abnormalities in the non-obese diabetic mouse. *Int Immunol 5:169.*

Lantz, C. S., J. Boesiger, C. H. Song, N. Mach, T. Kobayashi, R. C. Mulligan, Y. Nawa, G. Dranoff, and S. J. Galli (1998). Role for interleukin-3 in mast-cell and basophil development and in immunity to parasites. *Nature 392:90.*

Lee, M. S., L. Wogensen, J. Shizuru, M. B. Oldstone, and N. Sarvetnick (1994). Pancreatic islet production of murine interleukin-10 does not inhibit immune-mediated tissue destruction. *J Clin Invest 93:1332.*

Leenen, P. J., K. Radosevic, J. S. Voerman, B. Salomon, N. van Rooijen, D. Klatzmann, and W. van Ewijk (1998). Heterogeneity of mouse spleen dendritic cells: in vivo phagocytic activity, expression of macrophage markers, and subpopulation turnover. *J Immunol 160:2166.*

Lenardo, M. J. (1991). Interleukin-2 programs mouse alpha beta T lymphocytes for apoptosis. *Nature 353:858.*

Lenschow, D. J., K. C. Herold, L. Rhee, B. Patel, A. Koons, H. Y. Qin, E. Fuchs, B. Singh, C. B. Thompson, and J. A. Bluestone (1996). CD28/B7 regulation of Th1 and Th2 subsets in the development of autoimmune diabetes [published erratum appears in Immunity 1997 Feb;6(2):following 215]. *Immunity 5:285.*

Leonard, W. J., E. W. Shores, and P. E. Love (1995). Role of the common cytokine receptor gamma chain in cytokine signaling and lymphoid development. *Immunol Rev 148:97.*

Linsley, P. S., and J. A. Ledbetter (1993). The role of the CD28 receptor during T cell responses to antigen. *Annu Rev Immunol 11:191.*

Lord, J. D., B. C. McIntosh, P. D. Greenberg, and B. H. Nelson (1998). The IL-2 receptor promotes proliferation, bcl-2 and bcl-x induction, but not cell viability through the adapter molecule Shc. *J Immunol 161:4627.*

Love, J. M., A. M. Knight, M. A. McAleer, and J. A. Todd (1990). Towards construction of a high resolution map of the mouse genome using PCR-analysed microsatellites. *Nucleic Acids Res 18:4123.*

Ludewig, B., D. Graf, H. R. Gelderblom, Y. Becker, R. A. Kroczek, and G. Pauli (1995). Spontaneous apoptosis of dendritic cells is efficiently inhibited by TRAP (CD40-ligand) and TNF-alpha, but strongly enhanced by interleukin- 10. *Eur J Immunol 25:1943.*

Ludewig, B., B. Odermatt, S. Landmann, H. Hengartner, and R. M. Zinkernagel (1998). Dendritic cells induce autoimmune diabetes and maintain disease via de novo formation of local lymphoid tissue. *J Exp Med 188:1493.*

Lund, T., L. O'Reilly, P. Hutchings, O. Kanagawa, E. Simpson, R. Gravely, P. Chandler, J. Dyson, J. K. Picard, A. Edwards, and et al. (1990). Prevention of insulin-dependent diabetes mellitus in non-obese diabetic mice by transgenes encoding modified I-A beta-chain or normal I-E alpha- chain. *Nature 345:727.*

Lutz, M. B., N. Kukutsch, A. L. Ogilvie, S. Rossner, F. Koch, N. Romani, and G. Schuler (1999). An advanced culture method for generating large quantities of highly pure dendritic cells from mouse bone marrow. *J Immunol Methods 223:77.*

Lyman, S. D., L. James, T. Vanden Bos, P. de Vries, K. Brasel, B. Gliniak, L. T. Hollingsworth, K. S. Picha, H. J. McKenna, R. R. Splett, and et al. (1993). Molecular cloning of a ligand for the flt3/flk-2 tyrosine kinase receptor: a proliferative factor for primitive hematopoietic cells. *Cell 75:1157.*

Lyon M.F. and Searle A.G. (editors). Genetic Variants and Strains of the Laboratory Mouse (2nd Edition). Oxford University Press, New York, USA. © Commitee on Standardized Genetic Nomenclature for Mice 1989. First published 1989. Reprinted 1990.

Lyons, A. B., and C. R. Parish (1994). Determination of lymphocyte division by flow cytometry. *J Immunol Methods 171:131.*

Macatonia, S. E., A. J. Edwards, and S. C. Knight (1986). Dendritic cells and the initiation of contact sensitivity to fluorescein isothiocyanate. *Immunology 59:509.*

Macatonia, S. E., N. A. Hosken, M. Litton, P. Vieira, C. S. Hsieh, J. A. Culpepper, M. Wysocka, G. Trinchieri, K. M. Murphy, and A. O'Garra (1995). Dendritic cells produce IL-12 and direct the development of Th1 cells from naive CD4+ T cells. *J Immunol 154:5071.*

Mackay, I. R., A. Bone, T. Tuomi, R. Elliott, T. Mandel, C. Karopoulos, and M. J. Rowley (1996). Lack of autoimmune serological reactions in rodent models of insulin dependent diabetes mellitus. *J Autoimmun 9:705.*

Maldonado-Lopez, R., T. De Smedt, P. Michel, J. Godfroid, B. Pajak, C. Heirman, K. Thielemans, O. Leo, J. Urbain, and M. Moser (1999). CD8alpha+ and CD8alpha- subclasses of dendritic cells direct the development of distinct T helper cells in vivo. *J Exp Med 189:587.*

Manetti, R., P. Parronchi, M. G. Giudizi, M. P. Piccinni, E. Maggi, G. Trinchieri, and S. Romagnani (1993). Natural killer cell stimulatory factor (interleukin 12 [IL-12]) induces T helper type 1 (Th1)-specific immune responses and inhibits the development of IL-4-producing Th cells. *J Exp Med 177:1199.*

Maraskovsky, E., K. Brasel, M. Teepe, E. R. Roux, S. D. Lyman, K. Shortman, and H. J. McKenna (1996). Dramatic increase in the numbers of functionally mature dendritic cells in Flt3 ligand-treated mice: multiple dendritic cell subpopulations identified. *J Exp Med 184:1953.*

Mathis, D. J., C. Benoist, V. E. d. Williams, M. Kanter, and H. O. McDevitt (1983). Several mechanisms can account for defective E alpha gene expression in different mouse haplotypes. *Proc Natl Acad Sci U S A 80:273.*

Matsuno, K., T. Ezaki, S. Kudo, and Y. Uehara (1996). A life stage of particle-laden rat dendritic cells in vivo: their terminal division, active phagocytosis, and translocation from the liver to the draining lymph. *J Exp Med 183:1865.*

Mattner, F., S. Fischer, S. Guckes, S. Jin, H. Kaulen, E. Schmitt, E. Rude, and T. Germann (1993). The interleukin-12 subunit p40 specifically inhibits effects of the interleukin-12 heterodimer. *Eur J Immunol 23:2202.*

Maurer, D., C. Ebner, B. Reininger, E. Fiebiger, D. Kraft, J. P. Kinet, and G. Stingl (1995). The high affinity IgE receptor (Fc epsilon RI) mediates IgE-dependent allergen presentation. *J Immunol 154:6285.*

May, M. J., and S. Ghosh (1998). Signal transduction through NF-kappa B. *Immunol Today 19:80.*

Mayer, P., P. Valent, G. Schmidt, E. Liehl, and P. Bettelheim (1989). The in vivo effects of recombinant human interleukin-3: demonstration of basophil differentiation factor, histamine-producing activity, and priming of GM-CSF-responsive progenitors in nonhuman primates. *Blood 74:613.*

Mayordomo, J. I., T. Zorina, W. J. Storkus, L. Zitvogel, C. Celluzzi, L. D. Falo, C. J. Melief, S. T. Ildstad, W. M. Kast, A. B. Deleo, and et al. (1995). Bone marrow-derived dendritic cells pulsed with synthetic tumour peptides elicit protective and therapeutic antitumour immunity. *Nat Med 1:1297.*

McClive, P. J., A. G. Baxter, and G. Morahan (1994). Genetic polymorphisms of the non-obese diabetic (NOD) mouse. *Immunol Cell Biol 72:137.*

McEvoy, L., R. A. Schlegel, P. Williamson, and B. J. Del Buono (1988). Merocyanine 540 as a flow cytometric probe of membrane lipid organization in leukocytes. *J Leukoc Biol 44:337.*

McNiece, I. K., K. E. Langley, and K. M. Zsebo (1991). The role of recombinant stem cell factor in early B cell development. Synergistic interaction with IL-7. *J Immunol 146:3785.*

McWilliam, A. S., D. Nelson, J. A. Thomas, and P. G. Holt (1994). Rapid dendritic cell recruitment is a hallmark of the acute inflammatory response at mucosal surfaces. *J Exp Med 179:1331.*

McWilliam, A. S., S. Napoli, A. M. Marsh, F. L. Pemper, D. J. Nelson, C. L. Pimm, P. A. Stumbles, T. N. Wells, and P. G. Holt (1996). Dendritic cells are recruited into the airway epithelium during the inflammatory response to a broad spectrum of stimuli. *J Exp Med 184:2429.*

Metcalf, D., and N. A. Nicola (1992). The clonal proliferation of normal mouse hematopoietic cells: enhancement and suppression by colony-stimulating factor combinations. *Blood 79:2861.*

Metlay, J. P., M. D. Witmer-Pack, R. Agger, M. T. Crowley, D. Lawless, and R. M. Steinman (1990). The distinct leukocyte integrins of mouse spleen dendritic cells as identified with new hamster monoclonal antibodies. *J Exp Med 171:1753.*

Miller, B. J., M. C. Appel, J. J. O'Neil, and L. S. Wicker (1988). Both the Lyt-2+ and L3T4+ T cell subsets are required for the transfer of diabetes in nonobese diabetic mice. *J Immunol 140:52.*

Miyajima, A., A. L. Mui, T. Ogorochi, and K. Sakamaki (1993). Receptors for granulocyte-macrophage colony-stimulating factor, interleukin-3, and interleukin-5. *Blood 82:1960.*

Miyazaki, A., T. Hanafusa, K. Yamada, J. Miyagawa, H. Fujino-Kurihara, H. Nakajima, K. Nonaka, and S. Tarui (1985). Predominance of T lymphocytes in pancreatic islets and spleen of pre- diabetic non-obese diabetic (NOD) mice: a longitudinal study. *Clin Exp Immunol 60:622.*

Moll, H., H. Fuchs, C. Blank, and M. Rollinghoff (1993). Langerhans cells transport Leishmania major from the infected skin to the draining lymph node for presentation to antigen-specific T cells. *Eur J Immunol 23:1595.*

Morahan, G., P. McClive, D. Huang, P. Little, and A. Baxter (1994). Genetic and physiological association of diabetes susceptibility with raised Na+/H+ exchange activity. *Proc Natl Acad Sci U S A 91:5898.*

Morel, P. A., A. C. Vasquez, and M. Feili-Hariri (1999). Immunobiology of DC in NOD mice. *J Leukoc Biol 66:276.*

Moriggl, R., D. J. Topham, S. Teglund, V. Sexl, C. McKay, D. Wang, A. Hoffmeyer, J. van Deursen, M. Y. Sangster, K. D. Bunting, G. C. Grosveld, and J. N. Ihle (1999). Stat5 is required for IL-2-induced cell cycle progression of peripheral T cells. *Immunity 10:249.*

Moritani, M., K. Yoshimoto, F. Tashiro, C. Hashimoto, J. Miyazaki, S. Ii, E. Kudo, H. Iwahana, Y. Hayashi, T. Sano, and et al. (1994). Transgenic expression of IL-10 in pancreatic islet A cells accelerates autoimmune insulitis and diabetes in non-obese diabetic mice. *Int Immunol 6:1927.*

Mosmann, T. R., H. Cherwinski, M. W. Bond, M. A. Giedlin, and R. L. Coffman (1986). Two types of murine helper T cell clone. I. Definition according to profiles of lymphokine activities and secreted proteins. *J Immunol 136:2348.*

Mower, D. A., Jr., D. W. Peckham, V. A. Illera, J. K. Fishbaugh, L. L. Stunz, and R. F. Ashman (1994). Decreased membrane phospholipid packing and decreased cell size precede DNA cleavage in mature mouse B cell apoptosis. *J Immunol 152:4832.*

Murphy, K. M., A. B. Heimberger, and D. Y. Loh (1990). Induction by antigen of intrathymic apoptosis of CD4+CD8+TCRlo thymocytes in vivo. *Science 250:1720.*

Myers, M. A., M. R. Laks, S. J. Feeney, T. E. Mandel, M. Koulmanda, A. Bone, J. Barley, M. J. Rowley, and I. R. Mackay (1998). Antibodies to ICA512/IA-2 in rodent models of IDDM. *J Autoimmun 11:265.*

Nelson, B. H., and D. M. Willerford (1998). Biology of the interleukin-2 receptor. *Adv Immunol 70:1.*

Nepom, G. T. (1990a). A unified hypothesis for the complex genetics of HLA associations with IDDM. *Diabetes 39:1153.*

Nepom, G. T. (1990b). HLA and type I diabetes. *Immunol Today 11:314.*

Nishinakamura, R., N. Nakayama, Y. Hirabayashi, T. Inoue, D. Aud, T. McNeil, S. Azuma, S. Yoshida, Y. Toyoda, K. Arai, and et al. (1995). Mice deficient for the IL-3/GM-CSF/IL-5 beta c receptor exhibit lung pathology and impaired immune response, while beta IL3 receptor- deficient mice are normal. *Immunity 2:211.*

O'Hara, R. M., Jr., S. L. Henderson, and A. Nagelin (1996). Prevention of a Th1 disease by a Th1 cytokine: IL-12 and diabetes in NOD mice. *Ann N Y Acad Sci 795:241.*

O'Garra, A., and K. Murphy (1994). Role of cytokines in determining T-lymphocyte function. *Curr Opin Immunol 6:458.*

Ohashi, P. S., S. Oehen, K. Buerki, H. Pircher, C. T. Ohashi, B. Odermatt, B. Malissen, R. M. Zinkernagel, and H. Hengartner (1991). Ablation of "tolerance" and induction of diabetes by virus infection in viral antigen transgenic mice. *Cell 65:305.*

Ohteki, T., T. Fukao, K. Suzue, C. Maki, M. Ito, M. Nakamura, and S. Koyasu (1999). Interleukin 12-dependent interferon gamma production by CD8alpha+ lymphoid dendritic cells. *J Exp Med 189:1981.*

Oldstone, M. B. (1990). Viruses as therapeutic agents. I. Treatment of nonobese insulin-dependent diabetes mice with virus prevents insulin-dependent diabetes mellitus while maintaining general immune competence. *J Exp Med 171:2077.*

Oldstone, M. B., M. Nerenberg, P. Southern, J. Price, and H. Lewicki (1991). Virus infection triggers insulin-dependent diabetes mellitus in a transgenic model: role of anti-self (virus) immune response. *Cell 65:319.*

Ozato, K., N. Mayer, and D. H. Sachs (1980). Hybridoma cell lines secreting monoclonal antibodies to mouse H-2 and Ia antigens. *J Immunol 124:533.*

Ozato, K., N. M. Mayer, and D. H. Sachs (1982). Monoclonal antibodies to mouse major histocompatibility complex antigens. *Transplantation 34:113.*

Paglia, P., C. Chiodoni, M. Rodolfo, and M. P. Colombo (1996). Murine dendritic cells loaded in vitro with soluble protein prime cytotoxic T lymphocytes against tumor antigen in vivo. *J Exp Med 183:317.*

Palmer, J. P., C. M. Asplin, P. Clemons, K. Lyen, O. Tatpati, P. K. Raghu, and T. L. Paquette (1983). Insulin antibodies in insulin-dependent diabetics before insulin treatment. *Science 222:1337.*

Panina-Bordignon, P., R. Lang, P. M. van Endert, E. Benazzi, A. M. Felix, R. M. Pastore, G. A. Spinas, and F. Sinigaglia (1995). Cytotoxic T cells specific for glutamic acid decarboxylase in autoimmune diabetes. *J Exp Med 181:1923.*

Payvandi, F., S. Amrute, and P. Fitzgerald-Bocarsly (1998). Exogenous and endogenous IL-10 regulate IFN-alpha production by peripheral blood mononuclear cells in response to viral stimulation. *J Immunol 160:5861.*

Pennline, K. J., E. Roque-Gaffney, and M. Monahan (1994). Recombinant human IL-10 prevents the onset of diabetes in the nonobese diabetic mouse. *Clin Immunol Immunopathol 71:169.*

Petersen, J. S., S. Russel, M. O. Marshall, H. Kofod, K. Buschard, N. Cambon, A. E. Karlsen, E. Boel, W. A. Hagopian, K. R. Hejnaes, and et al. (1993). Differential expression of glutamic acid decarboxylase in rat and human islets. *Diabetes 42:484.*

Pettit, A. R., C. Quinn, K. P. MacDonald, L. L. Cavanagh, G. Thomas, W. Townsend, M. Handel, and R. Thomas (1997). Nuclear localization of RelB is associated with effective antigen- presenting cell function. *J Immunol 159:3681.*

Pierre, P., S. J. Turley, E. Gatti, M. Hull, J. Meltzer, A. Mirza, K. Inaba, R. M. Steinman, and I. Mellman (1997). Developmental regulation of MHC class II transport in mouse dendritic cells. *Nature 388:787.*

Pierre, P., and I. Mellman (1998). Developmental regulation of invariant chain proteolysis controls MHC class II trafficking in mouse dendritic cells. *Cell 93:1135.*

Pilstrom, B., and J. Bohme (1997). Alleviation of insulitis in NOD mice is associated with expression of transgenic MHC E molecules on primary antigen-presenting cells. *Immunology 90:483.*

Podolin, P. L., A. Pressey, N. H. DeLarato, P. A. Fischer, L. B. Peterson, and L. S. Wicker (1993). I-E+ nonobese diabetic mice develop insulitis and diabetes. *J Exp Med 178:793.*

Podolin, P. L., P. Denny, C. J. Lord, N. J. Hill, J. A. Todd, L. B. Peterson, L. S. Wicker, and P. A. Lyons (1997). Congenic mapping of the insulin-dependent diabetes (Idd) gene, Idd10, localizes two genes mediating the Idd10 effect and eliminates the candidate Fcgr1. *J Immunol 159:1835.*

Pozzilli, P., A. Signore, A. J. Williams, and P. E. Beales (1993). NOD mouse colonies around the world--recent facts and figures. *Immunol Today 14:193.*

Prins, J. B., J. A. Todd, N. R. Rodrigues, S. Ghosh, P. M. Hogarth, L. S. Wicker, E. Gaffney, P. L. Podolin, P. A. Fischer, A. Sirotina, and et al. (1993). Linkage on chromosome 3 of autoimmune diabetes and defective Fc receptor for IgG in NOD mice. *Science 260:695.*

Prochazka, M., E. H. Leiter, D. V. Serreze, and D. L. Coleman (1987). Three recessive loci required for insulin-dependent diabetes in nonobese diabetic mice [published erratum appears in Science 1988 Nov 11;242(4880):945]. *Science 237:286.*

Prochazka, M., D. V. Serreze, S. M. Worthen, and E. H. Leiter (1989). Genetic control of diabetogenesis in NOD/Lt mice. Development and analysis of congenic stocks. *Diabetes 38:1446.*

Pugliese, A., M. Zeller, A. Fernandez Jr., L. J. Zalcberg, R. J. Bartlett, C. Ricordi, M. Pietropaolo, G. S. Eisenbarth, S. T. Bennett, and D. D. Patel (1997). The insulin gene is transcribed in the human thymus and transcription levels correlated with allelic variation at the INS VNTR-IDDM2 susceptibility locus for type 1 diabetes. *Nat Genet 15:293.*

Pulendran, B., J. Lingappa, M. K. Kennedy, J. Smith, M. Teepe, A. Rudensky, C. R. Maliszewski, and E. Maraskovsky (1997). Developmental pathways of dendritic cells in vivo: distinct function, phenotype, and localization of dendritic cell subsets in FLT3 ligand- treated mice. *J Immunol 159:2222.*

Pulendran, B., J. L. Smith, G. Caspary, K. Brasel, D. Pettit, E. Maraskovsky, and C. R. Maliszewski (1999). Distinct dendritic cell subsets differentially regulate the class of immune response in vivo. *Proc Natl Acad Sci U S A 96:1036.*

Randen, I., O. J. Mellbye, O. Forre, and J. B. Natvig (1995). The identification of germinal centres and follicular dendritic cell networks in rheumatoid synovial tissue. *Scand J Immunol 41:481.*

Randolph, G. J., S. Beaulieu, S. Lebecque, R. M. Steinman, and W. A. Muller (1998). Differentiation of monocytes into dendritic cells in a model of transendothelial trafficking. *Science 282:480.*

Randolph, G. J., K. Inaba, D. F. Robbiani, R. M. Steinman, andW. A. Muller (1999). Differentiation of phagocytic monocytes into lymph node dendritic cells in vivo. *Immunity 11:753.*

Rapoport, M. J., A. Jaramillo, D. Zipris, A. H. Lazarus, D. V. Serreze, E. H. Leiter, P. Cyopick, J. S. Danska, and T. L. Delovitch (1993). Interleukin 4 reverses T cell proliferative unresponsiveness and prevents the onset of diabetes in nonobese diabetic mice. *J Exp Med 178:87.*

Razi-Wolf, Z., G. J. Freeman, F. Galvin, B. Benacerraf, L. Nadler, and H. Reiser (1992). Expression and function of the murine B7 antigen, the major costimulatory molecule expressed by peritoneal exudate cells. *Proc Natl Acad Sci U S A 89:4210.*

Refaeli, Y., L. Van Parijs, C. A. London, J. Tschopp, and A. K. Abbas (1998). Biochemical mechanisms of IL-2-regulated Fas-mediated T cell apoptosis. *Immunity 8:615.*

Reid, C. D., A. Stackpoole, A. Meager, and J. Tikerpae (1992). Interactions of tumor necrosis factor with granulocyte-macrophage colony-stimulating factor and other cytokines in the regulation of dendritic cell growth in vitro from early bipotent CD34+ progenitors in human bone marrow. *J Immunol 149:2681.*

Reis e Sousa, C., P. D. Stahl, and J. M. Austyn (1993). Phagocytosis of antigens by Langerhans cells in vitro. *J Exp Med 178:509.*

Rescigno, M., M. Martino, C. L. Sutherland, M. R. Gold, and P. Ricciardi-Castagnoli (1998). Dendritic cell survival and maturation are regulated by different signaling pathways. *J Exp Med 188:2175.*

Ridge, J. P., F. Di Rosa, and P. Matzinger (1998). A conditioned dendritic cell can be a temporal bridge between a CD4+ T- helper and a T-killer cell. *Nature 393:474.*

Roake, J. A., A. S. Rao, P. J. Morris, C. P. Larsen, D. F. Hankins,and J. M. Austyn (1995). Dendritic cell loss from nonlymphoid tissues after systemic administration of lipopolysaccharide, tumor necrosis factor, and interleukin 1. *J Exp Med 181:2237.*

Robb, L., C. C. Drinkwater, D. Metcalf, R. Li, F. Kontgen, N. A. Nicola, and C. G. Begley (1995). Hematopoietic and lung abnormalities in mice with a null mutation of the common beta subunit of the receptors for granulocyte-macrophage colony-stimulating factor and interleukins 3 and 5. *Proc Natl Acad Sci U S A 92:9565.*

Robert, C., R. C. Fuhlbrigge, J. D. Kieffer, S. Ayehunie, R. O. Hynes,G. Cheng, S. Grabbe, U. H. von Andrian, and T. S. Kupper (1999). Interaction of dendritic cells with skin endothelium: A new perspective on immunosurveillance. *J Exp Med 189:627.*

Robinson, C. P., S. Yamachika, C. E. Alford, C. Cooper, E. L. Pichardo, N. Shah, A. B. Peck, and M. G. Humphreys-Beher (1997). Elevated levels of cysteine protease activity in saliva and salivary glands of the nonobese diabetic (NOD) mouse model for Sjogren syndrome. *Proc Natl Acad Sci U S A 94:5767.*

Rothe, H., A. Hausmann, K. Casteels, H. Okamura, M. Kurimoto, V. Burkart, C. Mathieu, and H. Kolb (1999). IL-18 inhibits diabetes development in nonobese diabetic mice by counterregulation of Th1-dependent destructive insulitis. *J Immunol 163:1230.*

Sadlack, B., J. Lohler, H. Schorle, G. Klebb, H. Haber, E. Sickel, R. J. Noelle, and I. Horak (1995). Generalized autoimmune disease in interleukin-2-deficient mice is triggered by an uncontrolled activation and proliferation of CD4+ T cells.
Eur J Immunol 25:3053.

Sado, T., H. Kamisaku, and S. Aizawa (1980). Nature of T-cells resident in spleens of thymectomized, lethally irradiated, bone marrow-reconstituted mice. *Cell Immunol 49:51*

Sakamaki, K., I. Miyajima, T. Kitamura, and A. Miyajima (1992). Critical cytoplasmic domains of the common beta subunit of the human GM- CSF, IL-3 and IL-5 receptors for growth signal transduction and tyrosine phosphorylation. *Embo J 11:3541.*

Sallusto, F., and A. Lanzavecchia (1994). Efficient presentation of soluble antigen by cultured human dendritic cells is maintained by granulocyte/macrophage colony-stimulating factor plus interleukin 4 and downregulated by tumor necrosis factor alpha.
J Exp Med 179:1109.

Sallusto, F., M. Cella, C. Danieli, and A. Lanzavecchia (1995). Dendritic cells use macropinocytosis and the mannose receptor to concentrate macromolecules in the major histocompatibility complex class II compartment: downregulation by cytokines and bacterial products. *J Exp Med 182:389.*

Sallusto, F., C. Nicolo, R. De Maria, S. Corinti, and R. Testi (1996). Ceramide inhibits antigen uptake and presentation by dendritic cells. *J Exp Med 184:2411.*

Sallusto, F., P. Schaerli, P. Loetscher, C. Schaniel, D. Lenig, C. R. Mackay, S. Qin, and A. Lanzavecchia (1998). Rapid and coordinated switch in chemokine receptor expression during dendritic cell maturation. *Eur J Immunol 28:2760.*

Sallusto, F., B. Palermo, D. Lenig, M. Miettinen, S. Matikainen, I. Julkunen, R. Forster, R. Burgstahler, M. Lipp, and A. Lanzavecchia (1999). Distinct patterns and kinetics of chemokine production regulate dendritic cell function.
Eur J Immunol 29:1617.

Sato, N., K. Sakamaki, N. Terada, K. Arai, and A. Miyajima (1993). Signal transduction by the high-affinity GM-CSF receptor: two distinct cytoplasmic regions of the common beta subunit responsible for different signaling. *Embo J 12:4181.*

Scheicher, C., M. Mehlig, R. Zecher, and K. Reske (1992). Dendritic cells from mouse bone marrow: in vitro differentiation using low doses of recombinant granulocyte-macrophage colony-stimulating factor. *J Immunol Methods 154:253.*

Scheid, M. P., R. W. Lauener, and V. Duronio (1995). Role of phosphatidylinositol 3-OH-kinase activity in the inhibition of apoptosis in haemopoietic cells: phosphatidylinositol 3-OH-kinase inhibitors reveal a difference in signalling between interleukin-3 and granulocyte-macrophage colony stimulating factor. *Biochem J 312:159.*

Scheynius, A., R. L. Camp, and E. Pure (1993). Reduced contact sensitivity reactions in mice treated with monoclonal antibodies to leukocyte function-associated molecule-1 and intercellular adhesion molecule-1. *J Immunol 150:655.*

Schloot, N. C., S. Willemen, G. Duinkerken, R. R. de Vries, and B. O. Roep (1998). Cloned T cells from a recent onset IDDM patient reactive with insulin B- chain. *J Autoimmun 11:169.*

Schmidt, E. V. (1999). The role of c-myc in cellular growth control. *Oncogene 18:2988.*

Schoenberger, S. P., R. E. Toes, E. I. van der Voort, R. Offringa, and C. J. Melief (1998). T-cell help for cytotoxic T lymphocytes is mediated by CD40-CD40L interactions. *Nature 393:480.*

Schuler, G., and R. M. Steinman (1997). Dendritic cells as adjuvants for immune-mediated resistance to tumors. *J Exp Med 186:1183.*

Scott, C. L., D. A. Hughes, D. Cary, N. A. Nicola, C. G. Begley, and L. Robb (1998). Functional analysis of mature hematopoietic cells from mice lacking the betac chain of the granulocyte-macrophage colony-stimulating factor receptor. *Blood 92:4119.*

Serreze, D. V., E. H. Leiter, S. M. Worthen, and L. D. Shultz (1988). NOD marrow stem cells adoptively transfer diabetes to resistant (NOD x NON)F1 mice. *Diabetes 37:252.*

Serreze, D. V., J. W. Gaedeke, and E. H. Leiter (1993a). Hematopoietic stem-cell defects underlying abnormal macrophage development and maturation in NOD/Lt mice: defective regulation of cytokine receptors and protein kinase C. *Proc Natl Acad Sci U S A 90:9625.*

Serreze, D. V., H. R. Gaskins, and E. H. Leiter (1993b). Defects in the differentiation and function of antigen presenting cells in NOD/Lt mice. *J Immunol 150:2534.*

Serreze, D. V., E. H. Leiter, G. J. Christianson, D. Greiner, and D. C. Roopenian (1994). Major histocompatibility complex class I-deficient NOD-B2mnull mice are diabetes and insulitis resistant. *Diabetes 43:505.*

Serreze, D. V., H. D. Chapman, D. S. Varnum, M. S. Hanson, P. C. Reifsnyder, S. D. Richard, S. A. Fleming, E. H. Leiter, and L. D. Shultz (1996). B lymphocytes are essential for the initiation of T cell-mediated autoimmune diabetes: analysis of a new "speed congenic" stock of NOD.Ig mu null mice. *J Exp Med 184:2049.*

Serreze, D. V., S. A. Fleming, H. D. Chapman, S. D. Richard, E. H. Leiter, and R. M. Tisch (1998). B lymphocytes are critical antigen-presenting cells for the initiation of T cell-mediated autoimmune diabetes in nonobese diabetic mice. *J Immunol 161:3912.*

Sheehy, M. J. (1992). HLA and insulin-dependent diabetes. A protective perspective. *Diabetes 41:123.*

Shen, F. W., J. S. Tung, and E. A. Boyse (1986). Further definition of the Ly-5 system. *Immunogenetics 24:146.*

Shimonkevitz, R., J. Kappler, P. Marrack, and H. Grey (1983). Antigen recognition by H-2-restricted T cells. I. Cell-free antigen processing. *J Exp Med 158:303.*

Shreedhar, V., A. M. Moodycliffe, S. E. Ullrich, C. Bucana, M. L. Kripke, and L. Flores-Romo (1999). Dendritic cells require T cells for functional maturation in vivo. *Immunity 11:625.*

Shull, M. M., I. Ormsby, A. B. Kier, S. Pawlowski, R. J. Diebold, M. Yin, R. Allen, C. Sidman, G. Proetzel, D. Calvin, and et al. (1992). Targeted disruption of the mouse transforming growth factor-beta 1 gene results in multifocal inflammatory disease. *Nature 359:693.*

Siegal, F. P., N. Kadowaki, M. Shodell, P. A. Fitzgerald-Bocarsly, K. Shah, S. Ho, S. Antonenko, and Y. J. Liu (1999). The nature of the principal type 1 interferon-producing cells in human blood. *Science 284:1835.*

Singer, S. M., D. T. Umetsu, and H. O. McDevitt (1996). High copy number I-Ab transgenes induce production of IgE through an interluekin 4-dependent mechanism. *Proc Natl Acad Sci U S A 93:2947.*

Sitnicka, E., F. W. Ruscetti, G. V. Priestley, N. S. Wolf, and S. H. Bartelmez (1996). Transforming growth factor beta 1 directly and reversibly inhibits the initial cell divisions of long-term repopulating hematopoietic stem cells. *Blood 88:82.*

Slattery, R. M., L. Kjer-Nielsen, J. Allison, B. Charlton, T. E. Mandel, and J. F. Miller (1990). Prevention of diabetes in non-obese diabetic I-Ak transgenic mice. *Nature 345:724.*

Smith, K. M., D. C. Olson, R. Hirose, and D. Hanahan (1997). Pancreatic gene expression in rare cells of thymic medulla: evidence for functional contribution to T cell tolerance. *Int Immunol 9:1355.*

Smith, A. L., and B. Fazekas de St Groth (1999). Antigen-pulsed CD8alpha+ dendritic cells generate an immune response after subcutaneous injection without homing to the draining lymph node. *J Exp Med 189:593.*

Sobel, E. S., T. Katagiri, K. Katagiri, S. C. Morris, P. L. Cohen, and R. A. Eisenberg (1991). An intrinsic B cell defect is required for the production of autoantibodies in the lpr model of murine systemic autoimmunity. *J Exp Med 173:1441.*

Solimena, M., R. Dirkx Jr., J. M. Hermel, S. Pleasic-Williams, J. A. Shapiro, L. Caron, and D. U. Rabin (1996). ICA 512, an autoantigen of type I diabetes, is an intrinsic membrane protein of neurosecretory granules. *Embo J 15:2102.*

Song, W., H. L. Kong, H. Carpenter, H. Torii, R. Granstein, S. Rafii, M. A. Moore, and R. G. Crystal (1997). Dendritic cells genetically modified with an adenovirus vector encoding the cDNA for a model antigen induce protective and therapeutic antitumor immunity. *J Exp Med 186:1247.*

Sospedra, M., X. Ferrer-Francesch, O. Dominguez, M. Juan, M. Foz-Sala, and R. Pujol-Borrell (1998). Transcription of a broad range of self-antigens in human thymus suggests a role for central mechanisms in tolerance toward peripheral antigens. *J Immunol 161:5918.*

Sousa, C. R., S. Hieny, T. Scharton-Kersten, D. Jankovic, H. Charest, R. N. Germain, and A. Sher (1997). In vivo microbial stimulation induces rapid CD40 ligand-independent production of interleukin 12 by dendritic cells and their redistribution to T cell areas. *J Exp Med 186:1819.*

Specht, J. M., G. Wang, M. T. Do, J. S. Lam, R. E. Royal, M. E. Reeves, S. A. Rosenberg, and P. Hwu (1997). Dendritic cells retrovirally transduced with a model antigen gene are therapeutically effective against established pulmonary metastases. *J Exp Med 186:1213.*

Sprent, J., and S. R. Webb (1995). Intrathymic and extrathymic clonal deletion of T cells. *Curr Opin Immunol 7:196.*

* H. Strobl, E. Riedl, C. Scheinecker, C. Bello-Fernandez, W. F. Pickl, K. Rappersberger, O. Majdic and W. Knapp (1996). TGF-beta 1 promotes in vitro development of dendritic cells from CD34+ hemopoietic progenitors. *J Immunol.* 157: 1499-507.

* G. Stuhler, A. Zobywalski, F. Grunebach, P. Brossart, V. L. Reichardt, H. Barth, S. Stevanovic, W. Brugger, L. Kanz and S. F. Schlossman (1999). Immune regulatory loops determine productive interactions within human T lymphocyte-dendritic cell clusters. *Proc Natl Acad Sci U S A.* 96: 1532-5.

Springer, T., G. Galfre, D. S. Secher, and C. Milstein (1979). Mac-1: a macrophage differentiation antigen identified by monoclonal antibody. *Eur J Immunol 9:301.*

Springer, T. A. (1994). Traffic signals for lymphocyte recirculation and leukocyte emigration: the multistep paradigm. *Cell 76:301.*

Stanley, E., G. J. Lieschke, D. Grail, D. Metcalf, G. Hodgson, J. A. Gall, D. W. Maher, J. Cebon, V. Sinickas, and A. R. Dunn (1994). Granulocyte/macrophage colony-stimulating factor-deficient mice show no major perturbation of hematopoiesis but develop a characteristic pulmonary pathology. *Proc Natl Acad Sci U S A 91:5592.*

Steinman, R. M., and Z. A. Cohn (1973). Identification of a novel cell type in peripheral lymphoid organs of mice. I. Morphology, quantitation, tissue distribution. *J Exp Med 137:1142.*

Steinman, R. M., and Z. A. Cohn (1974). Identification of a novel cell type in peripheral lymphoid organs of mice. II. Functional properties in vitro. *J Exp Med 139:380.*

Steinman, R. M., D. S. Lustig, and Z. A. Cohn (1974). Identification of a novel cell type in peripheral lymphoid organs of mice. 3. Functional properties in vivo. *J Exp Med 139:1431.*

Steinman, R. M., and M. D. Witmer (1978). Lymphoid dendritic cells are potent stimulators of the primary mixed leukocyte reaction in mice. *Proc Natl Acad Sci U S A 75:5132.*

Steinman, R. M. (1991). The dendritic cell system and its role in immunogenicity. *Annu Rev Immunol 9:271.*

Steinman, R. M., M. Pack, and K. Inaba (1997). Dendritic cells in the T-cell areas of lymphoid organs. *Immunol Rev 156:25.*

Stoll, S., H. Jonuleit, E. Schmitt, G. Muller, H. Yamauchi, M. Kurimoto, J. Knop, and A. H. Enk (1998). Production of functional IL-18 by different subtypes of murine and human dendritic cells (DC): DC-derived IL-18 enhances IL-12-dependent Th1 development. *Eur J Immunol 28:3231.*

Stossel, H., F. Koch, E. Kampgen, P. Stoger, A. Lenz, C. Heufler, N. Romani, and G. Schuler (1990). Disappearance of certain acidic organelles (endosomes and Langerhans cell granules) accompanies loss of antigen processing capacity upon culture of epidermal Langerhans cells. *J Exp Med 172:1471.*

Strober, W., B. Kelsall, I. Fuss, T. Marth, B. Ludviksson, R. Ehrhardt, and M. Neurath (1997). Reciprocal IFN-gamma and TGF-beta responses regulate the occurrence of mucosal inflammation. *Immunol Today 18:61.*

Strunk, D., K. Rappersberger, C. Egger, H. Strobl, E. Kromer, A. Elbe, D. Maurer, and G. Stingl (1996). Generation of human dendritic cells/Langerhans cells from circulating CD34+ hematopoietic progenitor cells. *Blood 87:1292.*

Suss, G., and K. Shortman (1996). A subclass of dendritic cells kills CD4 T cells via Fas/Fas-ligand- induced apoptosis. *J Exp Med 183:1789.*

Svensson, M., B. Stockinger, and M. J. Wick (1997). Bone marrow-derived dendritic cells can process bacteria for MHC-I and MHC-II presentation to T cells. *J Immunol 158:4229.*

Swain, S. L. (1994). Generation and in vivo persistence of polarized Th1 and Th2 memory cells. *Immunity 1:543.*

* S. E. Townsend and C. C. Goodnow (1998). Abortive proliferation of rare T cells induced by direct or indirect antigen presentation by rare B cells in vivo. *J Exp Med.* 187: 1611-21.

Takahashi, K., M. C. Honeyman, and L. C. Harrison (1998). Impaired yield, phenotype, and function of monocyte-derived dendritic cells in humans at risk for insulin-dependent diabetes. *J Immunol 161:2629.*

Takatsu, K., A. Tominaga, N. Harada, S. Mita, M. Matsumoto, T. Takahashi, Y. Kikuchi, and N. Yamaguchi (1988). T cell-replacing factor (TRF)/interleukin 5 (IL-5): molecular and functional properties. *Immunol Rev 102:107.*

Takeda, S., T. Shimizu, and H. R. Rodewald (1997). Interactions between c-kit and stem cell factor are not required for B- cell development in vivo. *Blood 89:518.*

Takeda, K., H. Tsutsui, T. Yoshimoto, O. Adachi, N. Yoshida, T. Kishimoto, H. Okamura, K. Nakanishi, and S. Akira (1998). Defective NK cell activity and Th1 response in IL-18-deficient mice. *Immunity 8:383.*

Tang, H. L., and J. G. Cyster (1999). Chemokine Up-regulation and activated T cell attraction by maturing dendritic cells. *Science 284:819.*

Thome, M., P. Schneider, K. Hofmann, H. Fickenscher, E. Meinl, F. Neipel, C. Mattmann, K. Burns, J. L. Bodmer, M. Schroter, C. Scaffidi, P. H. Krammer, M. E. Peter, and J. Tschopp (1997). Viral FLICE-inhibitory proteins (FLIPs) prevent apoptosis induced by death receptors. *Nature 386:517.*

Thorsby, E., and K. S. Ronningen (1993). Particular HLA-DQ molecules play a dominant role in determining susceptibility or resistance to type 1 (insulin-dependent) diabetes mellitus. *Diabetologia 36:371.*

Tian, J., M. Clare-Salzler, A. Herschenfeld, B. Middleton, D. Newman, R. Mueller, S. Arita, C. Evans, M. A. Atkinson, Y. Mullen, N. Sarvetnick,A. J. Tobin, P. V. Lehmann, and D. L. Kaufman (1996a). Modulating autoimmune diabetes-prone mice. *Nat Med 2:1348.*

Tian, J., M. A. Atkinson, M. Clare-Salzler, A. Herschenfeld, T. Forsthuber, P. V. Lehmann, and D. L. Kaufman (1996b). Nasal administration of glutamate decarboxylase (GAD65) peptides induces Th2 responses and prevents murine insulin-dependent diabetes. *J Exp Med 183:1561.*

Tisch, R., X. D. Yang, S. M. Singer, R. S. Liblau, L. Fugger, and H. O. McDevitt (1993). Immune response to glutamic acid decarboxylase correlates with insulitis in non-obese diabetic mice. *Nature 366:72.*

Tisch, R., and H. McDevitt (1996). Insulin-dependent diabetes mellitus. *Cell 85:291.*

Todd, J. A., J. I. Bell, and H. O. McDevitt (1987). HLA-DQ beta gene contributes to susceptibility and resistance to insulin-dependent diabetes mellitus. *Nature 329:599.*

Todd, J. A., T. J. Aitman, R. J. Cornall, S. Ghosh, J. R. Hall, C. M. Hearne, A. M. Knight, J. M. Love, M. A. McAleer, J. B. Prins, and et al. (1991). Genetic analysis of autoimmune type 1 diabetes mellitus in mice. *Nature 351:542.*

Trembleau, S., G. Penna, E. Bosi, A. Mortara, M. K. Gately, and L. Adorini (1995). Interleukin 12 administration induces T helper type 1 cells and accelerates autoimmune diabetes in NOD mice. *J Exp Med 181:817.*

Trembleau, S., G. Penna, S. Gregori, M. K. Gately, and L. Adorini (1997). Deviation of pancreas-infiltrating cells to Th2 by interleukin-12 antagonist administration inhibits autoimmune diabetes. *Eur J Immunol 27:2330.*

* D. Vremec, J. Pooley, H. Hochrein, L. Wu and K. Shortman (2000). CD4 and CD8 expression by dendritic cell subtypes in mouse thymus and spleen. *J Immunol.* 164: 2978-86.

Trembleau, S., G. Penna, S. Gregori, H. D. Chapman, D. V. Serreze, J. Magram, and L. Adorini (1999). Pancreas-infiltrating Th1 cells and diabetes develop in IL-12-deficient nonobese diabetic mice. *J Immunol 163:2960.*

Trinchieri, G. (1995). Interleukin-12: a proinflammatory cytokine with immunoregulatory functions that bridge innate resistance and antigen-specific adaptive immunity. *Annu Rev Immunol 13:251.*

Tsuji, K., K. M. Zsebo, and M. Ogawa (1991). Murine mast cell colony formation supported by IL-3, IL-4, and recombinant rat stem cell factor, ligand for c-kit. *J Cell Physiol 148:362.*

Vafiadis, P., S. T. Bennett, J. A. Todd, J. Nadeau, R. Grabs, C. G. Goodyer, S. Wickramasinghe, E. Colle, and C. Polychronakos (1997). Insulin expression in human thymus is modulated by INS VNTR alleles at the IDDM2 locus. *Nat Genet 15:289.*

Van Parijs, L., Y. Refaeli, A. K. Abbas, and D. Baltimore (1999). Autoimmunity as a consequence of retrovirus-mediated expression of C- FLIP in lymphocytes. *Immunity 11:763.*

Van Parijs, L., Y. Refaeli, J. D. Lord, B. H. Nelson, A. K. Abbas, and D. Baltimore (1999). Uncoupling IL-2 signals that regulate T cell proliferation, survival, and Fas-mediated activation-induced cell death. *Immunity 11:281.*

Verge, C. F., D. Stenger, E. Bonifacio, P. G. Colman, C. Pilcher, P. J. Bingley, and G. S. Eisenbarth (1998). Combined use of autoantibodies (IA-2 autoantibody, GAD autoantibody, insulin autoantibody, cytoplasmic islet cell antibodies) in type 1 diabetes: Combinatorial Islet Autoantibody Workshop. *Diabetes 47:1857.*

Vermes, I., C. Haanen, H. Steffens-Nakken, and C. Reutelingsperger (1995). A novel assay for apoptosis. Flow cytometric detection of phosphatidylserine expression on early apoptotic cells using fluorescein labelled Annexin V. *J Immunol Methods 184:39.*

Vremec, D., M. Zorbas, R. Scollay, D. J. Saunders, C. F. Ardavin, L. Wu, and K. Shortman (1992). The surface phenotype of dendritic cells purified from mouse thymus and spleen: investigation of the CD8 expression by a subpopulation of dendritic cells. *J Exp Med 176:47.*

Vremec, D., and K. Shortman (1997). Dendritic cell subtypes in mouse lymphoid organs: cross-correlation of surface markers, changes with incubation, and differences among thymus, spleen, and lymph nodes. *J Immunol 159:565.*

Vremec, D., G. J. Lieschke, A. R. Dunn, L. Robb, D. Metcalf, and K. Shortman (1997). The influence of granulocyte/macrophage colony-stimulating factor on dendritic cell levels in mouse lymphoid organs. *Eur J Immunol 27:40.*

Vyse, T. J., and J. A. Todd (1996). Genetic analysis of autoimmune disease. *Cell 85:311.*

Wang, Y., O. Pontesilli, R. G. Gill, F. G. La Rosa, and K. J. Lafferty (1991). The role of CD4+ and CD8+ T cells in the destruction of islet grafts by spontaneously diabetic mice. *Proc Natl Acad Sci U S A 88:527.*

Wang, H. G., U. R. Rapp, and J. C. Reed (1996). Bcl-2 targets the protein kinase Raf-1 to mitochondria. *Cell 87:629.*

Wang, B., I. Andre, A. Gonzalez, J. D. Katz, M. Aguet, C. Benoist, and D. Mathis (1997). Interferon-gamma impacts at multiple points during the progression of autoimmune diabetes. *Proc Natl Acad Sci U S A 94:13844.*

Waters, C. M., T. D. Littlewood, D. C. Hancock, J. P. Moore, and G. I. Evan (1991). c-myc protein expression in untransformed fibroblasts. *Oncogene 6:797.*

Watson, J. (1979). Continuous proliferation of murine antigen-specific helper T lymphocytes in culture. *J Exp Med 150:1510.*

Weiner, H. L. (1997). Oral tolerance for the treatment of autoimmune diseases. *Annu Rev Med 48:341.*

Wherrett, D. K., S. M. Singer, and H. O. McDevitt (1997). Reduction in diabetes incidence in an I-Ag7 transgenic nonobese diabetic mouse line. *Diabetes 46:1970.*

Wicker, L. S., B. J. Miller, and Y. Mullen (1986). Transfer of autoimmune diabetes mellitus with splenocytes from nonobese diabetic (NOD) mice. *Diabetes 35:855.*

Wicker, L. S., B. J. Miller, L. Z. Coker, S. E. McNally, S. Scott, Y. Mullen, and M. C. Appel (1987). Genetic control of diabetes and insulitis in the nonobese diabetic (NOD) mouse. *J Exp Med 165:1639.*

Wicker, L. S., B. J. Miller, A. Chai, M. Terada, and Y. Mullen (1988). Expression of genetically determined diabetes and insulitis in the nonobese diabetic (NOD) mouse at the level of bone marrow-derived cells. Transfer of diabetes and insulitis to nondiabetic (NOD X B10) F1 mice with bone marrow cells from NOD mice. *J Exp Med 167:1801.*

Wicker, L. S., B. J. Miller, P. A. Fischer, A. Pressey, and L. B. Peterson (1989). Genetic control of diabetes and insulitis in the nonobese diabetic mouse. Pedigree analysis of a diabetic H-2nod/b heterozygote. *J Immunol 142:781.*

Wicker, L. S., M. C. Appel, F. Dotta, A. Pressey, B. J. Miller, N. H. DeLarato, P. A. Fischer, R. C. Boltz Jr., and L. B. Peterson (1992). Autoimmune syndromes in major histocompatibility complex (MHC) congenic strains of nonobese diabetic (NOD) mice. The NOD MHC is dominant for insulitis and cyclophosphamide-induced diabetes. *J Exp Med 176:67.*

Wicker, L. S., E. H. Leiter, J. A. Todd, R. J. Renjilian, E. Peterson, P. A. Fischer, P. L. Podolin, M. Zijlstra, R. Jaenisch, and L. B. Peterson (1994a). Beta 2-microglobulin-deficient NOD mice do not develop insulitis or diabetes. *Diabetes 43:500.*

Wicker, L. S., J. A. Todd, J. B. Prins, P. L. Podolin, R. J. Renjilian, and L. B. Peterson (1994b). Resistance alleles at two non-major histocompatibility complex-linked insulin-dependent diabetes loci on chromosome 3, Idd3 and Idd10, protect nonobese diabetic mice from diabetes. *J Exp Med 180:1705.*

Wicker, L. S., J. A. Todd, and L. B. Peterson (1995). Genetic control of autoimmune diabetes in the NOD mouse. *Annu Rev Immunol 13:179.*

Wicker, L. S. (1997). Major histocompatibility complex-linked control of autoimmunity [editorial; comment]. *J Exp Med 186:973.*

Wiktor-Jedrzejczak, W., E. Urbanowska, S. L. Aukerman, J. W. Pollard, E. R. Stanley, P. Ralph, A. A. Ansari, K. W. Sell, and M. Szperl (1991). Correction by CSF-1 of defects in the osteopetrotic op/op mouse suggests local, developmental, and humoral requirements for this growth factor. *Exp Hematol 19:1049.*

Williams, A. J., J. Krug, E. F. Lampeter, K. Mansfield, P. E. Beales, A. Signore, E. A. Gale, and P. Pozzilli (1990). Raised temperature reduces the incidence of diabetes in the NOD mouse. *Diabetologia 33:635.*

Witmer-Pack, M. D., W. Olivier, J. Valinsky, G. Schuler, and R. M. Steinman (1987). Granulocyte/macrophage colony-stimulating factor is essential for the viability and function of cultured murine epidermal Langerhans cells. *J Exp Med 166:1484.*

Witmer-Pack, M. D., D. A. Hughes, G. Schuler, L. Lawson, A. McWilliam, K. Inaba, R. M. Steinman, and S. Gordon (1993). Identification of macrophages and dendritic cells in the osteopetrotic (op/op) mouse. *J Cell Sci 104:1021.*

Wogensen, L., M. S. Lee, and N. Sarvetnick (1994). Production of interleukin 10 by islet cells accelerates immune-mediated destruction of beta cells in nonobese diabetic mice. *J Exp Med 179:1379.*

Wong, F. S., I. Visintin, L. Wen, R. A. Flavell, and C. A. Janeway Jr. (1996). CD8 T cell clones from young nonobese diabetic (NOD) islets can transfer rapid onset of diabetes in NOD mice in the absence of CD4 cells. *J Exp Med 183:67.*

Wong, B. R., R. Josien, S. Y. Lee, B. Sauter, H. L. Li, R. M. Steinman, and Y. Choi (1997). TRANCE (tumor necrosis factor [TNF]-related activation-induced cytokine), a new TNF family member predominantly expressed in T cells, is a dendritic cell-specific survival factor. *J Exp Med 186:2075.*

Wong, F. S., J. Karttunen, C. Dumont, L. Wen, I. Visintin, I. M. Pilip, N. Shastri, E. G. Pamer, and C. A. Janeway Jr. (1999). Identification of an MHC class I-restricted autoantigen in type 1 diabetes by screening an organ-specific cDNA library. *Nat Med 5:1026.*

Wu, L., A. D'Amico, K. D. Winkel, M. Suter, D. Lo, and K. Shortman (1998). RelB is essential for the development of myeloid-related CD8alpha- dendritic cells but not of lymphoid-related CD8alpha+ dendritic cells. *Immunity 9:839.*

Yagi, H., M. Matsumoto, K. Kunimoto, J. Kawaguchi, S. Makino, and M. Harada (1992). Analysis of the roles of CD4+ and CD8+ T cells in autoimmune diabetes of NOD mice using transfer to NOD athymic nude mice. *Eur J Immunol 22:2387.*

Yang, X. D., R. Tisch, S. M. Singer, Z. A. Cao, R. S. Liblau, R. D. Schreiber, and H. O. McDevitt (1994). Effect of tumor necrosis factor alpha on insulin-dependent diabetes mellitus in NOD mice. I. The early development of autoimmunity and the diabetogenic process. *J Exp Med 180:995.*

Yang, M., B. Charlton, and A. M. Gautam (1997). Development of insulitis and diabetes in B cell-deficient NOD mice. *J Autoimmun 10:257.*

Yasunaga, M., F. Wang, T. Kunisada, and S. Nishikawa (1995). Cell cycle control of c-kit+IL-7R+ B precursor cells by two distinct signals derived from IL-7 receptor and c-kit in a fully defined medium. *J Exp Med 182:315.*

Yokoyama, W. M., F. Koning, P. J. Kehn, G. M. Pereira, G. Stingl, J. E. Coligan, and E. M. Shevach (1988). Characterization of a cell surface-expressed disulfide-linked dimer involved in murine T cell activation. *J Immunol 141:369.*

Yoon, J. W., C. S. Yoon, H. W. Lim, Q. Q. Huang, Y. Kang, K. H. Pyun, K. Hirasawa, R. S. Sherwin, and H. S. Jun (1999). Control of autoimmune diabetes in NOD mice by GAD expression or suppression in beta cells.*Science 284:1183.*

Young, J. W., P. Szabolcs, and M. A. Moore (1995). Identification of dendritic cell colony-forming units among normal human CD34+ bone marrow progenitors that are expanded by c-kit-ligand and yield pure dendritic cell colonies in the presence of granulocyte/macrophage colony-stimulating factor and tumor necrosis factor alpha [published erratum appears in J Exp Med 1996 Mar 1;183(3):1283].
J Exp Med 182:1111.

Young, J. W., and K. Inaba (1996). Dendritic cells as adjuvants for class I major histocompatibility complex-restricted antitumor immunity. *J Exp Med 183:7.*

Zekzer, D., F. S. Wong, O. Ayalon, I. Millet, M. Altieri, S. Shintani, M. Solimena, and R. S. Sherwin (1998). GAD-reactive CD4+ Th1 cells induce diabetes in NOD/SCID mice. *J Clin Invest 101:68.*

Zha, J., H. Harada, E. Yang, J. Jockel, and S. J. Korsmeyer (1996). Serine phosphorylation of death agonist BAD in response to survival factor results in binding to 14-3-3 not BCL-X(L). *Cell 87:619.*

Zhan, Y., G. J. Lieschke, D. Grail, A. R. Dunn, and C. Cheers (1998). Essential roles for granulocyte-macrophage colony-stimulating factor (GM-CSF) and G-CSF in the sustained hematopoietic response of Listeria monocytogenes-infected mice.
Blood 91:863.

Zijlstra, M., E. Li, F. Sajjadi, S. Subramani, and R. Jaenisch (1989). Germ-line transmission of a disrupted beta 2-microglobulin gene produced by homologous recombination in embryonic stem cells. *Nature 342:435.*

Zitvogel, L., J. I. Mayordomo, T. Tjandrawan, A. B. DeLeo, M. R. Clarke, M. T. Lotze, and W. J. Storkus (1996). Therapy of murine tumors with tumor peptide-pulsed dendritic cells: dependence on T cells, B7 costimulation, and T helper cell 1-associated cytokines. *J Exp Med 183:87.*